WIND CLIMATOLOGY OF SOUTH AFRICA RELEVANT TO THE DESIGN OF THE BUILT ENVIRONMENT

by

ANDRIES COENRAD KRUGER

Dissertation presented for the Degree of Doctor of Engineering (Civil Engineering) at the University of Stellenbosch

Promotor: Prof JV Retief

Faculty of Engineering

Department of Civil Engineering

Co-promotor: Dr AM Goliger

CSIR

March 2011

DECLARATION

By submitting this dissertation electronically, I declare that the entirety of the work contained therein is my own, original work, that I am the sole author thereof (save to the extent explicitly otherwise stated), that reproduction and publication thereof by Stellenbosch University will not infringe any third party rights and that I have not previously in its entirety or in part submitted it for obtaining any qualification.

Signature: …….. Date: ……..

Abstract

In South Africa, wind constitutes the most critical environmental loading affecting the design of the built environment. The wind climatic information, which is currently incorporated in structural design standards, is based on the analysis of records from a limited number of wind recording stations, mainly located in large cities, and was done several decades ago. In view of the size and the climatological diversity of South Africa, this information cannot be deemed to be adequate. Therefore, the incorporation of well-distributed and updated information on wind climate is essential. The present study endeavoured to address this issue. A strong wind climatology was developed with the use of observed climate data, with the most significant result that a mixed strong wind climate is prevalent in the greater part of South Africa. Statistical approaches to estimate extreme wind speeds were investigated with applicable wind data, with the optimum approach guided by the unique climatological environment and the statistical properties of the utilised data set: For the wind gust analysis the Peak-Over-Threshold method with the exponential distribution is recommended, while in a mixed strong wind climate the “mixed climate” approach is preferred. For the analysis of the hourly mean wind speeds the choice is between the Gumbel distribution and the mixed climate approach, depending on the strong wind climate. The estimation and incorporation of environmental correction factors to the measured wind speeds were necessary as the surroundings of most weather stations did not correspond to the reference Terrain Category. For some of the weather stations it was impossible to compensate for the inadequate exposure and surrounding complex topography, so that a reduced number of weather stations were available for the strong wind analyses. The values estimated for the design wind speeds, adjusted for the short lengths of data records, as well as techniques developed to guide the spatial interpolation of the quantiles, were utilised to develop updated maps of the regional design wind speeds. A comparative study between the results of this study, and that of the previous study on which the current loading code in South Africa is based, indicates that the present study should produce more reliable quantile estimations.

Opsomming

Wind vorm die mees kritieke omgewingslading wat die ontwerp van die beboude omgewing in Suid-Afrika beïnvloed. Die windklimaat-inligting wat tans gebruik word in die ontwerp spesifikasies is gebaseer op die statistiese analiese van veskeie dekades gelede op ‘n beperkte aantal windmeting-stasies, hoofsaaklik gesentreer in groot stede. Indien die grootte sowel as die klimatologiese diversiteit van Suid-Afrika in ag geneem word kan hierdie inligting nie as voldoende gereken word nie. Die gebruik van heelwat beter verspreide en opgedateerde inligting oor die windklimaat is daarom noodsaaklik en die studie poog om hierdie leemte aan te spreek. ‘n Sterk-wind klimatologie van Suid-Afrika is ontwikkel deur die gebruik van waargenome klimaatdata, met die mees betekenisvolle bevinding dat ‘n gemengde sterk-wind klimaat in die grootste gedeelte van Suid-Afrika heers. Statistiese benaderings om ekstreme winde te beraam is ondersoek met die beskikbare winddata, met die optimale benadering wat sal afhang van die klimatologiese omgewing van die weerstasie en die statistiese eienskappe van die betrokke windrekord: Vir die wind-stoot analieses word die “Piek-Oor-Drumpel” metode met die eksponensïele verdeling aanbeveel, behalwe in ‘n gemengde sterk-wind klimaat waar die “gemengde klimaat” benadering gebruik word. Vir die analiese van die uurlikse gemiddelde winde is die keuse tussen die Gumbel verdeling en die gemengde klimaat benadering, afhangende van die sterk-wind klimaat. Die skatting en toepassing van omgewingskorreksiefaktore vir die windspoed was nodig, aangesien die omgewings waarin die meeste weerstasies is nie ooreenkom met die verwysings Terrein Kategorie nie. Vir sommige weerstasies was dit onmoontlik om vir die onvoldoende blootstelling te vergoed, met die gevolg dat minder stasies beskikbaar was vir die sterk wind analiese. Die geskatte waardes vir die ontwerp-windsnelhede, asook tegnieke ontwikkel vir ruimtelike interpolasie, is gebruik vir die ontwikkeling van kaarte van die omgewings-ontwerpsnelhede, na verstellings van die waardes om te vergoed vir die kort data rekords wat gebruik is. ‘n Kritiese vergelykingstudie wat gedoen is tussen die resultate van die huidige studie, en die vorige waarop die huidige laskodes vir Suid-Afrika gebaseer is, dui aan dat die huidige studie betroubaarder skattings van die kwantiele behoort op te lewer.

Acknowledgements

- My promoter, Prof Johan Retief, Part-time Senior Researcher, Department of Civil Engineering, University of Stellenbosch, for your insight and guidance towards the successful and timely completion of this research;
- My co–promoter, Dr Adam Goliger, structural engineer, Built Environment, CSIR, for your hands-on involvement in this study, as well as your willingness to share your vast knowledge on wind engineering;
- Snyman Sekele, researcher at the South African Weather Service, for assisting with a significant part of the data processing in the study;
- Other staff of the South African Weather Service, for assistance with the analysis of the wind data, as well as the supply of some of the weather station metadata information;
- ESKOM, for the funding of an extreme wind study of which some of the results could be utilised in the study;
- Nicolene, for everything else.

Table of Contents

List of Tables

List of Figures

Chapter 1

Introduction

1.1. Motivation

Wind constitutes the most critical environmental loading affecting the design (particularly structural safety aspects) of the built environment in South Africa. Over the years, several failures of buildings and structures due to wind actions have occurred, some of them resulting in loss of human lives, as well as significant financial losses (Goliger and Retief, 2002). These failures could be attributed to various factors e.g. improper design and/or construction, but also inadequate knowledge of the wind action; more specifically the wind characteristics at low elevations at a regional or local scale affecting the design of specific structures.

The Institute of Structural Engineering at Stellenbosch University and the Council for Scientific and Industrial Research (CSIR) are currently involved in the process of developing a set of new generation building design codes for South Africa. The wind climatic information, which is currently incorporated in the design specifications, is based on the statistical analysis of medium to long-term records from a very limited number of wind recording stations, mainly located in large cities (Milford 1985a, b). In view of the size, as well as the climatological diversity of South Africa, this information cannot be deemed to be adequate. This issue, as well as its impact on the design of the built environment, has been raised by Goliger (2007). Therefore, the incorporation of comprehensive and updated information on wind climate is essential, and of great relevance to the construction industry. The South African Weather Service (SAWS) (formerly known as the South African Weather Bureau (SAWB)), together with the above-mentioned institutions, cooperates in a process of determining a comprehensive statistical description of the occurrence of high wind speeds and associated wind direction for South Africa, which would be based mainly on the available reliable wind data measured by the SAWS. These analyses will form

the basis for wind loading requirements in the future design codes for the built environment.

1.2. Aims and approach

The main objective of this dissertation is to provide a comprehensive description of the extreme wind climate of South Africa. In this regard, two aims are identified; firstly an objective description of the observed strong wind climatology of South Africa, and secondly the development of updated and more comprehensive models and statistics for strong winds relevant to the design of the built environment.

The current available description of the strong wind climatology of South Africa (Goliger and Retief, 2002) is based on various sources of information, such as recorded lightning activity, specific documented extreme weather events, as well as the knowledge of SAWS experts. While it is thought that the current description provides a good overview of the causes of strong winds in South Africa, it should be seen as a "first approximation" study, as was acknowledged by the authors; the reasons being that the information utilised in the description was rather limited, and more importantly because no measured wind statistics were taken into account.

Therefore, to improve on this description, a more objective approach was followed by using measured wind data as the main source of information. Stations recording wind data, which are spatially well distributed over South Africa, and additional information on the synoptic or mesoscale weather conditions at the times of the wind measurements, were used. The weather conditions, at the times when the strong winds occurred, were then analysed.

For the development of updated wind statistics relevant to the design of the built environment, it is necessary that the utilised wind data ideally should be more comprehensive, both temporally and spatially, than what was available during the previous analyses. It is also imperative to utilise any useful metadata that can be incorporated into the analysis. Such metadata, which amongst others include information on the exposure of the climate station and the instrumentation, should be applied in the objective assessment of the data quality, as well as for the

development of correction factors to the wind data, where possible. Furthermore, the diverse wind climate of South Africa, with its different strong wind causes or mechanisms, is an important aspect to be taken into consideration in the statistical analysis of the wind data. In this regard the analysis of various sources of strong winds is critical. This dissertation sought to fulfil these requirements, with input from the additional climate data and related information that has been recorded and archived in recent decades.

1.3. Problem statement

The most important issues to be resolved in this research are related to the physical environment (i.e. strong wind climate), the data sources, and the proper statistical analysis thereof. Regarding the *physical environment* the following needs to be investigated:

- The diversity of the strong wind climate of South Africa, which is essentially determined by the various mechanisms producing strong winds in South Africa as well as other factors, such as topography, which produces the diversity observed;
- Whether the coverage of the weather stations is able to capture the full-scale strong wind climate;
- The presence of long-term cycles in the wind climate of South Africa, and the subsequent effect on the magnitude of the wind speeds;
- Interpretation of the wind data. In this regard high wind speeds need to be interpreted in terms of the strong wind mechanisms involved.

To properly investigate and describe the strong wind climate of South Africa, reliable and sufficient climate data is required, as well as proper analysis methods or approaches. Regarding the *climate data*, the following aspects are necessary to be assessed and addressed, before any proper analyses can be conducted:

- An audit of the available usable climate data;
- The quality of the available climate data, and the resolvement of any issues in this regard;

- An assessment of the sufficiency of the spatial distribution of the weather stations that can be utilised in the subsequent analysis.

The research requires the application of *proper analysis methods*, specifically the statistical methods required to estimate extreme values from the available wind data samples. In this regard the following are important:

- An investigation of available statistical techniques;
- The selection of proper analysis methods, which will take into account the sizes (which has a bearing on the representivity of the data samples), as well as other properties of the data sets which might have a bearing on the suitability of various analysis approaches.

The *desired outputs* of the dissertation are the following, to be able to provide a comprehensive description of the extreme wind climate of South Africa:

- A characterisation of the strong wind climate of South Africa, which comprises the identification and spatial distribution of the causes of strong winds;
- The relationships between the strong wind values and the mechanisms involved, which would entail proper analysis thereof;
- The statistical development of probability parameters (which could serve as input for subsequent reliability modeling or calibration of wind loads for purposes of design standards).

1.4. Structure of research and required information

A comprehensive update of the wind climatology and statistics of South Africa, relevant to the design of the built environment, is conducted. The dissertation follows a logical sequence to fulfil the main objectives, according to the key topics of the individual chapters, which are outlined below. The chapters are sequenced in such a way that the information or knowledge gained in the preceding chapters serves as input to the analyses included in the subsequent chapters.

Chapter 2 contains a general background to the research. Firstly, the relevance of this research to the built environment and wind engineering issues is discussed. Then the prevailing macroclimatic conditions are introduced, which indicate that

South Africa falls within a region where, for many areas, more than one cause of strong winds, i.e. a mixed strong wind climate exists. Related to this is a discussion of the approaches that are usually followed in the development of extreme wind statistics. In some regions of South Africa the possibility exists for the occurrence of extreme winds from infrequent meteorological events, such as tornadoes. The feasibility of the statistical incorporation of the likelihoods of extreme wind speeds from these events in the probability distributions of strong winds is also investigated. A brief overview of the previous extreme wind analyses for South Africa is then provided, and it will be pointed out how these analyses can be improved upon.

Measured climate data serves as the main input to the research. An overview of the assessment and selection of the available climate data is presented in Chapter 3. With the implementation of automatic weather station (AWS) technology in South Africa since the late 1980's, a vastly increased number of continuous wind speed records have become available. It is argued that the increased availability of wind data for South Africa would provide for a much better assessment of the wind climate of the country, mostly due to the increased spatial distribution of weather stations with relevant wind data records. However, it is not only the amount of available data that matters but also the quality of the data. It is therefore imperative that the homogeneity of the data be assessed, of which the various approaches followed will be discussed.

In Chapter 4, improved and detailed maps of the strong wind climatic zones for South Africa are developed, with the wind gust data being the main input. These maps can be referred to as a reference to the nature of the prevailing strong winds in a specific geographical region of the country. For regions where more than one strong wind mechanism is identified, the approaches taken to estimate extreme winds should then preferably take the mixed strong wind climate into account.

Various aspects of the development of the extreme wind climatology for South Africa are discussed in Chapters 5 to 7. Firstly, in Chapter 5, the application of different approaches or methods available in the statistical analyses of strong wind values, and subsequent analyses of the results, are presented. The advantages and disadvantages of these techniques are investigated, with the aim to find the most

appropriate statistical approaches to be adopted in the estimation of extreme winds in South Africa. For long time series in an environment where all strong winds have the same cause, fitting of the Gumbel distribution to annual maxima, is the usual method used to estimate the extremes. However, in the cases of shorter time series and mixed strong wind climates other approaches should also be considered.

The input values of the strong winds for the development of maps of regional design wind speeds should be estimated from data measured in an open terrain, which is free from significant obstructions to the wind flow. It is also crucial that the measurements should be taken in level terrain, without any complicated topographical features, such as mountains or valleys, for appreciable distances from the anemometer. In Chapter 6 an assessment is done of the exposure and surrounding environment of the weather stations which are utilised in the study. Various techniques are investigated for the correction of the measured wind data, in those cases where the exposures of the weather stations are not ideal. Where possible the correction factors are then developed and applied to the measured data.

Updated extreme wind climatology information for the country is presented in Chapter 7, which includes maps of the 1 in 50 year annual maximum wind gust and the 1 in 50 year annual maximum hourly mean wind speed. Firstly, the most appropriate and conservative approaches to the estimation of the extreme values are selected. Where applicable the correction factors developed in Chapter 6 are applied to the wind data, and the values recalculated. To enhance the conservativism of the values, the periods of record of the measurements are taken into account, as most of the lengths of the time series, which were utilised, are deemed to be short. The parameters of the selected distributions are adjusted accordingly and the extreme wind speed values re-estimated. These values were the wind speed quantiles to be utilised for the development of the maps of extreme winds. Subsequently methods are investigated to estimate the representative extreme values applicable between the geographical locations of the estimated values. Guidelines are developed for the optimal spacing of the extreme value contours included on the maps.

In Chapter 8 a regional assessment of the strong wind climate is performed, by integration of the results to obtain a condensed view. At this stage of the study it is

possible to spatially compare some of the wind characteristics of weather stations with one another. Of particular importance is the assessment of the distribution of strong wind values forthcoming from the various strong wind producing mechanisms, identified in Chapter 4 and analysed in Chapter 5, to characterise the effect of the mixed strong wind climate on the estimation of quantiles.

Chapter 9 contains a comparison of the results, data and methods of the current analysis with the previous most recent analysis by Milford (1985a and b). In this regard it is envisaged that the denser spatial distribution of weather stations employed in the current analysis, as well as the application of more appropriate statistical techniques, would lead to a more realistic presentation of the spatial distribution of extreme wind speed values in South Africa.

The revision of the extreme wind climatology of South Africa revealed that the estimation of extreme winds from the observed wind data is not merely a straight forward process of the application of a statistical model to the data.

Several aspects complicate the issue, such as:

- The diverse South African climate, where in some regions the strong winds are mostly caused by synoptic-scale processes, such as cold fronts and ridging highs, while in others the main cause is on the mesoscale, i.e. from thunderstorms.
- Regarding the observed wind data sets, the utilisation of short time series in the estimation of extreme wind quantiles for the typical 50-year design life of a structure, requires the consideration and investigation of various statistical approaches. The statistical models employed, should provide for the uncertainties which are inherent when short climate data series are used, to extrapolate the likely weather extremes which could occur over a much longer period of time.
- The location in which wind is measured determines whether those measurements are representative of the surrounding environment. To assure such representivity, the exposure of the measuring site is crucial and should be carefully considered.

In Chapter 10 the remedial actions to the above complications are summarised. In addition, the significance of the results in relation to wind engineering science, but also in terms of present climatological knowledge, is highlighted, by discussing the degree to which the challenges in the problem statement have been addressed or resolved. In addition, suggestions on how this research can be built upon in future are made.

Chapter 2

Background

2.1. Relevance of study to wind engineering science in South Africa

The existing building standard, SANS (South African National Standard) 10160-1989 (1989) (amended 1993), stipulates wind actions as the dominant environmental action on buildings within the South African climate. A recent review of the codification of wind-loading for structural design is presented by Goliger *et al*. (2009a). The basis for the implementation of these principles for the revised wind-loading design procedures of SANS 10160-3 (2010), The Draft South African Loading Code, is presented by Goliger *et al*. (2009b). In Goliger *et al.* (2009a and b) the relative importance of wind statistics to the built environment is emphasized: SANS 10160-3 (2010) continues to present the role of wind actions on buildings prominently, and use the Eurocode EN 1991-1-4 (2005) as reference. The dissertation will contribute to the knowledge of some of the wind-related issues which are raised in Goliger *et al*. (2009a and b), of which sections 2.1.1 and 2.1.2 present brief overviews.

2.1.1. The South African strong wind climate

In South Africa strong winds can be broadly categorized into two types, namely those of the synoptic scale origin (e.g. cold fronts), and those of convective origin (e.g. thunderstorms). The origins of the strong winds in South Africa are further discussed in section 2.2, and analysed in-depth in Chapter 4. For the areas dominated by strong winds from thunderstorms, an averaging time of 3 s or less is recommended for a meaningful determination of the extreme value design wind speeds. This is due to the short duration of the strong winds from thunderstorms, which are typically related to the passage of the gust front, defined as the leading

edge of the thunderstorm downdraft. The European wind climate is dominated by synoptic-scale mid-latitude cyclonic storms. The EN-1991-1-4 is based on these weather conditions, and therefore the basic wind speed (the extreme wind speed that can be expected every 50 years) is derived for an averaging period of 10 minutes, with fixed conversion factors between the different averaging time scales. Therefore, while the Eurocode is followed by deriving the basic wind speed for an averaging period of 10 minutes, this research investigates the design wind speeds at averaging times of 2-3 seconds and one hour. In a mixed strong wind climate an averaging time of 2-3 seconds is sufficiently short to capture the wind strengths of only the gust fronts from thunderstorms, while one hour is deemed a long enough averaging period not to be contaminated with these relatively strong wind gusts of very short duration. It is argued that from the analysis performed in this study, the 10 minute design wind speeds can be derived by applying appropriate conversion factors, which distinguish between thunderstorm- and synoptic-scale- dominated strong winds. However, such a conversion falls beyond the scope of this dissertation.

Strong winds produced by thunderstorms are usually of very short duration, and therefore the relationships between the mean wind strengths at the different time-scales in places dominated by thunderstorms are not as constant as in the case where the strong winds produced by synoptic-scale events are dominant. At the coast strong winds on the synoptic scale tend to dominate, while in the interior the thunderstorms tend to dominate. This issue is emphasised in the SANS 10160-1989, where the gust factor, i.e. the ratio between the 2-3 second wind gust and the hourly mean wind speed, for the interior is 2,0, while for the coast it is 1,6. The gust factors derived from the analyses in this research are discussed in Chapter 7. The differences in gust factors, and the fact that the analysis of strong winds in a mixed wind climate requires the assessment of the different causes of the strong winds, makes the recognition of mixed strong wind climates imperative in the statistical analysis of wind data.

2.1.2. Environment of wind measurements

Environmental influences on wind measurements include the terrain roughness, topography and the presence of prominent features or structures within the

immediate vicinity of the wind speed recorders. Loading codes stipulate correction factors to the design wind speed, for various categories of terrain roughness and topographical features upstream of the site under consideration. These correction factors require that the basic wind speed in an area be based on the wind speed that would have been measured under ideal conditions, i.e. in open, flat terrain with no significant obstacles or complex topographical features close-by. It therefore follows that the wind speeds, from which the extreme winds are estimated, should be measured under these ideal conditions. If the wind is not measured under these conditions, correction factors should be developed, where possible, to compensate for the inadequacies in the measuring environment. Also, the correction factor may depend on the nature of the strong winds and are different for synoptic and thunderstorm winds. The measuring environments of the weather stations utilised are analysed and discussed in depth in Chapter 6.

2.2. Prevailing macroclimatic conditions

From section 2.1 it follows that for the optimum analysis and subsequent interpretation of the extreme winds, an intimate knowledge of the nature or origin of strong winds of the region under consideration, is necessary. Here a discussion is presented on the prevailing weather systems in South Africa during different times of the year, but with the emphasis on those synoptic conditions which are conducive to the development of strong winds. These synoptic conditions may produce strong winds of a pure synoptic origin, e.g. from cold fronts or ridging high-pressure systems, or produce the conditions which are conducive to convective activity, where the strong winds originating from thunderstorms are likely to occur.

The seasonal differences in the near-surface circulation features of the atmosphere, over southern Africa and the surrounding oceans, are mainly the result of the northward displacement of the subtropical high-pressure belt by almost five degrees latitude from summer to winter. Usually these lower-level anticyclones on land are interrupted once to twice per week by cold-front troughs (Taljaard, 1995). Therefore, the influences of the subtropical high-pressure belt and the mid-latitude westerlies, with associated fronts, vary significantly during the course of the year over the subcontinent. The differences in the circulation features between the seasons, and

hence the likelihood of strong winds due to particular circulation features, can be summarised with reference to Hurry and Van Heerden (1987), who gave a detailed overview of the seasonal differences in the atmospheric circulation over southern Africa. From the pressure distribution and the basic movement of air masses, the following are noted with regards to the general synoptic circulation pattern in summer time, referring to Figure 2.1: The “westerlies”, a band of strong westerly winds surrounding the globe in which extratropical low-pressure systems develop, is situated well to the south of the continent. This implies that strong winds forthcoming from extratropical cyclones and their associated cold fronts will mostly be limited to the southern parts of the subcontinent. The Indian Ocean high-pressure system is situated more eastward, with frequent strong ridging over the subcontinent, where “ridging” refers to usually strong wind flow spiralling out from a high-pressure system. The associated south-eastern Trades (A) influence the north-eastern part of southern Africa. These winds can be strong, curving sometimes from Limpopo Province (L) into the Free State (F), or moving over the areas further to the north, such as Zimbabwe and Zambia (Z).

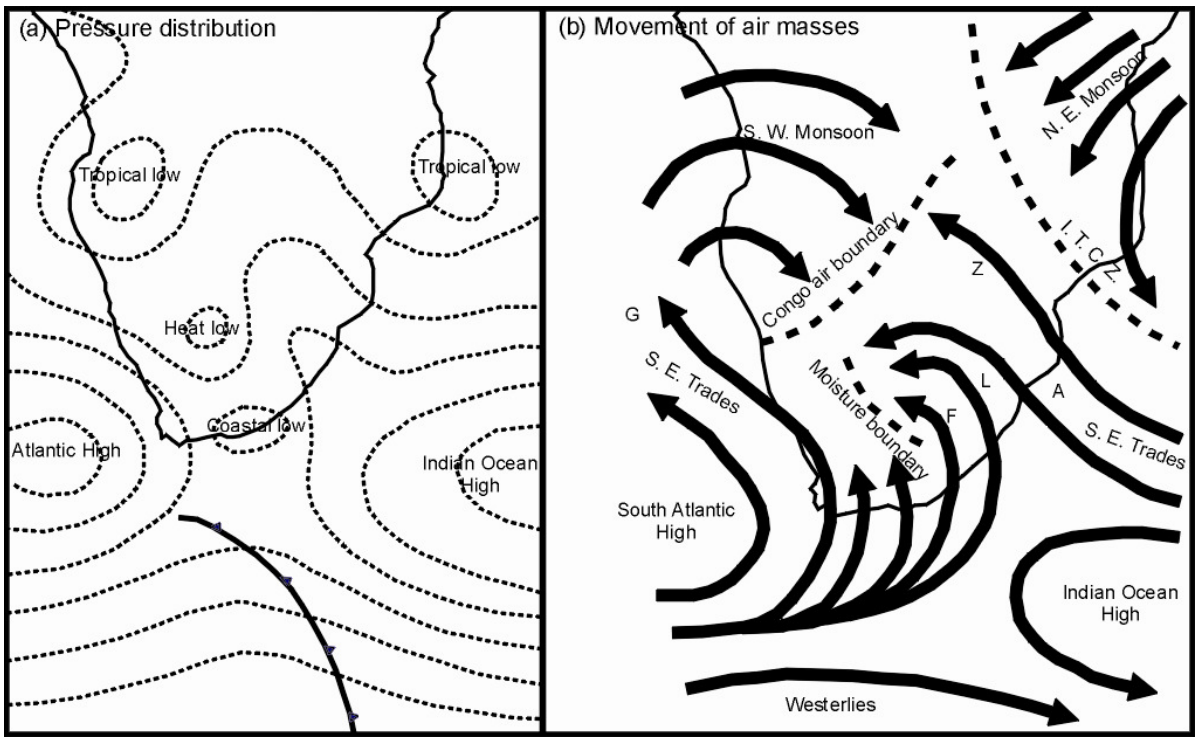

Figure 2.1. Features of the (a) pressure distribution and (b) basic movement of air masses over southern Africa during summer (after Hurry and Van Heerden, 1987).

The moist air transported into the subcontinent in this way can condense through uplift, e.g., from the topography or convection, with subsequent cloud formation and precipitation, often from thunderstorms which can produce strong wind gusts. The Atlantic Ocean high-pressure system, which is situated near the west coast, is a source of drier air which moves into the subcontinent from the southwest and southeast. The south-easterly wind blows mostly over the Cape Peninsula and is associated with unpleasant dryness and gustiness. It is locally known as the “Cape Doctor”, due to its effective removal of pollutants from the air. This wind can be quite persistent, as shown by an example in Figure 2.2, of the growth in a north-westerly direction of some trees in this region.

Figure 2.2. An example of the growth of a tree in the Cape Peninsula in a north-westerly direction, due to persistent strong south-easterly winds.

The “moisture boundary” is the area where the moist air from the east and the drier air from the southwest meet. The air from the Indian Ocean tends to move over the

Atlantic air, resulting in uplift and sometimes the formation of thunderstorms. When the moisture boundary is well to the south, widespread thunderstorms are possible. Summer heating causes a heat low to develop in the west or northwest of the subcontinent. The south-eastern Trades from the Atlantic Ocean high-pressure system (G) sometimes curve around this low, and change to the south-western Monsoon winds. Where these winds meet the south-eastern Trades the air masses converge to form the Congo air boundary, where thunderstorms are likely to develop. The north-eastern Trades from the north-eastern Monsoon system cross the equator, and where they meet the south-eastern Trades, convergence takes place. This convergence area determines the position of the Intertropical Convergence Zone (ITCZ) where heavy rainfall with associated thunderstorms frequently occur. Usually there is a shallow heat low over the Kalahari Desert, which sometimes influences the direction of the south-eastern Trades.

Therefore, in conclusion to the above discussion, gust fronts from thunderstorm activity are frequent over most of the country in summer, but less so in the southern and western parts. The heating of the earth's surface acts as a trigger for the development of thunderstorms, but additional factors play a role, such as the moisture boundaries, orographic uplift, frontal uplift, and large-scale convergence ahead of a trough (an elongated area of relatively low atmospheric pressure) or east of a low-pressure cell. In addition, line storms can form parallel to trough lines and are associated with strong wind gusts ahead, typically referred to as "line squalls".

From the basic pressure distribution and movement of air masses for winter, presented in Figure 2.3, it is observed that all circulation features are situated more to the north than in summer. The south-eastern trade winds still occur, but because the north-eastern Monsoon is absent, no convergence takes place. The ITCZ, as well as the Congo air boundary, move northwards and therefore the likelihood of thunderstorms to occur is diminished.

The "westerlies" influence the weather of the southern and central parts of the subcontinent to a large degree. Therefore, cold fronts, with associated strong winds, often move over these areas and may reach far to the north. Strong winds and gusts during winter are usually caused by intense cold fronts, moving mostly over the

southern half of South Africa, and also by the ridging of the high-pressure systems behind the fronts. During this time of the year, gale force winds are frequently experienced over the Cape Peninsula, as well as the southern and south-eastern coasts.

When the Atlantic Ocean high-pressure system moves more eastwards and stays strong, gale-force winds can spread to the KwaZulu-Natal coast as far north as the Mozambique Channel. However, when the Atlantic Ocean high-pressure system is situated south of the country, with the associated isobars lying almost parallel latitudinally, strong south-easterly to easterly winds can be experienced along the west coast and Cape south coast.

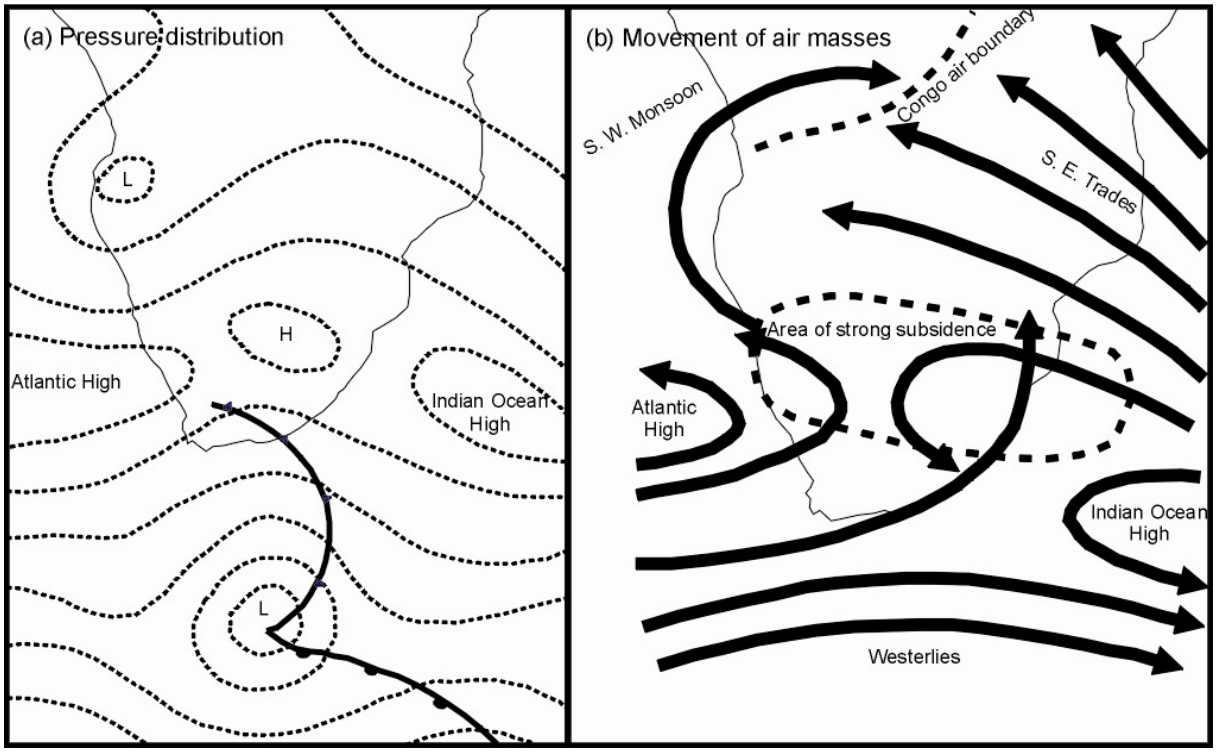

Figure 2.3. Features of the (a) pressure distribution and (b) basic movement of air masses over southern Africa during winter (after Hurry and Van Heerden, 1987).

It is noted that the prevailing macroclimatic conditions over the subcontinent are very similar to those on parts of other continents in the southern hemisphere, where the climate is influenced by both mid-latitude mature storms and the movement of the ITCZ. In these regions strong winds are caused by the passage of cold fronts and

the associated ridging, as well as thunderstorms which occur mainly in the summer months. These regions are the central and northern parts of Australia (Holmes, 2002; Oliver *et al.*, 2000), and Brazil in South America (Ponte and Riera, 2007). In section 2.3.3 that describes the mixed distributions, reference is made to studies of the different strong wind mechanisms in Australia, and the statistical treatment thereof – these are Twisdale and Vickery (1992), that distinguished between the strong winds caused by extratropical pressure systems and thunderstorms, and Gomes and Vickery (1978) who identified four strong-wind mechanisms, i.e. extratropical-pressure systems, thunderstorms, hurricanes and tornadoes.

2.3. Extreme value theory relevant to wind data modelling

The primary input to the development of an extreme wind climatology or atlas is observed wind data. This data should be analysed by the application of the most relevant statistical techniques available, by taking the underlying theoretical statistical distribution into account, and also the assumptions that are accompanied by the application of such a distribution.

Typical methodologies applied in the development of strong wind climatologies mainly comprise a broad discussion of statistical extreme value theory, but relevant to wind data. Discussions of the methodologies developed for special cases in extreme value analysis, such as those developed for short time series and time series subjected to an underlying mixed strong wind climate (where the sources of the measured strong wind values are forthcoming from more than one type of strong wind-producing mechanism), are also presented. The consideration of the latter methodologies is crucial, firstly because some of the time series to be utilised in this study can be considered to be quite short, but also due to the fact that a large part of South Africa exhibits a mixed strong wind climate.

Extreme-value theory comprises the statistical methodologies developed to determine the probabilities of specific extreme values to occur, from observed data sets. The optimum statistical method to be applied ultimately depends on the underlying features of these data sets. Most of the methodologies discussed in this

section could be applied to the wind data, of which the analyses are presented in Chapter 5.

2.3.1. The Weibull distribution

The Weibull distribution is considered to be a suitable model for the analysis of wind speed distributions (Hennessey, 1977; Perrin *et al.*, 2006). Therefore, in most cases this distribution can be fitted to all types of wind speed data, to estimate extreme wind speeds. A criticism of the Weibull method is that the extreme values in the data set have little influence on the estimated distribution (Perrin *et al.*, 2006). Therefore, the application of this method can cause inaccurate estimates of the tails of the distributions of wind speeds, and thus the statistical distribution of annual maximum wind speeds. Also, serial dependence of measurements often proves to be a problematic factor. These mentioned problems can compromise the assumptions that are made when fitting a distribution to a particular set of data to estimate extremes; these are serial independence of the recorded wind speeds, and that the fit of the distribution is good also in the extreme right tail, i.e. at relatively high values, of the distribution of wind speeds (Perrin *et al.*, 2006).

2.3.2. Generalized Extreme Value theory

The most widely used methods to estimate extreme wind speeds are based on the classical or Generalized Extreme Value (GEV) theory, of which a short review is presented by Palutikof *et al.* (1999). The difference between these methods and the Weibull method is that the Weibull distribution is fitted to all available data, while the GEV distribution is only fitted to the extreme values, usually the annual maxima.

In the annual maxima method, an Extreme Value (EV) distribution is fitted to the annual maximum wind speed values. By using this method both of the problems mentioned in section 2.3.1 are eliminated, as only independent annual extreme values are used in the fitting of the distribution. For sufficiently long sequences of independent and identically distributed random variables, the maxima of samples of size n, for large n, can be fitted to one of three basic families. These three families

were combined into a single distribution (Jenkinson, 1955), and is known as the GEV distribution, with cumulative distribution function (cdf):

$$F(x) = e^{-(1-\kappa y)^{1/k}} \qquad \kappa \neq 0 \tag{2.1a}$$

$$F(x) = e^{-e^{(-y)}} \qquad \kappa = 0 \tag{2.1b}$$

where κ is the shape parameter, which determines the type of extreme value distribution, and y is the standardised or reduced variate. The Gumbel or Fisher-Tippett Type I distribution has a value of $\kappa = 0$, the Fisher-Tippett Type II has $\kappa < 0$, while the Type III has $\kappa > 0$. Types I and II are unbounded at the upper end, while Type III is bounded. This means that there will be an upper bound for the quantile values estimated with the Type III distribution, while no upper bound exists for Types I and II.

The most often applied distribution is the Gumbel, not only because the calculations get simplified when $\kappa = 0$, but also because one of the parent distributions of the Gumbel distribution is the Weibull distribution. The Weibull distribution is, as mentioned in section 2.3.1, considered to be a good model for wind speed distributions. For the Gumbel distribution only two parameters, the mode and scale or dispersion parameters, are required. The standardized or reduced variate y is given by:

$$y = (x - \beta)/\alpha \tag{2.2}$$

where α is the scale or dispersion parameter, β is the mode of the extreme value distribution, and x is the extreme value.

There are various methods to estimate α and β, e.g. graphical methods, probability weighted moments, maximum likelihood solutions and the method of moments. All of these methods should produce similar results. The graphical method is based on equation 2.2, modified to

$$x = \alpha y + \beta \tag{2.3}$$

where the slope α gives the scale or dispersion, and β, the mode. To estimate a value for y, the Gumbel reduced variate

$$y_{Gumbel} = -ln[-ln(F(x))] \tag{2.4}$$

is used. $F(x)$ is empirically estimated for each of the observed annual maxima. For the Gumbel distribution, the most unbiased estimates are given by

$$F(x_m) = (m - 0.44)/(N + 0.12) \tag{2.5}$$

where x_m is the m^{th} ranked annual maximum wind speed, and N is the number of annual maxima (Gringorten, 1963, in Palutikof *et al.*, 1999). A value for y_{Gumbel} can be calculated for each value of x, and a least-squares fit is used to fit a straight line to this data set. From this straight line the parameters α and β can be found.

Another often used method is the method of moments, described by Wilks (2006), which only uses the sample mean and standard deviation to estimate the Gumbel parameters:

$$\alpha = s\sqrt{6}/\pi \tag{2.6}$$

and

$$\beta = \bar{x} - \gamma\alpha \tag{2.7}$$

where s is the standard deviation of the sample, x is the sample mean, and γ = 0,57721… is Euler's constant. While the estimations of the Gumbel parameters are simpler to calculate using the above method, the graphical method is often still preferred.

The quantile X_T, which is the value of X to be expected every T years, can now be calculated with

$$X_T = \beta - \alpha\, ln[-ln(1 - 1/T)] \tag{2.8}$$

So far the shape parameter κ has been assumed to be 0. If the extreme wind data follows an alternative form to the Type I, it is said to be GEV instead of Gumbel distributed. In that case three parameters need to be estimated, i.e. α, β and κ. The most often used numerical methods to estimate the parameter values are probability weighted moments (PWMs) (Hosking *et al.*, 1985), and maximum likelihood (ML) solutions (Davison, 1984; Smith, 1986; Davison and Smith, 1990; Wilks, 2006).

The PWMs are defined in terms of

$$b_R = E[xF(x)^R] \qquad R = 0, 1, 2... \tag{2.9}$$

Unbiased estimates of the first three PWMs are given by

$$b_0 = \bar{X} \quad (2.10a)$$

$$b_1 = \sum_{j=1}^{n-1} [(n-j)X_j/n(n-1)] \quad (2.10b)$$

$$b_2 = \sum_{j=1}^{n-1} [(n-j)(n-j-1)X_j]/[n(n-1)(n-2)] \quad (2.10c)$$

for sample size n.

The parameters α, β and κ can then be estimated as functions of the PWM's, namely: The shape parameter is estimated by

$$\hat{\kappa} = 7.859c + 2.9554c^2 \quad (2.11a)$$

where

$$c = [(2b_1 - b_0)/(3b_2 - b_0)] - [ln2/ln3] \quad (2.11b)$$

The scale and location parameters are estimated by

$$\hat{\alpha} = [(2b_1 - b_0)\kappa]/[\Gamma(1 - c^{-\hat{\kappa}})(1 + \hat{\kappa})] \quad (2.12a)$$

$$\hat{\beta} = b_0 + \{\hat{\alpha}[\Gamma(1 + \hat{\kappa}) - 1]\}/\hat{\kappa} \quad (2.12b)$$

where Γ is the gamma function (Press *et al.*, 1992).

Maximum likelihood methods require iterative procedures, and therefore can only be applied by the necessary programming or statistical software.

The GEV methods, including the Gumbel, employ only one value for each year of data, and therefore it is advisable that this method should only be used for long data sets for the estimation of the distribution parameters. Various authors suggest different lengths of time series that can safely be used, e.g. Cook (1985) suggests at least 20 years, and definitely not fewer than 10 years. It is assumed here that 10 years is the absolute minimum number of years of data for the application of the GEV methods. It should be noted that in the climatological community it is generally assumed that a time series of 30 years is sufficient to capture the variability of the climate. Taking this into consideration, there should, therefore, be a fair probability that the variability of the strength of the mechanisms leading to extreme wind values will not be reflected if less than 30 years of data is utilised. Also, if a short period of data is utilised and a very high extreme value is captured in the particular data set, the analysis of such a data set will produce unrealistic return values (Abild *et al.*, 1992; Brabson and Palutikof, 2000). This problem is further discussed in section 5.2.3, with reference to the application of the GEV method in section 5.2.2.

2.3.3. Mixed distributions

Data produced by different phenomena should preferably be treated separately to improve the extreme wind estimations (Palutikof *et al.*, 1999; Wilks, 2006). Although not taken into consideration in his determination of appropriate extreme value distributions, this concern was mentioned by Milford (1985a), who identified apparent mixed climatic conditions in the parent distributions of the wind data sets, which he analysed. Extreme wind data should be a natural candidate for mixed distributions, as it is highly probable for many locations that extreme winds can be caused by more than one strong wind producing mechanism. Some examples of studies that employed mixed distributions to estimate extreme winds in mixed strong wind climates are due to Twisdale and Vickery (1992) and Gomes and Vickery (1978), which are mentioned in section 2.2. In both these studies the combined distribution of the strong wind events was determined as the sum of the individual risks of exceedance, given as

$$F(x) \cong 1 - \left[1 - e^{-e^{-y_A}} + 1 - e^{-e^{-y_B}} + \cdots\right] \tag{2.13}$$

where y_A, y_B etc. are the reduced variates for the data sets related to the different strong wind producing mechanisms (Palutikof *et al.*, 1999). The above equation was first derived by Gomes and Vickery (1978), by noting that the combined cumulative probability distribution of the absolute annual maximum gust speed V_M is of the form

$$P(V_M < V) = \prod_{q=1}^{Q} P\left(V_q < V\right) \tag{2.14}$$

where V_M is the absolute annual maximum gust speed, V_q is the annual maximum gust speed for the q^{th} strong-wind producing mechanism, $P\ (V_M < V\ )$ and $P\ (V_q < V\ )$ are the cumulative probabilities of V_M and V_q , and Q is the number of significant phenomena.

To determine an equation that can be used to estimate maximum gust speeds for specific return periods and for a mixed strong wind climate, the following were taken into consideration, derived from Gomes and Vickery (1978): Mathematically

$$1 - (1/R) \approx e^{(-1/R)} \tag{2.15}$$

Therefore, for a return period of R years, the cumulative probability for a given gust speed V_R can be approximated by

$$P(V_M < V_R) = e^{(-1/R)} \tag{2.16}$$

Thus,

$$e^{(-1/R)} = \prod_{q=1}^{Q} P\left(V_q - V_R\right) \tag{2.17}$$

Therefore, for all strong wind producing mechanisms Gumbel distributed:

$$e^{(-1/R)} = \{e^{-e^{-[(V_R-\alpha_1)/\beta_1]}}\} * \{e^{-e^{-[(V_R-\alpha_2)/\beta_2]}}\} * \ldots \tag{2.18}$$

where α_1 and β_1 are the dispersion and the mode parameters of the first strong wind producing mechanism etc. Return period estimations for a specific wind speed in a mixed strong wind climate can be determined with the following equation:

$$R = 1/\{e^{[(\alpha_1-V_R)/\beta_1]} + e^{[(\alpha_2-V_R)/\beta_2]} + \cdots\} \tag{2.19}$$

It follows that for this methodology to be applied, the dispersion and mode parameters need to be determined for all the strong wind producing mechanisms. Firstly these mechanisms need to be identified, as well as the annual maximum wind gust values forthcoming from each strong wind mechanism. From the separate datasets for each strong wind mechanism, the distribution parameters are estimated according to the usual ways discussed for the Gumbel method.

2.3.4. Methodologies for short time series

2.3.4.1. More than one extreme value per epoch

The principal drawback to the classical GEV or Gumbel approach is that only one value is selected per epoch (Palutikof *et al.*, 1999), where the epoch is usually defined as one year. It is generally assumed that the estimations of distribution parameters become less reliable where less than 20 years of data are employed (Cook, 1985). Many wind time series, utilised for various wind analyses, have fewer than the optimum number of years, and to increase the number of cases for analysis, alternative approaches have been developed. The best known of these approaches are summarised in Palutikof *et al.* (1999):

- The concept of a single extreme value per epoch has been extended to include the *r*-largest values (Weissman, 1978).

- The Method of Independent Storms (MIS) uses a lull, or period of wind speeds below a selected threshold, to separate storms. The highest extreme value is selected from each storm.
- Peak-Over-Threshold (POT) maxima, which produce a series of extreme values above a chosen threshold. The Generalized Pareto Distribution (GPD) is then fitted to this data series.

The extension of a single extreme per epoch to the r-largest values firstly comprises the identification of these values for each epoch. The joint probability density function is given by

$$f(x_1 \dots x_{r)} = \alpha^{-r} e^{-e^{(-Z_r)-\sum_{j=1}^{r} Z_j}} \qquad \kappa = 0 \quad (2.20a)$$

$$f(x_1 \dots x_{r)} = \alpha^{-r} e^{\{-(1-\kappa Z_r)^{(1/\kappa)} + [(1/\kappa)-1]\sum_{j=1}^{r} \ln(1-\kappa Z_j)\}} \qquad \kappa \neq 0 \quad (2.20b)$$

where x_r is the r^{th}-largest value, $Z_r = (x_r - \beta)/\alpha$ and $Z_j = (x_j - \beta)/\alpha$. Smith (1986) gives the likelihood functions for the above equations, from which α and β can be estimated. The extremes selected for this method should be independent, which therefore have a bearing on the size of r. On the other hand, for more accurate estimations of distribution parameters, r should be made as large as possible to utilise as many extreme values as possible.

The MIS method was developed by Cook (1982, 1985). Firstly non-overlapping ten-hour means are calculated from the data series, by the application of a long-duration low-pass filter. The start of a lull is defined as the downward crossing of a 5 m/s threshold. The period between lulls define an epoch, for which independent storms are identified. The identified storm periods are searched for the maximum wind speed from the unfiltered data series. These selected extremes are fitted to a Gumbel distribution, of which the distribution parameters are estimated using the BLUE (Best Linear Unbiased Estimators) technique (Lieblein, 1974; Cook, 1985).

With POT methods, all values exceeding a specific threshold are used for analysis. A GPD is fitted to the selected values. The cdf of the GPD is

$$F(x) = 1 - [1 - (\kappa/\alpha)(x - \xi)]^{(1/\kappa)} \qquad (2.21)$$

where ξ is the selected threshold. For κ = 0, the GPD simplifies to the exponential (EXP) distribution

$$F(x) = 1 - e^{-[(x-\xi)/\alpha]} \tag{2.22}$$

The crossing rate of the threshold is defined as

$$\lambda = n/M \tag{2.23}$$

where n is the total number of exceedances, and M is the total number of years of the time series. Quantiles for specific return periods (in years) can be calculated from Abild *et al.* (1992):

$$X_T = \xi + (\alpha/\kappa)\,[1 - (\lambda T)^{-k}] \qquad \kappa \neq 0 \tag{2.24a}$$

$$X_T = \xi + \alpha \ln(\lambda T) \qquad \kappa = 0 \tag{2.24b}$$

The distribution parameters α and k can be estimated with the PWM method (section 2.3.2), by

$$\hat{\kappa} = [b_0/(2b_1 - b_0)] - 2 \tag{2.25a}$$

$$\hat{\alpha} = (1 + \hat{\kappa})b_0 \tag{2.25b}$$

which are valid within the range -0,5 < κ < 0,5. As with the other methods, selected extreme values should be independent. To ensure independence, choices have to be made between the threshold value and the separation time between the selected values. The choices of the separation time vary between authors, with e.g. Cook (1985) and Gusella (1991) using 48 hours for European wind climates and Walshaw (1994) using 60 hours for Sheffield data. The same applies for the selection of the threshold, where Cook (1985) decided on a threshold of 15 m/s for hourly mean wind speeds and 30 m/s for wind gusts, while Brabson and Palutikof (2000) found that a threshold of 32 to 36 m/s is most suitable for Shetland in the north of the United Kingdom. It therefore becomes clear that the optimum choices of threshold and separation time will depend on location and specifically the local wind climate. To aid in the threshold selection, various techniques exist, such as the Conditional Mean Exceedance (CME) graphs, which is a plot of the mean excess over threshold as a function of the threshold value (Davison, 1984; Ledermann *et al.*, 1990). If the CME graph indicates a straight line, the data is assumed to be GPD distributed. The threshold value is chosen as the lowest value above which the graph shows a straight line.

Brabson and Palutikof (2000) defined an independent event index

$$\varepsilon = (\text{independent events})/(\text{total events}) \quad (2.26)$$

and calculated the value of ε for various combinations of threshold and "dead time", i.e. the minimum period between selected values. An independent event can be defined as an event of which the cause is different than the other events before and after the particular event. The ideal is for ε to be as close as possible to unity, but a value for ε = 0,8 is sufficient to obtain accurate quantile estimates from the GPD.

2.3.4.2. Other methods

Some methods have specially been developed for estimating extreme wind speeds where there is a very limited length of meteorological records available, i.e. shorter than 10 years. Synthetic data generation includes normal and Weibull distributed independent random numbers, the partial duration series model (PDSM) (Gusella, 1991), the first- and second-order autoregressive models, the first-order Markov Chain method (Cheng and Chiu, 1985 and 1994), and a wind speed data generation scheme based upon wavelet transformation (Aksoy *et al*., 2004). Examples of these can be found in Cheng and Chiu (1985), who developed a stochastic model for generating long-term annual extreme winds from short period records. The assumption here is that the wind climate is "well behaved", meaning that there are no significant periodicities evident in the wind climate. For the South African climate such wind behaviour cannot readily be assumed, as there is cyclical behaviour evident in almost all the climate parameters over the region.

2.3.5. Goodness-of-fit testing

2.3.5.1. General

Goodness-of-fit tests are used to assess how well a statistical distribution fits to a data sample. Methods exist to visually, but subjectively, assess the goodness of fit. However, formal, quantitative tests are most often applied, and these are carried out within the framework of hypothesis testing. If evidence is obtained by the test conducted to be in favour of the null hypothesis, the result is interpreted as

confirmation that the data are not inconsistent with the hypothesized distribution (Wilks, 2006). There are many goodness-of-fit tests that have been devised, but the most common ones are the t-test, χ^2-test, Kolomogorov-Smirnov (K-S) test and the Anderson-Darling test. Of these the Anderson-Darling test, highlighted below, is deemed to be the most applicable for the purpose of the current study, as this test is more sensitive to deviations in the tails of the distribution than the other tests.

2.3.5.2. The Anderson-Darling goodness-of-fit test

The test statistic of the Anderson-Darling goodness-of-fit test (D'Agostino and Stephens, 1986) is usually given as A^2, and its value determined from

$$A^2 = -n - (1/n)\sum_{i=1}^{n}\{(2i-1)[(\ln(w_i) + \ln(1-w_{n-i+1})]\} \quad (2.27)$$

Where n is the sample size, and w is the cdf for the statistical distribution tested. For small samples A^2 is modified to

$$A_m^2 = A^2\left(1 + 0.2/\sqrt{n}\right) \quad (2.28)$$

where A_m indicates the modified value for A.

A_m^2 is compared to an appropriate critical value from Table 2.1 below.

Table 2.1. Critical values for the test statistic, A^2, of the Anderson-Darling goodness-of-fit test (D'Agostino and Stephens, 1986).

α	0,1	0,05	0,025	0,01
A^2	0,637	0,757	0,877	1,038

α indicates the level of significance.

Due to the nature of the hypothesis test, it is desired that the test statistic be as small as possible for evidence in favour of the null hypothesis, to indicate that the sample data is consistent with the statistical distribution under consideration. Therefore it is required that the value of A^2 be less than 0,757 for the null hypothesis to be accepted at the 5% level of significance.

2.3.6. Lengths of record and uncertainties of quantile estimations

The estimations of the distribution parameters from short periods of record, such as 10 years, are highly problematic. The uncertainty in estimations can be due to the arbitrary choice of statistical model, or sampling uncertainty (mostly due to a small sample size). Therefore, the estimated quantiles should also contain some information regarding the uncertainties of the estimates (Abild *et al*., 1992). In this regard it is essential that the confidence level of the estimates should also be assessed. In sections 5.4.2 and 7.4.1 this issue is further discussed, and statistical methodologies applied to estimate and compensate for these uncertainties.

2.4. Extreme winds originating from infrequent meteorological events

Infrequent meteorological events in South Africa, such as the occurrence of tornadoes, tropical cyclones and downbursts, are important to consider when estimating the likelihood of extreme winds. At a particular location, where the wind may have been measured over even a long period of time, the likelihood may exist for these infrequent meteorological events to occur, although not yet measured. It is only due to the small probability and/or limited spatial extent of these events, that their related extreme magnitude winds have never been recorded at the particular location. Furthermore, especially in the case of tornadoes, the associated winds are so strong that it is typically not possible to measure them directly. It is attempted in this chapter to roughly estimate the probability of these extreme events to occur over South Africa.

2.4.1. Tornadoes

The information about the spatial distribution, frequency and strength of tornadoes can only be inferred from a statistical analysis of the related wind damage reports (Goliger *et al*., 1997). Tornadoes occur in regions where thunderstorms are able to develop an organised internal structure of sufficient strength. The wind strengths of specific tornado events are based mainly on engineering estimation or the calculation of the wind force necessary to inflict various degrees of damage and/or the overturning or transporting of various other objects. One such estimate made on

the basis of an event in South Africa suggested a wind speed in the order of 100 m/s (Goliger, 1994). Currently a basic design wind speed of 40 m/s is specified for most of the country (SANS 10160-1989, 1989). A two-and-a-half-fold increase above the design wind speed is capable of inflicting substantial damage to the built environment. The only comprehensive study on the spatial distribution and probabilities of tornado-strength winds in South Africa were done by Goliger *et al.* (1997), to which the following analyses from sections 2.4.1.2 to 2.4.1.4 refer to.

2.4.1.1. Documentation of tornadoes in South Africa

The only database of tornadoes in South Africa was developed by the CSIR (Milford and Goliger, 1994), and covers the period 1905 up to mid-1996. This database is compiled from events published in the South African Weather Bureau (SAWB) newsletters (Viljoen, 1987-1988), the CAELUM publication and updates thereof (CAELUM, 1991), field trips, newspaper articles from the South African State Library, a survey of newspaper clippings collected since 1913 by the Weather Service library, and CSIR research reports. The database contains descriptions of nearly 200 tornado events.

2.4.1.2. Classification of tornadoes

The most commonly used method to classify tornadoes according to their strength is the Fujita-Pearson classification (Fujita, 1971; Fujita, 1973), which is presented in Table 2.2. The tornadoes are classified in terms of six intensities, ranging from F0 to F5, which are based on wind speeds inferred from visual evidence of the damage to structures. The Fujita-Pearson classification system has been applied to all the documented tornadoes in the CSIR database. The vast majority of events were not classified as F0, and no classifications were made of F4 or higher.

2.4.1.3. Probability of tornado occurrences

The mean rate of occurrence of tornadoes per unit area is a common measure of tornado risk (Fujita, 1971; Goliger and Milford, 1997; Goliger *et al.*, 1997). For South Africa, the mean rate of occurrence of tornadoes per square kilometre per year is

presented in Figure 2.4. Three zones are depicted, indicating different probabilities of occurrence, but excluding tornadoes of intensity F0.

Table 2.2. The Fujita and Pearson tornado scale (Goliger *et al.*, 1997; after Fujita, 1973).

Maximum wind speed (m/s)	Description of damage	Path length (km)	Path width (m)
F0 20 – 30	Light damage; Some damage to chimneys, branches of trees broken, shallow-rooted trees pushed over, sign boards damaged.	**P0** 0,5 – 1,5	5 – 15
F1 30 – 50	Moderate damage: Roof surfaces peeled off, mobile houses pushed off foundations and overturned, moving cars pushed off the road.	**P1** 1,5 – 5	15 – 30
F2 50 – 70	Considerable damage: Roofs torn off frame houses, mobile homes demolished, boxcars pushed over, large trees snapped or uprooted, light-object missiles generated.	**P2** 5 – 16	30 – 160
F3 70 – 90	Severe damage: Roofs and some walls torn off, well-constructed houses overturned, most trees in forested areas uprooted, heavy cars lifted off the ground and thrown around.	**P3** 16 – 50	160 – 510
F4 90 – 115	Devastating damage: Well-constructed houses levelled, structures with weak foundations blown some distance, cars thrown and large missiles generated.	**P4** 50 – 160	510 – 820
F5 115 – 140	Incredible damage: Strong-frame houses lifted off foundations and carried considerable distances to disintegrate, car-sized missiles fly through the air in excess of 100 m, trees debarked, other incredible phenomena.	**P5** 160 – 500	820 – 2800

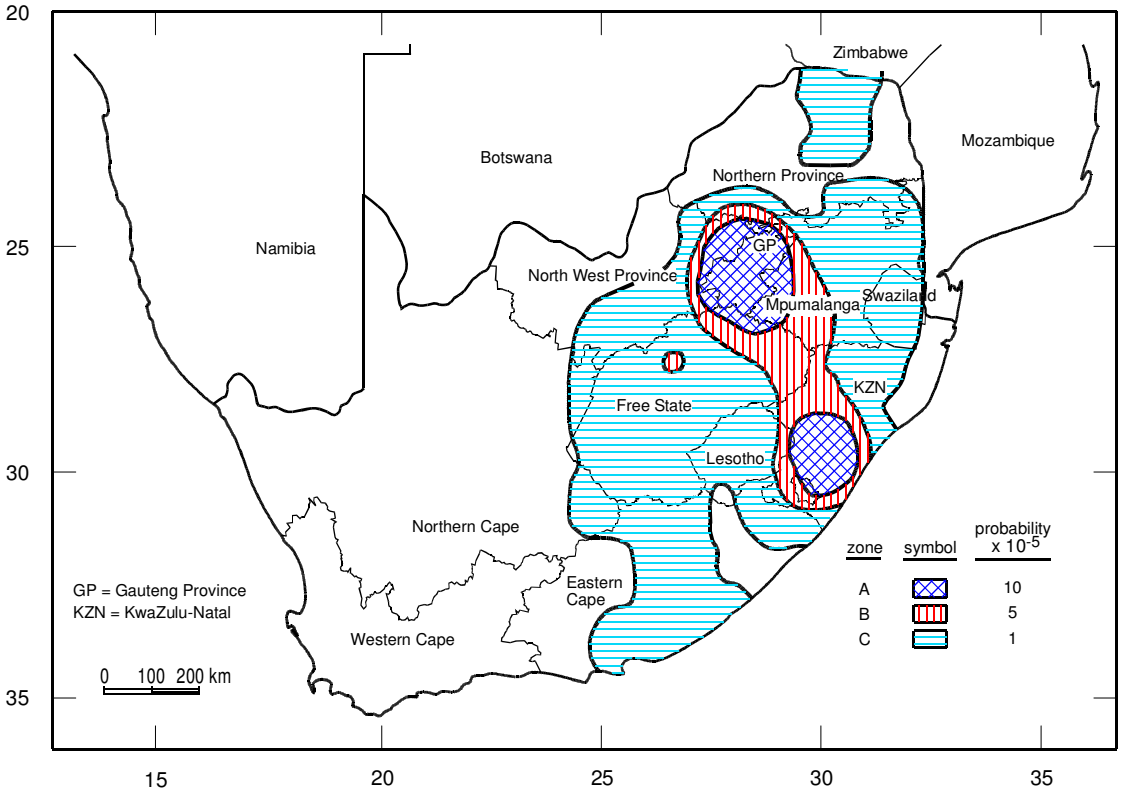

Figure 2.4. Mean rate of occurrence of tornadoes per annum, excluding tornadoes of intensity F0 (Goliger *et al.*, 1997).

2.4.1.4. Point probabilities of tornadic wind speeds

The risk of tornadic wind speeds at a specific geographical point can be estimated by tornado risk models. The McDonald type of model, amongst others, e.g. Twisdale and Dunn (1983), has been adopted for use in South Africa (McDonald, 1983). From this model, the probability of a tornado strike at a point in space, P_s, can be approximated by a geometric probability as

$$P_s(v \geq V_o) \approx E[\mu DA(V_o)] \tag{2.29}$$

where μ is the mean rate of occurrence of tornadoes per unit area, and $DA(V_o)$ is the damage area associated with a threshold wind speed V_o. If the mean occurrence rate is uniform across the area under consideration, the occurrence rate reduces to

$$P_s(v \geq V_o) \approx \mu E[DA(V_o)] \tag{2.30}$$

In a McDonald type model, the probability that a point within a local region will experience a wind speed that is contained in the F-scale interval is $P(v{=}V_i)$. For

tornadoes whose maximum wind speeds are contained in the F-scale interval, V_i is obtained as

$$P(v = V_i) = \mu \sum_{j=1}^{5} a_{ij} P\left(F = F_j\right) \tag{2.31}$$

where μ is the mean number of tornadoes within the local region per year, supplied in Figure 2.4, a_{ij} is the area within the damage path that experiences wind speeds within the F-scale interval V_i in a tornado whose maximum wind speed is in the interval V_j, $j \geq i$, and $P(F=F_j)$ is the probability distribution function of tornado intensity. The probability that a point within the local region will experience wind speeds greater than or equal to V_j is

$$P\left(v \geq V_j\right) = \sum_{i=j}^{5} P(v = V_i) \tag{2.32}$$

A single probability distribution for all regions where a likelihood of tornado occurrence exists was developed. This distribution, with corresponding wind speeds, is shown in Figure 2.5. The wind speed distribution is also assumed to follow directly from the Fujita classification system in Table 2.2:

$$F\left(v \geq V_j\right) = F\left(F \geq F_j\right) \tag{2.33}$$

The probability that a point within a local region will experience a wind speed contained in the F-scale interval V_i, $P(v=V_i)$, can now be obtained from the McDonald model. By neglecting wind direction and the width of a structure, the model can be simplified to

$$P\left(v \geq V_j\right) = \mu R_a\left(V_j\right) \tag{2.34}$$

Where $R_a(V_j)$ is the tornado damage function obtained as

$$R_a\left(V_j\right) = \sum_{i=j}^{5} \sum_{j=1}^{5} a_{ij} P\left(F = F_j\right) \tag{2.35}$$

and μ is the mean rate of occurrence of tornadoes given in Figure 2.2. The value of $R_a(V_j)$ for a range of V_j is presented in Figure 2.6.

For places where there is a possibility of tornadoes occurring, the probability of V_o being exceeded, can be given as

$$P(V \geq V_o) = P_o(V \geq V_o) + P_t(V \geq V_o) \tag{2.36}$$

where $P_o(V \geq V_o)$ is the probability of a wind speed V_o being exceeded as a result of strong-wind mechanisms occurring at least once a year, and $P_t(V \geq V_o)$ is the probability of a tornadic wind speed V_o being exceeded.

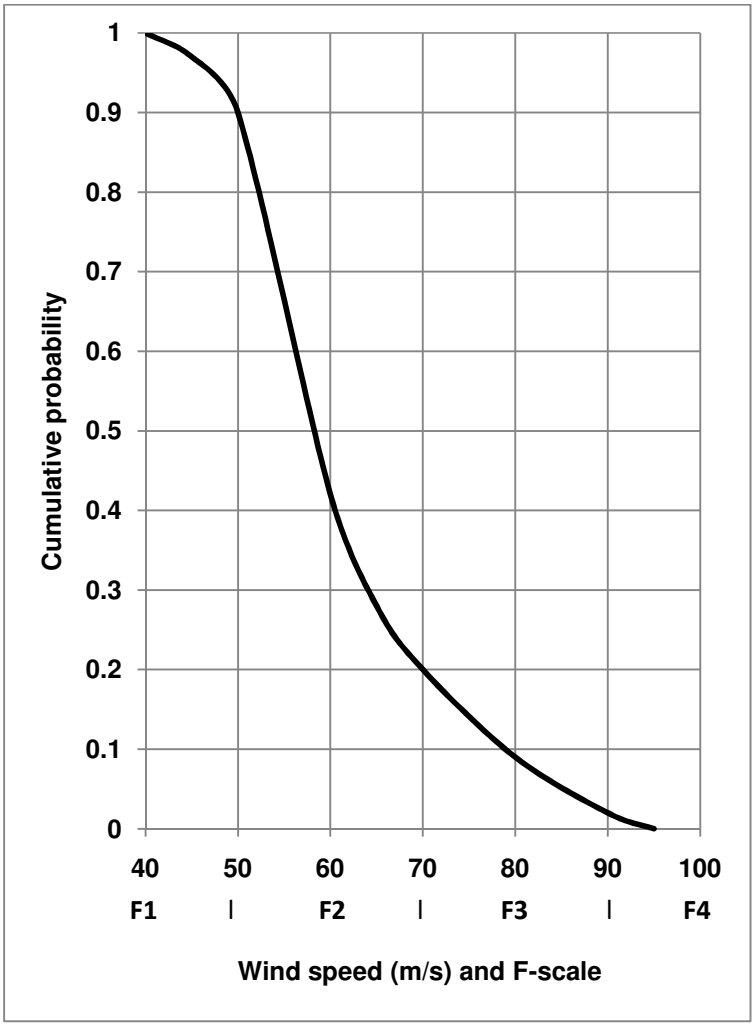

Figure 2.5. Cumulative tornado probability/intensity relationship (after Goliger *et al.*, 1997).

The annual maximum probability distribution $P_o(V \geq V_o)$ for the 2-3 second gust speed is estimated with the methods described in section 2.3, which are applied in Chapter 5. The value of $P_t(V \geq V_o)$ is calculated with equation 2.34, where the value of μ is obtained from the map in Figure 2.4, and the value of $R_a(V_j)$ can be read off the graph presented in Figure 2.6.

Following is an example in the application of equation 2.36, to incorporate the probabilities of tornadic wind speeds. The whole Gauteng Province, which includes Johannesburg, falls in region A in Figure 2.4. Therefore μ is equal to 1 x 10^{-4}/km^2.

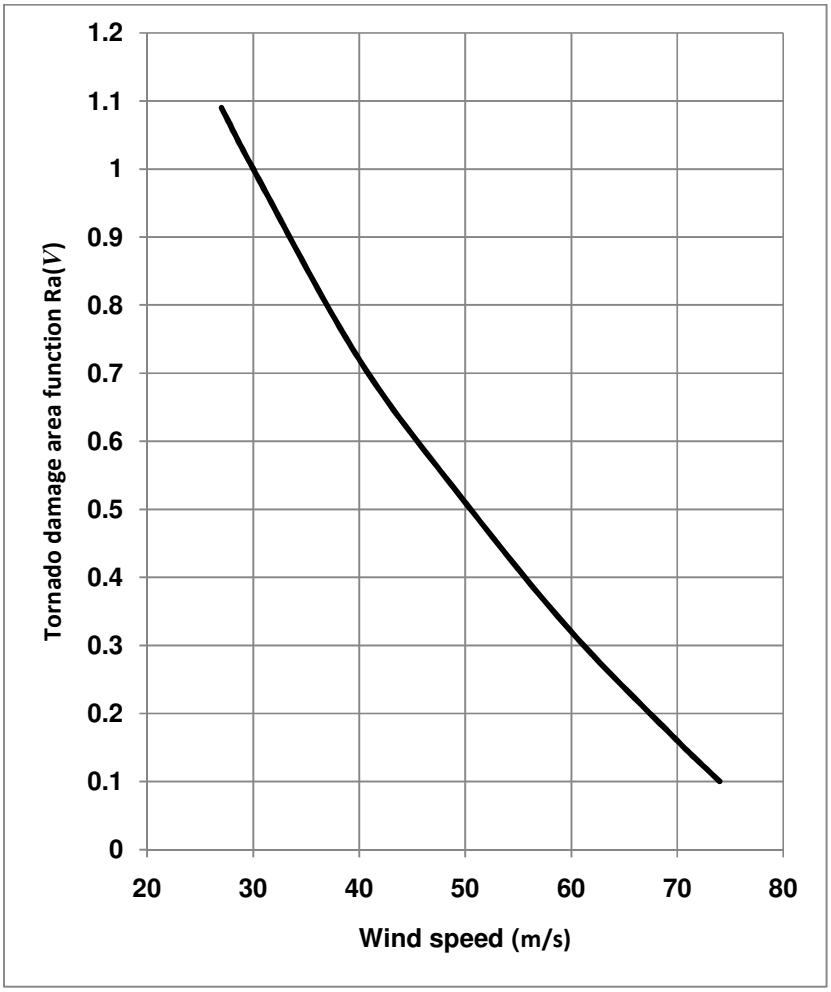

Figure 2.6. Tornado damage area function $R_a(V)$ (after Goliger *et al.*, 1997).

The values of $P_t(V \geq V_o)$ for different values of V_o is given in Table 2.3, while $P_o(V \geq V_o)$ is determined by fitting the Gumbel distribution to the data set of annual maximum wind gusts.

Table 2.3. Values of $P_t(V \geq V_o)$ for different values of V_o in zone A in Figure 2.4.

V_o	$R_a(V_o)$	$P_t(V \geq V_o)$
30	1	1×10^{-4}
40	0,72	$7,2 \times 10^{-5}$
50	0,5	5×10^{-5}
60	0,32	$3,2 \times 10^{-5}$
70	0,16	$1,6 \times 10^{-5}$

The estimations of $P(V \geq V_o)$ is presented graphically in Figure 2.7. The blue line indicates $P_o(V \geq V_o)$ and the red line $P(V \geq V_o)$ where it deviates from $P_o(V \geq V_o)$. One can see that for probabilities of less than one in 1000 years $P_t(V \geq V_o)$ does not play a role, showing that for design purposes of single structures, tornadic wind speeds do not need to be taken into consideration due to their low annual probability. However, one should keep in mind that for line structures which can cover large areas or distances, such as power transmission lines, it is advisable that consideration should be given for the occurrence of tornadoes (Milford and Goliger, 1994).

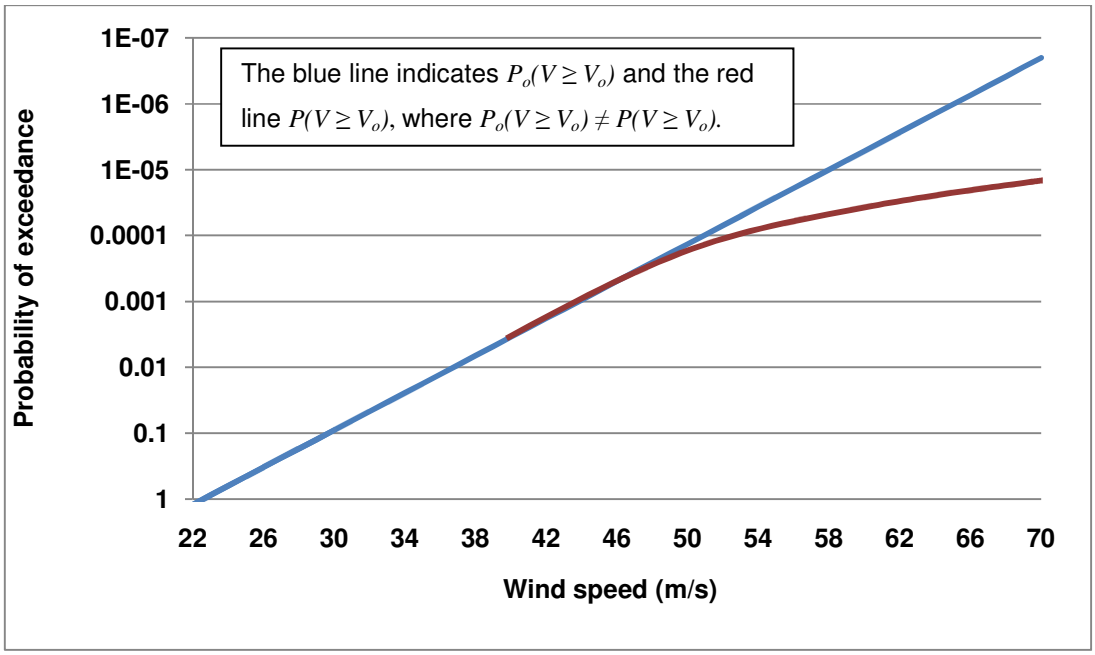

Figure 2.7. Annual probability of exceeding threshold wind gust for Johannesburg Weather Office.

2.4.2. Tropical cyclones

A total of 11 cyclones significantly affected the weather of the eastern parts of South Africa in some or other ways, in the 60-year period from 1950 to 2009 (CAELUM (1991), and updates thereof). One should note, however, that almost all of these tropical cyclones did not enter the South African borders. The two exceptions are the tropical cyclones Domoina (29-31 January 1984) and Imboa (10-20 February 1984). Domoina moved into the southern part of the Kruger National Park from

Mozambique, turning south-eastwards and moved over Swaziland and northern KwaZulu-Natal, before dissipating in the Indian Ocean. Imboa moved south-westwards along the coastline of KwaZulu-Natal, and touched the coast just north of Durban.

No weather station in South Africa has ever recorded extreme wind speeds which were caused directly by a tropical cyclone. It can therefore be concluded from the available historical information that there is a risk, albeit remote, of hurricane-strength winds to occur over the eastern parts of South Africa.

2.5. The previous extreme wind analyses for South Africa

Previous analyses of extreme wind data include May (1972), Louw and Katsiambirtas (1974), South African Weather Bureau (1974 and 1975, Department of Transport (1981), Milford (1985a and b) and Milford (1987). Therefore, more than two decades have passed since the last analysis of extreme wind data relevant to the built environment of South Africa. Only this fact makes the need for an updated analysis compelling. Wind climate information which is currently utilized in the design process of the built environment for South Africa (SANS 10160-1989, 1989) is based on the historical wind data from a limited number of long-term climate stations, which are mostly based in large cities. Based on this analysis, Figure 2.8 shows maps of the 50-year hourly mean and 50-year gust speeds, on which the currently used wind speeds for design purposes are based.

These maps show isolines reflecting simple interpolation between the 50-year values, estimated from observed wind data from 15 sites in South Africa. From Figure 2.8(a) one can see that the southern half of South Africa is prone to higher mean wind speeds than the north, probably due to the frequent passage of strong cold fronts, especially during the winter. While the differences in the magnitude of the mean wind speeds can usually be explained by the simple determination of prevalent synoptic conditions, the strengths of wind gusts can often only be explained by considering the prevalence of weather conditions at the mesoscale as well. As one moves northwards in South Africa, thunderstorms become more important as the causes of high wind gusts. This is argued to be the reason why the isolines in Figure

2.8(b), which indicates the 50-year maximum wind gust, do not closely correspond to the isolines in Figure 2.8(a), particularly in the north.

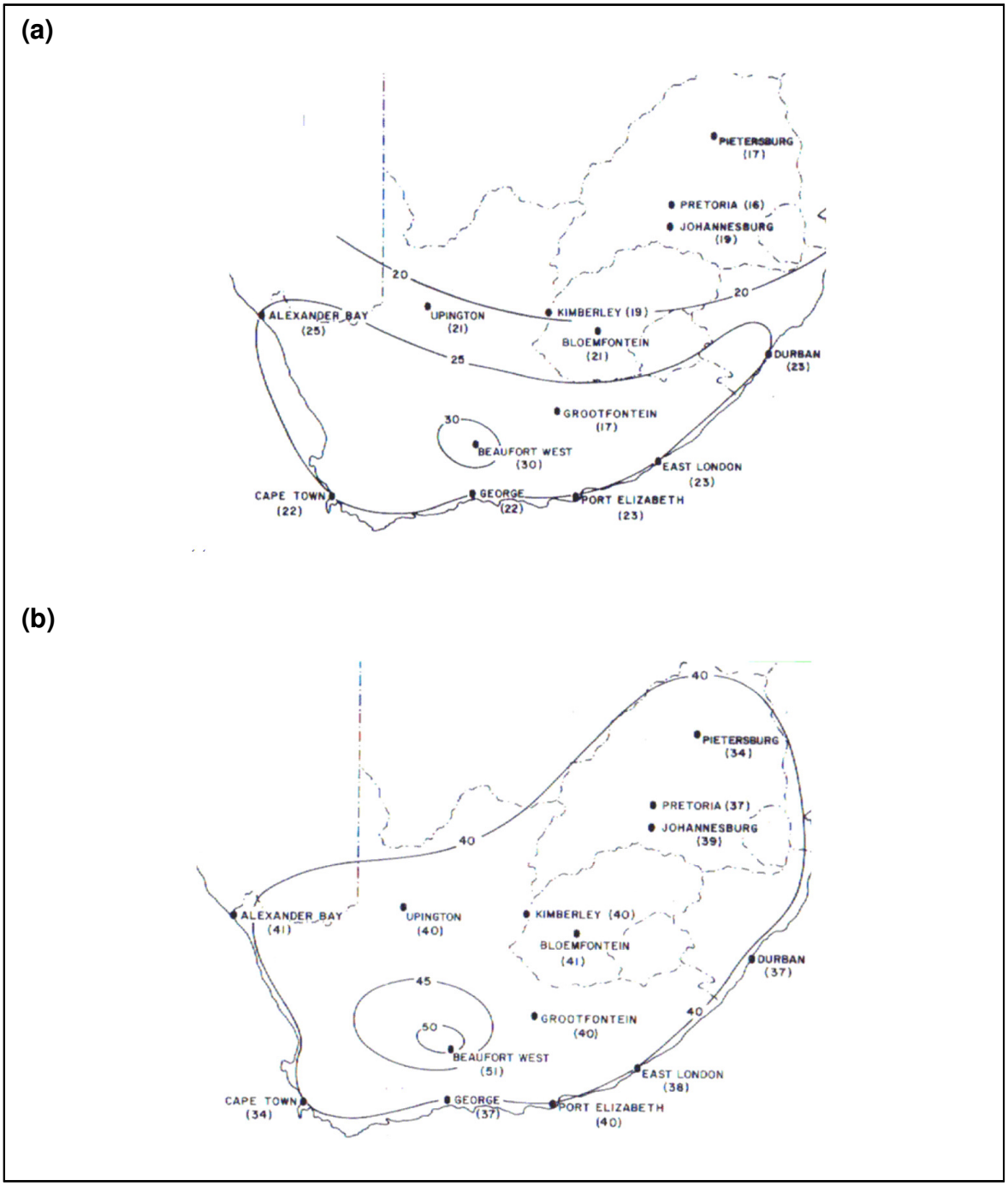

Figure 2.8. Maps of the (a) 50-year mean hourly wind speed and (b) 50-year gust speeds currently utilized for design purposes in South Africa (Milford, 1985a and b).

Some issues which will be addressed, to improve on the analysis of Milford (1985a, b), is the utilization of the data from a larger number of climate stations (Chapter 3), investigations into the mechanisms which cause the extreme winds (Chapter 4), assessments of various statistical analysis techniques (Chapter 5), and the assessments of the exposure of climate stations which are available for the analyses (Chapter 6).

The choice of the averaging period is retained in this study for the sake of continuity and comparative purposes. What alternative averaging periods are concerned, eventually objective 10-minute design maps will have to be developed, on which the revised South African loading code is based. An averaging time of 2-3 seconds is used in the one Milford assessment, which is the typical response time of the Dines anemograph. This averaging time is retained, but it is noted that the response time of the newer instrumentation is much lower, in the region of 1 s. This newer high-resolution data will therefore be adequate to capture the short time scale events, such as the passage of thunderstorm gust fronts.

Chapter 3

Measured Wind data in South Africa

3.1. General

As mentioned in the previous chapters, the main objective is to make an improved statistical assessment of the likelihood of extreme wind speed occurrence in South Africa. For such an assessment, the primary source of data is the observed wind records. The SAWS is the custodian of most climate data in South Africa. Data measurements are, where possible, performed according to World Meteorological Organization (WMO) standards, as stipulated in WMO-No. 8 (WMO, 1996). This chapter discusses the available wind data, as well as the quality assessments and selection processes of the data.

3.2. Measurement and storage of wind data

The Dines pressure tube anemograph was the original instrumentation employed to continuously measure the wind. The wind speed was deduced from wind pressure in a tube facing the direction of the wind. This wind-measuring instrument required a shelter to protect its sensitive parts, such as the recording mechanism, a float carrying a pen, and a revolving drum with graph paper. The assembly of the Dines anemograph is shown in Figure 3.1. In comparison with the modern instrumentation, it was a costly as well as labour intensive exercise to set up and maintain weather stations with these instruments. Because of this, Dines pressure tube anemographs were usually situated at aerodromes of big cities, and were only operated by personnel of the SAWB regional weather offices.

Since the early 1990's, the SAWS started in earnest to implement automatic weather station (AWS) technology. This technology made it more cost-effective to set up a larger number of weather stations that are able to continuously record the weather. An effort was also made to place the AWSs in more remote areas to improve the spatial distribution of the weather measurements. With the AWS setup in South Africa, wind speed and direction are measured by an RM Young sensor, which is shown in Figure 3.2. Data forthcoming from these weather stations have mostly uninterrupted records of the mean wind speed and wind direction, as well as the maximum wind gust and direction, for each recording time interval. In South Africa the recording time intervals are five minutes long.

The SAWS stores all of its historical climate data in a database, the SAWS climate databank. Three data tables in the database contain wind data. These tables provide the following:

- Daily maximum 2-3 second wind gust speed, with direction and time;
- Hourly mean wind speed and direction;
- Five-minute mean wind speed and direction; and
- Strongest 2-3 second wind gust, with direction and time, for each five-minute time interval.

For the older data sets, which were measured with the Dines anemograph, no 5-minute data is available. It is also important to note that it is only since 1995 (the specific month depends on the particular geographic region) that 5-minute climate data from AWSs have been stored on the climate database. Therefore, where climate analysis is done with 5-minute data as input, these analyses can on most occasions only be undertaken with data time series that start at the earliest some time during 1995.

Figure 3.1. Dines pressure tube anemograph (www.campbellsci.ca).

Figure 3.2. The RM Young wind sensor (www.youngusa.com).

3.3. Audit and geographical coverage of wind data

Since the systematic implementation of modern AWS technology, especially since 1992, the number of weather stations that measures wind on a continuous basis has increased substantially. This increase can be illustrated by comparing the number of weather stations which were operational in January 1987 (14), versus January 2007 (172), of which the positions are presented in the maps in Figure 3.3.

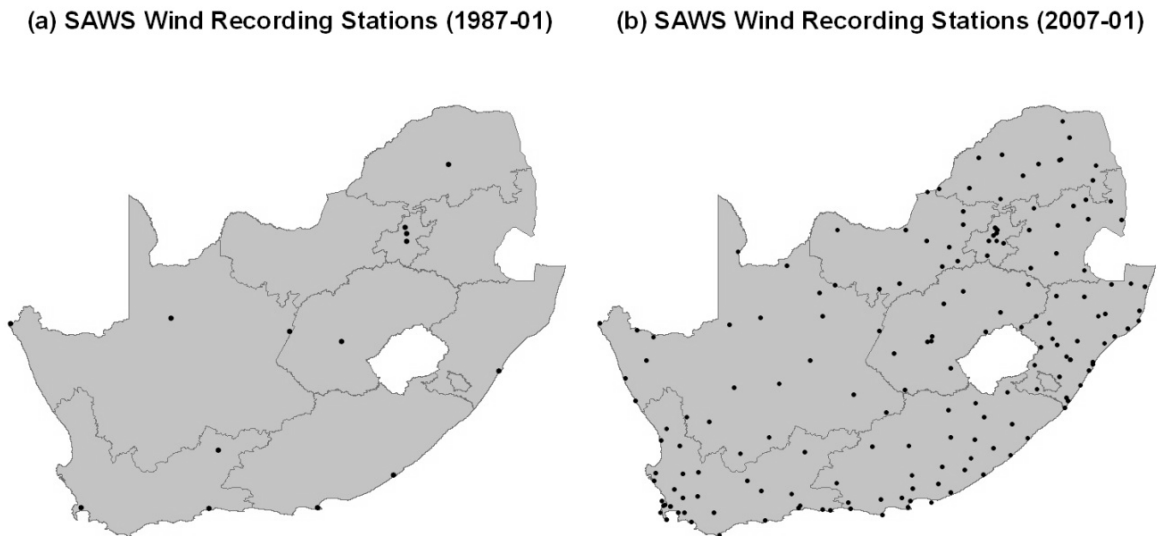

Figure 3.3. Spatial distribution of climate stations which measures wind continuously in (a) January 1987, and (b) January 2007.

The significant increase in the annual number of daily maximum wind gust values archived in the SAWS climate database can be demonstrated further by comparing the measurements for the years from 1961 to 2007, as presented in Figure 3.4.

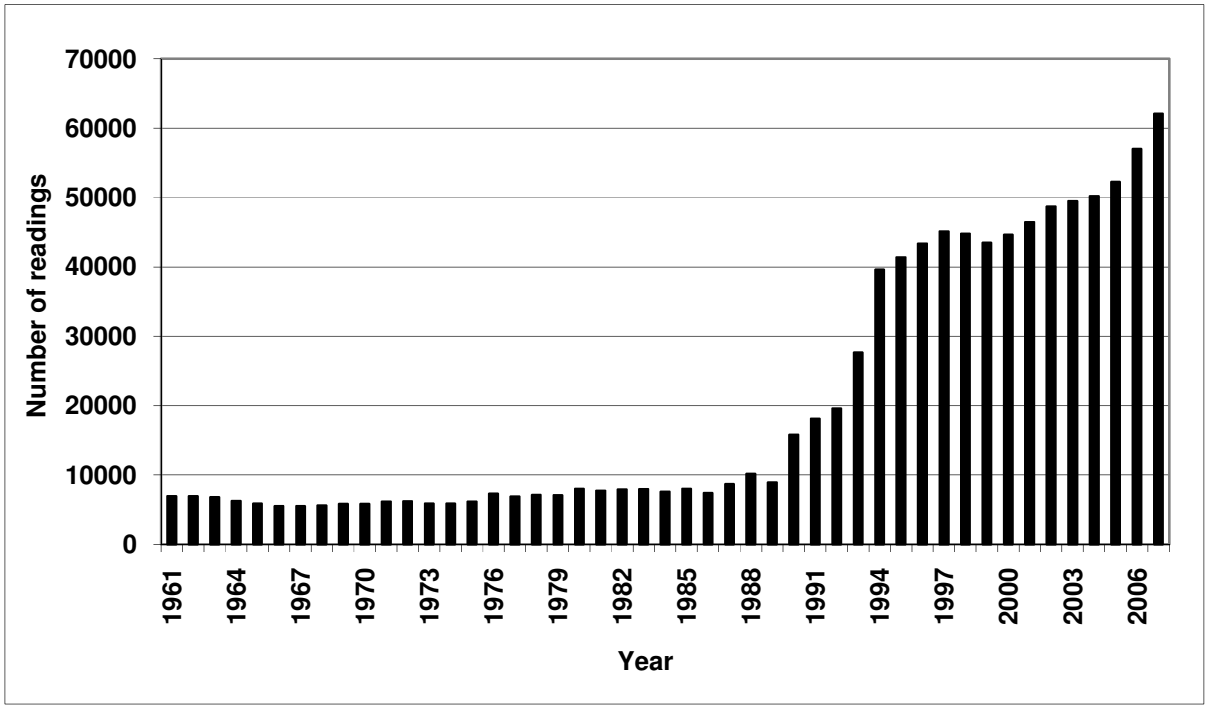

Figure 3.4. Annual number of daily maximum wind gust readings available in the SAWS climate database for the years from 1961 to 2007.

3.4. Homogeneity of wind data

The amount of available data does not necessarily reflect the eventual amount of data which would be useful to this study. The most important factor determining the usefulness of data is whether it is of sufficient quality, and if not, whether the specific quality problems in the data can be addressed. The SAWS endeavours to undertake sufficient quality control of all data stored on the climate database, but with various degrees of success. However, it is understandable that there will be some quality issues in datasets that are continuously updated, and that undergo transfers between electronic storage facilities, due to the modernisation efforts through the years. The quality or homogeneity problems encountered in the historical climate data sets are typically due to the following factors:

- Change in location of the climate station;
- Change in measuring units, e.g. knots to meters per second;

- Change in instrumentation;
- Different data coding techniques in the different databases employed;
- Change in the exposure of the instrumentation;
- Faulty, wrongly calibrated, neglected or damaged instrumentation;
- Incorrect digitization of data; and
- Problems in the electronic transfer of data from regional weather offices to the central climate database, or from one database to another during modernisation.

These data problems caused some wind time series to be inhomogeneous. Climate data sets should, therefore, be thoroughly checked for erroneous data values, before statistical analyses can be conducted. Following are brief discussions on, as well as some typical examples of, the wind data inhomogeneities which were detected.

During a change of the type of measuring instrumentation, the data time series before and after the changeover can exhibit noticeably different characteristics, which can often be observed by the visual inspection of the time series plots of the data. From Figure 3.5 it is noticeable, from the time series of mean monthly wind speed at Durban Weather Office, when a changeover of instrumentation from the Dines pressure tube anemograph to the AWS occurred, which was on 1 September 1992. From the changeover date the time series exhibits a pattern which apparently looks like a low-frequency cyclic behaviour. This recent pattern can be deemed to be an acceptable climatological behaviour, as time series of other climate variables, such as temperature and rainfall, also exhibit similar kind of cyclical behaviour. Some aspects of the pattern of the time series before September 1992 is however harder or impossible to justify climatologically, e.g. the relatively low mean monthly wind speeds between 1969 and 1978, and the relatively large changes in mean monthly wind speed between 1982 and 1988. In general it seems that substantially lower wind speeds were recorded before 1 September 1992 than thereafter, due to several possible reasons, which are difficult to establish retrospectively. It could have been that the Dines anemograph was situated at a site which is not optimal for wind measurements, e.g. with obstacles close to the anemometer. Another reason could be the changes in the digitization of the measured

wind data. The Dines anemograph data values were entered manually, with all hourly mean readings lower than 1,5 m/s entered as zero, which is not the case for the wind data from the recent AWS. Another reason could be the incorrect calibration of the Dines anemograph.

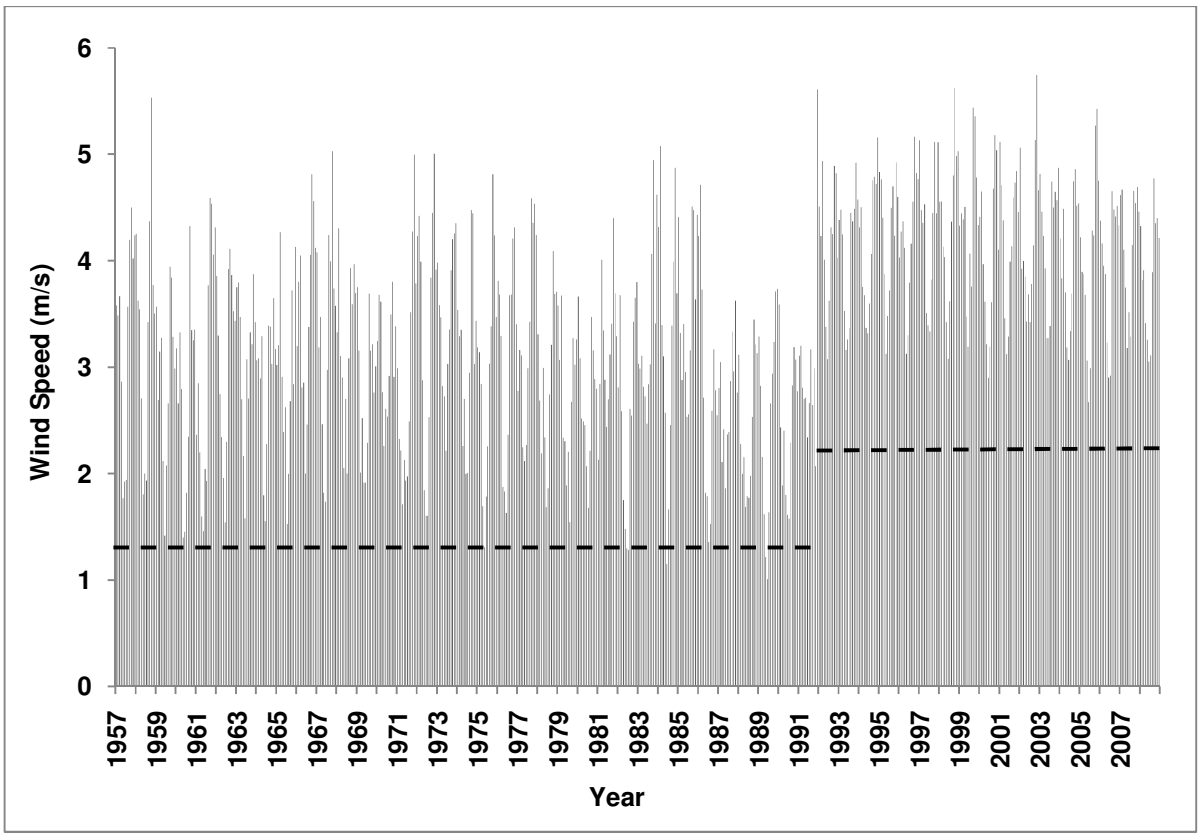

Figure 3.5. Monthly mean wind speed (m/s) for Durban Weather Office, for the period 1956 to 2008.

Some data inhomogeneities are not always easy to detect visually from plotted time series, as illustrated by the time series of monthly mean wind speeds for Johannesburg Weather Office, from 1953 to 2007, which is presented in Figure 3.6. At Johannesburg Weather Office, the same changeover to AWS instrumentation took place, on 1 June 1989. Here an increase in monthly mean wind speeds was recorded, but it is not as pronounced as it is in the case for Durban Weather Office. The low monthly mean wind speed for June 2007 is due to missing and incorrect data during the particular month.

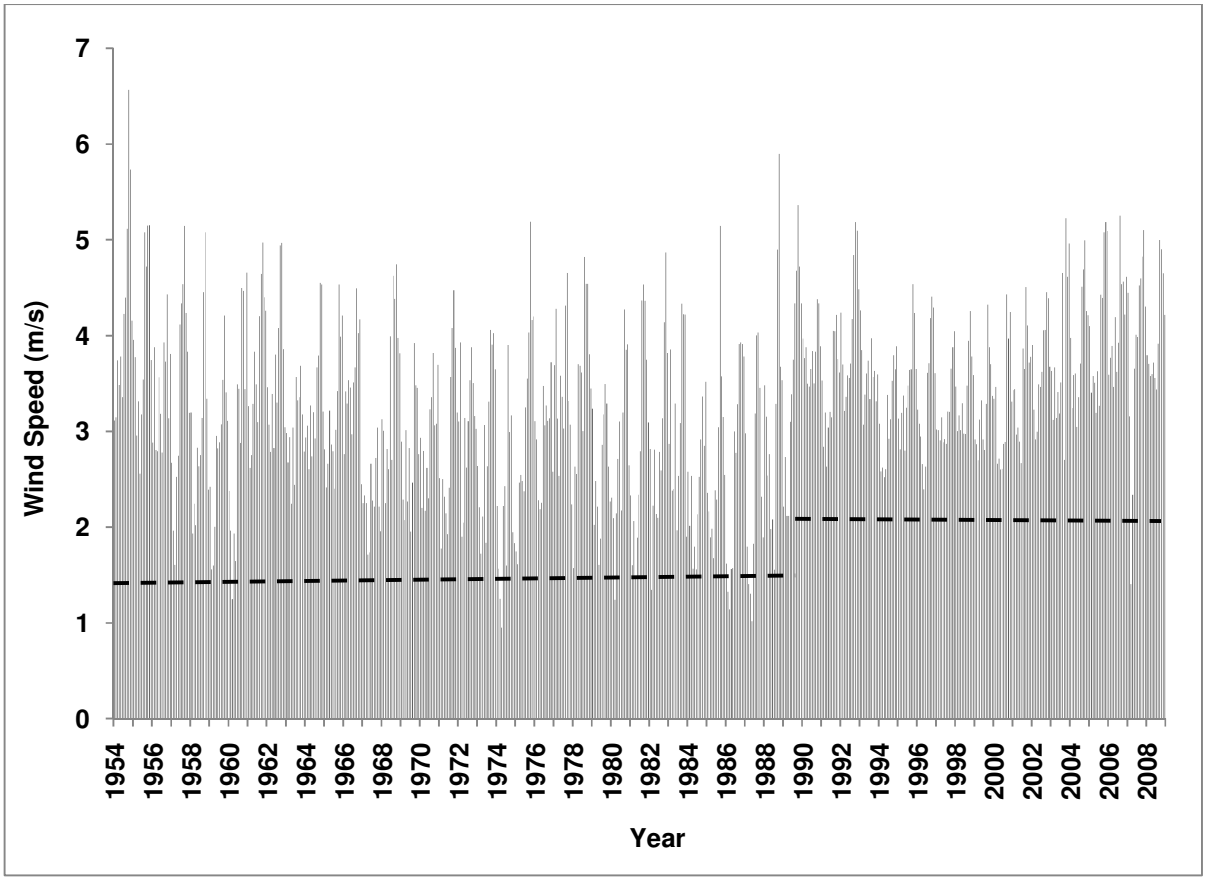

Figure 3.6. Monthly mean wind speed (m/s) for Johannesburg Weather Office, for the period 1953 to 2008.

Calibration errors or malfunctions of instrumentation are often not easy to detect, as the problem can be intermittent or of a short duration. An example of such data inhomogeneities is presented for the Brandvlei weather station in the Northern Cape province. Figure 3.7 presents the time series of the monthly mean wind speed, for the years 1995 to 2008. Apparent from the time series is a malfunction or calibration problem of the anemometer during 1997, due to the recording of wind speeds which were about twice as high as during the remainder of the recording period. The wind data for the year 1997 were therefore excluded from further statistical analysis.

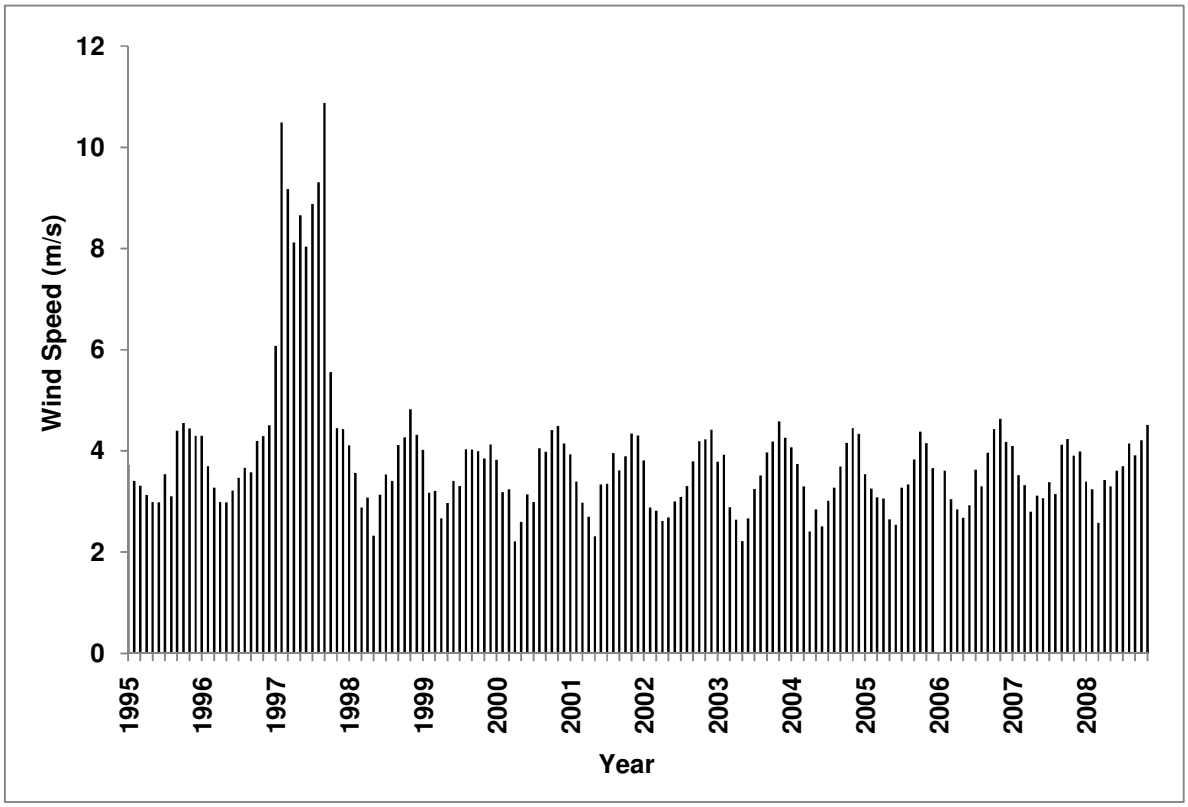

Figure 3.7. Monthly mean wind speed (m/s) for Brandvlei weather station, for the period 1995 to 2008.

In some cases the time series of wind data may look acceptable, but only after further investigation into the correctness of specific wind gusts, quality problems in the data may become apparent. Figure 3.8 shows the monthly mean wind speed for Bethlehem Weather Office in the east of the Free State province, for the years 1995 to 2008. The time series of the monthly mean wind speeds looks acceptable. However, further investigations into the validity of particular daily maximum wind gusts, with the daily time series of 5-minute climate data, revealed a malfunction of the anemometer for extended periods during 2008. Erroneous wind gust values are usually presented in the form of “spikes”, where a particular 5-minute maximum gust is significantly stronger than the gust values that were recorded before and after the measurement. A spike is also easily identifiable due to the fact that the other recorded weather parameters do not support the occurrence of such a high wind speed. An example of such a data spike is shown in Figure 3.9, which shows the plots of the daily 5-minute time series of

the maximum wind gust, mean wind speed, mean wind direction and mean temperature, for 22 December 2008. On this day a maximum wind gust of 28,5 m/s was recorded. It can be seen from the time series that the mean wind speed values did not reflect an increase during the particular time of the recorded gust.

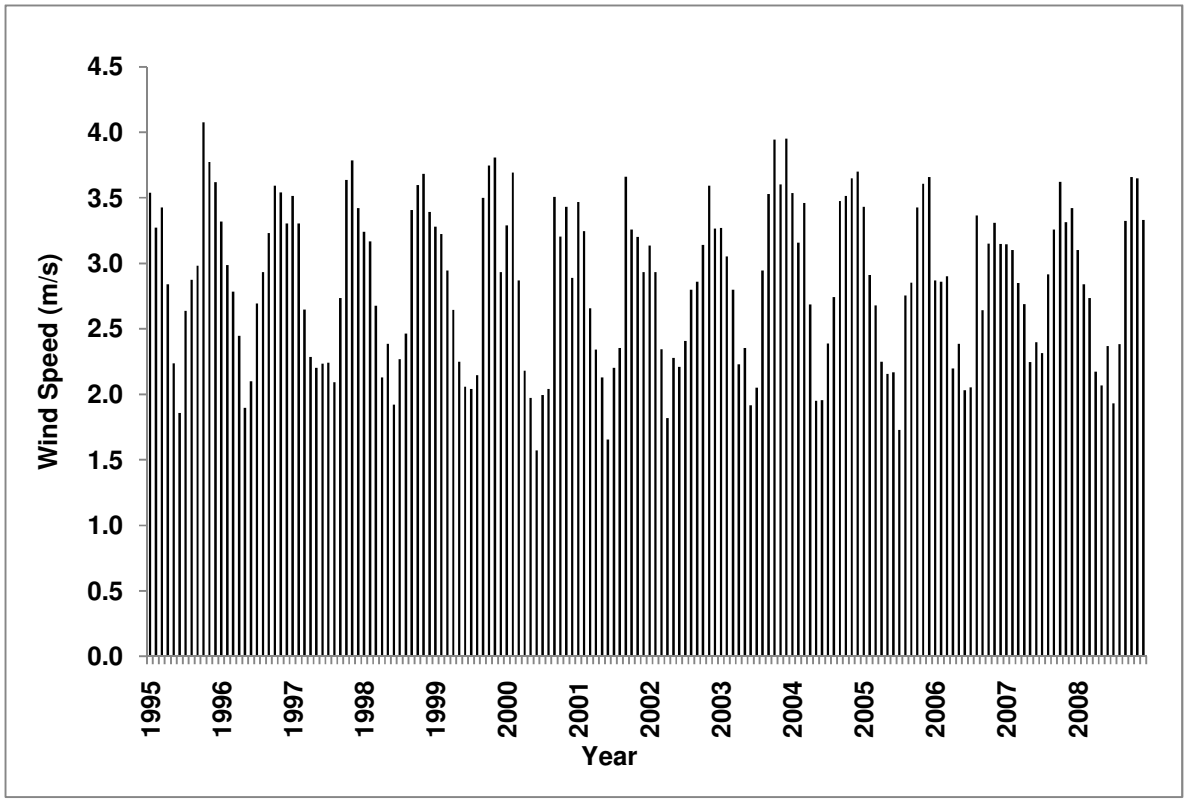

Figure 3.8. Monthly mean wind speed (m/s) for Bethlehem Weather Office, for the period 1995 to 2008.

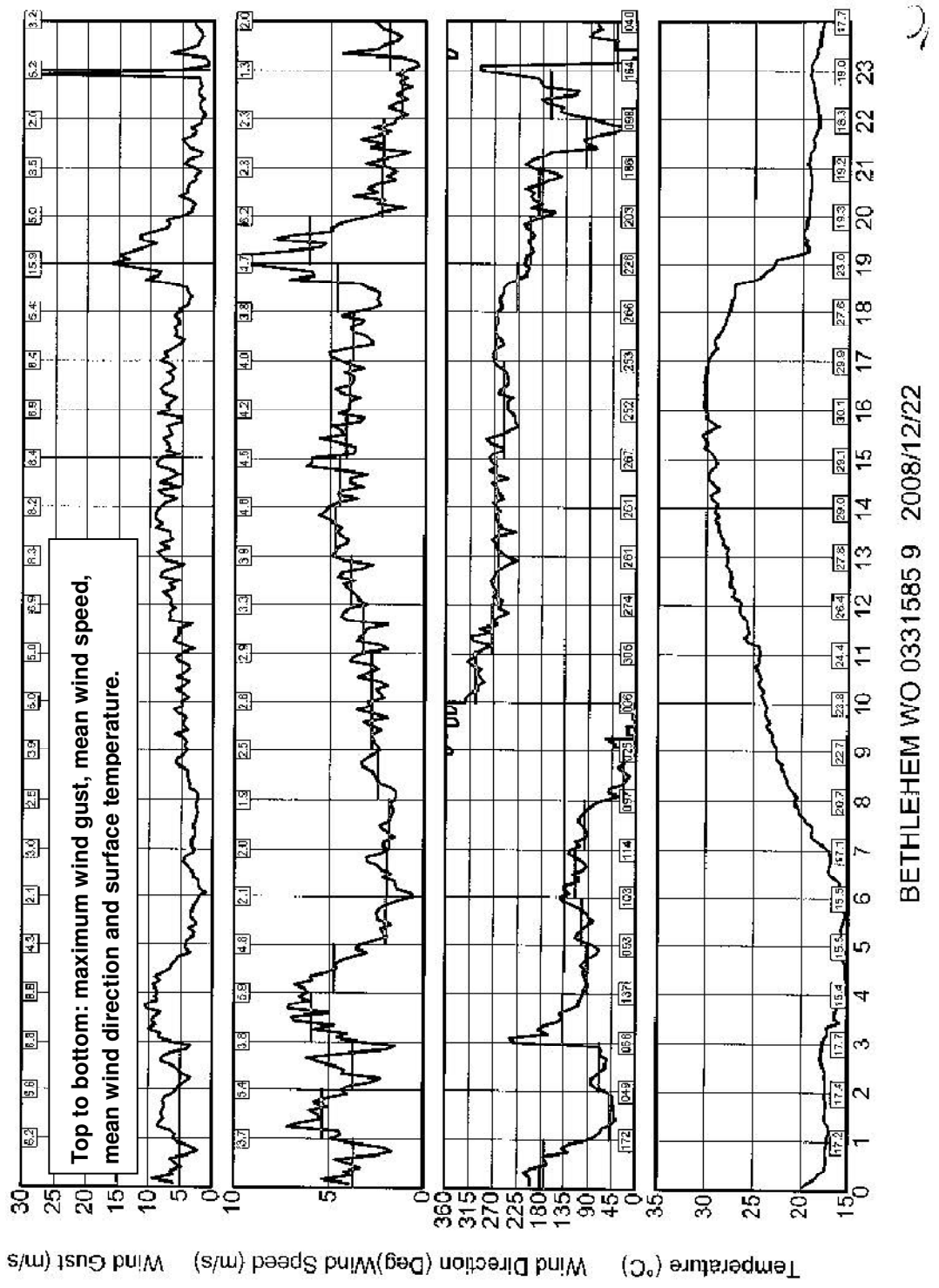

Figure 3.9. Plots of the 5-minute time series measured at Bethlehem Weather Office for 22 December 2008 for maximum wind gust, mean wind speed, mean wind direction and surface temperature.

From the discussed examples it is apparent that many, if not most, wind data inhomogeneities are unique for a particular data series. Experience has shown that only adjustments or deletions of data on the basis of well-known inhomogeneities common to all data sets are not sufficient to make sure that the data is of a reasonable quality. The best way to check the quality of the wind data sets identified for this study were, therefore, to scrutinize the data sets for inhomogeneities on an individual basis, for each station, in a systematic manner.

The following system was used to detect inhomogeneities in the wind data:

- To aid in the detection of data inhomogeneities, metadata is essential. Metadata can be defined as data or information on data sets, which for climate services are an essential input in the quality control of climate data. From the metadata, information can be gained on aspects of the history of the climate station, such as changes in the location, changes of the type or replacement of the instrumentation, and calibration of the instruments. The metadata of the identified weather stations were scrutinized for any time periods where problems could have existed which might have influenced the anemometer readings.

- Plots of the time series of monthly mean wind speeds were checked for the following:

  Climatic discontinuity, is defined as a climatic shift that consists of a rather abrupt and permanent change during the period of record from one average value to another. Discontinuities usually occur due to change of instrumentation or position of the station. Where such discontinuities occur, the data before and after the discontinuity should be assessed to determine the cause. It was found that the assessed wind time series tend to show discontinuities at the changeover from the old Dines anemograph to AWS technology. Mean wind speeds recorded by AWSs are generally higher but wind gusts lower compared to those recorded by the Dines anemograph. However, this was not the case for all the weather stations. Therefore, a decision was made that the time series

should be separated at the changeover date of instrumentation, as it would not be possible to deduce an accurate correction factor to the old data from the available information.

Climatic oscillation, is defined as a fluctuation in which the variable tends to move gradually and smoothly between successive maxima and minima. In the wind time series these were usually in the form of climatic rhythms, which are oscillations or vacillations in which the successive maxima and minima occur at approximately equal intervals of time. Further investigations revealed probable climatic periodicities, where the time interval between successive maxima and minima are nearly constant throughout the record. Most climate time series exhibit periodicities. Periodicities in monthly time series for wind will be most evident on a seasonal time-scale. Especially in the interior the strongest winds usually occur during summer and the weakest during winter. Lower frequency periodicities are also evident, and most pronounced on a decadal time scale.

Climatic trend, is defined as a climatic change characterized by a smooth monotonic increase or decrease of the average value over the period of record. No evidence of significant climatic trends was found in the wind time series investigated.

Climatic vacillation, is defined as a fluctuation in which the climatic variable tends to dwell alternately around two (or more) average values, and to drift from one average value to another at regular or irregular intervals. An example of this behavior can be found in the time series for Brandvlei, presented in Figure 3.7. This pattern is usually caused by the malfunction of the anemometer during a fixed period of time. After re-calibration or replacement, the data values return again to normal, to the mean state before the problem occurred.

- Individual outliers in the data sets were determined separately for hourly mean wind speeds and 2-3 second wind gusts. The annual maxima for these values were validated with the aid of daily plots of 5-minute values of maximum wind gust, mean wind speed, mean wind direction, surface temperature, rainfall,

relative humidity and surface pressure. Strong hourly mean wind speeds usually occur because of the occurrence of particular synoptic systems, such as cold fronts, strong ridges and deep troughs. Strong 2-3 second wind gusts also have particular synoptic phenomena as cause, but also gust fronts from thunderstorms. *The knowledge of the internal relations between meteorological parameters, or cross-over testing, was applied to validate the strong wind speeds.* For example, during the occurrence of a gust front, an abrupt drop in temperature, onset of rainfall, increase in humidity, and sometimes even surface pressure, is evident. Further discussion on the identification of strong wind producing mechanisms, and therefore in turn the validation of strong winds, can be found in section 4.2.

3.5. Selected wind data

The selected data sets of wind time series had to fulfil the following two requirements, in terms of the lengths of the record and completeness, after the data quality issues have been addressed:

- The time series of daily maximum wind gust data should have been at least 10 years long to ensure that a reasonable estimation by most statistical strong wind estimation methodologies can be made.
- Each year of the utilised time series should contain at least 90% data, taking into consideration which times of the year the annual maximum wind gusts are most likely to occur. As an example, over the interior, where it is expected that annual maximum wind gusts are usually caused by thunderstorm activity, all spring, summer and autumn months had to be complete for a specific year of the wind data to be utilised for statistical analyses.

The eventual list of weather stations utilised in the study is presented in Table 3.1, listed according to the climate number. The climate number is a unique number assigned to every weather station, according to its geographical position. For this assignment of the climate numbers, South Africa was divided into sections of size 0,25º x 0,25º, as

presented in Figure 3.10. The number of the section represents the first four digits of the climate number. The remaining digits of the climate number are assigned in a similar fashion by the further subdivision of the sections into subsections, which are not shown here. The geographical positions of the weather stations are presented in Figure 3.11.

Table 3.1. List of stations, with geographical coordinates, to be utilised in the study. The stations are ordered according to the SAWS climate numbering system.

Station Number	Station Name	Latitude (ºS)	Longitude (ºE)	Height above sea level (m)	Year/month AWS measurements commenced
0003108	STRUISBAAI	34,80	20,06	4	1991/11
0005609	STRAND	34,14	18,85	10	1996/06
0006386	HERMANUS	34,43	19,22	14	1996/09
0007699	TYGERHOEK	34,15	19,90	151	1990/12
0010682	STILBAAI	34,37	21,40	102	1993/10
0012661	GEORGE WO	34,02	22,38	191	1992/09
0014123	KNYSNA	34,06	23,09	53	1996/07
0014545	PLETTENBERGBAAI	34,09	23,33	137	1986/03
0015692	TSITSIKAMMA	34,03	23,91	7	1991/05
0020618	ROBBENEILAND	33,80	18,37	3	1992/11
0021178	CAPE TOWN WO	33,97	18,60	46	1992/10
0021823	PAARL	33,72	18,97	104	1993/07
0022729	WORCESTER-AWS	33,66	19,42	199	1998/12
0031650	JOUBERTINA AWS	33,84	23,86	545	1997/04
0033556	PATENSIE	33,77	24,82	85	1988/03
0034763	UITENHAGE	33,71	25,44	158	1985/09
0035209	PORT ELIZABETH	33,98	25,61	59	1992/08
0040192	GEELBEK	33,20	18,12	4	1997/03
0041388	MALMESBURY	33,47	18,72	101	1990/06
0041841	PORTERVILLE	33,01	18,98	122	1990/06
0045642	LAINGSBURG	33,20	20,87	655	1995/11
0056917	GRAHAMSTOWN	33,29	26,50	642	1985/07
0059572	EAST LONDON WO	33,03	27,83	116	1997/02
0061298	LANGEBAANWEG	32,97	18,16	31	1991/05
0063807	EXCELSIOR CERES	32,96	19,43	945	1990/07
0078227	FORT BEAUFORT	32,79	26,63	455	1997/05
0083572	LAMBERTSBAAI	32,03	18,33	93	1994/11
0092081	BEAUFORT-WES	32,36	22,58	902	1993/01
0096072	GRAAFF - REINET	32,19	24,54	791	1992/07
0123685	QUEENSTOWN	31,92	26,88	1105	1991/07
0127272	UMTATA WO	31,53	28,67	743	1996/12
0134479	CALVINIA WO	31,48	19,76	975	1992/05

Station Number	Station Name	Latitude (ºS)	Longitude (ºE)	Height above sea level (m)	Year/month AWS measurements commenced
0144791	NOUPOORT	31,19	24,97	1496	1993/08
0148517	JAMESTOWN	31,12	26,81	1601	1989/05
0150620	ELLIOT	31,34	27,85	1463	1993/11
0155394	PORT EDWARD	31,07	30,23	7	1989/03
0169880	DE AAR WO	30,67	24,00	1287	1993/03
0182465	PADDOCK	30,75	30,26	515	1992/12
0182591	MARGATE	30,85	30,33	154	1993/03
0184491	KOINGNAAS	30,20	17,29	99	1991/08
0190868	BRANDVLEI	30,47	20,48	923	1994/07
0214700	SPRINGBOK WO	29,67	17,89	1006	1993/08
0224400	PRIESKA	29,67	22,73	947	1992/11
0239698	PIETERMARITZBURG	29,63	30,40	672	1985/01
0239699	ORIBI AIRPORT	29,65	30,40	725	1998/04
0240808	DURBAN WO	29,97	30,95	8	1992/09
0241072	MT EDGECOMBE	29,70	31,05	91	1992/10
0241076	VIRGINIA	29,77	31,05	10	1994/12
0261307	BLOEMFONTEIN	29,12	26,18	1408	1993/10
0261516	BLOEMFONTEIN WO	29,10	26,30	1354	1992/05
0268016	GAINTS CASTLE	29,27	29,52	1754	1988/10
0270155	GREYTOWN	29,08	30,60	1029	1993/03
0274034	ALEXANDERBAAI	28,57	16,54	21	1986/01
0290468	KIMBERLEY WO	28,80	24,77	1197	1992/05
0300454	LADYSMITH	28,57	29,77	1069	1993/01
0304357	MTUNZINI	28,95	31,70	39	1992/02
0317475	UPINGTON WO	28,41	21,26	841	1992/05
0321110	POSTMASBURG	28,35	23,09	1323	1992/11
0331585	BETHLEHEM WO	28,25	28,33	1686	1980/11
0333682	VAN REENEN	28,37	29,38	1680	1993/03
0337738	ULUNDI	28,30	31,42	522	1997/03
0339732	CHARTERS CREEK	28,20	32,42	3	1994/01
0356880	KATHU	27,67	23,01	1187	1991/07
0360453	TAUNG	27,55	24,77	1110	1996/06
0362189	BLOEMHOF	27,65	25,62	1228	1991/04
0364300	WELKOM	27,99	26,67	1343	1990/11
0365398	KROONSTAD	27,63	27,23	1434	1992/10
0370856	NEWCASTLE	27,77	29,98	1238	1994/04
0410175	PONGOLA	27,41	31,59	312	1989/08
0427083	VAN ZYLSRUS	26,88	22,05	938	1991/08
0438784	VEREENIGING	26,57	27,95	1481	1991/11
0441416	STANDERTON	26,93	29,23	1563	1996/05
0472278	LICHTENBURG	26,13	26,17	1487	1992/07
0475879	JHB BOT TUINE	26,15	28,00	1622	1994/06

Station Number	Station Name	Latitude (ºS)	Longitude (ºE)	Height above sea level (m)	Year/month AWS measurements commenced
0476399	JOHANNESBURG	26,15	28,23	1695	1989/06
0479870	ERMELO WO	26,50	29,98	1766	1993/07
0508047	MAFIKENG WO	25,81	25,54	1282	1984/05
0511399	RUSTENBURG	25,65	27,23	1151	1992/07
0513346	PRETORIA UNISA	25,77	28,20	1439	1994/05
0513385	IRENE WO	25,91	28,21	1524	1993/08
0515320	WITBANK	25,84	29,19	1550	1993/11
0520691	KOMATIDRAAI	25,52	31,90	183	1990/08
0548375	PILANESBERG	25,26	27,23	1086	1995/08
0554816	LYDENBURG	25,11	30,48	1434	1992/10
0587725	THABAZIMBI	24,58	27,42	977	1992/10
0594626	GRASKOP AWS	24,93	30,85	1436	1992/07
0633882	POTGIETERSRUS	24,21	29,01	1097	1995/09
0638081	HOEDSPRUIT	24,35	31,05	524	1996/09
0674341	ELLISRAS	23,68	27,70	841	1992/08
0675666	MARKEN	23,60	28,38	998	1992/04
0677802	PIETERSBURG WO	23,87	29,45	1237	1992/05
0723664	THOHOYANDOU WO	23,09	30,38	614	1996/08

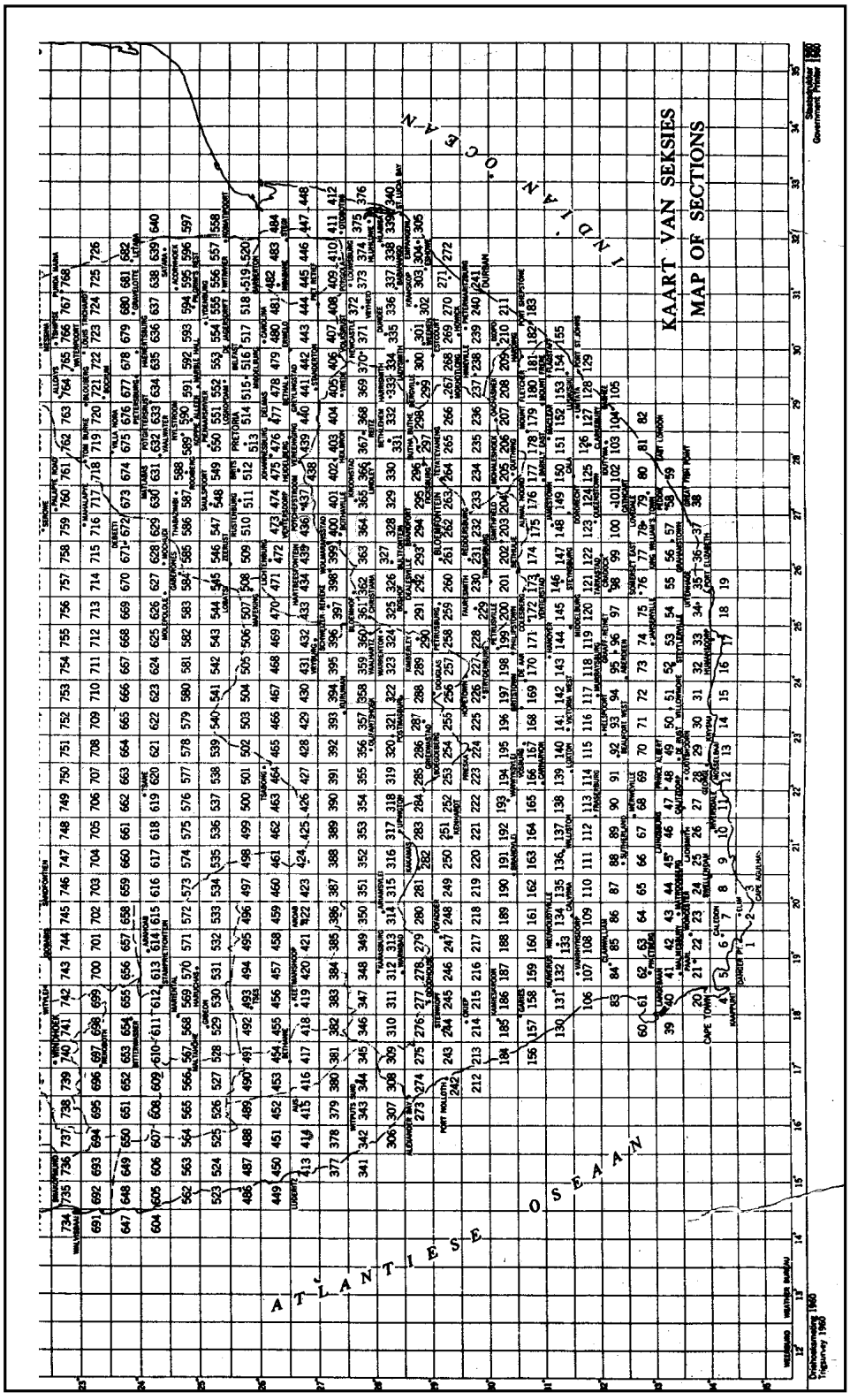

Figure 3.10. Map of sections for the assignment of the first four digits of the SAWS climate station numbers.

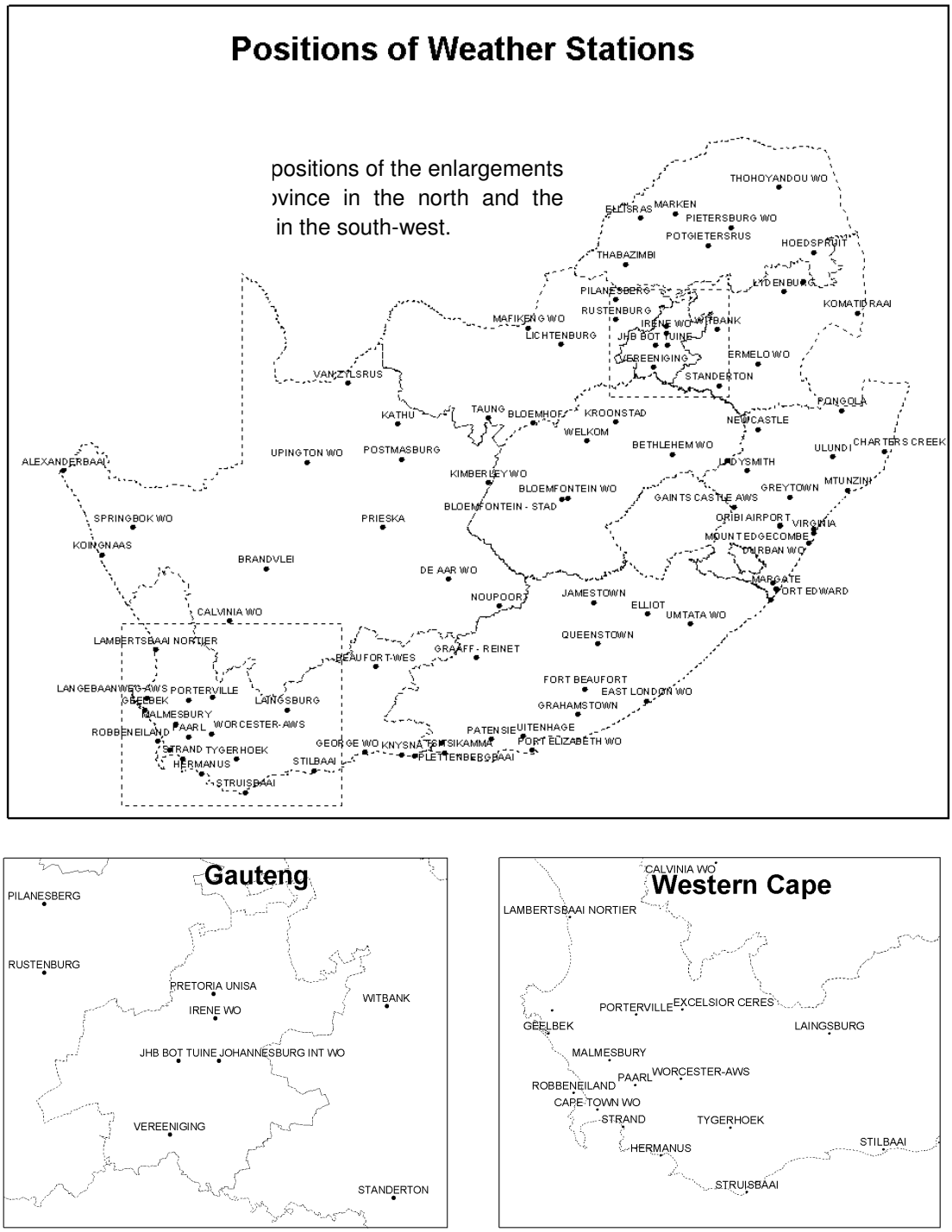

Figure 3.11. Positions of the weather stations to be utilised in the study.

Chapter 4

Strong Wind Climatology of South Africa

4.1. General

The aim of the work presented in this chapter is to develop the zoning of South Africa into geographical regions that are indicative of the most likely cause of strong winds, particularly the annual maxima of the 2-3 second wind gusts. The awareness of different sources or mechanisms of extreme winds is recommended in the subsequent statistical analysis of high wind speeds in Chapter 5, as it is an important factor in the selection or development of the most appropriate extreme value distributions to be fitted to the wind data. In mixed strong wind climates, alternative methods to the traditional Gumbel analysis method of estimating extreme wind speed probabilities, are advised. Such methods tend to yield more accurate estimates of annual wind speed maxima for long return periods greater than 50 years (Gomes and Vickery, 1978; Palutikof *et al.*, 1999; Twisdale and Vickery, 1992).

In the past South Africa has been classified into climatic zones by various authors, by the application of various criteria (Schulze, 1947, 1965; Jackson, 1951; Kruger, 2004). All of these climate regionalisations used the rainfall data as the primary factor in the delineation of the regions. Other climatological factors, such as temperature and humidity, were also considered in some cases. None of the already developed climatic regions consider the prevailing winds as an explicit factor in the delineation of different zones.

The only attempt to divide South Africa into strong wind regions was undertaken by Goliger and Retief (2002), who identified geographic zones where various types of

strong wind events are likely to be dominant. The recorded lightning activity, specific documented extreme weather events, the “Lemon Technique” (which serves as an aid to weather forecasters), as well as the knowledge of the relevant SAWS experts were used as the input information. However, no wind climate statistics were taken into account, and the zones, which were identified, were referred to as the “first approximations”, based on the limited information utilised in the investigation. Figure 4.1 presents the spatial extent of two strong wind types identified by Goliger and Retief (2002), which they regard as the types that cause the most damage and adverse wind conditions in South Africa.

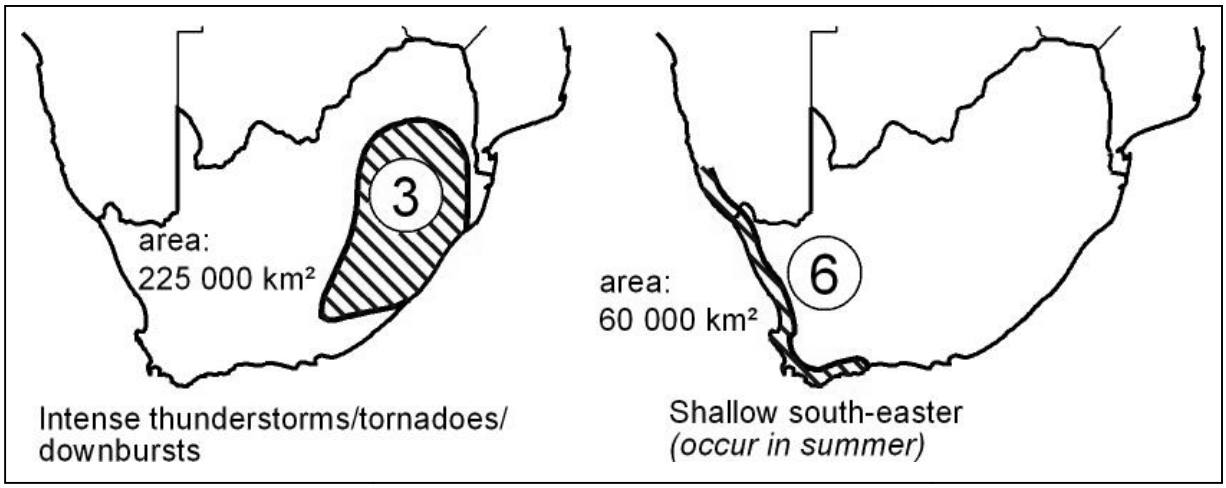

Figure 4.1. The spatial extent of two strong wind types, from Goliger and Retief (2002), which they regard as the types that cause the most damage and adverse wind conditions in South Africa.

A map of the strong wind climatic zones can be described as a basic diagram indicating the spheres of influence of specific weather systems that are likely to cause strong winds. Therefore, some resemblances between a general climate region and a wind climate region can be found, as mean precipitation, temperature, humidity and other climate variables are also, to a large degree, determined by the prevailing weather systems.

In this study the emphasis is on *the weather systems which have the potential to cause very strong or extreme winds in a specific location*, i.e., those climatic formations that are the usual causes of annual maximum wind gusts. In essence, a strong wind climatic zone, in this study, is defined as a geographical area which indicates a type of weather system that has the potential to be the cause of an annual maximum wind gust.

One should keep in mind that regional climatic boundaries are usually indefinite, except where they coincide with prominent physical features, such as mountain ranges, which then should be regarded as zones where the climates sometimes change rapidly from the type shown on the one side to that on the other (Jackson, 1951). Therefore, a measure of subjectivity and uncertainty will usually be present in the process of the delineation of climatic zones. The delineation of strong wind zones in this chapter will also have some measure of subjectivity, but it is thought that the large number of weather stations utilised, and the good spatial spread of the stations, will reduce the subjectivity to a large degree. To strengthen the objectivity of the spatial extent of the different strong wind zones, the topography, especially the position of the escarpment, has been taken into account where deemed relevant.

4.2. Analysis of data

The data that were utilised for the determination of the possible sources of annual maximum wind gusts are from the weather stations listed in Table 3.1, of which their positions are presented in Figure 3.11. Since 1995 the SAWS archives weather measurements in 5-minute intervals; this is some years after the implementation of the AWS technology. This means that although an AWS station might have started recording before 1995, 5-minute high-resolution data will not be available for the particular station.

These high resolution data measurements and averaging times are necessary to identify the causes of strong wind gusts with a high confidence. Therefore, for the purpose of this study, *data before 1995 could not be considered in most cases*. Where

data before 1995 was considered, there was sufficient evidence from synoptic maps that the occurrence of the particular extreme wind was due to a synoptic scale mechanism.

Sources of annual maximum wind gusts were identified with the following procedure:

- The annual maximum 2-3 second wind gust values were identified for each year of the time series.
- The 5-minute time series of the climatic data, of which the variables are the maximum wind gust, mean wind speed, mean wind direction, surface temperature, rainfall, relative humidity and surface pressure, were plotted for those days that the annual maximum gusts occurred, to enable the identification of the causes of extreme winds.

An example of such a plot, generated by the SAWS quality control software, is presented in Figure 4.2, which shows the 5-minute time series from Cape Town Weather Office for 15 July 2008. On this day the annual maximum wind gust speed of 25,0 m/s for 2008 was recorded at 17:25 South African Standard Time (SAST). From the time series it is apparent that the wind gust was caused by the passage of a cold front, *inter alia* evidenced by north-westerly winds, a significant decrease in temperature, and the onset of rainfall between 17:00 and 18:00 SAST.

Evidence of the prevailing weather systems, identified from synoptic charts published in the SAWS Daily Weather Bulletin (South African Weather Service, 1992-2008), were used to confirm the strong-wind producing mechanisms identified from the plots of the 5-minute time series. The synoptic chart for southern Africa for 15 July 2008 at 14:00 SAST is presented in Figure 4.3, from which one can see that a cold front was approaching the south-western Cape from the west.

The above procedure was sufficient to identify all sources of wind gusts which were caused by synoptic scale phenomena, such as cold fronts, ridging of high-pressure systems and convergence towards troughs. However, evidence of mesoscale phenomena, such as thunderstorms, cannot be easily gained from synoptic charts.

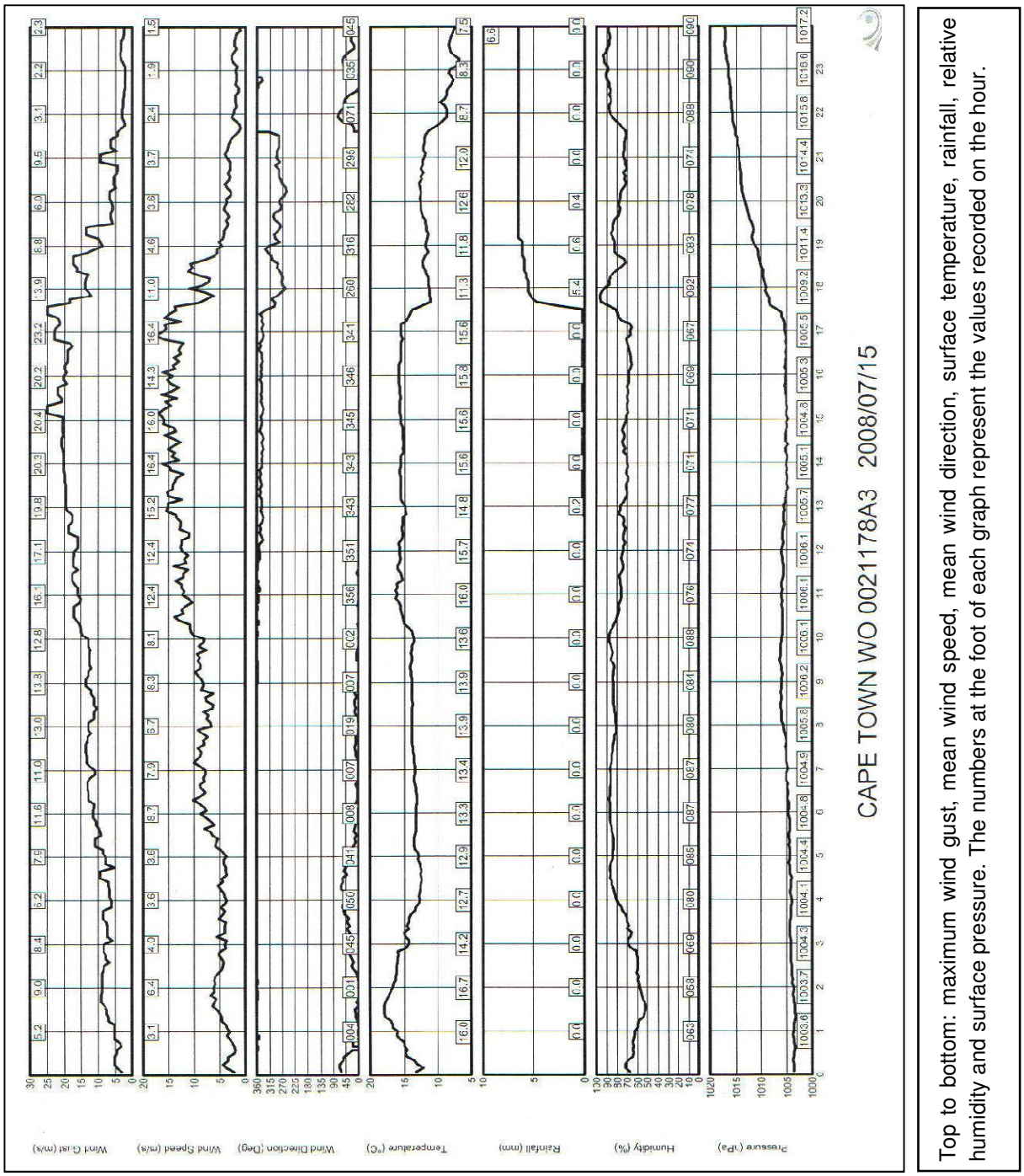

Top to bottom: maximum wind gust, mean wind speed, mean wind direction, surface temperature, rainfall, relative humidity and surface pressure. The numbers at the foot of each graph represent the values recorded on the hour.

Figure 4.2. Plots of the 5-minute time series recorded at Cape Town Weather Office for 15 July 2008 for maximum wind gust, mean wind speed, mean wind direction, surface temperature, rainfall, relative humidity and surface pressure.

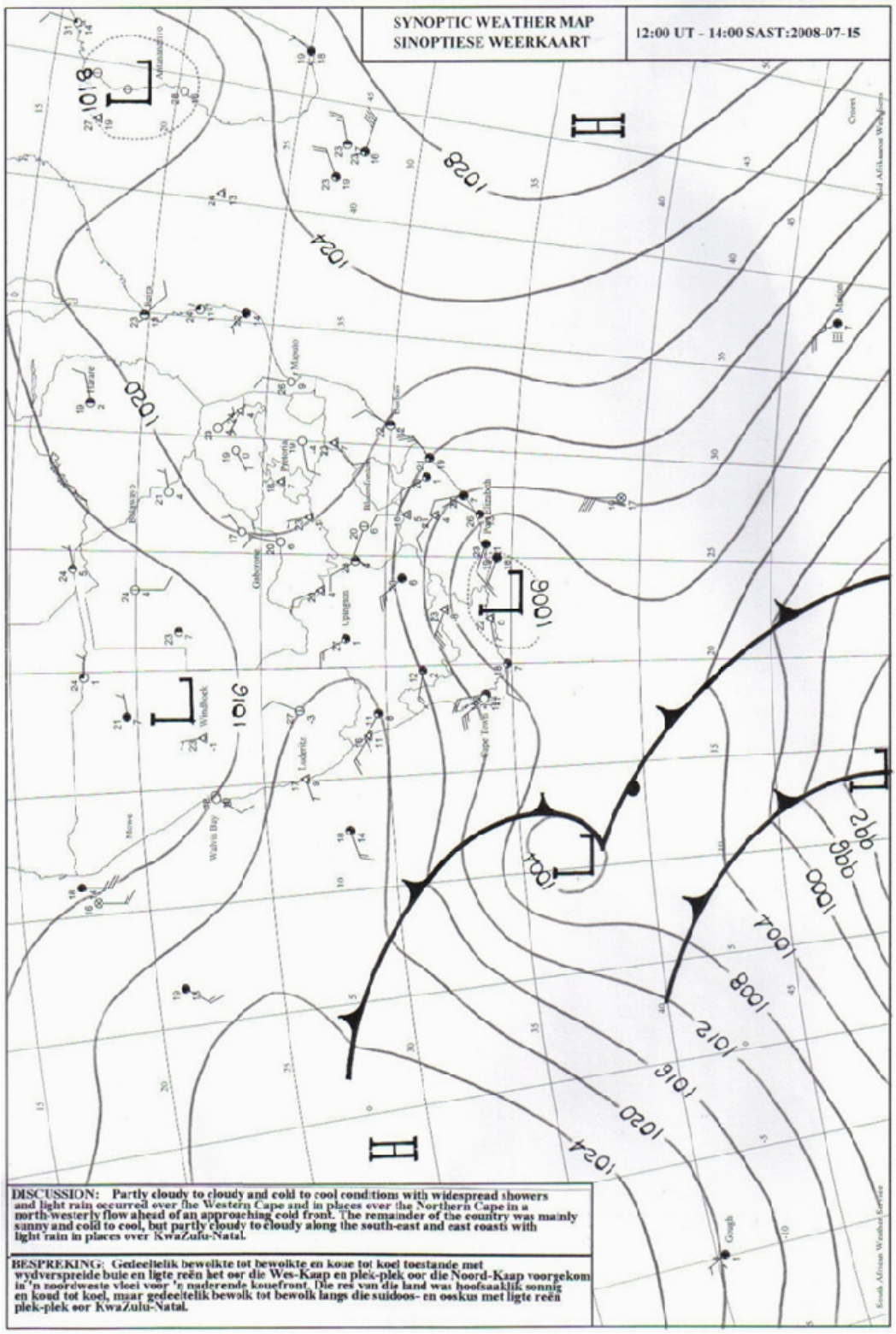

Figure 4.3. Synoptic chart for southern Africa for 15 July 2008 at 14:00 SAST (South African Weather Service, 1992-2008).

Therefore, where it was suspected that a particular wind gust was caused by, e.g., a thunderstorm; mostly evidence from the 5-minute time series plots was used for the purpose of identification. An example of a typical 5-minute time series plot which shows evidence of a strong wind gust caused by thunderstorm activity is presented in Figure 4.4. The plot, for 27 December 2004, shows the annual maximum wind gust at 14:40 SAST in Johannesburg, when a wind speed of 26,3 m/s was recorded.

The strongest winds forthcoming from thunderstorms are usually caused by the "gust front", the leading edge of the downdraft of cold air from the thunderstorm cloud. These gust fronts are associated with the following (Lee, 1996; Uyeda and Zrnic, 1986), which can be recognised from the 5-minute plots:

- Strong wind gust;
- Sharp drop in temperature;
- Usually but not always an increase in the humidity;
- Most often the onset of rain; and
- Often a slight increase in air pressure.

All of these signs can be observed in Figure 4.4. In cases in which the evidence of gust fronts was not as clear as in this typical example, evidence was sought from synoptic charts, to ascertain whether surface pressure patterns were conducive to the development of thunderstorms, such as a well-developed surface trough to the immediate west. In addition, manned weather offices provide reports of observed weather. These reports are stored on the SAWS climate database and were interrogated for any evidence of thunderstorms on the day that the annual maximum gust occurred; for the specific weather station as well as those surrounding it.

However, the possibility exists that on some occasions thunderstorms are imbedded in cold fronts, which makes it impossible to ascertain whether the wind gust under investigation was mainly caused by the cold front or thunderstorms. In these cases cold fronts were assumed as being the primary strong-wind producing mechanism. One should also note that, in cases where thunderstorms are embedded in the frontal zones, the wind profiles are usually similar to the wind profiles of passages of cold fronts

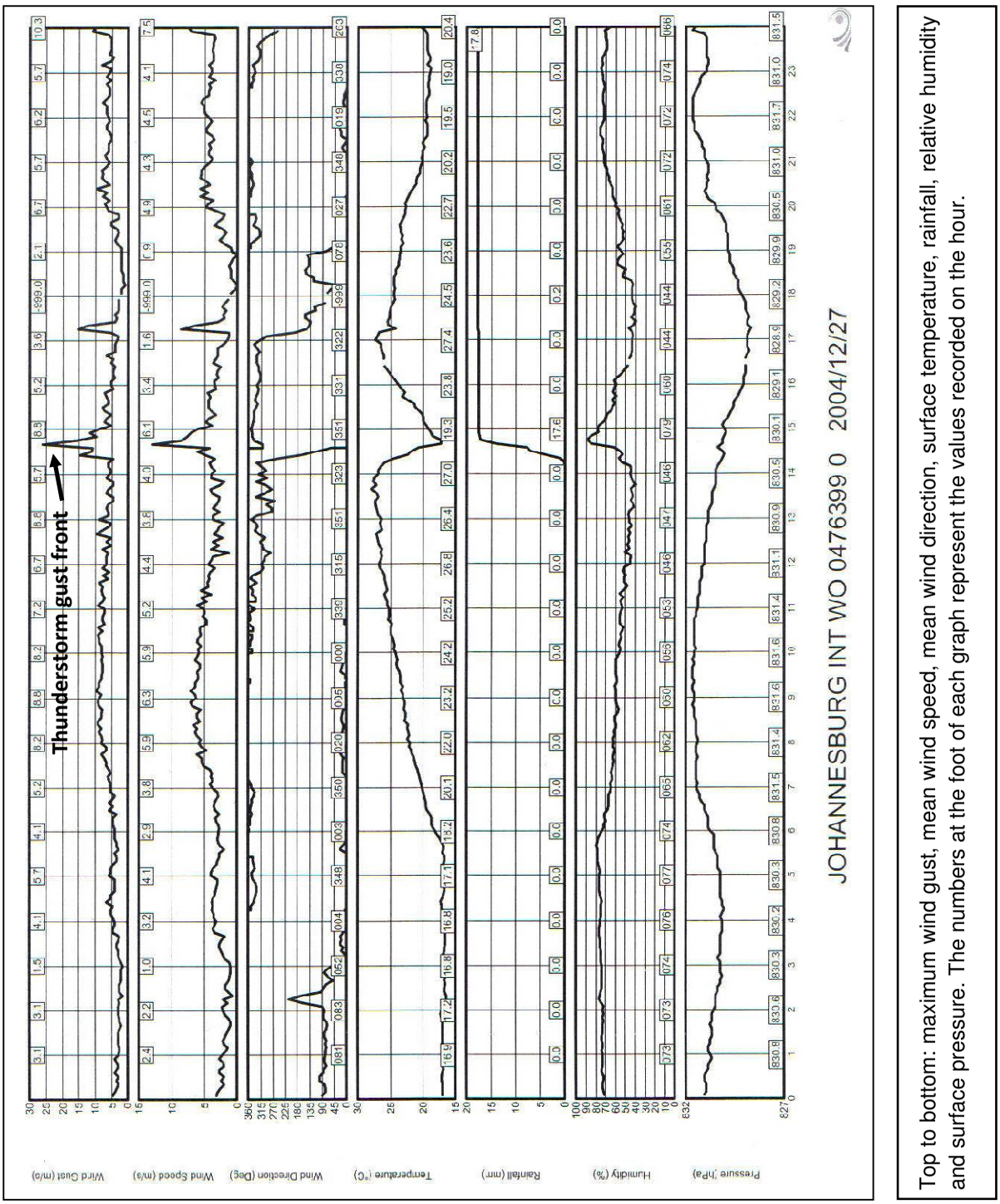

Top to bottom: maximum wind gust, mean wind speed, mean wind direction, surface temperature, rainfall, relative humidity and surface pressure. The numbers at the foot of each graph represent the values recorded on the hour.

Figure 4.4. Plots of the 5-minute time series measured at Johannesburg Weather Office for 27 December 2004 for maximum wind gust, mean wind speed, mean wind direction, surface temperature, rainfall, relative humidity and surface pressure.

without imbedded thunderstorms. Due to these similar wind profiles, there should then not be any significant implications for the analysis, of the winds so grouped.

Eventually all causes of the annual maximum wind gusts were listed for each weather station. Some examples are presented in Table 4.1, in which the values, as well as the causes, of each annual maximum wind gust recorded at Cape Town in the Cape Peninsula, Grahamstown in the south-eastern interior, De Aar in the central interior, and Johannesburg in the northern interior, are presented:

Table 4.1. Annual maximum wind gusts speeds (m/s) recorded at Cape Town (a), Grahamstown (b), De Aar (c), and Johannesburg (d) and their causes, for the available years for the period 1993 – 2008.

Year	(a) Cape Town		(b) Grahamstown		(c) De Aar		(d) Johannesburg	
	Wind Gust (m/s)	Cause	Wind Gust (m/s)	Cause	Wind Gust (m/s)	Cause	Wind Gust (m/s)	Cause
1993	30,5	CF	-	-	-	-	-	-
1994	35,5	CF	-	-	32,4	TS	21,0	CF
1995	28,5	CF	22,4	CF	32,1	TS	26,5	TS
1996	33,4	CF	27,6	CF	29,3	R/T	23,0	TS
1997	35,5	CF	19,7	CF	29,7	R/T	26,5	TS
1998	26,2	R	28,7	TS	33,0	TS	24,0	TS
1999	25,2	R	24,7	CF	30,7	TS	19,5	CF
2000	23,6	CF	22,3	CF	35,7	TS	22,5	TS
2001	28,9	CF	21,2	CF	34,7	TS	22,1	TS
2002	25,2	CF	28,7	CF	31,6	TS	23,2	TS
2003	26,2	CF	28,6	TS	30,8	TS	23,0	TS
2004	21,6	R	22,7	CF	31,8	TS	26,3	TS
2005	25,2	CF	22,3	TS	29,8	TS	29,4	TS
2006	23,7	CF	26,9	CF	29,4	TS	23,1	TS
2007	28,8	CF	22,9	CF	40,2	TS	-	-
2008	25,0	CF	24,4	CF	32,0	TS	34,1	TS

CF: Cold Front, R: Ridging, R/T: Ridging from the east with a deep trough to the west, TS: Thunderstorm.

- The main causes of the annual maximum wind gusts in Cape Town are the passage of cold fronts (13 out of 16 years, or 81%), and the ridging of the Atlantic Ocean high-pressure systems, i.e., strong south-easterly winds (three out of 16 years, or 19%); contrary to a general belief that most strong winds in Cape Town are south-easterly.
- At Grahamstown the main cause of the annual maximum wind gusts are cold fronts (11 out of 14 years, or 79%) and thunderstorms (three out of 14 years, or 21%).
- At De Aar the main cause of annual maximum wind gusts are thunderstorms (13 out of 15 years, or 87%) with, as a secondary cause, a synoptic situation which is characterized by ridging from the east with a deep surface trough to the west (two out of 15 years, or 13%).
- In Johannesburg most of the annual maximum wind gusts are caused by thunderstorms (12 out of 14 years, or 86%) with, as a secondary cause, the passage of cold fronts (two out of 14 years, or 14%).

4.3. Results and discussion

The determination of the causes of annual maximum wind gusts (according to six possibilities) as well as corresponding percentages of years of occurrence, were done for all weather stations utilised in the study, with the results as presented in Table 4.2.

The fractions of annual maximum wind gusts caused by these sources are presented in the maps in Figure 4.5(a-c), for each station utilised in the study (see Table 4.2 for full list of results). For most weather stations more than one source of annual extreme wind gusts were found, with one weather station where as many as four separate mechanisms contribute to the annual strong winds.

Table 4.2. Percentage of annual maximum wind gusts caused by the six identified sources.

Station Number	Station Name	TS	CF	R	T	TW	LP
0003108	STRUISBAAI		100				
0005609	STRAND		8	92			
0006386	HERMANUS		100				
0007699	TYGERHOEK		100				
0010682	STILBAAI		100				
0012661	GEORGE WO		100				
0014123	KNYSNA		100				
0014545	PLETTENBERGBAAI		100				
0015692	TSITSIKAMMA		100				
0020618	ROBBENEILAND		47	53			
0021178	CAPE TOWN WO		81	19			
0021823	PAARL		13	87			
0022729	WORCESTER-AWS		100				
0031650	JOUBERTINA AWS	20	70				10
0033556	PATENSIE	38	38				24
0034763	UITENHAGE	27	73				
0035209	PORT ELIZABETH		100				
0040192	GEELBEK		55	45			
0041388	MALMESBURY		57	43			
0041841	PORTERVILLE		13	53			34
0045642	LAINGSBURG		75				25
0056917	GRAHAMSTOWN	21	79				
0059572	EAST LONDON WO		100				
0061298	LANGEBAANWEG		91	9			
0063807	EXCELSIOR CERES		100				
0078227	FORT BEAUFORT	55	45				
0083572	LAMBERTSBAAI		36			64	
0092081	BEAUFORT-WES	8	69				23
0096072	GRAAFF - REINET	15	38				47
0123685	QUEENSTOWN	42	58				
0127272	UMTATA WO	50	50				
0134479	CALVINIA WO		53				47
0144791	NOUPOORT	57	21				22
0148517	JAMESTOWN	38	62				
0150620	ELLIOT	64	36				
0155394	PORT EDWARD		100				
0169880	DE AAR WO	86			14		
0182465	PADDOCK	7	80				13
0182591	MARGATE		100				

Station Number	Station Name	TS	CF	R	T	TW	LP
0184491	KOINGNAAS		27	40		33	
0190868	BRANDVLEI	67			33		
0214700	SPRINGBOK WO	15	54			31	
0224400	PRIESKA	62	8		30		
0239698	PIETERMARITZBURG	69	23				8
0239699	ORIBI AIRPORT	78	11				11
0240808	DURBAN WO		100				
0241072	MT EDGECOMBE		100				
0241076	VIRGINIA		100				
0261307	BLOEMFONTEIN	100					
0261516	BLOEMFONTEIN WO	100					
0268016	GAINTS CASTLE		100				
0270155	GREYTOWN	69	31				
0274034	ALEXANDERBAAI		72			28	
0290468	KIMBERLEY WO	100					
0300454	LADYSMITH	77	23				
0304357	MTUNZINI	62	38				
0317475	UPINGTON WO	100					
0321110	POSTMASBURG	100					
0331585	BETHLEHEM WO	38	46	16			
0333682	VAN REENEN	33	67				
0337738	ULUNDI	70	30				
0339732	CHARTERS CREEK	40	50	10			
0356880	KATHU	100					
0360453	TAUNG	100					
0362189	BLOEMHOF	64	36				
0364300	WELKOM	62	38				
0365398	KROONSTAD	83	17				
0370856	NEWCASTLE	64	36				
0410175	PONGOLA	80	20				
0427083	VAN ZYLSRUS	92					8
0438784	VEREENIGING	83	17				
0441416	STANDERTON	82	9	9			
0472278	LICHTENBURG	77			23		
0475879	JHB BOT TUINE	92	8				
0476399	JOHANNESBURG	86	14				
0479870	ERMELO WO	64	29				7
0508047	MAFIKENG WO	75			25		
0511399	RUSTENBURG	92			8		
0513346	PRETORIA UNISA	73	9	9	9		
0513385	IRENE WO	71	21	8			
0515320	WITBANK	86	14				

Station Number	Station Name	TS	CF	R	T	TW	LP
0520691	KOMATIDRAAI	100					
0548375	PILANESBERG	82	9		9		
0554816	LYDENBURG	62	9	29			
0587725	THABAZIMBI	90		10			
0594626	GRASKOP AWS	60	40				
0633882	POTGIETERSRUS	90					10
0638081	HOEDSPRUIT	50		50			
0674341	ELLISRAS	86	7				7
0675666	MARKEN	58		42			
0677802	PIETERSBURG WO	100					
0723664	THOHOYANDOU WO	75	8				17

TS: thunderstorms, CF: Cold fronts, R: Ridging, T: Trough to the west with strong ridging from the east, TW: Trough on the West Coast, LP: Isolated low-pressure systems.

It is argued that the availability of more years of wind data would result in an even more complex set of results, as the strong wind mechanisms that do not occur often; for example the isolated lows, might be more prevalent in longer data series. This is because some of the weather stations fairly close to one another might indicate only one dominant strong wind mechanism for all the years for the one weather station, while the other weather station might also indicate the presence of a strong wind mechanism which does not occur that often (e.g. the Pietersburg and Potgietersrus weather stations which are only about 50 km apart). This should be kept in mind in the exercise of delineating the different strong wind zones by being not too conservative in the approximations of the spatial extents of the zones. Figure 4.6 presents a summary of the percentage of stations associated with different numbers of contributing strong wind mechanisms.

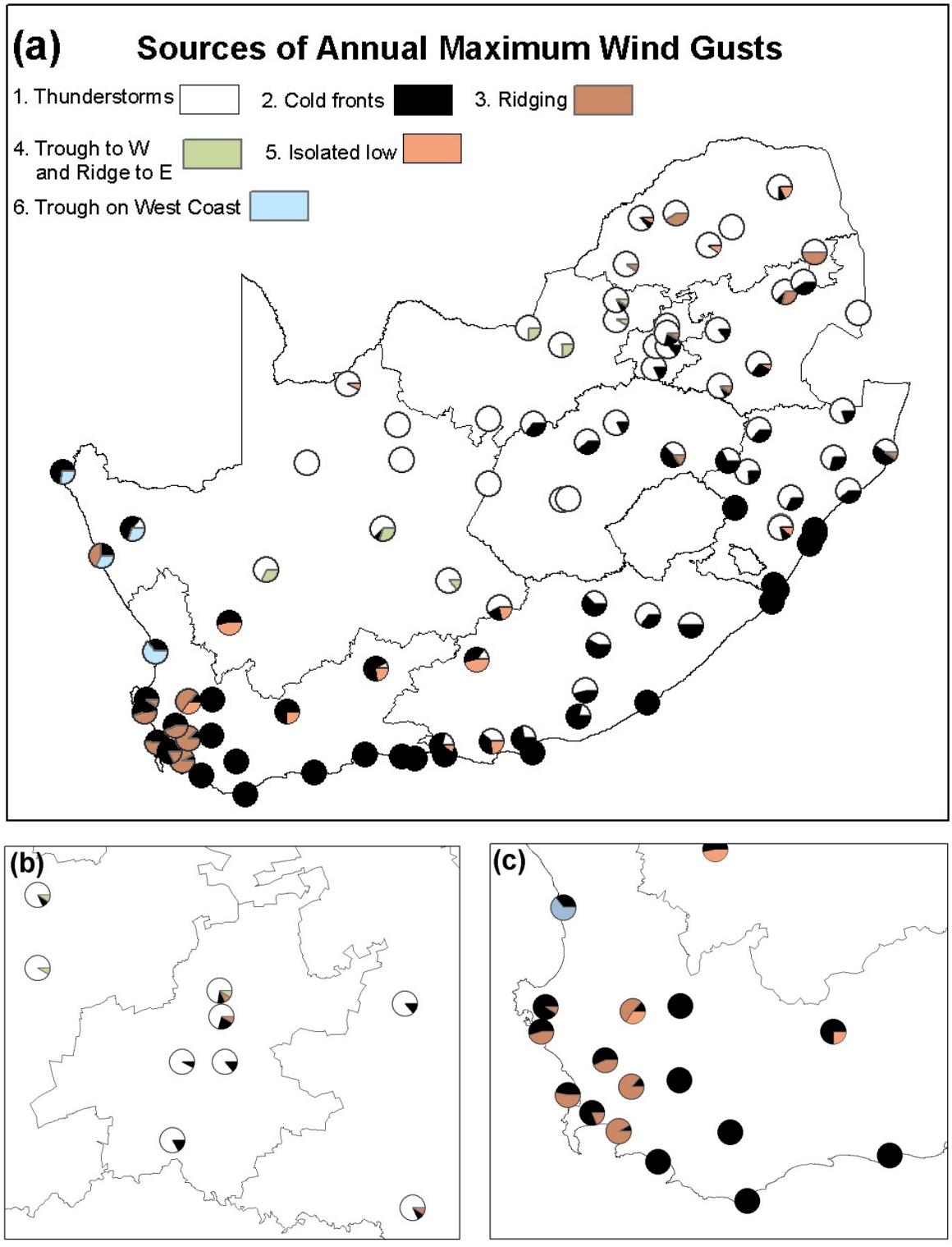

Figure 4.5. Fractions of annual maximum wind gusts caused by six identified sources, for each station utilised in the study (a), Gauteng province in the north (b) and the Western Cape Province in the south-west (c).

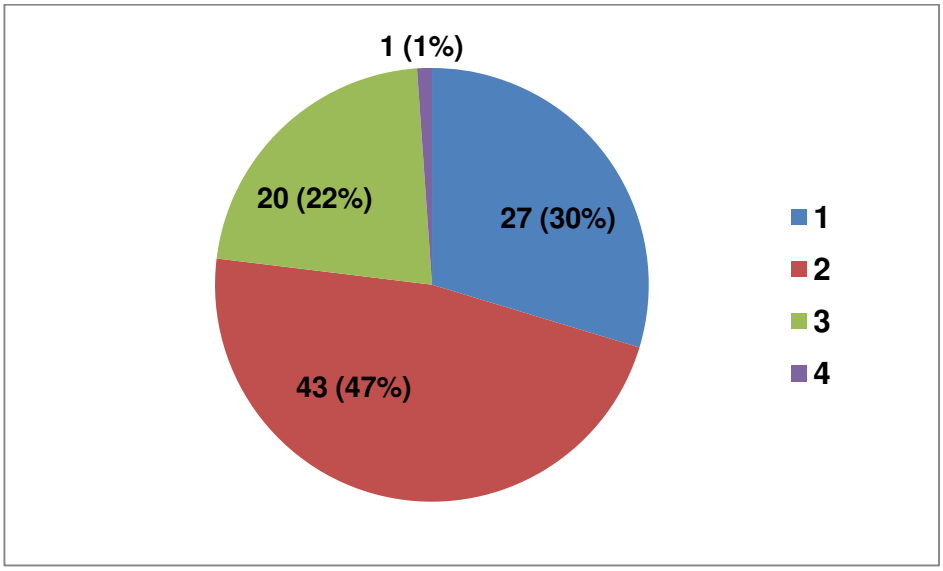

Figure 4.6. Numbers (percentage) of stations with one to four identified strong wind mechanisms.

However, regardless of the complexity of the results, one can see that the cold fronts and the other strong wind mechanisms derived from mature storms dominate the coastline and the adjacent interior, while the thunderstorms dominate further inland. Also, it is clear that the different strong wind zones that can be derived from this information will overlap. These derived zones are depicted on separate maps, which are presented in Figure 4.7(a-f). Following are the descriptions of these sources, ordered in approximate level of dominance:

1. Thunderstorms:

   Most annual maximum wind gusts in the interior are caused by thunderstorm activity during the summer months. This is especially true in the central interior where annual maximum wind gusts at many weather stations were solely caused by thunderstorms (10% of the total number of stations). The strongest gusts from thunderstorms are usually recorded during the passages of “gust fronts” over the weather station, which in turn usually precedes the first rainfall from the thunderstorm cell. Figure 4.7(a) presents the area in the interior, but very close to

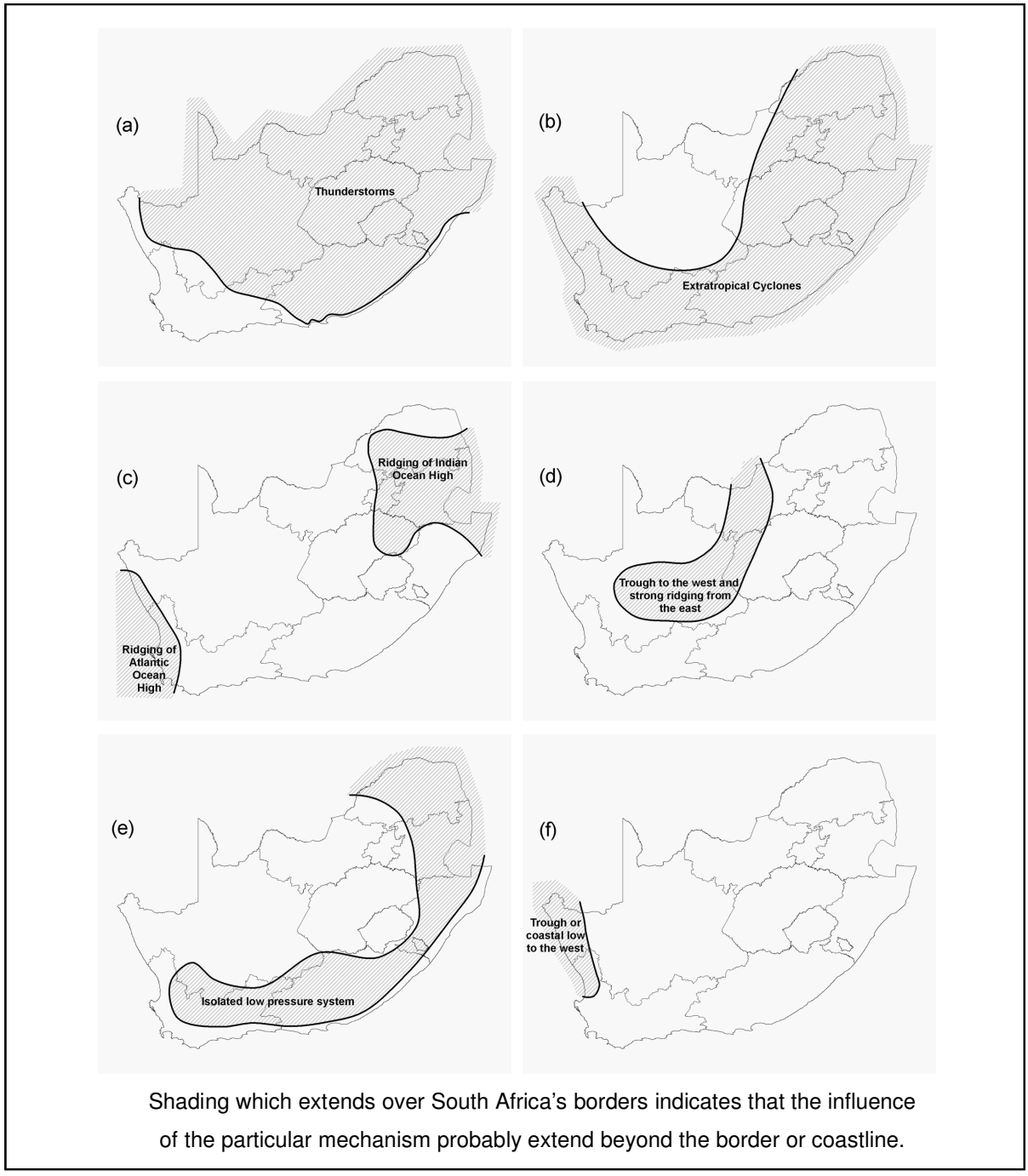

Figure 4.7. Zones with extreme winds possible as a result of (a) thunderstorms, (b) cold fronts, (c) ridging of the Atlantic or Indian Ocean high-pressure systems, (d) a surface trough to the west and strong ridging from the east, (e) convergence towards isolated low-pressure systems or deep coastal low-pressure systems on the coast, and (f) a deep surface trough to the west on the West Coast.

the coastline in the south-east, where the annual maximum gust speeds can also occur due to thunderstorms.

2. Cold fronts:

   Most annual maximum gusts along the coastline and adjacent interior are caused by the passage of cold fronts. The spatial extent of the annual maximum wind gusts, occurring as a result of the extratropical cyclones, i.e., the passage of cold fronts, is presented in Figure 4.7(b). From the analysis of the synoptic maps it was observed that along the western and southern coasts strongest winds mostly occur in the vicinity of the actual front. However, along the south-eastern and eastern coasts the winds are usually strongest just behind the coastal low-pressure system preceding the front. Finally, in the central to northern interior strong wind gusts usually occur well east of the actual fronts, which move in from the west, and are also associated with deep coastal low-pressure systems on the south-eastern and eastern coasts. This results in a strong flow of the air towards the east. Along the coast and adjacent interior the annual maximum wind gusts of many stations were caused by cold fronts only (19% of the total).

   From the above one could argue that the cold front mechanism can be subdivided into three processes, which can provide an even more complex presentation of the strong wind mechanisms than that presented in Figure 4.5. However, this was not done as in all three cases the cold front itself was assumed to be the dominant cause of the observed strong winds. On the southern and eastern coastline the cold front mechanism makes up 100% of the cases, but from Hermanus towards the west, the ridging of the Atlantic Ocean high-pressure system starts to play a significant role.

3. Ridging of the quasi-stationary Atlantic and Indian Ocean high-pressure systems over the subcontinent:

   The annual maximum wind gusts caused by the ridging of the Atlantic Ocean high-pressure system are evident along the western and south-western Cape

coasts and adjacent interior. Figure 4.7(c) presents the areas experiencing extreme winds as a result of the ridging of the Atlantic Ocean and Indian Ocean high-pressure systems. This ridging is strongest during the summer months, and as previously mentioned, the associated wind in the south-western Cape is locally known as the “Cape Doctor”. Ridging in the eastern interior is associated with either the Atlantic Ocean high-pressure system ridging around the coast from west to east behind a cold front, or with the Indian Ocean high-pressure system to the east of the subcontinent.

4. A synoptic situation in the central interior, characterised by a deep surface trough which is situated to the west, and ridging of the Atlantic or Indian Ocean high-pressure systems from the east:

   Some annual maximum wind gusts in the central and western interior occur just east of deep surface troughs, usually together with strong ridging by the Indian Ocean high-pressure system from the east. These synoptic conditions are usually conducive to the development of thunderstorms due to convergence, and often occur in summer. However, sometimes the necessary moisture is not available so that the only effect is the occurrence of strong, gusty and dry winds. Figure 4.6(d) presents the area in the southern to central interior where extreme wind gusts due to these conditions are likely to occur. It is interesting to note that this zone is congruent to the northern boundary of the cold front zone presented in Figure 4.7(b). This is because the occurrence of the troughs in the interior are usually accompanied or coupled with the passage of the cold fronts along the coastal regions, as evidenced from synoptic maps.

5. Strong isolated low-pressure systems, also including unusually strong coastal low-pressure systems:

   Often synoptic situations occur when strong isolated low-pressure systems develop, usually along the coast, but also on occasion in the interior in summer. Occurrences of the annual maximum wind gusts due to the convergence around isolated low-pressure systems, as well as around very deep coastal low-pressure systems ahead of a cold front (where the strong low-pressure system is considered to be the overwhelming cause of the strong winds occurring), were

grouped together. A significant fraction of annual maximum wind gusts at some weather stations in the south-western and southern interior are caused by these weather systems, but other cases were also identified for weather stations along the escarpment towards the north. Therefore, while isolated low-pressure systems tend to be the cause of a sizeable number of annual maximum wind gusts in the south, these systems can also cause extreme winds elsewhere, of which the area is presented in Figure 4.7(e). Notable from Figure 4.7(e) is that the area close to the coast under the influence of isolated low-pressure systems does not include the coastline itself. This is because strong winds, which are caused by these systems, occur due to a strong horizontal pressure gradient towards the low-pressure system. Such isolated low-pressure systems are most often situated very close or on the coastline itself.

6. A synoptic situation on the west coast and adjacent interior, characterised by a coastal low, and sometimes a deep surface trough, developing ahead of the passage of a cold front:

   Along the west coast and adjacent interior, annual maximum wind gusts are sometimes caused by convergence towards a deep trough to the west, which is associated with the occurrence or development of a coastal low-pressure system ahead of the passage of a cold front. Figure 4.7(f) presents the area that can experience extreme wind conditions under the influence of these synoptic conditions, which can occur during anytime of the year.

It is only the first two dominant strong-wind producing mechanisms (thunderstorms and extratropical cyclones) which are, for many weather stations, the sole causes of annual maximum wind gusts. The weather stations where either thunderstorms or extratropical cyclones are the only causes of annual extreme wind gusts make up 23% of the total number of stations. For 29% of the stations the only causes of strong winds are both the thunderstorms and the extratropical cyclones, which can thus be regarded as the most prevalent case. At the remaining 48% of stations the other four strong-wind producing mechanisms also play a role, which are for most of these weather stations of a

secondary nature. The percentage of weather stations, where three or more mechanisms are the causes of strong winds, is 22%.

The secondary strong-wind producing mechanisms are associated with synoptic scale processes, often of a frontal origin. These mechanisms are classified as secondary to cold fronts because, while they are synoptic in scale, their strong winds are not directly caused by the strength of a cold front. However, together with the strong winds directly attributed to the passages of cold fronts, these strong winds are usually more persistent in nature due to the relatively slow changes of the synoptic-scale flow patterns. This is in contrast to strong winds produced by thunderstorms, which in many cases may last only a few minutes.

For some applications e.g. the statistical modelling for wind load predictions, a broad differentiation can be made between strong winds attributed to thunderstorms, and strong winds caused by the remainder of the mechanisms, i.e. the synoptic-scale systems. This is possible because the gust profiles induced by synoptic-scale storms are similar, and much lower than for thunderstorms (see the discussion in section 7.3.2.1 and Figure 7.8). This will have an effect on the conversion factors to be applied between different averaging periods (see also the discussion in section 2.1.1). Figure 4.8 presents the spatial distribution of the regions where the thunderstorms dominate on the one hand, and the mature storms on the other. In this regard the specific methodologies applied in the treatment of mixed distributions are important, where in some cases broad groupings into only synoptic and non-synoptic origins are recommended. The application of the mixed distribution method to estimate the quantiles are discussed in section 5.5.1, where it is shown that such an approach leads to higher estimated quantile values, in comparison to when a single strong wind climate is assumed. For South Africa this is an important issue in the estimation of reliable quantile estimates, and distinguishes it from the European reference procedures.

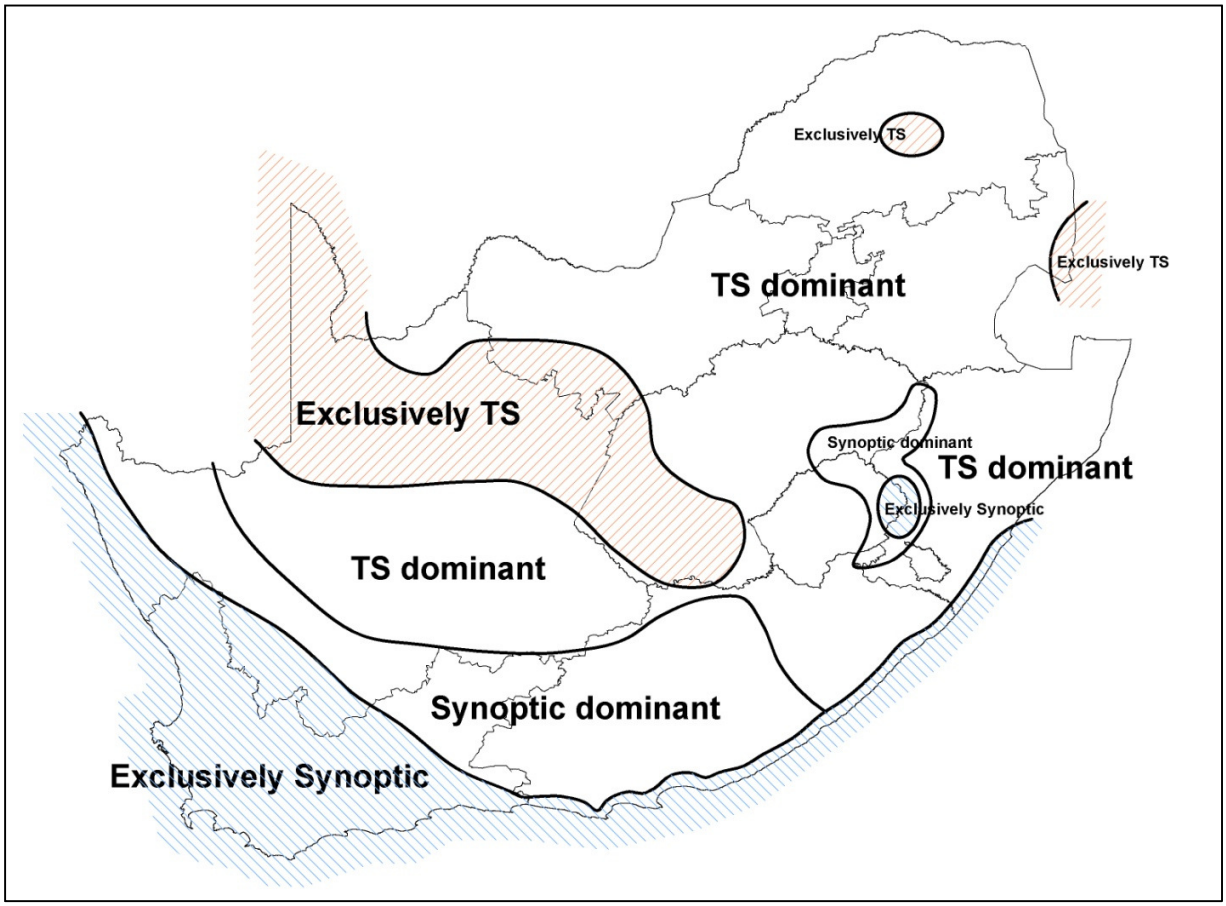

Figure 4.8. Regions where the strong winds from thunderstorms (TS) and synoptic storms dominate.

4.4. Concluding remarks

By analysing the annual extreme wind gust data from 94 weather stations, which are spatially well distributed over the South African territory, it was possible to develop the climatology of strong wind zones for South Africa. The strong wind climate of South Africa appears to show similarities with South America (e.g. Brazil) and Australia (Holmes, 2002; Oliver *et al.*, 2000; Ponte and Riera, 2007), but the considerations of the mixed strong wind climates in the estimation of wind quantiles have been limited. In these regions mixed strong wind climates are also evident, with the southern regions dominated by the synoptic-scale systems while the northern regions by thunderstorms. Between these northern and southern regions a mixed strong wind climate exists. It is

therefore no coincidence that the first recognition of the need of the separate treatment of the different strong wind mechanisms in the estimation of the quantiles, and the development thereof, came forth from Australia (Gomes and Vickery, 1978). The application of the mixed distribution method in section 5.5.2 builds upon these methodologies, and goes beyond by the classifying and analysing of the synoptic-scale winds into more sub-groupings.

Six strong-wind producing mechanisms were identified by classifying the causes of the annual maximum wind gust speeds. Two of those mechanisms, namely thunderstorms and extratropical cyclones (the passage of cold fronts) are dominant, while the other four mechanisms are of a secondary importance.

The geographic distribution of strong wind climates was established, and is in general agreement with the strong wind zones developed by Goliger and Retief (2002). As examples, Figure 4.1 (zone 6) and Figure 4.7(c) show strong similarity between the regions that indicate strong south-easterlies and ridging, which refer to the same strong-wind mechanism. Figure 4.1 (zone 3) indicates the zone for the intense thunderstorms, which is almost covered by the area depicted in Figure 4.7(a), except for the coastal region. This is due to the fact, which was referred to in the analysis section, that thunderstorms that occur over the coastal parts are usually embedded in cold fronts, and therefore reveal a similar wind profile.

It is shown that in most parts of South Africa overlapping of strong wind zones derived, occur. This is especially true for the two dominant strong-wind producing mechanisms, i.e., the extratropical cyclones and thunderstorms. Where these two mechanisms dominate in a particular region, strong winds produced by extratropical cyclones usually occur during the winter months, while strong winds from thunderstorms occur during the summer season. There are only two regions in South Africa where the annual maximum wind gusts are associated with only one type of strong-wind producing mechanism. For the south-western, southern, south-eastern and eastern coasts as well as their immediate adjacent interior, the annual maximum gusts are only caused by extratropical

cyclones. On the other hand, parts of the central and far northern interior are dominated exclusively by thunderstorms. The regional dominance of these two mechanisms is best illustrated by the map presented in Figure 4.8. Sub-regions where there are overlapping between the thunderstorms and the cold fronts are also shown, with the dominant mechanism depicted.

When considering the entire country, some of the mechanisms secondary to thunderstorms and extratropical cyclones still tend to dominate regionally. Examples of these are the south-easterly winds in the south-western Cape, caused by the ridging of the Atlantic Ocean high-pressure system, and the strong winds produced by deep troughs or strong coastal lows on the West Coast, where their influences dominate over isolated areas.

The accuracy of the extreme wind speed estimations and therefore wind design parameters can be compromised, usually by underestimating the wind speed values for the long return periods, if the wind values used to determine the shape of the extreme values distributions are forthcoming from more than one source (Gomes and Vickery, 1978; Milford, 1985a; Palutikof *et al*., 1999). This is especially true where differentiation is needed between strong winds of thunderstorm and synoptic scale origins (Gomes and Vickery, 1978; Twisdale and Vickery, 1992). It is therefore recommended that the estimations of extreme winds for most locations in South Africa employ methods which take the mixed strong wind climate into account, especially where these estimations are done for the design of structures that should have very low probabilities of failure (e.g. power stations and hospitals).

Another aspect of the strong wind producing mechanisms to keep in mind is that the footprints of the different strong wind producing mechanisms differ. In the case of strong winds produced by thunderstorms, the footprints or the size of areas subject to the strong winds tend to be much smaller than for example with cold fronts, of which the footprint can be hundreds of kilometres. These larger footprints have ramifications for

the risk analysis of structures such as transmission line networks, which cover a sizable area.

However, more relevant to the present analysis is the density of the network required to pick up representative occurrences of strong winds. The present network may be sufficient for synoptic winds; however, a much denser network and/or longer observation period is required to provide a proper “sample” of strong winds originating from thunderstorms. It could therefore be argued that there is a systematic underestimation of the magnitudes of strong winds caused by thunderstorms.

Chapter 5

Statistical Analysis of Strong Wind Data

5.1. General considerations

The most recent analysis of South African extreme wind values was performed by Milford (1985 a and b). One of the findings of this study was that the annual extreme mean hourly wind data were in most cases best fitted to the Gumbel (Fisher-Tippet Type I) distribution, if compared to the Fisher-Tippett Type II and Type III distributions (Milford 1985a). In the case of Milford (1985a and b), the extreme wind analysis was applied to the SAWS wind data which were still measured by the Dines anemographs. It is not certain whether the exposures of the installations of all the Dines anemographs were ideal, and whether the anemographs were always correctly calibrated. All of these instruments were phased out during 1992, and replaced by RM Young sensors in conjunction with the AWS technology.

In Chapter 3 it was shown that the wind data from the Dines anemographs and the AWSs are not compatible. Therefore, the analysis of extreme winds in this chapter will focus on the wind data forthcoming from AWSs (RM Young sensors) only, from the weather stations listed in Table 3.1 in Chapter 3. These weather stations all have near-complete data series of between 10 and 16 years duration, when the wind was measured using the RM Young wind sensors. In section 8.4 some comparisons are made between the results from the extreme wind analyses of the data series from the different types of wind instrumentation, and observation periods.

The analyses performed in this chapter does not take the exposure of the anemometers into account, the purpose being the identification of the most appropriate extreme wind

estimation methods to be applied to the available wind speed data. The overview of the statistical methodologies to estimate extreme winds is to be found in Chapter 2. More or less the same sequence, in which these methods are presented, is followed in the current chapter.

In the fitting of the various statistical distributions, the Anderson-Darling goodness-of-fit test has been applied (see section 2.3.5.2). The results from this test implied that all the applied statistical distributions fitted the data well.

5.2. Application of GEV distributions

5.2.1. The Gumbel method

As mentioned in section 2.3.2, the Gumbel method is the most often applied method to estimate extreme wind speeds. This is firstly because of the fact that the shape parameter, κ, of the Gumbel distribution is equal to zero, and therefore simplifies the calculations. The second reason is that one of the parent distributions of the Gumbel distribution is the Weibull distribution, which is considered to be a good model for the distribution of the wind speed, as raised in section 2.3.1.

As discussed in section 2.3.2, there are different options of methodologies which are often applied to estimate the parameters of the Gumbel distribution, i.e. the scale or shape α, and the mode β. Some of the most often used methods are (i) the graphical method and (ii) the method of moments.

A graphical solution to the estimation of α and β is often preferred (Palutikof *et al.*, 1999). As an example, the graphical method is applied to the annual extreme wind gust data for Struisbaai, on the southern Cape coast, which is presented in Table 5.1. In the third column the wind gust values are shown in increasing order, x_m, from the smallest to the largest, from which the plotting positions $F(x_m)$ were determined from equation 2.5. Values for the reduced variate, y_{Gumbel}, could then be calculated with equation 2.4.

Table 5.1. Available annual extreme wind gust values (m/s) (a) and reduced variates for Struisbaai (b), for the period 1997 to 2008.

(a)

Year	Annual maximum wind gust (m/s)
1997	26,6
1998	25,9
1999	41,9
2000	27,4
2001	31,5
2002	Not available
2003	26,6
2004	26,1
2005	28,0
2006	24,2
2007	24,9
2008	29,3

(b)

Annual maximum wind gust (m/s) in increasing order	Reduced variate y_{Gumbel}
24,2	-1,1
24,9	-0,7
25,9	-0,4
26,1	-0,1
26,6	0,1
26,6	0,4
27,4	0,6
28,0	1,0
29,3	1,3
31,5	1,9
41,9	3,0
-	-

Figure 5.1 presents the Gumbel plot, y_{Gumbel} against x (the annual maximum wind gust values), as well as the least-squares fit to the plotted values. The fitted straight line has equation $y = 3{,}8x + 26{,}4$, from which the estimations for α and β are then acquired as 3,8 and 26,4 respectively.

Alternatively, the estimation of the Gumbel parameters by the method of moments simply consists of applying equations 2.6 and 2.7 to the data set in Table 5.1, which then produce estimations for α as 3,7 and β as 26,3. The estimated 1:50 year quantiles are 40,8 m/s and 40,6 m/s for these two methods respectively. Comparisons of the results between the two methods for the data sets of other weather stations produce similar small differences between the results. According to Abild (1994) and Hosking *et al.* (1985), in Larsén and Mann (2009), this method yields less bias and variance on the parameter estimates, and has been proven highly efficient even for small sample sizes.

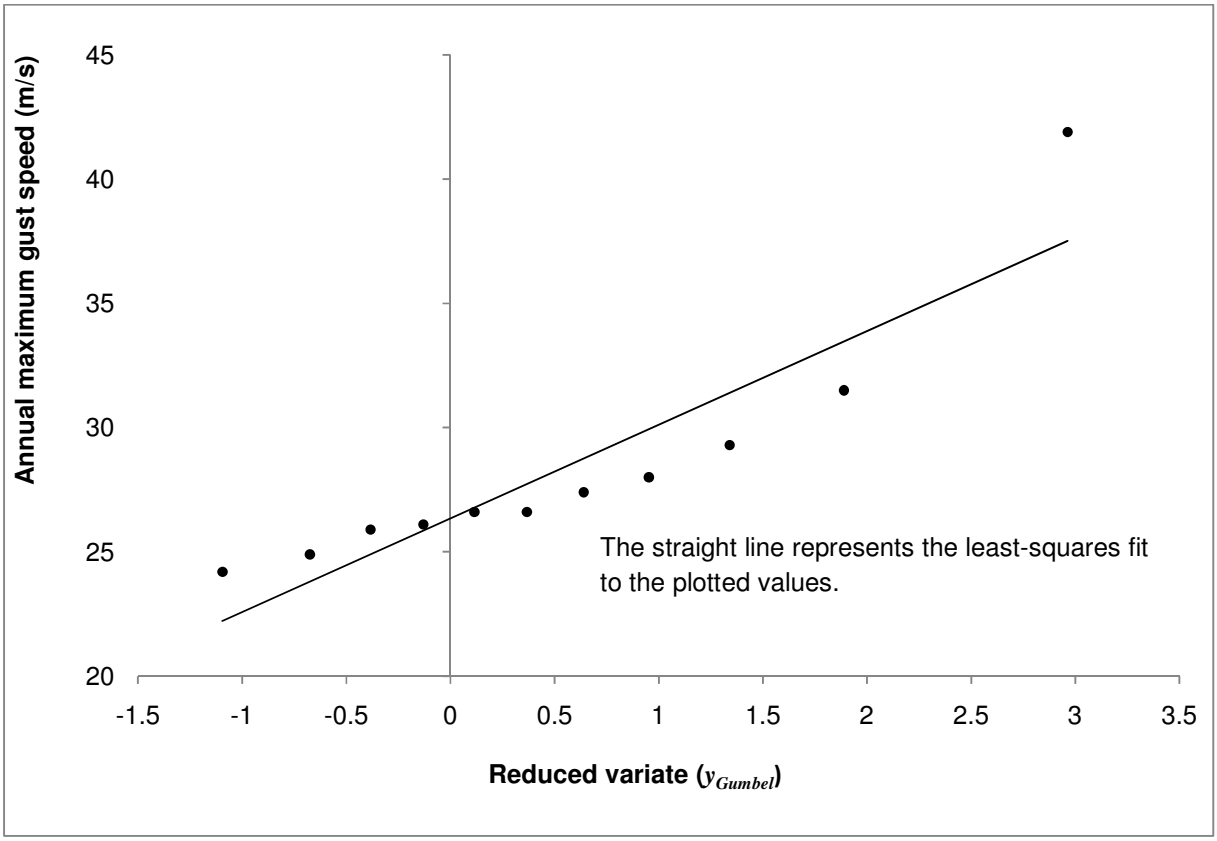

Figure 5.1. Gumbel plot for Struisbaai, for the period 1997 to 2008.

Considering the above, it was decided to estimate the coefficients of all the fitted Gumbel distributions with the method of moments. To be noted, the level of confidence of the estimations, and therefore the uncertainties, as pointed out in section 2.3.6, is not taken into consideration here. This issue is addressed in section 7.4.1, where the estimated quantiles are adjusted by the upward adjustment of the distribution parameters by an appropriate confidence limit. The quantiles of the annual maximum gust speeds and annual maximum hourly wind speeds, with return periods 50, 100 and 500 years, were then calculated with equation 2.8. It is recognized that there should be substantial reservations in the estimations of quantiles for long return periods such as 100 and 500 years with the short time series; these are only estimated for comparative purposes between the different methodologies. For illustrative purposes, the degree of extrapolation of the quantiles beyond the data record for Struisbaai is presented in Figure 5.2.

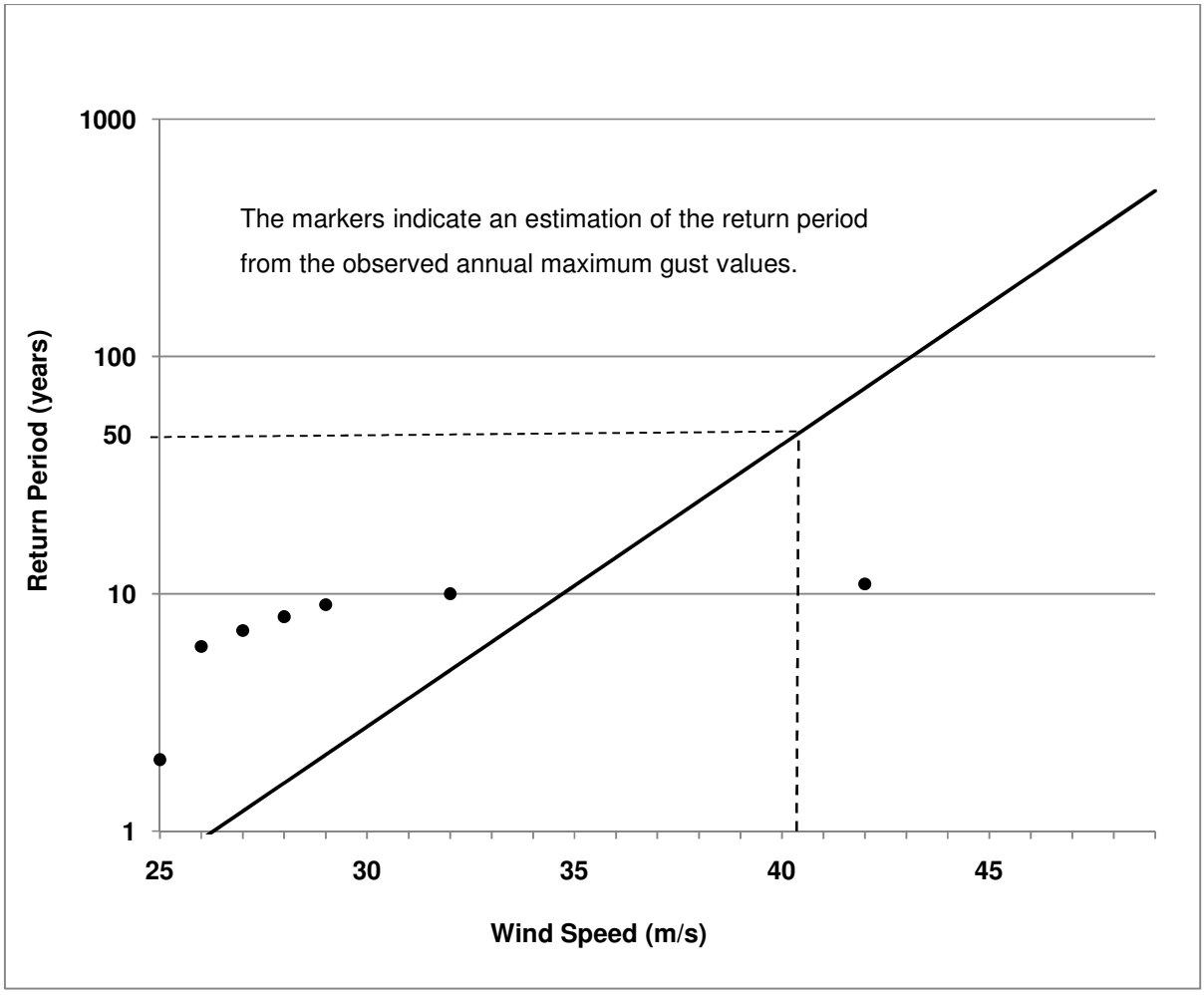

Figure 5.2. Gumbel estimation of the quantiles for Struisbaai.

The Gumbel results for the main centres in South Africa, as well as other significant stations, are presented in Table 5.2. The results for the complete set of selected weather stations are included in Table A.1 in Appendix A.

Table 5.2. Estimations of the quantiles X_T (m/s) with return periods T equal to 50, 100 and 500 years, with the Gumbel method.

Station Number	Station Name	Annual maximum wind gust (m/s)					Annual maximum hourly wind speed (m/s)				
		α	β	X_{50}	X_{100}	X_{500}	α	β	X_{50}	X_{100}	X_{500}
0012661	GEORGE WO	1,81	25,16	32,2	33,5	36,4	1,63	14,32	20,9	22,0	24,6
0021178	CAPE TOWN WO	3,18	25,85	38,3	40,5	45,6	1,64	16,00	22,4	23,5	26,2
0035209	PORT ELIZABETH	2,09	29,90	38,1	39,5	42,9	1,55	18,68	24,7	25,8	28,3
0059572	EAST LONDON WO	1,50	25,89	31,8	32,8	35,2	0,80	15,68	18,8	19,4	20,7
0092081	BEAUFORT-WES	2,28	29,65	38,6	40,1	43,8	1,88	18,39	25,8	27,1	30,1
0127272	UMTATA WO	3,44	27,07	40,5	42,9	48,5	1,50	14,58	20,5	21,5	23,9
0182591	MARGATE	1,63	24,18	30,6	31,7	34,3	0,75	13,67	16,6	17,1	18,3
0239698	PIETERMARITZBURG	1,89	19,65	27,0	28,3	31,4	0,87	7,62	11,0	11,6	13,0
0240808	DURBAN WO	2,16	24,85	33,3	34,8	38,2	1,21	14,66	19,4	20,2	22,2
0261516	BLOEMFONTEIN WO	2,60	24,30	34,5	36,3	40,5	0,72	11,40	14,2	14,7	15,9
0274034	ALEXANDERBAAI	1,43	25,76	31,3	32,3	34,6	0,80	19,03	22,2	22,7	24,0
0290468	KIMBERLEY WO	2,37	27,10	36,4	38,0	41,8	0,87	13,36	16,8	17,4	18,8
0317475	UPINGTON WO	3,11	25,30	37,5	39,6	44,6	0,75	13,68	16,6	17,1	18,3
0476399	JOHANNESBURG	2,82	22,96	34,0	35,9	40,5	0,96	11,68	15,4	16,1	17,6
0508047	MAFIKENG WO	1,99	24,14	31,9	33,3	36,5	1,20	14,26	19,0	19,8	21,7
0513385	IRENE WO	2,48	23,22	32,9	34,6	38,6	0,91	12,42	16,0	16,6	18,1
0677802	PIETERSBURG WO	2,40	22,82	32,4	34,0	37,9	0,90	11,37	14,9	15,5	16,9

5.2.2. Fitting of the GEV distribution

In fitting the Gumbel distribution to a set of data, it is assumed that the shape parameter, κ, of the GEV distribution equals zero. Various authors dispute this, and often give a choice between the Type I ($\kappa = 0$) and Type III form ($\kappa > 0$) of the GEV distribution.

It is assumed that the Type II form ($\kappa < 0$) is usually indicative of a wind data series composed of wind speeds forthcoming from different strong-wind producing mechanisms (Gomes and Vickery, 1978), producing a thicker tail to the distribution,

which can cause unrealistically high values for wind speed quantiles at longer return periods. Such wind series should ideally be decomposed, and the wind speeds forthcoming from the different strong-wind producing mechanisms treated separately, as presented in the analyses in section 5.5.

The biggest criticism of the application of the Type III form is that the distribution is bounded from above, and Palutikof *et al.* (1999) argue that there is no physical justification for a natural upper bound for wind speed, especially at the order of magnitude at which wind speeds are naturally observed. However, Walshaw (1994) argues that a Type III distribution should be fitted if it fits the data better than a Type I. Lechner *et al.* (1992) showed that for 100 wind time series in the United States, 36 showed a Type I form, three a Type II form, and 61 a Type III form.

By assuming that the shape parameter, κ, is not equal to zero, GEV distributions were fitted to the annual maximum wind gusts, as well as the annual maximum mean hourly wind speeds, of the set of weather stations. Three distribution parameters, κ, α, and β, therefore needed to be estimated, i.e. the shape parameter, the scale or dispersion parameter, and the mode, respectively. The estimations of these values can be mathematically intensive and therefore the use of applicable software is advisable. In this case the EasyFit software (www.mathwave.com) was employed, which estimate the distribution parameters by the ML solutions. This method follows an iterative procedure until the iterations reach a specified maximum, in this case 1000 iterations, which are deemed sufficient to obtain accurate estimates.

Figure 5.3 presents the fitting of the GEV distribution to the annual maxima of the wind gusts of Struisbaai, for which the value of the κ parameter was estimated as -0,47, i.e. a very strong form of Type II. Interesting to note is that, while the quantile estimations for the Type II is much higher than Type I for the longer return periods, the quantile estimations for the shorter return periods, e.g. 10 years, are actually lower, due to the shape of the distribution.

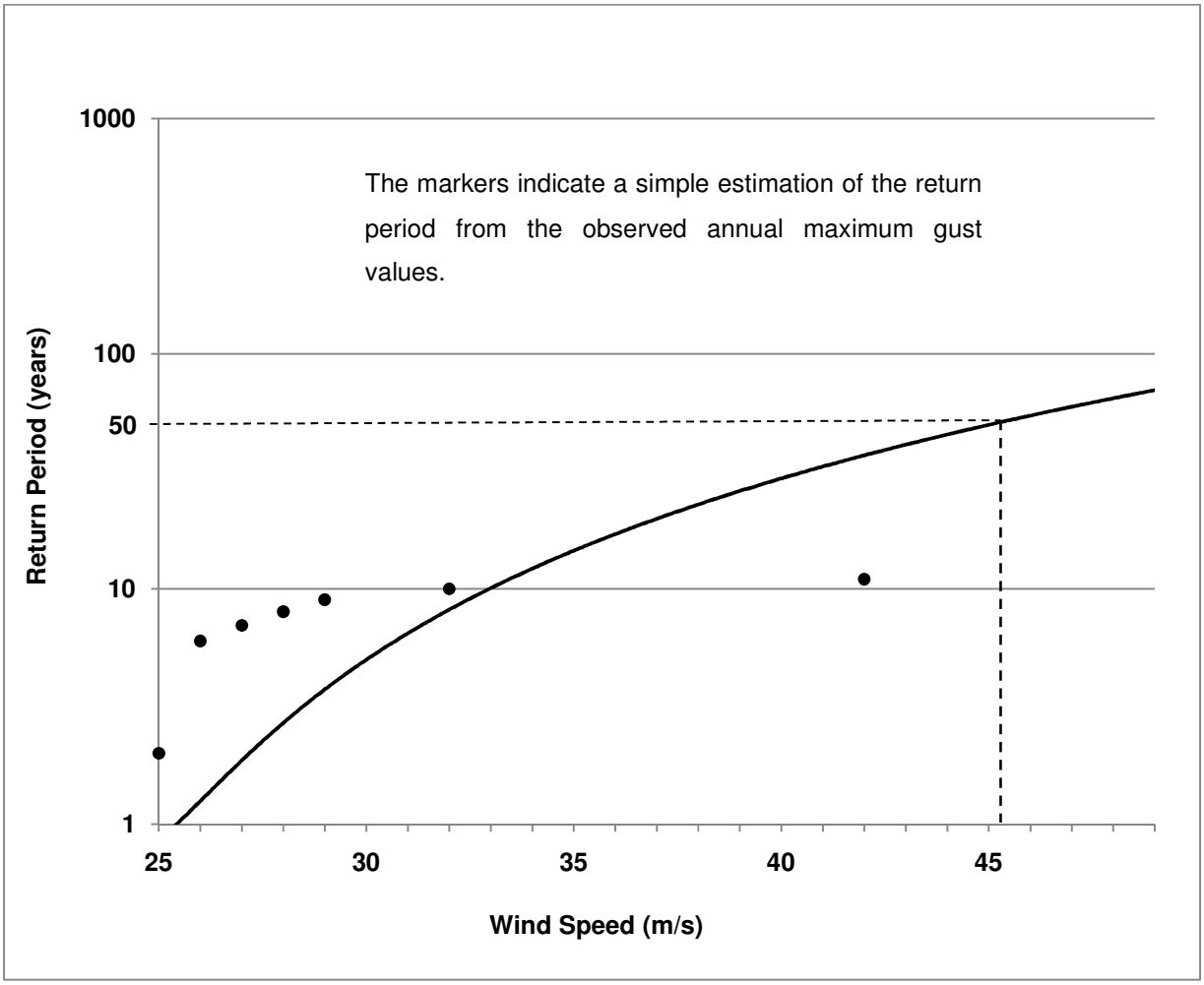

Figure 5.3. GEV Type II estimation of the quantiles for Struisbaai.

Tables 5.3 and 5.4 present the results of the estimations of the annual maximum gusts and annual maximum hourly wind speeds, for the quantiles of the same return periods as those estimated with the Gumbel distribution, presented in Table 5.2. The complete sets of results are included in Tables A.2 and A.3 respectively, in Appendix A.

Table 5.3. Estimations of the quantiles X_T of the annual maximum wind gusts, with return periods T equal to 50, 100 and 500 years, by fitting of the GEV distribution.

Station Number	Station Name	Distribution parameters			Annual maximum wind gust (m/s)		
		κ	α	β	X_{50}	X_{100}	X_{500}
0012661	GEORGE WO	+0,23	2,39	25,26	31,4	32,0	33,2
0021178	CAPE TOWN WO	-0,06	3,25	25,61	39,9	42,8	50,1
0035209	PORT ELIZABETH	-0,13	1,94	29,69	39,6	42,0	48,3
0059572	EAST LONDON WO	-0,09	2,39	26,01	37,3	39,8	46,2
0092081	BEAUFORT-WES	-0,01	2,36	29,59	38,9	40,6	44,5
0127272	UMTATA WO	-0,19	3,08	26,58	44,4	49,2	63,0
0182591	MARGATE	+0,01	1,70	24,16	30,7	31,8	34,5
0239698	PIETERMARITZBURG	-0,05	2,20	19,72	29,2	31,1	35,8
0240808	DURBAN WO	-0,14	2,00	24,62	35,0	37,5	44,4
0261516	BLOEMFONTEIN WO	-0,24	2,01	24,02	37,1	41,0	53,1
0274034	ALEXANDERBAAI	+0,09	1,70	25,75	31,3	32,1	33,7
0290468	KIMBERLEY WO	+0,20	3,07	27,21	35,6	36,5	38,2
0317475	UPINGTON WO	-0,17	2,82	24,90	40,5	44,6	56,1
0476399	JOHANNESBURG	-0,16	2,46	22,70	36,1	39,5	49,1
0508047	MAFIKENG WO	+0,20	2,65	24,20	31,4	32,3	33,8
0513385	IRENE WO	+0,03	2,82	23,11	33,5	35,2	39,0
0677802	PIETERSBURG WO	+0,36	3,43	23,39	30,5	31,1	31,8

5.2.3. Further analysis and discussion of results

From the results presented in Tables 5.3 and 5.4 it is apparent that fitting of the GEV distribution to the available data sets led to the shape parameter, κ, almost as a rule, to be estimated not close to zero. For the whole set of annual maximum gusts in Table A.2, the estimated values for κ range from -0,47 to 1,07; and for the annual maximum hourly mean wind speeds in Table A.3, from -0,35 to 0,55.

Table 5.4. Estimations of the quantiles X_T of the annual maximum hourly mean wind speeds, with return periods T equal to 50, 100 and 500 years, by fitting of the GEV distribution.

Station Number	Station Name	Distribution parameters			Annual maximum hourly wind speed (m/s)		
		κ	α	β	X_{50}	X_{100}	X_{500}
0012661	GEORGE WO	+0,27	2,2	14,6	20,0	20,5	21,3
0021178	CAPE TOWN WO	-0,20	1,4	15,8	23,9	26,1	32,7
0035209	PORT ELIZABETH	-0,11	1,5	18,5	25,8	27,4	31,9
0059572	EAST LONDON WO	+0,45	1,2	15,8	18,1	18,2	18,4
0092081	BEAUFORT-WES	-0,04	2,6	15,7	26,6	28,7	33,9
0127272	UMTATA WO	-0,05	1,6	14,4	21,4	22,8	26,2
0182591	MARGATE	-0,03	0,8	12,0	16,7	17,2	18,5
0239698	PIETERMARITZBURG	-0,03	0,9	7,6	11,3	12,0	13,8
0240808	DURBAN WO	-0,13	1,1	14,6	20,2	21,5	25,1
0261516	BLOEMFONTEIN WO	+0,13	0,9	11,4	14,1	14,5	15,2
0274034	ALEXANDERBAAI	+0,22	1,0	19,1	21,7	22,0	22,5
0290468	KIMBERLEY WO	+0,07	1,0	13,3	16,8	17,3	18,4
0317475	UPINGTON WO	+0,55	1,1	13,9	15,7	15,8	15,9
0476399	JOHANNESBURG	+0,11	1,1	11,7	15,3	15,8	16,8
0508047	MAFIKENG WO	-0,04	1,3	14,2	19,6	20,7	23,3
0513385	IRENE WO	+0,11	1,1	12,4	15,9	16,4	17,4
0677802	PIETERSBURG WO	+0,39	1,3	11,5	14,1	14,2	14,5

Figures 5.4 and 5.5 illustrate the annual extreme wind gusts and annual maximum hourly mean wind speeds estimated with the GEV and Gumbel distributions (section 5.2.1) differ as a function of the value of κ. As can be expected, a negative value of κ corresponds to a quantile value estimated with the GEV distribution to be higher than that estimated with the Gumbel distribution. This is because a negative shape parameter implies a thicker tail of the GEV distribution, compared to the Gumbel distribution.

A positive value of κ corresponds to a quantile value estimated with the GEV distribution to be lower than that estimated with the Gumbel distribution, as a positive shape

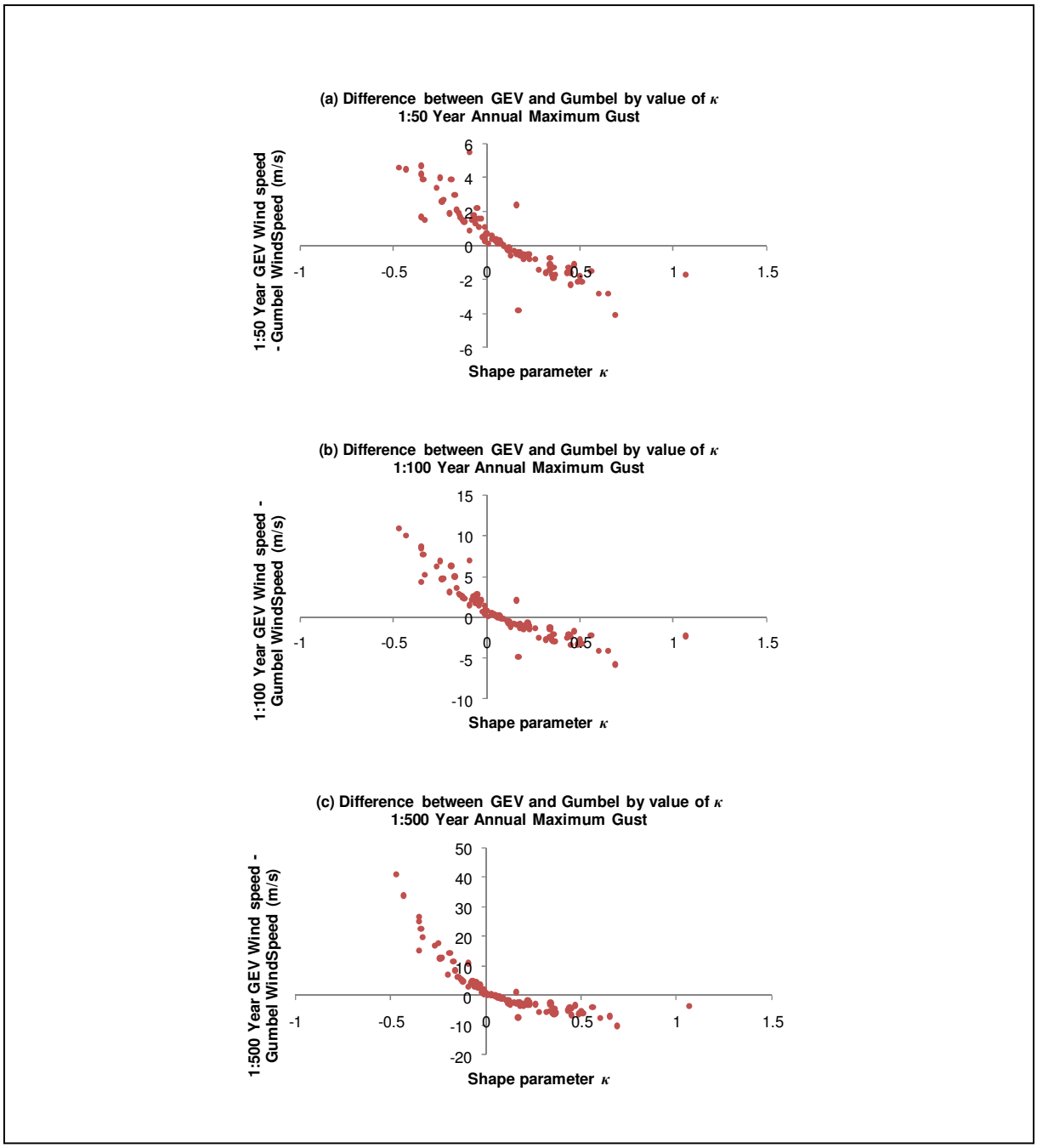

Figure 5.4. Differences between the values of the annual extreme wind gusts estimated with the GEV and Gumbel distributions for (a) 1:50, (b) 1:100 and (c) 1:500 year quantiles, with varying shape parameter κ**.**

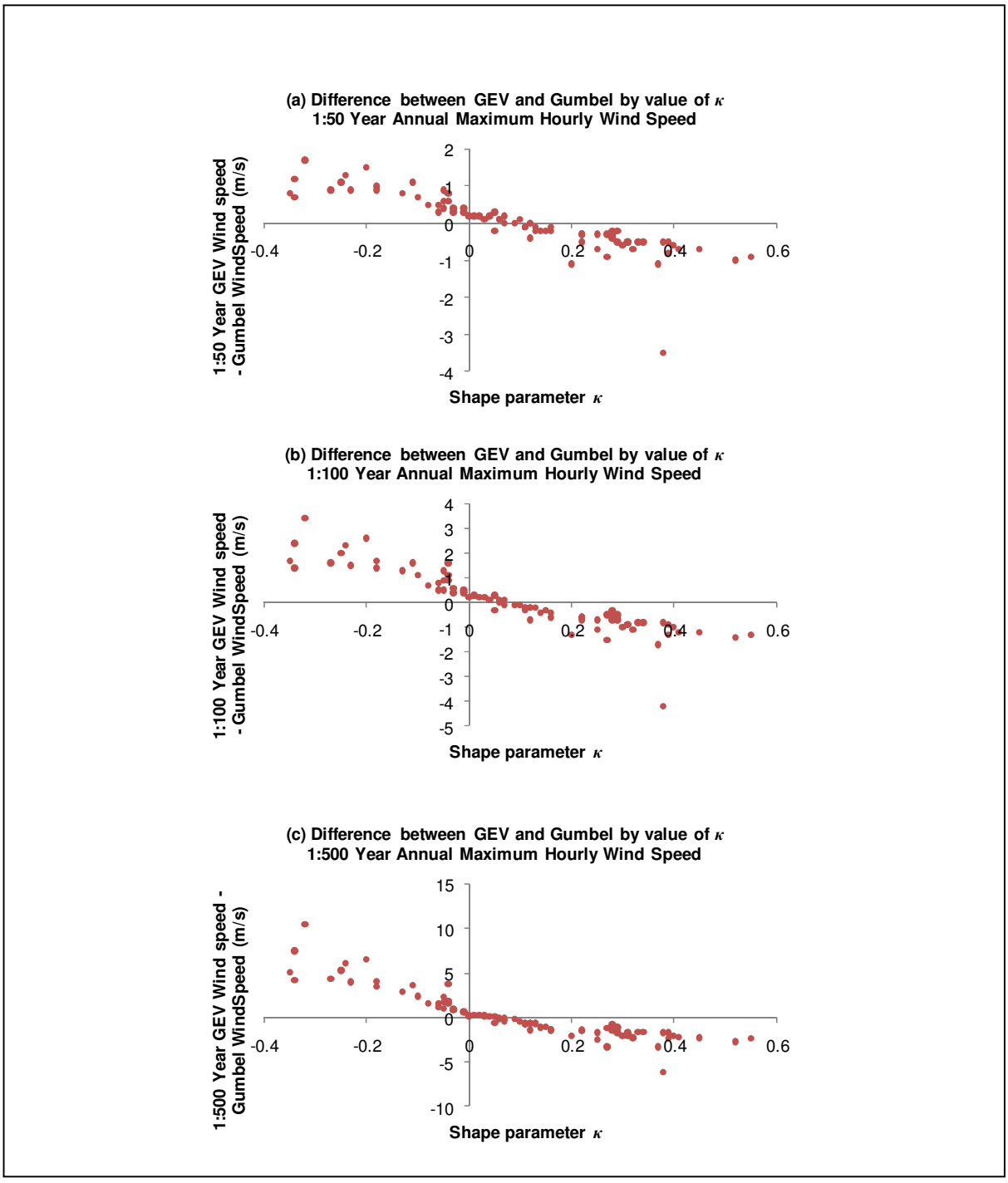

Figure 5.5. Differences between the values of the annual extreme hourly wind speeds estimated with the GEV and Gumbel distributions for (a) 1:50, (b) 1:100 and (c) 1:500 year quantiles, with varying shape parameter κ.

parameter implies that there is an upper bound to the quantile values which are estimated with the GEV distribution. As the deviations of the values of κ from zero become larger, the differences between the values of the quantile values estimated with the GEV distribution and that estimated with the Gumbel distribution also become larger. This is especially true when the quantiles for annual extreme wind gusts are estimated for long return periods, with negative values for κ.

As mentioned before in the literature, the Type II distribution is seldom resolved from a GEV analysis, and might indicate a mixed wind series (Abild *et al.*, 1992; Brabson and Palutikof, 2000; Palutikof *et al.*, 1999). However, the data analysed suggest quite a high percentage of weather stations with annual maximum wind series exhibiting negative values for κ. For the annual maximum wind gusts 39 % of weather stations had negative values for κ, while for annual maximum hourly wind speeds the figure is 32 %. Also, negative κ values were found for weather stations where strong winds are caused by only one strong wind producing mechanism. No link between the sign of κ and the particular strong wind producing mechanisms could be found.

It is argued here that another possible cause for negative values for κ can be anomalous values, where the annual maximum values for one or a few years are much higher than the other values in a particular data set. These values are not regarded as possibly incorrect, as the data values utilised in these analyses have been thoroughly quality controlled. The fitting of a GEV distribution to data series is affected by these values, and can therefore indicate a Type II distribution when it is physically not justifiable – this is particularly relevant to short time series. To take Cape Town (κ = -0,20) as an example, the quantiles are estimated from strong winds measured during the passages of cold fronts. One should therefore assume that the quantile estimations for Cape Town should fall within the range expected from the strongest winds that can be generated by cold fronts, even for long return periods. However, this is not the case as the 1:500 year quantile from the GEV method, for the hourly mean wind speeds shows: The estimated quantile of 32,7 m/s falls in the maximum wind category of the

Beaufort wind scale, an empirical measure to describe wind speed, which indicates hurricane strength winds. However, the Gumbel estimate for the 1:500 year hourly mean wind speed for the same station is 24,6 m/s, which falls into the category for a storm or gale; consistent with wind strengths to be expected during a strong cold front.

Brabson and Palutikof (2000) illustrated the effect of the addition of four very large annual maxima, when the time series for Sumburgh (UK) was extended from a 13 year sample to a 25 year sample. The addition of these values dramatically raised the 100 year quantile value from 45,3 m/s to 56,8 m/s, well outside the standard errors calculated on the basis of the 13-year sample. However, the Gumbel predictions were less affected by the addition of the new data. It is also important to note from that analysis that the extension of the data set caused the difference between the quantile estimations with the GEV and Gumbel to be smaller, than with the shorter time series (0,1 m/s compared to 6,4 m/s). Brabson and Palutikof also showed, using additional weather stations, that the longer the time series utilised, the closer the value for κ is estimated to zero. With additional analyses they concluded that the generalized models, whether GEV or GPD, if brought to rely on 13 years of data, fail to predict the actual maximum gust speeds observed over a longer 25-year period. They attributed this failure largely to the non-stationarity in the wind climate in the region. This has the effect that the extreme values are not evenly distributed in a wind time series – this of course will apply to South Africa, as well, because of the cyclical behaviour of the climate (see Chapter 3).

The median of a data set is robust to outliers or anomalous values, while the average is not. The difference between the median and the average can therefore provide an indication of the magnitude of anomalous values in a data set. Figure 5.6 presents the relationship between κ and the difference between the median and the average, of all the data sets of the annual maximum wind gusts. The graph illustrates the fact that there is a statistically significant correlation between the value of the difference between the median and the average, and the value of κ.

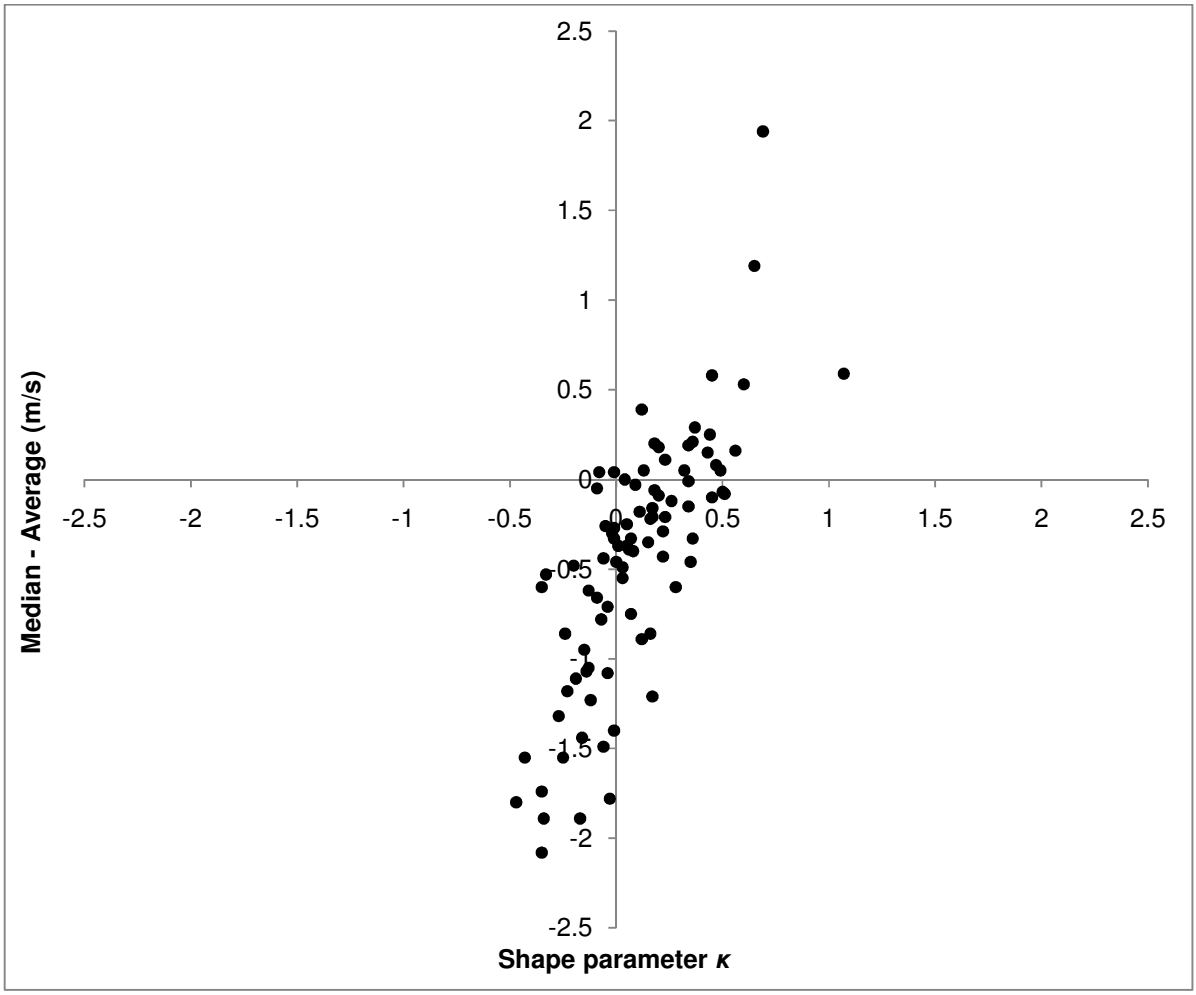

Figure 5.6. The relationship between the difference between the median and average (m/s) and the shape parameter κ, for the GEV distribution fitted to the annual maximum gust data.

An example of how an anomalous value in a data set can make a significant difference in the values of the estimated quantiles, is for the data set for Umtata. The annual maximum gust speed for Umtata for 1999 is a verified 39,3 m/s, which was measured on 3 November 1999. This value is much higher than the mean of the annual maximum gust speeds, which is 27,8 m/s. If, for illustrative purposes, the value of 39,3 m/s is removed from the data set, the 1:50 year quantile for the wind gust becomes 35,6 m/s, compared to the 40,5 m/s with the high value included. It is concluded here, with the analyses presented in this section and those by Brabson and Palutikof (2000), that the

fitting of the GEV distribution to small data sets of annual extreme winds should be treated with caution, and is in general not recommended.

5.3. Methods for short time series

The problems in fitting the GEV distribution will be more pronounced for smaller data sets, such as those utilised in this research, which are all shorter than 20 years. Therefore other approaches to estimate the extreme wind speeds, specifically developed for shorter time series, were investigated to compare the results with those from the traditional methods and, by doing so to identify the most appropriate statistical method to apply to the available wind data sets.

The well known approaches to estimate extreme winds for shorter time series are discussed in Palutikof *et al.* (1999), of which the methodologies are summarised in section 2.3.4. With all of these methods decisions are required which in most cases contain some elements of subjectivity. At the same time, it has to be ensured that wind speed values extracted from the original wind data sets, for fitment to the statistical distributions, should be as independent and identically or evenly distributed as possible (Palutikof *et al.*, 1999).

Regarding the extension of a single extreme value per epoch to include the r-largest values (Weissman, 1978), decisions have to be taken on the size of r, as well as the minimum separation distance or time between extreme values. The separation distance might depend on the type of wind data, whether wind gusts or mean wind speeds over longer periods, as well as the type of strong winds experienced at the location where the wind measurements were taken.

Using the Method of Independent Storms (MIS) a decision has to be taken on the threshold value which separates individual storms. This value should be high enough to ensure that the storms identified are independent and eliminate the possibility of one larger storm which contains a lull in wind speed during the period it occurred. Also,

individual storms might be separated by lulls with wind speeds of different values, complicating the choice of the threshold value.

With the Peak-Over-Threshold (POT) method a decision also has to be taken regarding the threshold value as well as the separation distance, similar to the method that employs the r-largest values. However, if a separation distance is deemed sufficient by taking the prevailing weather systems into account, the threshold value can be inferred or derived without deciding on a specific value beforehand. The POT approach is the most widely used method to estimate extreme winds from short wind data time series and, due to the above considerations, it was decided to apply this method to the available wind data sets.

5.3.1. Application of peak-over-threshold (POT) method

With POT methods, all values exceeding a specific threshold are used for analysis, providing that the threshold value ensures a sufficient separation time between selected strong winds to avoid the interdependence of values. A separation time of 48 hours was selected by various authors for European wind climates (Cook, 1985; Gusella, 1991). The European wind climate is dominated by synoptic-scale strong-wind producing mechanisms, especially the passages of extratropical cyclones. In South Africa the situation is similar for hourly mean wind speeds and gusts in many regions, and therefore this separation time was deemed to be appropriate. However, in a large part of the country, most strong wind gusts are produced by thunderstorms in which individual systems can easily be separated by a period of one day only. Therefore, in the analysis of hourly mean wind speeds, the separation time was strictly deemed to be 48 hours, while for wind gusts, more flexibility was allowed by taking the particular strong-wind mechanism and synoptic conditions into account.

To obtain a sufficient number of strong wind data values, one must accept that not all of the data values will be independent. In this regard the finding by Brabson and Palutikof (2000) was taken into account, in which the value of the independent event index, ε,

defined in equation 2.26, can be as low as 0,8 to obtain accurate quantile estimates from the GPD.

In analysing the wind data, a range of threshold values were selected in 2,5 m/s increments. The data sets extracted according to these thresholds were then checked to identify the data set with the largest number of wind speed values and a value of ε that is at least 0,8. The GPD was then fitted to the selected series of values, contained in the Data Appendix. Unfortunately the POT method did not seem to be compatible with hourly mean wind speed data, with too high percentages of values, even with very high thresholds, showing dependency. This method could therefore not be applied to the hourly mean wind speeds. Table 5.5 presents the quantiles X_T of the annual maximum wind gusts, for return periods T equal to 50, 100 and 500 years, for the weather stations in Table 5.2, by application of the POT method. The results for the whole set of stations are included in Table A.4. The number of values n that could be selected varies widely between stations, with λ (the average number of values per year) ranging from 1,50 to 19,20. A high value for λ indicates a better separation of individual storms than when λ is low, because a larger number of independent strong wind values could be utilized. A low value of λ indicates that the strong winds tend to be clustered in the time series. It is, therefore, not surprising that the weather stations in those regions in the interior where thunderstorms are likely to occur frequently, exhibit in general higher λ values than those closer to the coast, where synoptic scale systems tend to cause most strong winds. The advantage of the POT method above methods which employ only one value per epoch, is that usually significantly more values can be utilised, which will in turn result in more confident estimates of the extreme wind quantiles. On the other hand it can be argued that a very large number of values can dilute the effect of the more extreme values in the data. However, it is assumed here that in general greater confidence can be given to quantiles estimated with values of λ much larger than 1, compared to a situation when only one value per epoch is utilized, as long as the values are independent and therefore Poisson distributed.

Table 5.5. Estimations of the quantiles X_T of the annual maximum wind gusts, with return periods T equal to 50, 100 and 500 years, by application of the POT method.

Station Number	Station Name	Distribution parameters					Annual maximum wind gust (m/s)		
		κ	α	t	n	λ	X_{50}	X_{100}	X_{500}
0012661	GEORGE WO	+0,19	2,7	22,4	62	3,88	31,3	32,0	33,2
0021178	CAPE TOWN WO	-0,19	2,2	24,8	49	3,06	42,7	46,8	58,4
0035209	PORT ELIZABETH	+0,21	2,8	25,1	193	12,06	35,2	35,7	36,6
0059572	EAST LONDON WO	+0,12	2,6	20,2	167	15,18	32,3	33,1	34,7
0092081	BEAUFORT-WES	+0,10	3,0	24,9	83	5,53	38,0	39,2	41,6
0127272	UMTATA WO	+0,03	3,2	20,0	103	10,30	38,3	40,1	44,2
0182591	MARGATE	0,10	2,4	20,1	125	8,33	30,8	31,7	33,5
0239698	PIETERMARITZBURG	0,04	2,6	15,0	118	8,43	28,8	30,1	33,2
0240808	DURBAN WO	-0,05	2,0	20,0	151	9,44	34,3	36,2	40,8
0261516	BLOEMFONTEIN WO	0,03	2,8	20,1	112	8,00	35,1	36,6	40,0
0274034	ALEXANDERBAAI	0,11	1,7	22,6	138	9,86	30,3	30,9	32,0
0290468	KIMBERLEY WO	0,00	2,9	20,0	158	11,29	38,0	40,0	44,5
0317475	UPINGTON WO	0,02	2,6	20,1	140	10,00	35,1	36,7	40,2
0476399	JOHANNESBURG	-0,05	2,2	17,8	158	11,29	34,3	36,4	41,7
0508047	MAFIKENG WO	-0,04	1,9	20,3	97	8,08	33,3	35,0	39,2
0513385	IRENE WO	0,11	2,8	17,5	188	13,43	30,7	31,7	33,6
0677802	PIETERSBURG WO	0,19	3,7	17,4	117	9,00	30,7	31,4	32,9

κ and α are the distribution parameters, while t refers to the threshold value, as determined by the software.

5.3.2. Fitting of the exponential distribution

When the POT method is applied with the GPD, one of the parameters to be estimated is the shape parameter κ, similar to the GEV distribution. However, it was shown with the results of the fitting of the GEV distribution to a small number of data values, that κ can then be under- or overestimated. In fact, Brabson and Palutikof (2000) show in their analyses that the value of κ varies with a varying threshold value. From Table 5.5 it can be seen that the number of data values available for POT analysis, and the threshold values deemed most appropriate, vary substantially between the weather stations. In

this section we fit the same data sets to which the GPD was fitted to the Exponential (EXP) distribution, i.e. the GPD with κ = 0. Table 5.6 presents the results of the analyses, also with estimations of the quantiles X_T, with return periods T equal to 50, 100 and 500 years, for the same weather stations as in Table 5.2. The full set of results is included in Table A.5 in Appendix A.

Table 5.6. Estimations of the quantiles X_T of the annual maximum wind gusts, with return periods T equal to 50, 100 and 500 years, by application of the EXP method.

Station Number	Station Name	Distribution parameters				Annual maximum wind gust (m/s)		
		α	t	n	λ	X_{50}	X_{100}	X_{500}
0012661	GEORGE WO	2,0	22,6	62	3,88	33,3	34,7	38,0
0021178	CAPE TOWN WO	2,3	25,2	49	3,06	36,7	38,2	41,9
0035209	PORT ELIZABETH	2,4	25,1	193	12,06	40,4	42,1	45,9
0059572	EAST LONDON WO	2,4	20,1	167	15,18	36,1	37,8	41,7
0092081	BEAUFORT-WES	2,5	25,1	83	5,53	39,0	40,7	44,7
0127272	UMTATA WO	3,0	20,1	103	10,30	39,0	41,1	46,0
0182591	MARGATE	2,2	20,1	125	8,33	33,3	34,8	38,3
0239698	PIETERMARITZBURG	2,3	15,1	118	8,43	29,1	30,8	34,5
0240808	DURBAN WO	2,0	20,1	151	9,44	32,6	34,0	37,3
0261516	BLOEMFONTEIN WO	2,7	20,1	112	8,00	36,3	38,2	42,5
0274034	ALEXANDERBAAI	1,5	22,6	138	9,86	32,1	33,2	35,7
0290468	KIMBERLEY WO	2,8	20,1	158	11,29	37,7	39,6	44,1
0317475	UPINGTON WO	2,6	20,1	140	10,00	36,0	37,8	41,9
0476399	JOHANNESBURG	2,5	17,6	158	11,29	33,4	35,1	39,2
0508047	MAFIKENG WO	2,2	20,1	97	8,08	33,0	34,5	38,0
0513385	IRENE WO	2,5	17,6	188	13,43	33,6	35,3	39,3
0677802	PIETERSBURG WO	2,9	17,6	117	9,00	35,0	37,0	41,6

α indicates the distribution parameter, while t refers to the threshold value, as determined by the software.

5.3.3. Further analysis and discussion of results

As with the comparison between the results of the Gumbel and GEV methods, it can be seen that the estimated quantiles are sensitive to the value of κ, which confirms the finding of Simiu and Heckert (1996). The general result is that with the GPD method, positive values of κ renders quantile values lower, while negative values of κ renders quantile values higher, than that estimated with the EXP method. Figure 5.7 illustrates how the difference between annual extreme wind gusts estimated with the GPD and EXP distributions differ, with the estimated value of κ. The trends which can be observed are similar to those in the analysis which was presented in Figure 5.4. Because the GPD method is more flexible than the EXP method, the GPD distribution should fit the data better than the EXP distribution, as demonstrated by Brabson and Palutikof (2000). However, it was also illustrated by these authors that the downside of this flexibility is that estimated values of κ which are highly positive, strongly truncate the tail of the distribution causing a low bound at the upper end. Unlikely low extreme quantile values are then predicted. On the other hand, highly negative estimations of κ predict extreme speeds that are unrealistically strong for the longer return periods. The same argument than that developed in section 5.2.3 applies here, that short time series tend to render unrealistic values for κ. See also the discussion in section 5.4.1, which compares the values of κ_{GPD} and κ_{GEV}., as well as the relationship between λ and κ_{GPD}.

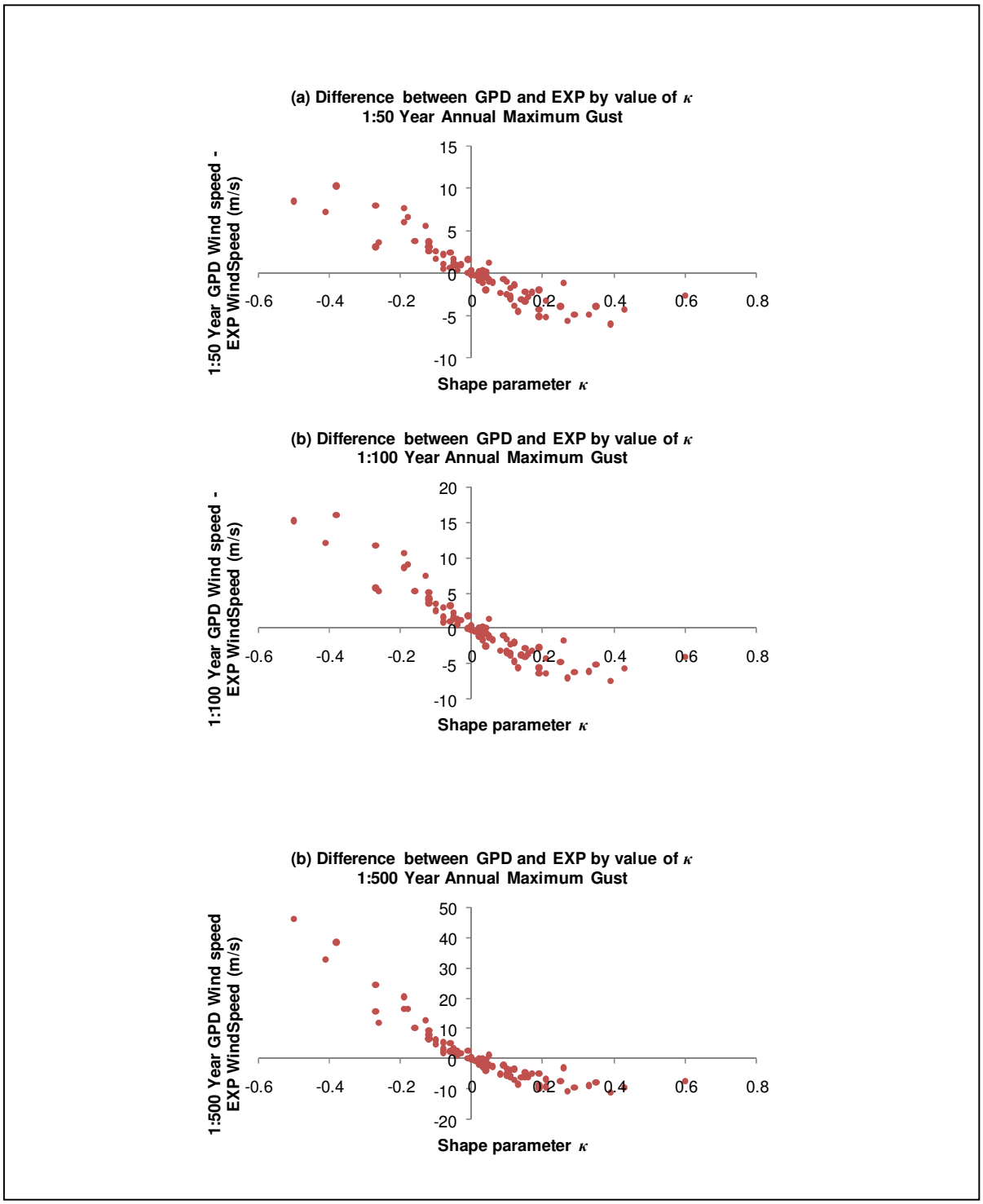

Figure 5.7. Differences between the values of the annual extreme wind gusts estimated with the GPD and EXP distributions for (a) 50, (b) 100 and (c) 500 year quantiles, with varying shape parameter κ.

5.4. Comparison of the annual maxima and POT methods

5.4.1. The κ parameter

If the gust speed extremes are well described by a single GPD distribution, then κ_{GPD} (κ estimated with the GPD) should equal κ_{GEV} (κ estimated with the GEV), or approach this value with increase in the threshold value (Brabson and Pautikof, 2000). However, this can of course only be true if the estimations for κ_{GPD} and κ_{GEV} are realistic, which may ultimately depend on the size of the data sets utilised to estimate the distribution parameters with. Figure 5.8 presents a scatterplot comparison between κ_{GPD} and κ_{GEV} for the weather stations utilised in the research. One can see that there is no apparent relationship between the two parameters. This can be due to either the inaccurate estimations of κ_{GPD} or κ_{GEV}, or both.

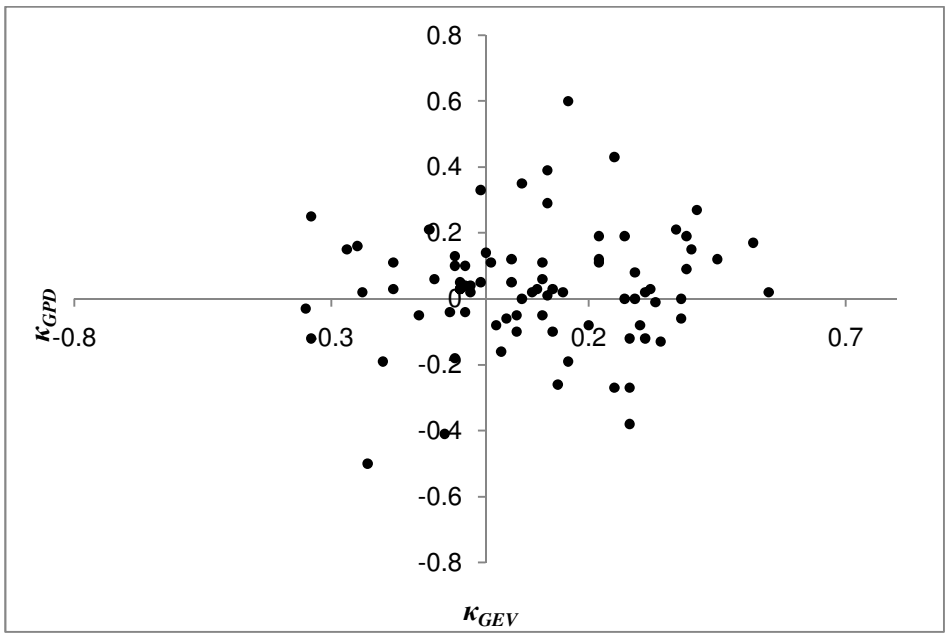

Figure 5.8. Comparison between κ_{GPD} and κ_{GEV}, as estimated for all the data sets utilised in the study.

From the above discussion it is becoming apparent that the value of the shape parameter should be treated with suspicion when generalized distributions are applied to short time series. However, the sizes of the data sets utilised in the application of the GPD distribution vary a lot between weather stations, with λ ranging from 1,5 to 19,2, with a median value of 7. It is assumed that the larger the data set utilised, the more accurate the estimated distribution parameters. Figure 5.9 presents the relationship between κ_{GPD} and λ. It is apparent that the values for κ_{GPD} tend to be clustered around zero; in fact, the average for the values is 0,05. Another observation is that the values for κ_{GPD} show lower variability for the upper half of the data pairs where λ > 7, compared to where λ < 7. The standard deviation for the values of κ_{GPD} where λ > 7 is equal to 0,12, while for κ_{GPD} where λ < 7 the standard deviation is equal to 0,22; the difference of which is statistically significant.

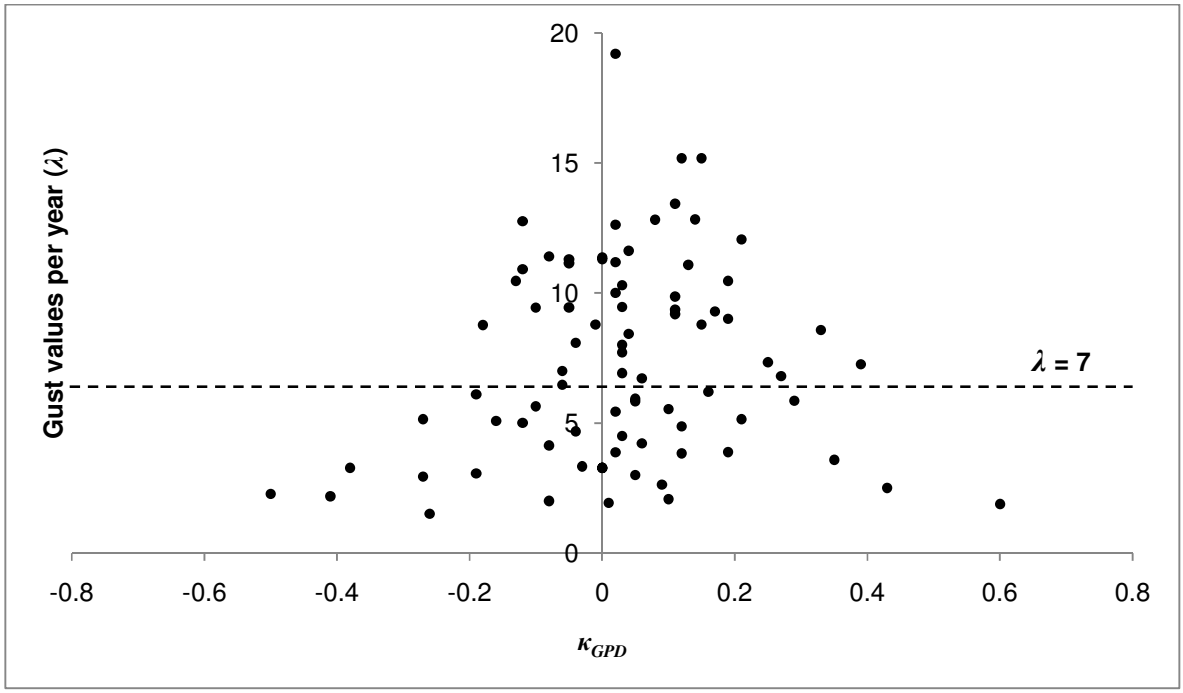

Figure 5.9. The relationship between the shape parameter κ_{GPD} and λ as presented in Table A.4.

From the above, and results elsewhere in the chapter, it follows then that it can be assumed that, with the available data for this study, the safest estimation for the value of κ is zero. This is consistent with Brabson and Palutikof (2000) who, after analysing shorter and longer periods of data for the same location, came to the conclusion that the $\kappa = 0$ versions of the models make more accurate predictions of extreme wind speeds, even when a shorter period of data is utilised (in their case 13 years).

Abild *et al.* (1992) came to a similar conclusion, namely that, while the GPD and GEV distributions are powerful in detecting outliers, and a possible two-component population in exponential data, the tail behaviour is strongly influenced by the estimation of κ, and will therefore not provide reliable estimates of upper quantiles when fitted to a short record. Put in another way, the poor behaviour of κ is indicative of the insufficiency of the short time series.

5.4.2. Gumbel and exponential distributions

The Gumbel and the EXP distributions are restrictive forms of the GEV and GPD distributions respectively, having less flexibility as κ is assumed to be zero. It was concluded in the previous section that, while the GEV and GPD distributions provide a better fit to the data, they do not necessarily make accurate predictions of high wind speeds, when based on a short period of data, or a small average number of data values per year. Figure 5.10 presents the relationship between X_{100} estimated by the Gumbel and EXP methods, with the correlation statistically significant at the 95% level of confidence. There is a general tendency for X_{100} to be estimated higher by the EXP method than with the Gumbel method, when X_{100} is estimated by the Gumbel method to be below about 38 m/s. This observation applies to about 82% of the X_{100} Gumbel estimates.

The question arises now which estimates, by the Gumbel or EXP method, can be considered to be the most reliable. Abild *et al.* (1992) suggests that T-year estimates

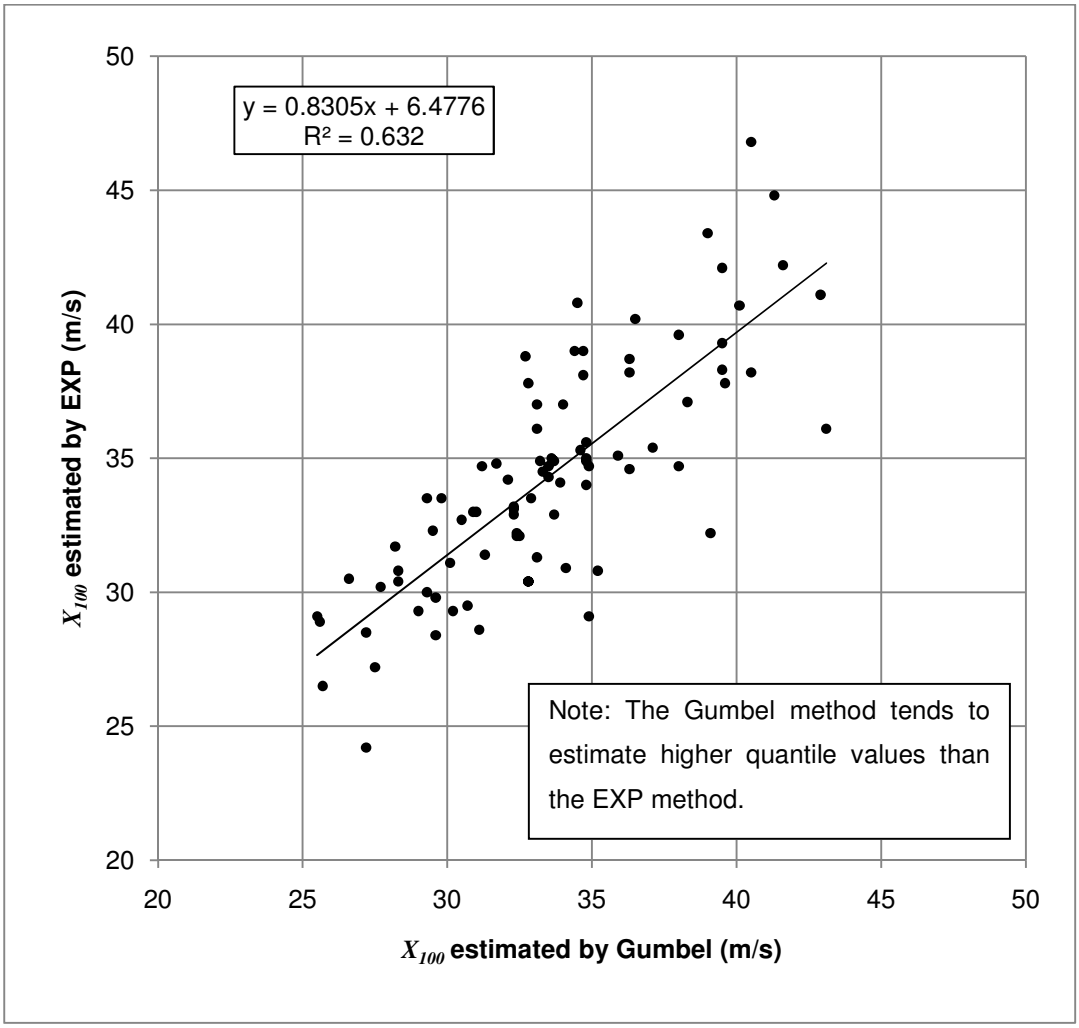

Figure 5.10. The correlation between estimations of X_{100} by the Gumbel and EXP methods.

should never be given only as point estimates but at least also contain some information regarding the uncertainty of the estimate related to the statistical model chosen. Brabson and Palutikof (2000) state that critical to the usefulness of maximum gust speed predictions are their associated standard errors. Calculation procedures for the standard errors of the T-year estimates are described by Hosking *et al.* (1985) and Abild *et al.* (1992). The derivations of the equations for the calculations of the standard deviations or variances will not be repeated here, but for the Gumbel distribution

(5.1)

and for the EXP distribution

$$Var\left[\hat{X}_T\right] \cong (\alpha^2/n)\{1 + [\ln(\lambda T)]^2\} \quad (5.2)$$

where α is the scale or dispersion parameter, n is the number of wind speed values utilised (in the case of the Gumbel distribution the number of years), T is the return period, and λ is the cross-over rate per year in the case of the POT. It follows then that the standard errors of the quantiles for a specific return period, which express the precision of the estimates of the quantiles, essentially depend on the variability of the wind speed values of the sample, and the number of values in the sample. Table 5.7 presents the standard deviations S_{50}, S_{100} and S_{500} associated with the estimated annual maximum wind gust quantiles X_{50}, X_{100}, and X_{500} by the Gumbel and EXP distributions, as presented in Tables 5.2 and 5.6 respectively.

Table 5.7. The standard deviations S_{50}, S_{100} and S_{500} associated with the estimated quantiles X_{50}, X_{100}, and X_{500} by the Gumbel and EXP methods.

Station Number	Station Name	Gumbel			EXP		
		S_{50}	S_{100}	S_{500}	S_{50}	S_{100}	S_{500}
0012661	GEORGE WO	1,6	1,8	2,4	1,4	1,6	2,0
0021178	CAPE TOWN WO	2,8	3,2	4,2	1,7	1,9	2,4
0035209	PORT ELIZABETH	1,8	2,1	2,8	1,1	1,2	1,5
0059572	EAST LONDON WO	2,1	2,4	3,2	1,3	1,4	1,7
0092081	BEAUFORT-WES	2,1	2,4	3,1	1,5	1,7	2,2
0127272	UMTATA WO	3,8	4,3	5,7	1,9	2,1	2,6
0182591	MARGATE	1,5	1,8	2,3	1,2	1,3	1,6
0239698	PIETERMARITZBURG	1,8	2,1	2,7	1,3	1,5	1,8
0240808	DURBAN WO	1,9	2,2	2,9	1,0	1,1	1,4
0261516	BLOEMFONTEIN WO	2,4	2,8	3,7	1,6	1,7	2,1
0274034	ALEXANDERBAAI	1,3	1,5	2,0	0,8	0,9	1,1
0290468	KIMBERLEY WO	2,3	2,6	3,4	1,4	1,6	1,9
0317475	UPINGTON WO	2,9	3,3	4,4	1,4	1,5	1,9
0476399	JOHANNESBURG	2,6	3,0	3,9	1,3	1,4	1,7
0508047	MAFIKENG WO	2,0	2,3	3,0	1,3	1,5	1,8
0513385	IRENE WO	2,4	2,7	3,5	1,2	1,3	1,6
0677802	PIETERSBURG WO	2,3	2,7	3,5	1,6	1,8	2,2

The full set of results is included in Table B.1 in Appendix B, from which it is shown that only seven of the 91 weather stations, i.e. Hermanus, Plettenbergbaai, Paarl, Lambertsbaai, Queenstown, Brandvlei and Bethlehem, indicate standard errors of the Gumbel method to be smaller than that of the EXP method. For all these stations α was estimated larger for the EXP distribution than for the Gumbel distribution which, referring to equations 5.1 and 5.2, caused the larger values. However, one can conclude that in general more confidence can be put on the quantile values estimated by the EXP method than by the Gumbel method.

5.5. Mixed strong wind climates

As previously mentioned, in the application of the GEV and GPD methods, the estimation of a negative value for the shape parameter κ is often seen as an indication of a mixed strong wind climate, i.e. the data set contains values from two or even more populations, i.e. types of events. While these methods are powerful in detecting outliers or a possible two (or more)-component population in exponential data, they will not provide reliable estimates of upper quantiles when fitted to a short record (Abild *et al.*, 1992). Twisdale and Vickery (1992), in their analysis of the wind speed data of four weather stations, came to the conclusion that places where thunderstorms dominate the extreme wind climatology, the traditional approach by the Gumbel or POT methods will tend to underestimate the design wind speeds. These methods assume that all of the winds used to describe the probability distribution of wind speed are produced by the same phenomena, such as large-scale extratropical storms. However, this is not always the case, especially for the 2-3 second wind gusts, as in the greater part of the interior of South Africa thunderstorms tend to dominate the strong wind climate (see Chapter 4). Therefore, for such data sets extreme wind estimation methodologies should be explored that explicitly take the mixed strong wind climatology into account.

5.5.1. Application of a mixed distribution method

The optimum application or fitting of the mixed speed distribution, described by Gomes and Vickery (1978), is discussed in section 2.3.3. This method requires preferably the identification of all strong wind producing mechanisms, which will probably be the cause of the occurrence of an annual extreme wind at a specific station. Gomes and Vickery (1978) disaggregated four extreme wind generating mechanisms, i.e. extratropical low-pressure systems, thunderstorms, hurricanes and tornadoes, while Twisdale and Vickery (1992) distinguished between two mechanisms, i.e. extratropical low-pressure systems and thunderstorms.

In this study the causes of each of the annual maximum wind gusts and annual maximum hourly mean wind speeds were identified for the individual weather stations. The methodology to identify the causes is discussed in section 4.2 for wind gusts, but it has been expanded, in the current section, to hourly mean wind speeds as well. To be noted, the thunderstorms were not considered to be a possible cause of high hourly mean wind speeds, due to their strong winds of usual short duration. Strong winds during a thunderstorm are usually shorter than 10 minutes; therefore only the underlying synoptic-scale situation was taken into account. The descriptions of the different strong wind mechanisms are presented in section 4.3. The identified causes for each weather station were then considered to be the main strong wind producing mechanisms at a particular station. The results are presented in Table 5.8 for both the annual maximum wind gusts and the annual maximum hourly mean wind speeds. The full list of results is presented in Table A.6 in Appendix A. The disaggregations of the strong wind sources, in the synoptic scale, in the current research are more detailed than in both of the examples of Gomes and Vickery (1978) and Twisdale and Vickery (1992). This approach may improve the accuracy of the extreme wind estimations, and additional information can also be gained from the extreme wind analyses, such as the most likely causes, directions, and the time of year of extreme wind estimations for specific return periods. For the annual extreme wind gusts 86% of the weather stations exhibited a mixed strong wind climate by application of the disaggregation procedure (also see

section 4.3 and Table 4.2), while for the annual extreme hourly mean wind speeds the fraction is much lower at 57%.

Table 5.8. The identified sources of the annual maximum wind gusts and the annual maximum hourly mean wind speeds.

Station Number	Station Name	Annual maximum wind gusts						Annual maximum hourly mean wind speeds				
		TS	CF	R	T	LP	TW	CF	R	T	LP	TW
0003108	STRUISBAAI		•					•	•			
0005609	STRAND		•	•				•	•			
0006386	HERMANUS		•					•	•			
0007699	TYGERHOEK		•					•				
0010682	STILBAAI		•					•				
0012661	GEORGE WO		•					•				
0014123	KNYSNA		•					•				
0014545	PLETTENBERGBAAI		•					•			•	
0015692	TSITSIKAMMA		•					•				
0020618	ROBBENEILAND		•	•				•	•			
0021178	CAPE TOWN WO		•	•				•	•			
0021823	PAARL		•	•				•				
0022729	WORCESTER-AWS		•					•				
0031650	JOUBERTINA AWS	•	•			•		•			•	
0033556	PATENSIE	•	•			•		•	•		•	
0034763	UITENHAGE	•	•					•				
0035209	PORT ELIZABETH		•					•				
0040192	GEELBEK		•	•				•	•			
0041388	MALMESBURY		•	•				•	•			
0041841	PORTERVILLE		•	•		•		•	•		•	
0045642	LAINGSBURG		•			•		•				
0056917	GRAHAMSTOWN	•	•					•				
0059572	EAST LONDON WO		•					•				
0061298	LANGEBAANWEG		•	•				•	•			

Station Number	Station Name	Annual maximum wind gusts						Annual maximum hourly mean wind speeds				
		TS	CF	R	T	LP	TW	CF	R	T	LP	TW
0063807	EXCELSIOR CERES		•					•	•			
0078227	FORT BEAUFORT	•	•					•				
0083572	LAMBERTSBAAI		•			•		•	•			
0092081	BEAUFORT-WES	•	•			•		•				
0096072	GRAAFF - REINET	•	•			•		•			•	
0123685	QUEENSTOWN	•	•					•				
0127272	UMTATA WO	•	•					•				
0134479	CALVINIA WO		•			•		•			•	
0144791	NOUPOORT	•	•			•			•		•	
0148517	JAMESTOWN	•	•					•				
0150620	ELLIOT	•	•					•				
0155394	PORT EDWARD		•					•				
0169880	DE AAR WO	•			•			•		•		
0182465	PADDOCK	•	•			•		•			•	
0182591	MARGATE		•					•				
0184491	KOINGNAAS		•	•		•			•		•	
0190868	BRANDVLEI	•			•			•			•	
0214700	SPRINGBOK WO	•	•			•		•				•
0224400	PRIESKA	•	•		•			•		•		
0239698	PIETERMARITZBURG	•	•			•		•			•	
0239699	ORIBI AIRPORT	•	•			•		•			•	
0240808	DURBAN WO		•					•				
0241072	MT EDGECOMBE		•					•	•			
0241076	VIRGINIA		•					•	•			
0261307	BLOEMFONTEIN	•						•		•		
0261516	BLOEMFONTEIN WO	•						•		•		
0268016	GIANTS CASTLE		•					•				
0270155	GREYTOWN	•	•					•				
0274034	ALEXANDERBAAI		•				•					•

Station Number	Station Name	Annual maximum wind gusts						Annual maximum hourly mean wind speeds				
		TS	CF	R	T	LP	TW	CF	R	T	LP	TW
0290468	KIMBERLEY WO	•						•		•		
0300454	LADYSMITH	•	•					•				
0304357	MTUNZINI	•	•					•				
0317475	UPINGTON WO	•						•		•		
0321110	POSTMASBURG	•						•		•		
0331585	BETHLEHEM WO	•	•	•				•	•			
0333682	VAN REENEN	•	•					•				
0337738	ULUNDI	•	•					•				
0339732	CHARTERS CREEK	•	•	•				•	•			
0356880	KATHU	•						•		•		
0360453	TAUNG	•						•		•		
0362189	BLOEMHOF	•	•					•				
0364300	WELKOM	•	•					•		•		
0365398	KROONSTAD	•	•					•		•		
0370856	NEWCASTLE	•	•					•				
0410175	PONGOLA	•	•					•				
0427083	VAN ZYLSRUS	•				•		•		•		
0438784	VEREENIGING	•	•					•		•		
0441416	STANDERTON	•	•	•				•		•		
0472278	LICHTENBURG	•			•			•				
0475879	JHB BOT TUINE	•	•					•	•			
0476399	JOHANNESBURG	•	•					•	•			
0479870	ERMELO WO	•	•			•		•				
0508047	MAFIKENG WO	•			•				•			
0511399	RUSTENBURG	•			•			•				
0513346	PRETORIA UNISA	•	•	•	•				•			
0513385	IRENE WO	•	•	•				•	•			
0515320	WITBANK	•	•					•				
0520691	KOMATIDRAAI	•						•				

Station Number	Station Name	Annual maximum wind gusts						Annual maximum hourly mean wind speeds				
		TS	CF	R	T	LP	TW	CF	R	T	LP	TW
0548375	PILANESBERG	•	•		•				•			
0554816	LYDENBURG	•	•	•				•	•			
0587725	THABAZIMBI	•		•				•	•			
0594626	GRASKOP AWS	•	•					•				
0633882	POTGIETERSRUS	•				•		•	•			
0638081	HOEDSPRUIT	•		•					•			
0674341	ELLISRAS	•	•			•		•	•			
0675666	MARKEN	•		•					•			
0677802	PIETERSBURG WO	•						•	•			
0723664	THOHOYANDOU WO	•	•			•		•	•			

Columns indicate winds caused by TS: Thunderstorms, CF: Cold fronts, R: Ridging, T: Trough to the west with strong ridging from the east, LP: Isolated low-pressure systems, and TW: Trough on the West Coast.

After the identification of the strong wind mechanisms involved at each weather station, the strongest wind gusts and hourly mean wind speeds were determined which were caused by each of the identified mechanisms, for each year of available data. An example of the results of this procedure is presented in Table 5.9, for the weather station at Robben Island. Here the annual maximum wind gusts, as well as the annual maximum hourly winds, are caused by two mechanisms, namely the passage of cold fronts and the ridging of the Atlantic Ocean high-pressure system. The maximum wind gust values and hourly mean wind speeds produced by each of the mechanisms are also given.

The method to estimate quantiles from the data in Table 5.9 is discussed in section 2.3. For both the wind gusts and the hourly mean wind speeds, assuming that the values are Gumbel distributed, the combined distribution of these events is, from equation 2.13

$$F(x) = 1 - \left[1 - e^{-e^{-y_{CF}}} + 1 - e^{-e^{-y_R}}\right] \tag{5.3}$$

where y_{CF} and y_R are the reduced variates for the data sets for the cold fronts and ridging respectively.

Table 5.9. The maximum wind gust values and hourly wind speeds produced by the passage of cold fronts and the ridging of the Atlantic Ocean high-pressure system at Robben Island, for 1992-2008.

Year	Annual maximum wind gust (m/s)		Annual maximum hourly mean wind speed (m/s)	
	Cold Front	Ridging	Cold Front	Ridging
1994	27,3	21,6	12,9	11,9
1995	22,5	22,7	11,6	12,1
1996	21,4	20,8	11,6	13,3
1997	23,2	22,6	12,9	11,6
1998	19,9	20,0	9,6	11,9
1999	18,2	22,3	11,0	12,1
2000	20,9	21,7	10,8	13,1
2001	24,4	22,0	12,9	11,0
2002	21,5	20,6	12,2	12,4
2003	20,2	21,8	11,4	11,3
2004	16,4	20,2	8,3	11,6
2005	24,3	21,6	11,9	10,8
2006	18,4	23,5	10,8	11,9
2007	26,3	20,4	14,1	13,3
2008	24,0	25,4	10,7	14,5

Therefore,

$$e^{(-1/T)} = \{e^{-e^{-[(V_R-\alpha_{CF})/\beta_{CF}]}}\} * \{e^{-e^{-[(V_R-\alpha_R)/\beta_R]}}\} \quad (5.4)$$

where T is the return period, α_{CF} and β_{CF} are the dispersion and the mode parameters of the cold front values, α_R and β_R are the dispersion and the mode parameters of the values associated with ridging, and V_R is the wind speed associated with the return period T. The return period estimations for a specific wind speed could then be determined by

$$T = 1/\{e^{[(\alpha_{CF}-V_R)/\beta_{CF}]} + e^{[(\alpha_R-V_R)/\beta_R]}\} \quad (5.5)$$

Figure 5.11 presents the quantile estimates for the annual maximum wind gusts as well as the annual maximum hourly mean wind speeds, by the method for mixed strong wind climates and the Gumbel method. Also shown are the quantile estimates where the Gumbel method has been applied to the data sets for cold fronts and ridging, presented in Table 5.9. One can see that the distribution patterns are similar for extreme wind gusts and hourly mean wind speeds. One may also assume that from a return period of about 50 years for the wind gusts, and 100 years for the hourly mean wind speeds, the annual extreme winds will probably be caused by the passage of cold fronts, of which the strongest usually occur during the winter months. The wind directions of these winds are usually north-westerly.

An example of a weather station where thunderstorms are one of the main causes of extreme wind gusts is Jamestown in the Eastern Cape Province. Figure 5.12 presents the annual maximum wind gust distribution for this weather station, from which one notices large difference between the quantile estimates by the mixed climate method and the conventional Gumbel method.

This procedure to estimate quantiles with the mixed distribution method was undertaken for all weather stations, where more than one strong wind producing mechanism could be identified. Table 5.10 presents the values for the quantiles X_{50}, X_{100}, and X_{500}, as estimated by the mixed distribution method, for both annual maximum wind gusts and mean hourly wind speeds, for the weather stations listed in Table 5.2 which exhibit a mixed strong wind climate (cells are empty where a single mechanism applies). The full set of results for all the weather stations is presented in Table A.6 in Appendix A.

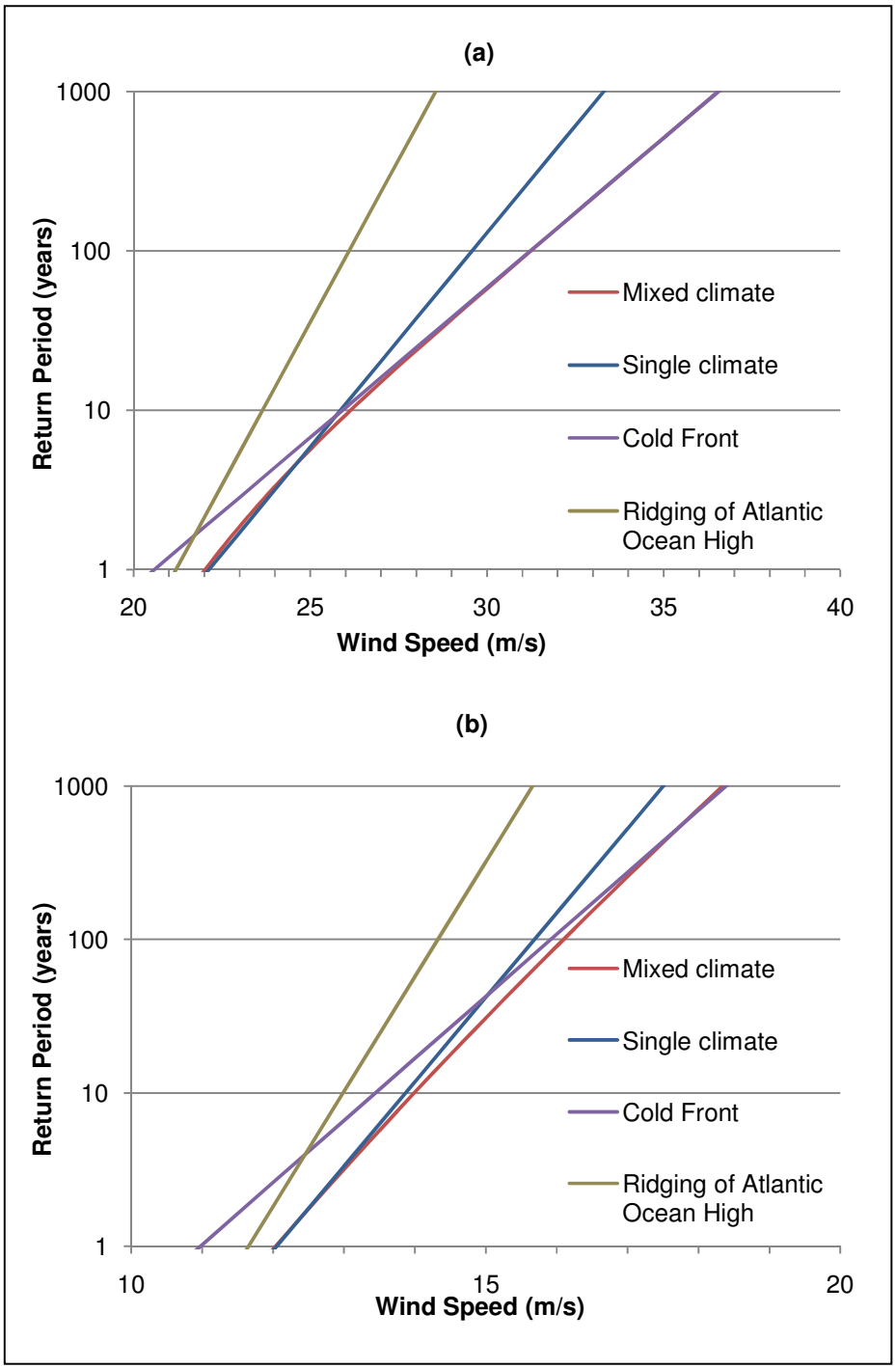

Figure 5.11. Annual maximum wind gust distribution (a) and annual maximum hourly mean wind speed distribution (b) for Robben Island.

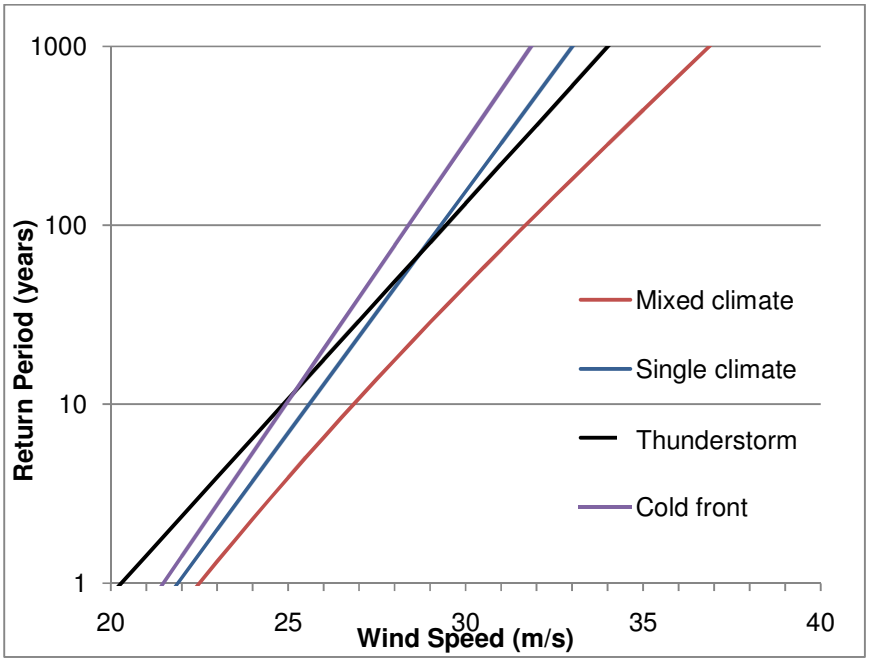

Figure 5.12. Annual maximum wind gust distribution for Jamestown.

Table 5.10. Values for the quantiles X_{50}, X_{100}, and X_{500}, as estimated by the mixed distribution method for weather stations with more than one strong wind producing mechanism.

Station Number	Station Name	Annual maximum wind gust (m/s)			Annual maximum hourly wind speed (m/s)		
		X_{50}	X_{100}	X_{500}	X_{50}	X_{100}	X_{500}
0021178	CAPE TOWN WO	38,7	41,0	46,3	22,8	24,0	26,8
0092081	BEAUFORT-WES	38,8	40,4	44,1			
0127272	UMTATA WO	41,9	44,7	51,2			
0239698	PIETERMARITZBURG	28,6	30,1	33,6	11,0	11,6	13,0
0261516	BLOEMFONTEIN WO				14,4	14,9	16,1
0274034	ALEXANDERBAAI	32,2	33,6	37,4			
0290468	KIMBERLEY WO				16,9	17,5	19,0
0317475	UPINGTON WO				17,0	17,7	19,2
0476399	JOHANNESBURG	34,6	36,8	41,7	15,8	16,5	18,2
0508047	MAFIKENG WO	31,8	33,3	36,7			
0513385	IRENE WO	33,3	35,1	39,4	16,5	17,2	18,9
0677802	PIETERSBURG WO				15,0	15,7	17,3

Cells are empty where a single mechanism applies.

5.5.2. Further analyses and discussion of results

5.5.2.1. The κ parameter and mixed distributions

The assumption that a negative shape parameter κ, estimated by fitting of the GEV distribution, or GPD distribution with the POT method, might indicate a mixed distribution of the wind values in the data samples is here investigated further. With the data sets utilised in this study, more than one strong wind mechanism was identified for 23 of the 35 weather stations with $\kappa < 0$, estimated by fitting of the GEV distribution to annual maximum gust speeds. For mean hourly winds, 15 of the 29 weather stations with $\kappa < 0$, estimated by the fitting of the GEV distribution to annual maximum mean hourly wind speeds, had more than one identified strong wind mechanism. It is therefore apparent that mixed distributions are not the only cause for negative estimations of κ, as not all weather stations with $\kappa < 0$ have mixed strong wind climates.

The GEV distribution was fitted to the data samples for each strong wind mechanism, e.g. to the data sets in the four columns of Table 5.9 for Robben Island. The results of these analyses are presented in Table 5.11, for the same weather stations as in Table 5.2. It can be noted that there are no real consistency between weather stations in the sign or magnitude of κ for specific strong wind mechanisms. The full set of results is presented in Table C.1 in Appendix C.

From the above results a conclusion can be made that the values of κ, for the data samples utilised, probably depend in most cases on the internal variability of the values in the data samples, and not on the strong wind mechanisms involved. Therefore it is reiterated again that for shorter time series, the estimation of quantiles should be based on the application of a method restricting the value of κ to zero, as suggested in section 5.2.3. It might be possible, that if the time series utilised were significantly longer, that there would be some consistencies evident in the sign and magnitude of κ between the different weather stations, and specific strong wind producing mechanisms.

Table 5.11. Values of the κ parameter for the different strong wind mechanisms, estimated by fitting of the GEV distribution.

Station Number	Station Name	Annual maximum wind gust (m/s)				Annual maximum hourly wind speed (m/s)		
		κ_{TS}	κ_{CF}	κ_{R}	κ_{OTHER}	κ_{CF}	κ_{R}	κ_{OTHER}
0012661	GEORGE WO		+0,23			+0,27		
0021178	CAPE TOWN WO		-0,04	-0,14		-0,16	-0,01	
0035209	PORT ELIZABETH		-0,13			-0,11		
0059572	EAST LONDON WO		+0,59			+0,45		
0092081	BEAUFORT-WES	+0,32	-0,05		-0,30	-0,04		
0127272	UMTATA WO	-0,35	+0,57			-0,05		
0182591	MARGATE		+0,01					
0239698	PIETERMARITZBURG	-0,13	-0,17		-0,24	-0,23		-0,03
0240808	DURBAN WO		-0,14			-0,13		
0261516	BLOEMFONTEIN WO	-0,24				+0,21		-0,09
0274034	ALEXANDERBAAI		+0,09		-0,04			+0,22
0290468	KIMBERLEY WO	+0,20				+0,21		-0,07
0317475	UPINGTON WO	-0,17				+0,23		+0,20
0476399	JOHANNESBURG	+0,01				+0,27		-0,03
0508047	MAFIKENG WO	-0,12						-0,04
0513385	IRENE WO	+0,09				-0,15		+0,21
0677802	PIETERSBURG WO	+0,36				+0,24	-0,10	

κ_{TS} is the shape parameter for the data set for thunderstorms, κ_{CF} for cold fronts and κ_{R} for ridging. κ_{OTHER} indicates an additional strong wind mechanism at a specific weather station, which can be found in Table 5.8. Cells are empty where a single mechanism applies.

5.5.2.2. Comparison between quantile estimations of Gumbel and mixed distribution methods

The differences between the values of the quantiles X_{50}, X_{100}, and X_{500}, estimated by the method for mixed distributions and the Gumbel method, e.g. $X_{50}^{mixed} - X_{50}^{G}$ for the 1:50 year quantiles, is presented in Table 5.12, for the weather stations in Table 5.10. The full set of results is presented in Table D.1 in Appendix D.

Table 5.12. Differences between the estimates for the quantiles X_{50}, X_{100}, and X_{500} estimated by the mixed distribution and Gumbel methods (i.e. $X_{50}^{mixed} - X_{50}^{G}$).

Station Number	Station Name	Annual maximum wind gust (m/s)			Annual maximum hourly wind speed (m/s)		
		X_{50}	X_{100}	X_{500}	X_{50}	X_{100}	X_{500}
0021178	CAPE TOWN WO	0,4	0,5	0,7	0,4	0,5	0,6
0092081	BEAUFORT-WES	0,2	0,3	0,3			
0127272	UMTATA WO	1,4	1,8	2,7			
0239698	PIETERMARITZBURG	1,6	1,8	2,2	0,0	0,0	0,0
0261516	BLOEMFONTEIN WO				0,2	0,2	0,2
0274034	ALEXANDERBAAI	0,9	1,3	2,8			
0290468	KIMBERLEY WO				0,1	0,1	0,2
0317475	UPINGTON WO				0,4	0,6	0,9
0476399	JOHANNESBURG	0,6	0,9	1,2	0,4	0,4	0,6
0513385	IRENE WO	0,4	0,5	0,8	0,5	0,6	0,8
0677802	PIETERSBURG WO				0,1	0,2	0,4

Cells are empty where a single mechanism applies.

As expected, and also noted by Gomes and Vickery (1978), quantile estimations by the mixed distribution method are usually larger than the estimations by the Gumbel method, with the differences increasing with increasing return periods. For X_{50}, the mixed distribution method estimates are, on average, 0,7 m/s larger than the Gumbel method for annual maximum wind gusts, and 0,2 m/s larger for annual maximum hourly mean wind speeds. For longer return periods the mean differences become larger. For X_{100}, the mean differences are 1,0 m/s and 0,3 m/s, while for X_{500} the mean differences are 1,7 m/s and 0,5 m/s respectively.

Where there are large differences between the estimates of the two methods it is usually because the strong wind mechanism that is causing the most extreme wind speeds is underrepresented in the sample of annual maximum wind speeds of a weather station. The dispersion of the annual maximum values of this particular strong wind mechanism is then also always larger than that for the other strong wind mechanism(s) taken into account. To illustrate this, the annual maximum wind gust

distribution for Uitenhage and the annual maximum hourly mean wind speed distribution for Malmesbury are discussed.

In the case of Uitenhage the most extreme wind gusts are caused by thunderstorms. Table 5.13 presents the annual maximum wind gust values, as well as the annual maximum values produced by the passage of cold fronts and the occurrence of thunderstorms at Uitenhage for the period 1996 to 2008.

Table 5.13. The annual maximum wind gust values produced by the passage of cold fronts and the occurrence of thunderstorms at Uitenhage, for 1996-2008.

Year	Annual maximum wind gust (m/s)		Annual maximum wind gust (m/s) caused by either a cold front or thunderstorm
	Cold front	Thunderstorm	
1996	30,3	15,9	30,3
1997	22,1	29,5	29,5
1998	22,8	16,3	22,8
1999	25,5	15,9	25,5
2000	25,1	18,5	25,1
2001	23,0	24,7	24,7
2002	-	-	-
2003	-	-	-
2004	26,5	18,2	26,5
2005	23,3	20,8	23,3
2006	27,1	24,3	27,1
2007	26,0	13,4	26,0
2008	24,7	25,8	25,8
Average	**25,2**	**19,8**	**26,1**

The measurements for 2002 and 2003 are unreliable and therefore omitted from the analysis.

Cold fronts are the causes of the annual maximum wind gusts on eight of the available 11 years of data. The average of the values for cold fronts is 25,2 m/s, which is higher than the average of the values for thunderstorms at 19,8 m/s. However, the value of the dispersion parameter, α, is 1,8 for cold fronts and 3,8 for thunderstorms. This larger

value for α results in a shallower slope in the extreme wind gust distribution graph for thunderstorms, as well as for the mixed climate, as presented in Figure 5.13.

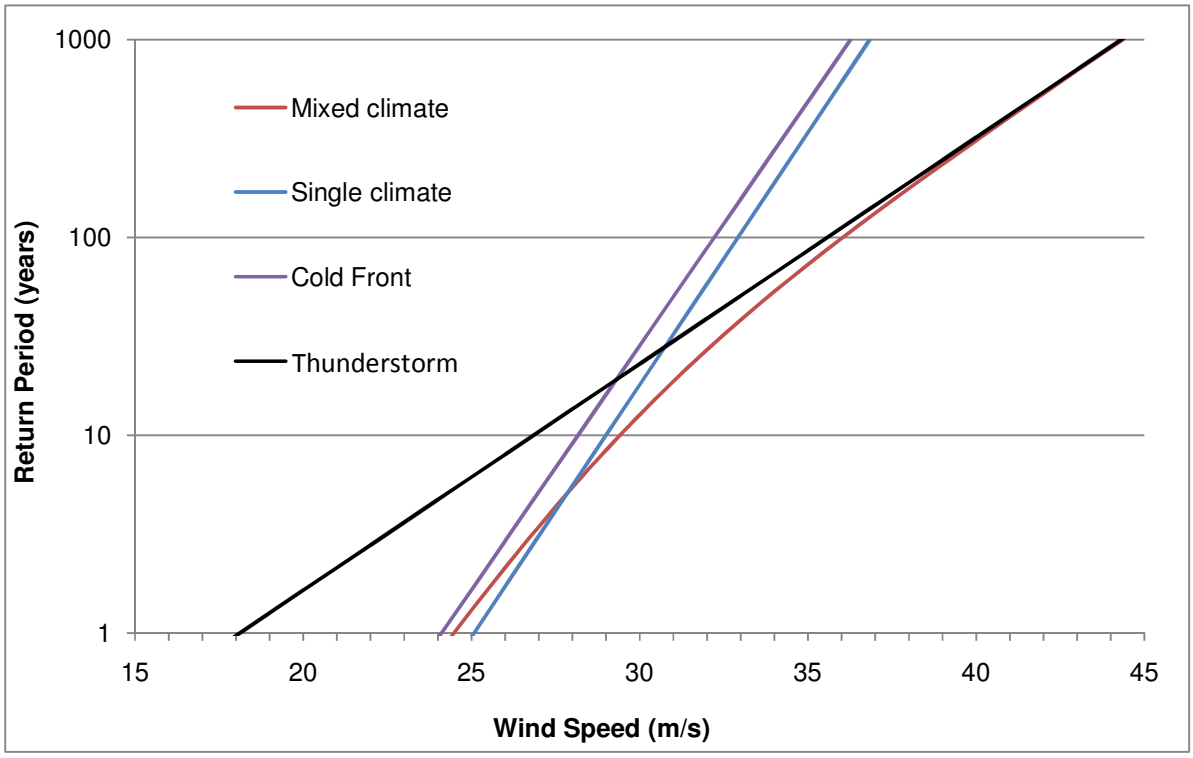

Figure 5.13. Extreme wind gust distribution for Uitenhage.

Another interesting example is that for the extreme hourly mean wind speed distribution for Malmesbury. Table 5.14 presents the maximum hourly mean wind speed values produced by the passage of cold fronts and the ridging of the Atlantic Ocean high-pressure system at Malmesbury, for the period 1992 to 2008. Cold fronts are the causes of the annual maximum hourly mean wind speeds on six of the available 17 years of data, while the ridging of the Atlantic Ocean high-pressure system is the cause for the remaining 11 years. The average of the annual maximum values for the cold fronts is 8,6 m/s, while for the ridging it is 9,0 m/s. The value of α for the cold fronts is 0,9, while for the ridging it is 1,0. Therefore the extreme hourly wind distributions for cold fronts and ridging are very similar. However, the mean of the annual maximum hourly mean wind speeds, regardless of the cause, is 9,4 m/s and α is equal to 0,7. The result is an extreme wind distribution as presented in Figure 5.14. The slope of the mixed climate

distribution is similar to the distributions for cold fronts and ridging, while the single climate slope for the traditional Gumbel method is much steeper, causing a significant underestimation of wind speeds for the longer return periods.

Table 5.14. The annual maximum hourly mean wind speed values produced by the passage of cold fronts and the ridging of the Atlantic Ocean high-pressure system at Malmesbury, for 1992-2008.

Year	Annual maximum hourly mean wind speed (m/s)		Annual maximum hourly mean wind speed (m/s) caused by either a cold front or ridging
	Cold front	Ridging	
1992	9,9	9,5	9,9
1993	9,3	11,1	11,1
1994	11,1	10,1	11,1
1995	8,2	9,9	9,9
1996	9,4	9,3	9,4
1997	10,1	10,2	10,2
1998	7,1	9,0	9,0
1999	7,7	9,8	9,8
2000	7,2	9,1	9,1
2001	8,8	9,0	9,0
2002	8,3	9,3	9,3
2003	8,8	9,7	9,7
2004	6,1	8,4	8,4
2005	8,1	6,5	8,1
2006	8,0	7,0	8,0
2007	8,8	6,5	8,8
2008	8,8	9,0	9,0
Average	**8,6**	**9,0**	**9,4**

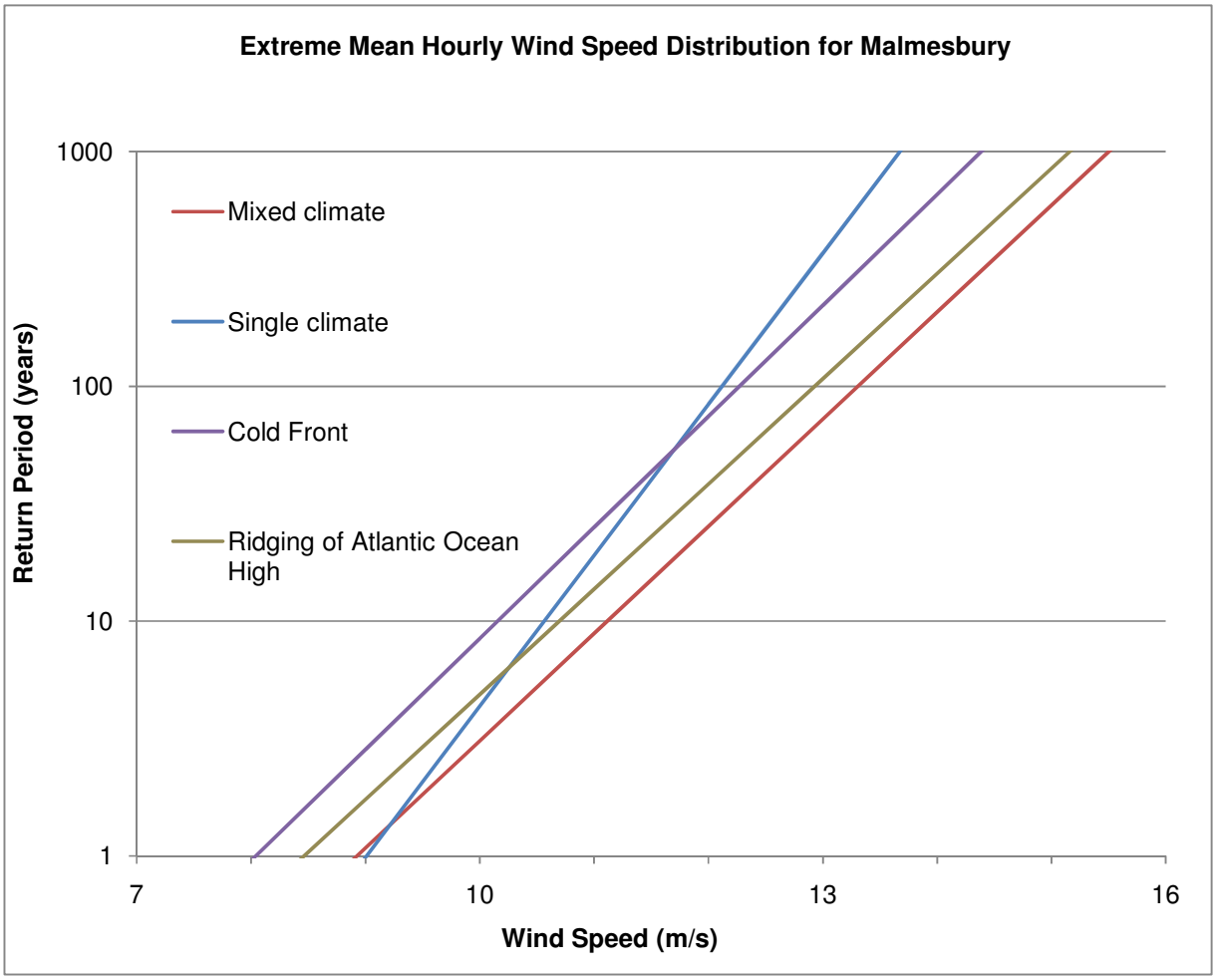

Figure 5.14. Annual maximum mean hourly wind speed distribution for Malmesbury.

The conclusion is that, for the estimation of quantiles for long return periods, it is advisable or "safer" to follow a mixed distribution approach. This is especially applicable to strong wind estimations in South Africa, where most of the land area is influenced by more than one strong wind producing mechanism.

The disaggregated data sets developed in this analysis also make it possible to predict extreme wind estimations caused by the different strong wind mechanisms. For the above examples, the estimated wind gust quantiles X_{50}, X_{100} and X_{500} for the strong wind mechanisms identified for Uitenhage is shown in Table 5.15. Table 5.16 presents

hourly mean wind speed quantiles for the same return periods for the strong wind mechanisms identified for Malmesbury.

Table 5.15. Estimations of extreme wind gusts of cold fronts and thunderstorms for Uitenhage.

Strong wind mechanism	X_{50}	X_{100}	X_{500}
Cold front	31,0	32,2	35,0
Thunderstorm	33,0	35,6	41,7

Table 5.16. Estimations of extreme hourly mean wind speeds of cold fronts and ridging of the Atlantic Ocean high-pressure system for Malmesbury.

Strong wind mechanism	X_{50}	X_{100}	X_{500}
Cold front	11,6	12,3	13,7
Ridging	12,3	12,9	14,5

5.6. Concluding remarks

The various steps taken in the analysis of the strong wind data can be summarised as presented in the overview in Figure 5.15. Firstly all the data sets were analysed with the traditional Gumbel method. As it cannot readily be assumed that κ = 0, the data sets were subsequently analysed with the GEV approach, and from the results it was seen that no spatial consistency between stations in terms of the value of κ is evident. This indicated that the GEV approach is not recommended for the analysis of short time series, as are utilised in the present study.

The POT method, specifically developed for the analysis of short time series, was then applied. It was seen that this method is not applicable to hourly mean wind speeds, and therefore only the data sets for the wind gusts were analysed. With the POT method applied to the GPD, again no spatial consistency between stations in terms of the value of κ was evident. The POT method was then applied with the EXP distribution, which is essentially the GPD distribution with κ = 0. This approach is deemed to produce the

best estimates of extreme wind values from the methods investigated, if a single strong wind climate is assumed.

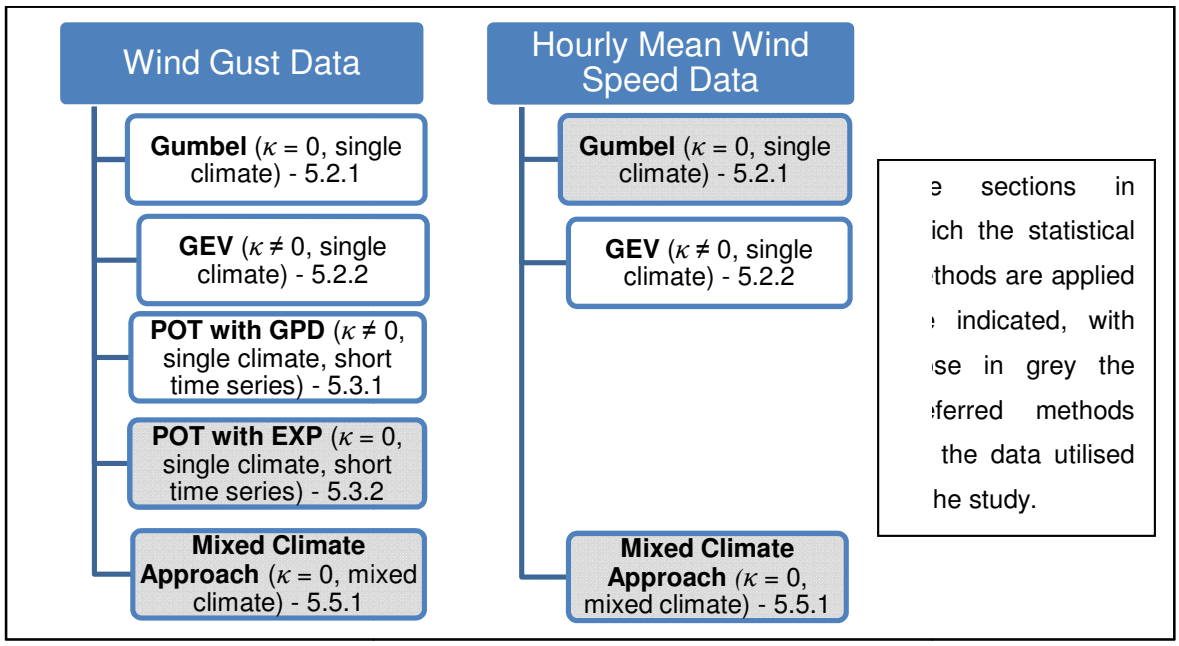

Figure 5.15. The analysis approach of strong winds taken in Chapter 5.

Subsequently a method for analysing mixed strong wind climates was applied to the wind gust as well as the hourly mean wind speed data sets. For both these data sets almost all of the weather stations showed increased quantile estimates. It is concluded that, for the wind data of single climatic origin utilised in the study, the POT approach applied with the EXP method is the preferred method to use in the case of wind gusts. In the case of a strong wind climate of various origins the mixed strong wind climate approach is preferred, especially for longer return periods where the quantile estimations by the mixed climate method become much larger than that with the traditional Gumbel method. It is not feasible to apply the POT method to a mixed climate approach, due to the large number of strong winds of which the causes would have to be determined.

For hourly mean wind speeds the traditional Gumbel approach is satisfactory. However, in the case of a strong wind climate of various origins, the method for a mixed strong

wind climate is preferred, also due to the much larger quantiles estimated with this method, compared to the Gumbel method as was the case for the wind gusts.

Chapter 6

Exposure of Weather Stations

6.1. General

The investigation of the exposures of the weather stations utilized in the study is imperative because of the fact that the standardization of the wind information is necessary for consistent results and the further development of a map of design wind speeds. All data which forms the inputs to the analysis has to be captured by a wind anemometer positioned in an 'open terrain category', at a standard elevation of 10 m above the ground level. This is the requirement of all international engineering design standards. In most cases non-standard surroundings lead to wind speed recordings which are lower than would be measured in open terrain. For engineers wind data which is representative of the environment is crucial, due to the quadratic relationship between wind speed and the wind load on structures.

Various definitions of the open terrain category are stipulated in different sources, but in essence they refer to an open flat grassland with few well scattered obstructions, with heights and plan dimensions not larger than 10 m. This category includes open farmlands or parklands with few trees or undeveloped land, with an overall roughness length of between 0,03 and 0,05 m. The roughness length, z_0, can be interpreted as the theoretical height above ground level at which the horizontal wind speed will become zero, under assumption of a logarithmic wind profile (Wever and Groen, 2009). Partly because of this requirement, wind anemometer installations across the world are often located at airports, but primarily it needs to fulfill the civil aviation requirements for a flat and undeveloped terrain. Table 6.1 presents different terrain categories, as well as the

corresponding roughness lengths, as described in the building standard Eurocode 1 (EN 1991-1-4, 2005), which is applicable to the European Union.

Table 6.1. Terrain categories and terrain parameters from EN 1991-1-4 (2005).

Terrain category	Description	z_0 Roughness length (m)
0	Sea or coastal area exposed to the open sea	0,003
I	Lakes or flat and horizontal area with negligible vegetation and without obstacles	0,01
II	Area with low vegetation such as grass and isolated obstacles (trees, buildings) with separations of at least 20 obstacle heights	0,05
III	Area with regular cover of vegetation or buildings or with isolated obstacles with separations of maximum 20 obstacle heights (such as villages, suburban terrain, permanent forest)	0,3
IV	Area in which at least 15 % of the surface is covered with buildings and their average height exceeds 15 m	1,0

Further of importance to note is that the wind speeds increase with elevation (i.e. distance from the ground) and all design standards define this increase in terms of the growth of the boundary layer profile. Boundary layer theory indicates that it develops over several kilometers of the approach terrain, the distance from the measurement site, and this implies a requirement for the surroundings of the wind anemometers also to be consistent in its character over several kilometers.

The general guideline for the placement of anemometers is based on established WMO standards, which are consistent of those of everyday practise. The measurements should take place over level, open terrain at a height of 10 m above the ground. In the

WMO context “open terrain” is defined as an area where the distance between the anemometer and any obstruction is at least 10 times the height of the obstruction. This differs from the definition of Terrain Category II in Table 6.1, which requires a distance of 20 obstacle heights, i.e. 10x vs. 20x. This means that an anemometer which measures wind velocity at a height of 10 m should be free from significant obstructions over a distance of at least 100 m. However, in some instances it is not possible to strictly meet these requirements, e.g. weather stations erected close to built-up areas where space is limited. Buildings and structures can then limit the exposure of the anemometers.

It follows then that a weather station might be erected according to the WMO standards, but that the wind speed measured at that station might not fulfil the exposure requirements of the basic wind speed. There might be various reasons for such a situation, e.g. while the WMO standards require a radius of about 100 m around an anemometer to be free of obstructions, a built-up area, for example, influences the wind-flow for several kilometres downwind. It is also possible that the terrain around the anemometer is not of the required roughness due to e.g. the variability in vegetation cover of the South African landscape, or due to the fact that a weather station can be located close to the coastline.

Another aspect of the placement of weather station to keep in mind is that some weather stations in South Africa are erected between hills and mountains, on their slopes or peaks, or close to forests which deviates significantly from the Terrain II category. The research into the effects of topography indicates that the boundary layer profile can be influenced significantly by prominent topographical features. For example, wind-tunnel measurements of the Cape Town topography indicates that, in terms of the mean wind speed profile, the influence of Table Mountain (with an elevation of about 1 000 m), is still significant about 5 km downwind, while the peak wind speed profile at low elevations could be increased between 10% and 50% (Goliger *et al*., 1990). A similar study into the wind flow influences of an undulated topography in Pretoria, indicate that the influence of a 160 m high, relatively smooth ridge, tends to

dissipate only about 2 km downwind, although the magnitude of peak wind speeds at low elevations tends to reach the magnitude of the free-stream flow within a distance of about 500 m downwind (i.e. about 3 times the height of the ridge) (Goliger and Milford, 1988).

6.2. Assessment of exposure of weather stations

To assess the possible shortcomings in the exposure of the South African weather stations an attempt was made to compare the exposures of the weather stations to that required for the direct calculation of the basic wind speed. The exposures of the anemometers at the weather stations were then categorised according to set criteria, which are numbered and summarised below. All measurements are taken at the reference height of 10 m:

1. **Reasonable positioning:** The anemometer is erected at a height of 10 m, strictly according to WMO standards. This means that no obstructions exist at least 100 m from the anemometer. No built up areas are evident for at least 2 km from the anemometer. The topography around the anemometer is flat, with no prominent hills or mountains closer than 3 km. The terrain, for at least 2 km around the anemometer, is in the region of the required roughness, i.e. 0.03 to 0,05 m. The exposure of the station conforms closely to that required for the calculation of the basic wind speed.
2. **Influence of surface roughness:** The anemometer is erected at a height of 10 m, strictly according to WMO standards. This means that no obstructions exist at least 100 m from the anemometer. Some built up areas are evident closer than 2 km from the anemometer, or the terrain around the anemometer is not always of the required roughness e.g. if situated at the coastline or surrounded by sandy or bare soil. This means that the surface roughness length can be as high as 0,3 m or as low as 0,003 m. The topography around the anemometer is flat, with no prominent hills or mountains closer than 3 km.
3. **Influence of obstructions:** The anemometer is erected at a height of 10 m. However, some obstructions exist that are probably closer than 100 m from the

anemometer. The topography around the anemometer is flat, with no prominent hills or mountains closer than 3 km.

4. **Influence of topography:** The anemometer is erected at a height of 10 m, strictly according to WMO standards. However, the topography around the anemometer is not flat, with some prominent slopes, hills or mountains closer than 3 km.

6.3. Methodology

The most important step in the assessment of the surroundings of a weather station is to be sure of the exact position of the weather station, as well as the positions and distances from the anemometer of the features that might influence the wind flow. Various sources are available in the SAWS to locate an approximate position of a particular weather station, e.g. the information files available for each weather station which include 1:50 000 topographical maps with markers for the approximate positions of the weather stations. These files also contain photographs of the weather stations, usually taken from different directions.

Another source is the climate database, where the geographical coordinates of each weather station are available, at an accuracy of a hundredth of a degree latitude and longitude. However, the abovementioned information is not sufficient to locate the exact positions of the weather stations, to the accuracy required to assess the exact distances and the orientations of possible obstructions that may compromise the wind. To address this problem, regional weather offices were supplied with GPS devices and required to determine the exact locations of all open weather stations. Mixed results were obtained with the collection of this updated information, with some offices supplying the information timeously and accurately and others not. Where this information was not forthcoming or inaccurate, there had to be relied on the available geographical coordinate data, topographical maps and photographs to determine the positions of the weather stations as closely as possible. Fortunately the latter option of determining the exact positions was only necessary for a small number of the weather stations.

Google Earth (http://earth.google.com), together with the mentioned photographs in the station files, were used to obtain a general idea of the characteristics of the landscape around the weather stations, i.e. the surface roughness, the possible obstacles and built up areas close to the anemometer, as well as the surrounding topography. The maps from Google Earth are of variable quality in terms of resolution, so that in some instances it was a challenging process to obtain sufficient information on the surroundings of the anemometers, which obviously requires a high resolution. Appendix E contains the relevant downloaded Google maps, with markers identifying the weather station positions. Short summaries discussing the surroundings of the weather stations and the prevailing strong winds in the vicinity of the weather station are also included.

6.4. Results of exposure assessments

Table 6.2 presents a summary of the information which is contained in Appendix E. Of the 91 stations assessed from the exposure point of view, 40 of the weather stations, or 43%, have surrounding exposures close to that required for the direct estimation of the basic wind speed. An additional eight weather stations, or 9%, have exposures which will probably lead to an overestimation of the basic wind speed, if no exposure corrections are made. Reasons for this are the proximity to the ocean or other large water bodies, or the surrounding landscape which will, during the larger part of an average year, consist of bare soil or very sparse vegetation (all of which will reduce the roughness well below the required value of 0,03 to 0,05 m). However, the overestimation of the basic wind speed cannot be deemed as critical for building design purposes as will be for the case of underestimations. In this context one can make the assumption that 52% of the weather stations utilised in the study have adequate exposure.

Table 6.2. Categorization of the exposure of the weather stations, and likely effect on the measured wind data.

Station Number	Station Name	Category				Likely effect on wind speed (from wind direction)
		1	2	3	4	
0003108	STRUISBAAI		•	•		Overestimation (NE to E and NW), underestimation (SW to NW)
0005609	STRAND		•			Overestimation (SW), over- or underestimation (NW or SE), underestimation (NW).
0006386	HERMANUS		•	•	•	Over- or underestimation (NE to E, and W to NW)
0007699	TYGERHOEK				•	Underestimation (NW)
0010682	STILBAAI	•				
0012661	GEORGE WO	•				
0014123	KNYSNA		•		•	Underestimation (NW)
0014545	PLETTENBERGBAAI	•				
0015692	TSITSIKAMMA		•	•	•	Overestimation (SW), underestimation (NW)
0020618	ROBBENEILAND		•	•		Under- or overestimation (SE), overestimation (SW to NW)
0021178	CAPE TOWN WO			•		Underestimation
0021823	PAARL		•		•	Underestimation
0022729	WORCESTER	•				
0031650	JOUBERTINA				•	Underestimation
0033556	PATENSIE	•				
0034763	UITENHAGE				•	Underestimation (NW)
0035209	PORT ELIZABETH WO	•				
0040192	GEELBEK		•			Overestimation
0041388	MALMESBURY		•			Underestimation (W to N)
0041841	PORTERVILLE	•				
0045642	LAINGSBURG				•	Underestimation
0056917	GRAHAMSTOWN	•				
0059572	EAST LONDON WO	•				
0061298	LANGEBAANWEG	•				
0063807	EXCELSIOR CERES		•	•	•	Underestimation
0078227	FORT BEAUFORT	•				
0083572	LAMBERTSBAAI			•		Underestimation (W to NW)

Station Number	Station Name	Category				Likely effect on wind speed (from wind direction)
		1	2	3	4	
0092081	BEAUFORT-WES				•	Overestimation
0096072	GRAAFF-REINET	•				
0123685	QUEENSTOWN		•	•		Underestimation, except from E
0127272	UMTATA WO	•				
0134479	CALVINIA WO	•				
0144791	NOUPOORT		•	•		Underestimation (SW to NW)
0148517	JAMESTOWN		•	•	•	Underestimation
0150620	ELLIOT	•				
0155394	PORT EDWARD		•			Overestimation (SW)
0169880	DE AAR WO				•	Overestimation
0182465	PADDOCK	•				
0182591	MARGATE	•				
0184491	KOINGNAAS		•			Overestimation
0190868	BRANDVLEI		•			Overestimation
0214700	SPRINGBOK WO		•	•	•	Underestimation
0224400	PRIESKA	•				
0239698	PIETERMARITZBURG		•			Underestimation
0239699	ORIBI AIRPORT		•			Underestimation
0240808	DURBAN WO	•				
0241072	MOUNT EDGECOMBE		•	•		Underestimation
0241076	VIRGINIA	•				
0261307	BLOEMFONTEIN-STAD		•	•		Underestimation
0261516	BLOEMFONTEIN WO	•				
0268016	GAINTS CASTLE AWS				•	Underestimation or overestimation
0270155	GREYTOWN			•		Underestimation
0274034	ALEXANDERBAAI		•			Overestimation
0290468	KIMBERLEY WO	•				
0300454	LADYSMITH			•		Underestimation (NW)
0304357	MTUNZINI	•				
0317475	UPINGTON WO		•			Overestimation
0321110	POSTMASBURG	•				
0331585	BETHLEHEM WO		•	•		Underestimation
0333682	VAN REENEN	•				
0337738	ULUNDI	•				
0339732	CHARTERS CREEK		•			Underestimation, overestimation (NE - SE)

Station Number	Station Name	Category				Likely effect on wind speed (from wind direction)
		1	2	3	4	
0356880	KATHU	•				
0360453	TAUNG	•				
0362189	BLOEMHOF	•				
0364300	WELKOM		•			Overestimation
0365398	KROONSTAD					Position not accurately determined
0370856	NEWCASTLE	•				
0410175	PONGOLA	•				
0427083	VAN ZYLSRUS		•			Overestimation
0438784	VEREENIGING	•				
0441416	STANDERTON		•			Underestimation, except from W
0472278	LICHTENBURG	•				
0475879	JHB BOT TUINE		•	•		Underestimation
0476399	JOHANNESBURG WO		•			Underestimation
0479870	ERMELO WO		•			Underestimation
0508047	MAFIKENG WO	•				
0511399	RUSTENBURG		•			Underestimation
0513346	PRETORIA UNISA		•	•	•	Underestimation or overestimation
0513385	IRENE WO		•	•		Underestimation (S to SW)
0515320	WITBANK		•	•		Underestimation (S and NW)
0520691	KOMATIDRAAI	•				
0548375	PILANESBERG	•				
0554816	LYDENBURG					Position not accurately determined
0587725	THABAZIMBI		•		•	Underestimation
0594626	GRASKOP AWS		•	•		Underestimation
0633882	POTGIETERSRUS		•			Underestimation
0638081	HOEDSPRUIT	•				
0674341	ELLISRAS	•				
0675666	MARKEN	•				
0677802	PIETERSBURG WO		•			Underestimation (S)
0723664	THOHOYANDOU WO	•				

Column numbers indicate: 1. *Exposure is approximately that required for direct calculation of the basic wind speed,* ***2.*** *Roughness not close to the required 0,03 m,* ***3.*** *Obstructions exist which are closer than 100 m from the anemometer and* ***4.*** *The terrain or topography around the anemometer is not close to flat. The last column indicates the likely effects of these distortions on the wind speed measurements (from wind direction), or whether the position of the station could not be determined accurately enough (see section 6.2).*

The majority of weather stations with exposure problems have these problems because of the surrounding landscape in the direction of the prevailing strong winds not conforming to the required surface roughness of approximately 0,03 to 0,05 m. A total of 39 weather stations, or 43%, can be deemed to be located in areas where the surrounding landscape does not conform to the required surface roughness. These problems are usually due to the fact that many weather stations are located close to, or even within, built-up areas. But, if one omits the eight weather stations with surrounding surface roughness which will probably lead to overestimations of the basic wind speed, which were mentioned previously, the percentage of weather stations with surroundings of inadequate surface roughness reduces to 34%.

Further assessment reveals that a total of 21 weather stations, or 23%, have some kind of obstruction closer than 100 m from the anemometer, in the directions of the prevailing strong winds. The effects of these obstructions are difficult to quantify without the use of full-scale or wind tunnel measurements.

The cases of weather stations on uneven terrain or surrounded by complex topography are not confined to the more mountainous regions, but also occur due to the inadequate positioning of weather stations in relation to their surroundings, e.g. the AWS at the De Aar Weather Office which is located on a hill. The surrounding areas of a total of 16, or 18%, of the weather stations, showed problems with very uneven surrounding terrain and/or close-by hills, mountains or valleys. From the above discussion of Table 6.2, one can see that in many weather stations more than one category of inadequate exposure are applicable.

6.5. Development of correction factors

Three factors which can cause distortions in the measured data could be identified in the surroundings of the weather stations, namely:

- the incorrect terrain roughness at the approach to the anemometer, i.e. the approach is not in the open terrain category,

- the presence of structures in the immediate vicinity of the AWS, i.e. affecting the flow approaching the anemometer, and
- the impact of the surrounding topography, i.e. the approach terrain not being flat and level.

The results of the assessments indicate that the above factors influence a large proportion of the weather stations, to such a degree that for several weather stations it is not possible to calculate a fair estimate of the basic wind speeds directly from the measured data**.** Therefore, if a map should be constructed of design wind speeds, the results of these weather stations should rather be omitted from the analysis, if no physical adjustments to the measured wind speed values can be made.

However, for some weather stations the deviations from the open terrain category are only caused by the surface roughness, which does not resemble the Terrain Category II in Table 6.1. For these cases a simple correction factor is sought that can be applied to the wind data, so that close estimates of the basic wind speeds applicable for the specific locations of the weather stations can be obtained.

6.5.1. Estimation of surface roughness z_0

To develop correction factors to the measured wind data, z_0 needs to be assessed. Several approaches exist to estimate z_0. These are

- approximations derived from the measured data,
- the application of the logarithmic wind profile to specific site measurements at different heights, and
- visual assessment by comparison with standard reference values given in textbooks.

The first approach by approximations from the measured data requires high-resolution measurements of the standard deviations of wind speed (Verkaik, 2000), which is not available from the wind measurements stored on the SAWS climate database. The second approach involving the logarithmic profile implies measurement of the wind

speeds at different heights, which are also not possible in this study. Therefore, the only remaining method is to estimate the surface roughness visually. This method is not necessarily inferior to the other methods, as shown in a study by Barthelmie *et al.* (1993). They found that the roughness lengths derived by the various methods can vary considerably. The terrain-derived roughness lengths gave reasonable results, while the gust-derived and standard deviation roughness lengths both predicted wind speeds which were lower than those observed.

Morphometric models are often used to estimate roughness. These models use as input the averages of terrain descriptors, such as obstacle height, the cross-flow width and frontal area density, i.e. the density of the obstacle in the direction of the wind. The results of this modelling are often disappointing (Grimmond and Oke, 1999). This is because the variances of the descriptors, as well as other factors such as orientation, roof shape, and the presence of trees in cities, are not included. Therefore the option of estimating average roughness visually, using the eye as integrator, cannot be disregarded. When the judgement is supported by a clearly-worded classification, the error will not be more than a single roughness class-width (Davenport *et. al*, 2000).

The visual estimation of the roughness from terrain data is usually done by studying and interpreting the land surface from spatial land-cover data or aerial photographs, such as the Google Earth maps included in Appendix E, over a distance of several kilometres from the anemometer. The land surface is then compared to the descriptions of land cover, such as in Table 6.1. Each type of land cover is associated with a typical roughness length. For more accurate estimations of the roughness length, than the information provided in Table 6.1, which is basically the classification developed by Davenport (1960), a revision of the rougher terrain part of the classification was done in 2001. This revision takes into account more than 40 experiments over homogeneous terrain, and 35 experiments at sufficient height over inhomogeneous terrain and over cities (Wieringa *et al.*, 2001). This is presented in Table 6.3. With the use of eight classes, as in Table 6.3., the resulting error in the estimation of potential wind speed will not exceed 6% (Wieringa, 1992).

Table 6.3. Typical surface roughness length (z_0) associated with terrain type (Wieringa *et al.*, 2001).

Terrain	Landscape Description	z_0 (m)	Additional analysis requirement
I. Sea	Open sea or lake (irrespective of wave size), tidal flat, snow-covered flat plain, featureless desert, tarmac and concrete, with a free fetch of several kilometres	0,002	-
II. Smooth	Featureless land surface without any noticeable obstacles and with negligible vegetation, e.g. beaches, pack ice with large ridges, marsh, and snow-covered or fallow open country.	0,005	-
III. Open	Level country with low vegetation (e.g. grass) and isolated obstacles with separations of at least 50 obstacle heights, e.g. grazing land without windbreaks, heather, moor and tundra, runway area of airports. Ice with ridges across-wind.	0,03	-
IV. Roughly open	Cultivated or natural area with low crops or plant cover, or moderately open country with occasional obstacles (e.g. low hedges, isolated low buildings or trees) at relative horizontal distances of at least 20 obstacle heights.	0,1	-
V. Rough	Cultivated or natural area with high crops or crops of varying height, and scattered obstacles at relative distances of 12 to 15 obstacle heights for porous objects (e.g. shelterbelts) or 8 to 12 obstacle heights for low solid objects (e.g. buildings).	0,25	May need z_d
VI. Very rough	Intensively cultivated landscape with many rather large obstacle groups (large farms, clumps of forest) separated by open spaces of about 8 obstacle heights. Low densely-planted major vegetation like bushland, orchards, young forest. Also, area moderately covered by low buildings with interspaces of 3 to 7 building heights and no high trees.	0,5	Requires z_d
VII. Skimming	Landscape regularly covered with similar-size large obstacles, with open spaces of the same order of magnitude as obstacle heights, e.g. mature regular forests, densely built-up area without much building height variation.	1	Requires z_d
VIII. Chaotic	City centres with mixture of low-rise and high-rise buildings, or large forests of irregular height with many clearings.	≥ 2	Analysis by wind tunnel advised

The last column in Table 6.3 refers to any additional requirements when the roughness length of a particular area is assessed, specifically regarding the displacement height, z_d, which is the separation height between the flow regime between obstacles near the surface and the boundary layer above. When such a situation develops, the wind flow is called “skimming”, and z_d is usually taken as two thirds of the obstacle heights. The displacement height is taken into account when the terrain surface fraction covered by obstacles is above 20%, as the mutual sheltering of the obstacles then becomes dominant (Davenport *et al.*, 2000).

The effective roughness lengths around the anemometers of the weather stations were therefore estimated visually. For the purposes of this study the assessments of roughness categories around the anemometers were done for a distance of about 2 km, which is reasonable for the purpose of roughness corrections of the measurements of extreme winds (Hansen, pers. comm.).The area around a particular weather station was divided into 16 sectors of 22,5º around the compass directions; i.e. N, NNE, NE, ENE, E, ESE, SE, SSE, S, SSW, SW, WSW, W, WNW, NW and NNW. The roughness assessments were then made for each of these sectors which are then each about 2 km long. To err on the conservative side, most often the roughest area were taken as representative of the sector under consideration. As an example, the procedure is illustrated for the weather station at Grahamstown. The position of the station with the indication of the 16 sectors is presented in Figure 6.1, imposed on an aerial image of the area which was extracted from Google Earth and also included in Appendix E. The surface roughness lengths of these 16 sectors were then assessed as objectively as possible. From the N to NNE a number of isolated hangars and other airport buildings are situated about 500 m from the weather station. Apart from these the terrain is flat, and a value for z_0 of 0,25 was assigned. From NE to ENE there are some built-up areas at a distance of 700 m to 1,4 km from the weather station, and a value for z_0 of 0,25 m was also assigned. The E sector is fairly open, except for the built-up area in the south-eastern corner of the sector; therefore $z_0 \approx$ 0,1 m. The ESE to SE sectors possesses built-up areas, especially towards ESE, where it is assumed that flow separation takes place. Therefore for ESE $z_0 \approx$ 0,1 m, and for SE $z_0 \approx$ 0,5 m, with $z_d \approx$ 3,5 m, which is

typical of a residential area. From SSE to NNW the terrain is flat and open ($z_0 \approx 0{,}03$ m). In the NE direction are some very low buildings (not clear on the image) situated in the vicinity of the anemometer, with $z_0 \approx 0{,}25$ m.

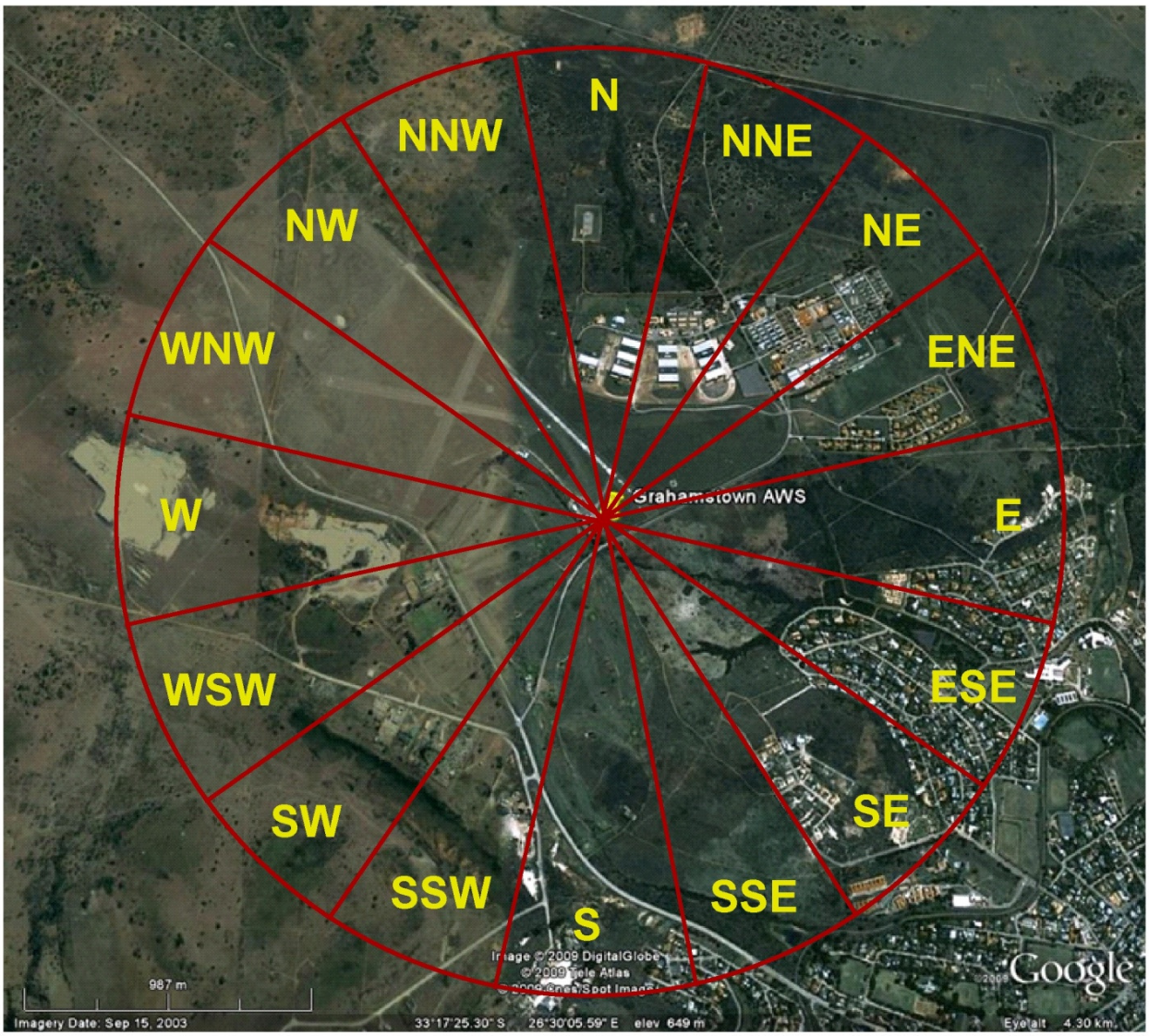

Figure 6.1. Aerial image of the weather station at Grahamstown with the 16 sectors superimposed which were assessed for surface roughness.

The results of the assessments of all the weather stations are presented in Table 6.4. Where it was impossible to make fair assessments of the probable roughness length, due to factors such as hilly terrain or close-by buildings or obstructions, the cells for the

particular directions were left empty. Where it was deemed applicable, z_d was also estimated and noted in the table.

Table 6.4. Assessments of z_0 (m) around the weather stations.

Station Number	Station Name	N	NNE	NE	ENE	E	ESE	SE	SSE	S	SSW	SW	WSW	W	WNW	NW	NNW
0003108	STRUISBAAI	0,0002	0,0002	0,0002	0,0002	0,0002	0,005	0,25	0,25	0,5 (3,5)	0,5 (3,5)	0,25 (3,5)	0,25 (3,5)	0,5 (3,5)	0,005	0,005	0,0002
0005609	STRAND	1 (3,5)	1 (3,5)	1 (3,5)	0,5 (3,5)	0,5 (3,5)	0,5	0,5	0,0002	0,0002	0,0002	0,0002	0,0002	-	-	0,25	0,5 (3,5)
0006386	HERMANUS	-	0,5 (3,5)	0,5 (3,5)	0,0002	-	-	-	-	0,1	-	-	-	0,25	0,5 (3)	0,25	-
0007699	TYGERHOEK	-	-	-	-	0,25	0,25	0,1	0,1	0,1	0,1	0,1	0,1	0,1	0,1	0,1	-
0010682	STILBAAI	0,03	0,03	0,03	0,25 (3,5)	0,5 (3,5)	0,5 (3,5)	0,25 (3,5)	0,03	0,03	0,03	0,03	0,03	0,03	0,03	0,03	0,03
0012661	GEORGE WO	0,03	0,03	0,1	0,1	0,1	0,1	0,1	0,1	0,1	0,1	0,03	0,03	0,03	0,1	0,1	0,03
0014123	KNYSNA	-	-	-	-	-	-	0,25	0,25	0,5 (3,5)	0,5 (3,5)	0,25(3,5)	0,1	0,1	1 (4)	-	-
0014545	PLETTENBERGBAAI	0,03	0,03	0,03	0,03	0,03	0,03	0,03	0,03	0,03	0,03	0,03	0,03	0,03	0,03	0,03	0,03
0015692	TSITSIKAMMA	-	-	-	-	0,0002	0,0002	0,0002	0,0002	0,0002	0,0002	0,0002	0,0002	-	-	-	-
0020618	ROBBENEILAND	0,0002	0,0002	0,0002	0,0002	0,0002	0,0002	0,005	0,03	0,03	0,03	0,03	0,1 (3,5)	0,03	0,01	0,01	0,0002
0021178	CAPE TOWN WO	0,1	0,1	0,1	0,03	0,1	0,03	0,03	0,03	0,03	0,25	0,5 (4)	0,25	0,25	0,1	0,1	0,03

Station Number	0063807	0061298	0059572	0056917	0045642	0041841	0041388	0040192	0035209	0034763	0033556	0031650	0022729	0021823
Station Name	EXCELSIOR CERES	LANGEBAANWEG	EAST LONDON WO	GRAHAMSTOWN	LAINGSBURG	PORTERVILLE	MALMESBURY	GEELBEK	PORT ELIZABETH	UITENHAGE	PATENSIE	JOUBERTINA	WORCESTER	PAARL
N	-	0,03	0,25	0,1	-	0,1	0,5 (3,5)	0,03	0,1	0,5 (1,5)	0, 5 (1,5)	-	0,03	0,25
NNE	-	0,03	0,25	0,1	-	0,1	0,5 (3,5)	0,03	0,1	0,5 (1,5)	-	-	0,03	0,25
NE	-	0,03	0,25	0,25	-	0,1	0,25 (3,5)	0,03	0,1	0,5 (1,5)	-	-	0,03	0,5 (3,5)
ENE	0,25	0,03	0,25	0,25	-	0,25	0,5 (3,5)	0,03	0,25	0,25	-	-	0,03	0,5 (3,5)
E	0,25 (2,5)	0,03	0,25	0,1	-	0,25	0,5 (3,5)	0,03	0,25	0,1	-	-	0,03	0,5 (3,5)
ESE	0,25 (2,5)	0,03	0,25	0,5 (3,5)	-	0,25	0,25 (3)	0,03	0,25	0,1	-	-	0,25 (3)	1 (3,5)
SE	0,1	0,1	0,25	0,25	-	0,25	0,1	0,03	0,1	0,1	-	-	0,25 (3)	1 (3,5)
SSE	0,25 (2,5)	0,03	0,25	0,03	-	0,25	0,1	0,03	0,03	0,25 (1,5)	0,1	-	0,03	0,5 (3,5)
S	0,25 (2,5)	0,03	0,25	0,03	-	0,25	0,1	0,03	0,03	0,5 (1,5)	0,5 (1,5)	-	0,03	1 (3,5)
SSW	0,25 (2,5)	0,03	0,25	0,03	-	0,25	0,1	0,03	0,25	0,5 (1,5)	0,5 (1,5)	-	0,03	1 (3,5)
SW	0,25 (2,5)	0,1	0,1	0,03	-	0,1	0,1	0,03	0,25	0,5 (1,5)	0,5 (1,5)	-	0,03	1 (3,5)
WSW	-	0,25	0,1	0,03	-	0,1	0,1	0,03	0,03	0,5 (1,5)	0,5 (1,5)	-	0,03	-
W	-	0,25 (4)	0,03	0,03	-	0,1	0,1	0,03	0,03	0,5 (1,5)	0,5 (1,5)	-	0,03	-
WNW	-	0,25 (4)	0,1	0,03	-	0,1	0,25 (3)	0,03	0,1	0,5 (1,5)	0,5 (1,5)	-	0,03	-
NW	-	0,1	0,25	0,25	-	0,1	0,25 (3)	0,03	0,25 (4)	0,5 (1,5)	0,5 (1,5)	-	0,03	-
NNW	-	0,03	0,25	0,03	-	0,1	0,25	0,03	0,1	0,5 (1,5)	0,5 (1,5)	-	0,03	0,5 (3,5)

Station Number	0078227	0083572	0092081	0096072	0123685	0127272	0134479	0144791	0148517	0150620	0155394	0169880	0182465	0182591
Station Name	FORT BEAUFORT	LAMBERTSBAAI	BEAUFORT-WES	GRAAFF-REINET	QUEENSTOWN	UMTATA WO	CALVINIA WO	NOUPOORT	JAMESTOWN	ELLIOT	PORT EDWARD	DE AAR WO	PADDOCK	MARGATE
N	0,25	0,03	-	0,03	0,5 (3,5)	0,03	0,03	0,25	-	0,1	0,25	-	0,25	0,1
NNE	0,25	0,03	-	0,03	0,5 (3,5)	0,03	0,1	0,25	-	0,25	0,03	-	0,25	0,25
NE	0,1	0,03	-	0,03	0,25 (3,5)	0,03	0,25	0,1	-	0,25 (3,5)	0,0002	-	0,25	0,25
ENE	0,03	0,03	-	0,03	0,1	0,03	0,1	0,03	-	0,25 (3,5)	0,0002	-	0,25	0,25
E	0,03	0,03	-	0,03	0,03	0,03	0,1	0,03	-	0,25	0,0002	-	0,25	0,25
ESE	0,03	0,03	-	0,03	0,03	0,03	0,03	0,03	-	0,1	0,0002	-	0,25	-
SE	0,03	0,03	-	0,03	0,03	0,03	0,03	0,03	0,03	0,03	0,0002	-	0,25	-
SSE	0,03	0,03	-	0,03	0,03	0,03	0,03	0,03	0,03	0,1	0,0002	-	0,25	0,25
S	0,03	0,03	-	0,03	0,1	0,03	0,03	0,03	0,1	0,1	0,0002	-	0,25	0,25
SSW	0,1	0,03	-	0,03	0,1	0,03	0,03	0,03	0,25	0,1	0,0002	-	0,25	0,25
SW	0,1	0,03	-	0,03	0,25	0,1	0,03	0,1	0,25	0,1	0,1	-	0,25	0,25
WSW	0,03	0,1	-	0,03	0,25	0,25	0,03	0,25 (4)	0,25	0,1	0,25 (3,5)	-	0,25	0,1
W	0,03	0,1	-	0,03	0,25	0,25	0,03	0,25 (4)	0,25	0,1	0,25	-	0,25	0,1
WNW	0,1	0,1	-	0,03	0,25	0,1	0,03	0,25	0,25	0,1	0,25	-	0,25	0,1
NW	0,25	0,1	-	0,03	0,25	0,03	0,03	0,25	0,25	0,1	0,25	-	0,25	0,1
NNW	0,25	0,03	-	0,03	0,5 (3,5)	0,03	0,03	0,1	-	0,1	0,25	-	0,25	0,1

Station Number	0184491	0190868	0214700	0224400	0239698	0239699	0240808	0241072	0241076	0261516	0268016	0270155	0274034	0290468	0300454
Station Name	KOINGNAAS	BRANDVLEI	SPRINGBOK WO	PRIESKA	PIETERMARITZBURG	ORIBI AIRPORT	DURBAN WO	MOUNT EDGECOMBE	VIRGINIA	BLOEMFONTEIN WO	GAINTS CASTLE AWS	GREYTOWN	ALEXANDERBAAI	KIMBERLEY WO	LADYSMITH
N	0,1	0,03	-	0,1	-	0,25	0,25	-	0,25	0,03	-	0,25	0,005	0,03	0,1
NNE	0,1	0,1	-	0,1	-	0,25	0,25	-	0,1	0,03	-	0,25	0,005	0,03	0,1
NE	0,03	0,25	-	0,1	-	0,25 (3,5)	0,25	-	0,03	0,03	-	0,25	0,005	0,1	0,1
ENE	0,03	0,25	-	0,25	-	0,25	0,25	-	0,0002	0,1	-	0,25	0,005	0,03	0,1
E	0,03	0,25	-	0,1	-	0,25	0,25	0,1	0,0002	0,1	-	0,1	0,005	0,03	0,1
ESE	0,03	0,1	-	0,03	-	0,25	0,25	0,1	0,0002	0,1	-	0,1	0,005	0,03	0,1
SE	0,03	0,03	-	0,03	-	0,1	0,25	0,25	0,0002	0,03	-	0,1	0,005	0,03	0,03
SSE	0,03	0,03	-	0,03	-	0,1	0,1	0,25	0,0002	0,03	-	0,1	0,005	0,03	0,03
S	0,03	0,03	-	0,03	0,25	0,1	0,1	-	0,0002	0,03	-	0,1	0,03	0,03	0,03
SSW	0,03	0,03	-	0,03	0,25	0,25	0,03	0,25	0,0002	0,03	-	0,25 (2)	0,03	0,03	0,03
SW	0,03	0,03	-	0,03	0,25	0,25	0,03	0,25	0,03	0,1	-	-	0,03	0,03	0,03
WSW	0,03	0,03	-	0,03	0,25	0,25	0,1	0,5 (4)	0,1	0,03	-	-	0,03	0,03	0,03
W	0,03	0,03	-	0,03	0,5 (3,5)	0,25	0,25	0,5 (4)	0,25	0,03	-	-	0,005	0,03	0,03
WNW	0,1	0,03	-	0,03	0,5 (3,5)	0,25	0,25	-	0,25	0,03	-	-	0,005	0,03	0,03
NW	0,1	0,03	-	0,1	0,5 (3,5)	0,25	0,25	-	0,25	0,03	-	-	0,005	0,03	0,03
NNW	0,1	0,03	-	0,1	0,5 (3,5)	0,25	0,25	-	0,25	0,03	-	-	0,005	0,03	0,1

Station Number	Station Name	0304357 MTUNZINI	0317475 UPINGTON WO	0321110 POSTMASBURG	0331585 BETHLEHEM WO	0333682 VAN REENEN	0337738 ULUNDI	0339732 CHARTERS CREEK	0356880 KATHU	0360453 TAUNG	0362189 BLOEMHOF	0364300 WELKOM	0365398 KROONSTAD	0370856 NEWCASTLE	0410175 PONGOLA
N		0,25 (1,5)	0,03	0,25	0,1	0,1	0,25	0,25 (2)	0,03	0,1	-	0,03	-	0,25	0,1
NNE		0,25 (1,5)	0,03	0,25	0,03	0,1	0,25	0,25 (2)	0,03	-	-	0,03	-	0,25	0,1
NE		0,25 (1,5)	0,03	0,25	0,03	0,1	0,25	0,25 (2)	0,03	-	-	0,03	-	0,1	0,1
ENE		0,25 (1,5)	0,03	0,1	0,03	-	0,1	0,0002	0,03	-	-	0,03	-	0,03	0,1
E		0,25 (1,5)	0,03	0,03	0,03	-	0,25	0,0002	0,03	0,1	-	0,03	-	0,03	0,1
ESE		0,25 (1,5)	0,03	0,03	0,03	0,1	0,25	0,0002	0,03	0,1	0,03	0,03	-	0,03	0,1
SE		0,25 (1,5)	0,03	0,03	0,1	0,1	0,25	0,0002	0,03	0,1	0,03	0,03	-	0,03	0,1
SSE		0,25 (1,5)	0,03	0,03	0,1	-	0,25	0,03	0,03	0,1	0,03	0,03	-	0,03	0,1
S		0,25 (1,5)	0,03	0,03	0,1	-	0,25	0,25 (2)	0,03	0,1	0,03	0,03	-	0,03	0,1
SSW		0,25 (1,5)	0,03	0,03	0,1	-	0,03	0,25 (2)	0,03	0,1	0,03	0,03	-	0,03	0,1
SW		0,25 (1,5)	0,1	0,03	0,1	-	0,03	0,25 (2)	0,03	0,1	0,03	0,03	-	0,03	0,1
WSW		0,25 (1,5)	0,1	0,03	0,1	-	0,03	0,25 (2)	0,03	0,1	0,03	0,03	-	0,03	0,1
W		0,25 (1,5)	0,03	0,03	0,25	-	0,03	0,25 (2)	0,03	0,1	0,1	0,03	-	0,03	0,1
WNW		0,25 (1,5)	0,03	0,03	0,25	0,1	0,25	0,25 (2)	0,03	0,1	0,25	0,03	-	0,03	0,1
NW		0,25 (1,5)	0,03	0,03	0,25	0,1	0,25	0,25 (2)	0,03	0,1	0,1	0,03	-	0,03	0,1
NNW		0,25 (1,5)	0,03	0,1	0,25	0,1	0,25	0,25 (2)	0,03	0,1	0,1	0,03	-	0,1	0,1

Station Number	Station Name	0438784	0441416	0472278	0475879	0476399	0479870	0508047	0511399	0513346	0513385	0515320	0520691	0548375
		VEREENIGING	STANDERTON	LICHTENBURG	JHB BOT TUINE	JOHANNESBURG WO	ERMELO WO	MAFIKENG WO	RUSTENBURG	PRETORIA UNISA	IRENE WO	WITBANK	KOMATIDRAAI	PILANESBERG
N		0,03	-	0,03	1 (3,5)	0,1	0,03	0,03	1 (3,5)	-	0,1	0,03	0,25 (1,5)	0,1
NNE		0,03	1 (3,5)	0,03	0,25	0,03	0,03	0,03	1 (3,5)	-	0,1	0,03	0,25 (1,5)	0,1
NE		0,03	1 (3,5)	0,03	0,5 (3,5)	0,03	0,03	0,03	1 (3,5)	-	0,1	0,1	0,25 (1,5)	0,25
ENE		0,03	1 (3,5)	0,03	1 (3,5)	0,03	0,03	0,03	0,5 (3,5)	-	0,03	0,1	0,25 (1,5)	0,25 (3,5)
E		0,03	1 (3,5)	0,03	1 (3,5)	0,03	0,1	0,03	0,5 (3,5)	-	0,03	0,1	0,25 (1,5)	0,25 (3,5)
ESE		0,03	1 (3,5)	0,03	1 (3,5)	0,03	0,25	0,03	1 (4)	-	0,1	0,1	0,25 (1,5)	0,1
SE		0,03	1 (3,5)	0,03	1 (3,5)	0,03	0,25	0,03	1 (4)	-	0,1	0,25	0,25 (1,5)	0,03
SSE		0,03	1 (3,5)	0,03	-	0,03	0,1	0,03	1 (3,5)	-	0,1	0,1	0,25 (1,5)	0,03
S		0,1	1 (3,5)	0,03	0,25	0,03	0,25	0,03	1 (3,5)	-	0,1	0,1	0,25 (1,5)	0,1
SSW		0,25 (3,5)	1 (3,5)	0,03	-	0,1	0,25	0,03	0,5 (3,5)	-	0,1	0,1	0,25 (1,5)	0,1
SW		0,25	0,25	0,03	-	0,25	0,25	0,03	0,25	-	0,25 (3,5)	0,1	0,25 (1,5)	0,1
WSW		0,25	0,1	0,03	0,25	0,5 (5)	0,25	0,03	0,25	-	0,25 (3,5)	0,1	0,25 (1,5)	0,1
W		0,1	0,03	0,03	0,25	0,5 (8)	0,1	0,1	0,5 (3,5)	-	0,25 (3,5)	0,1	0,25 (1,5)	0,1
WNW		0,25	0,03	0,03	1 (3,5)	0,5 (8)	0,03	0,1	1(3,5)	-	0,1	0,1	0,25 (1,5)	0,03
NW		0,03	0,1	0,03	1 (3,5)	0,25	0,03	0,03	1 (3,5)	-	0,1	0,25	0,25 (1,5)	0,1
NNW		0,03	-	0,03	1 (3,5)	0,5 (8)	0,03	0,03	1 (3,5)	-	0,1	0,25	0,25 (1,5)	0,1

Station Number	Station Name	N	NNE	NE	ENE	E	ESE	SE	SSE	S	SSW	SW	WSW	W	WNW	NW	NNW
0587725	THABAZIMBI	0,25	0,25	0,25	0,25	0,25	0,25 (3,5)	0,25 (3,5)	-	-	-	-	-	-	-	0,1	-
0594626	GRASKOP AWS	0,25 (3,5)	0,25 (3,5)	0,25	0,25	0,25	0,25	0,25	0,25	0,25	0,25 (3,5)	0,25 (3,5)	0,25 (3,5)	0,25 (3,5)	0,25	0,25	0,25
0638081	HOEDSPRUIT	0,03	0,03	0,03	0,03	0,03	0,03	0,03	0,03	0,03	0,03	0,03	0,03	0,03	0,03	0,03	0,03
0674341	ELLISRAS	0,1	0,1	0,1	0,1	0,1	0,1	0,1	0,1	0,1	0,25	0,25	0,25	0,25	0,1	0,1	0,1
0675666	MARKEN	0,25	0,25	0,25	0,25	0,25	0,25	0,25	0,25	0,25	0,25	0,25	0,25	0,25	0,25	0,25	0,25
0677802	PIETERSBURG WO	0,03	0,03	0,03	0,1	0,25	0,25	0,25	0,25	0,25	0,25	0,1	0,1	0,03	0,03	0,03	0,03
0723664	THOHOYANDOU WO	0,03	0,03	0,03	0,1	0,1	0,1	0,1	0,1	0,1	0,03	0,03	0,03	0,03	0,1	0,1	0,03

Empty cells indicate that it was impossible to make an accurate visual assessment of the roughness length. Where applicable, z_d (m) is given in brackets.

6.5.2. Correction factors for mean wind speed due to terrain category

The logarithmic wind profile, which gives the relationship between mean wind speed and the height above the surface in the planetary boundary layer, is the best representation of wind speeds at low elevations (Wever and Groen, 2009). The wind speed u, at height z, is given by

$$u_z = (u_*/\kappa)\{\ln[(z - z_d)/z_0] + \psi(z, z_0, L)\} \quad (6.1)$$

where u_* is the friction velocity, κ is Von Karmann's constant ($\approx 0{,}4$), and ψ is a stability term where L is the Monin-Obukhov stability parameter (Monin and Obukhov, 1954). During strong winds a neutral atmosphere can be assumed, and the stability corrections

in the logarithmic wind profile become unimportant (De Rooy and Kok, 2004). The stability term can then be ignored.

If a logarithmic wind profile is assumed, the wind speed can be estimated up to the blending height, which is defined as the height at which the wind speed will not vary significantly horizontally, in spite of local surface roughness variations (Wieringa, 1986). Therefore, if the wind speed at the blending height is known, the "potential wind speed", u_p, can be estimated, which is defined as the wind speed over a hypothetical flat open surface at a specific reference height (Wieringa, 1986). By applying the logarithmic wind profile

$$u_p = u_b\{[\ln(z_r/z_{0,r})]/[\ln(z_b/z_{0,r})]\} \quad (6.2)$$

where u_b is the wind speed at the blending height, z_r is the reference height, $z_{0,r}$ is the roughness length of the hypothetical surface, and z_b is the blending height. From Wieringa (1986), and applied by Wever and Groen (2009) and others, when the local roughness length is known, the Exposure Correction Factor (ECF) due to improper terrain category can now be calculated, by using

$$ECF = [\ln(z_b/z_0)\ln(z_r/z_{0,r})]/[\ln(z_m/z_0)\ln(z_b/z_{0,r})] \quad (6.3)$$

where z_m is the measuring height, usually 10 m. The blending height z_b is typically taken as 60 m. Several authors suggest that the exact blending height is not very critical, because vertical gradients are small at these heights (De Rooy and Kok, 2004); e.g. McNaughton and Jarvis (1984) used 100 m, Wieringa (1986), Wever and Groen (2009) and others used 60 m, and De Rooy and Kok (2004) used 120 m. For a typical example, where z_0 = 0,25 m, the value of the ECF is equal to 1,14 for z_b equal to 60 m, and 1,17 for z_b equal to 120 m. This corresponds to a difference in ECF of only 0,03.

The reference roughness length $z_{0,r}$ is taken as 0,03 m. In the case where z_d comes into play, z_m should be reduced by the height of z_d. This is because the wind profiles and similarity relations in the boundary layer are only realistic when related to a "ground" surface located at z_d (Davenport, 2000). The ECF is therefore modified to

$$ECF = [\ln(z_b/z_0)\ln(z_r/z_{0,r})]/[\ln(z_m - z_d/z_0)\ln(z_b/z_{0,r})] \quad (6.4)$$

Table 6.5 presents the ECF for the 22,5º sectors for which z_0 and z_d were derived, by the application of equation 6.4. It can be seen that for most stations and most wind sectors, a correction factor is need to increase the measured wind speeds. While most of the ECF values are close to unity, there are instances where high correction factors are required. The highest correction factors are for those stations located in urban or built-up areas, or on the fringes thereof. The values of the ECF can then be as high as 1,67, e.g. the weather station in Strand.

Table 6.5. Terrain exposure correction factors for the 16 wind directions around the weather stations.

Station Number	Station Name	N	NNE	NE	ENE	E	ESE	SE	SSE	S	SSW	SW	WSW	W	WNW	NW	NNW
0003108	STRUISBAAI	1,00	1,00	1,00	1,00	0,89	0,89	0,89	0,89	1,00	1,00	1,00	0,89	0,89	1,00	1,00	1,00
0005609	STRAND	-	-	-	-	-	-	-	-	-	-	-	-	-	-	-	-
0006386	HERMANUS	1,00	1,00	1,00	1,00	1,00	1,00	1,00	1,00	1,00	1,00	1,00	1,00	1,00	1,00	1,00	1,00
0007699	TYGERHOEK	-	-	-	-	-	-	-	-	-	-	-	-	-	-	-	-
0010682	STILBAAI	1,00	1,00	1,00	1,29	1,43	1,43	1,29	1,00	1,00	1,00	1,00	1,00	1,00	1,00	1,00	1,00
0012661	GEORGE WO	1,00	1,00	1,06	1,06	1,06	1,06	1,06	1,06	1,06	1,06	1,00	1,00	1,00	1,06	1,06	1,06
0014123	KNYSNA	-	-	-	-	-	-	1,14	1,14	1,43	1,43	1,29	1,06	1,06	1,75	-	-
0014545	PLETTENBERGBAAI	1,00	1,00	1,00	1,00	1,00	1,00	1,00	1,00	1,00	1,00	1,00	1,00	1,00	1,00	1,00	1,00
0015692	TSITSIKAMMA	-	-	-	-	0,89	0,89	0,89	0,89	0,89	0,89	0,89	0,89	-	-	-	-

Station Number	0020618	0021178	0021823	0022729	0033556	0034763	0035209	0040192	0041388	0041841	0045642	0056917	0059572
Station Name	ROBBENEILAND	CAPE TOWN WO	PAARL	WORCESTER	PATENSIE	UITENHAGE	PORT ELIZABETH	GEELBEK	MALMESBURY	PORTERVILLE	LAINGSBURG	GRAHAMSTOWN	EAST LONDON WO
N	0,89	1,06	1,14	1,00	-	1,29	1,06	1,00	1,43	1,06	-	1,00	1,14
NNE	0,89	1,06	1,14	1,00	-	1,29	1,06	1,00	1,43	1,06	-	1,06	1,14
NE	0,89	1,06	1,43	1,00	-	1,29	1,06	1,00	1,29	1,06	-	1,14	1,14
ENE	0,89	1,00	1,43	1,00	-	1,14	1,14	1,00	1,43	1,14	-	1,14	1,14
E	0,89	1,06	1,43	1,00	-	1,06	1,14	1,00	1,43	1,14	-	1,00	1,14
ESE	0,89	1,00	1,67	1,26	-	1,06	1,14	1,00	1,26	1,14	-	1,14	1,14
SE	0,94	1,00	1,67	1,26	-	1,06	1,06	1,00	1,06	1,14	-	1,43	1,14
SSE	1,00	1,00	1,43	1,00	1,06	1,19	1,00	1,00	1,06	1,14	-	1,14	1,14
S	1,00	1,00	1,67	1,00	1,29	1,29	1,00	1,00	1,06	1,14	-	1,00	1,14
SSW	1,00	1,14	1,67	1,00	1,29	1,29	1,14	1,00	1,06	1,14	-	1,00	1,14
SW	1,00	1,67	1,67	1,00	1,29	1,29	1,14	1,00	1,06	1,06	-	1,00	1,06
WSW	1,17	1,14	-	1,00	1,29	1,29	1,00	1,00	1,06	1,06	-	1,00	1,06
W	1,00	1,14	-	1,00	1,29	1,29	1,00	1,00	1,06	1,06	-	1,00	1,00
WNW	0,96	1,06	-	1,00	1,29	1,29	1,06	1,00	1,26	1,06	-	1,00	1,06
NW	0,96	1,06	-	1,00	1,29	1,29	1,32	1,00	1,26	1,06	-	1,14	1,14
NNW	0,89	1,00	1,43	1,00	1,29	1,29	1,06	1,00	1,14	1,06	-	1,00	1,14

Station Number	Station Name	N	NNE	NE	ENE	E	ESE	SE	SSE	S	SSW	SW	WSW	W	WNW	NW	NNW
0061298	LANGEBAANWEG	1,00	1,00	1,00	1,00	1,00	1,00	1,06	1,00	1,00	1,00	1,06	1,14	1,32	1,32	1,06	1,00
0063807	EXCELSIOR CERES	-	-	-	1,14	1,23	1,23	1,06	1,23	1,23	1,23	1,23	-	-	-	-	-
0078227	FORT BEAUFORT	1,14	1,14	1,06	1,00	1,00	1,00	1,00	1,00	1,00	1,06	1,06	1,00	1,00	1,06	1,14	1,14
0083572	LAMBERTSBAAI	1,00	1,00	1,00	1,00	1,00	1,00	1,00	1,00	1,00	1,00	1,00	1,06	1,06	1,06	1,06	1,00
0092081	BEAUFORT-WES	-	-	-	-	-	-	-	-	-	-	-	-	-	-	-	-
0096072	GRAAFF-REINET	1,00	1,00	1,00	1,00	1,00	1,00	1,00	1,00	1,00	1,00	1,00	1,00	1,00	1,00	1,00	1,00
0123685	QUEENSTOWN	1,43	1,43	1,29	1,06	1,00	1,00	1,00	1,00	1,06	1,06	1,14	1,14	1,14	1,14	1,14	1,43
0127272	UMTATA WO	1,00	1,00	1,00	1,00	1,00	1,00	1,00	1,00	1,00	1,00	1,06	1,14	1,14	1,06	1,00	1,00
0134479	CALVINIA WO	1,00	1,06	1,14	1,06	1,06	1,00	1,00	1,00	1,00	1,00	1,00	1,00	1,00	1,00	1,00	1,00
0144791	NOUPOORT	1,14	1,14	1,06	1,00	1,00	1,00	1,00	1,00	1,00	1,00	1,06	1,32	1,32	1,14	1,14	1,06
0148517	JAMESTOWN	-	-	-	-	-	-	1,00	1,00	1,06	1,14	1,14	1,14	1,14	1,14	1,14	-
0150620	ELLIOT	1,06	1,14	1,29	1,29	1,14	1,06	1,00	1,06	1,06	1,06	1,06	1,06	1,06	1,06	1,06	1,06
0155394	PORT EDWARD	1,14	1,00	0,89	0,89	0,89	0,89	0,89	0,89	0,89	0,89	1,06	1,29	1,14	1,14	1,14	1,14

Station Number	Station Name	N	NNE	NE	ENE	E	ESE	SE	SSE	S	SSW	SW	WSW	W	WNW	NW	NNW
0169880	DE AAR WO	-	-	-	-	-	-	-	-	-	-	-	-	-	-	-	-
0182465	PADDOCK	1,14	1,14	1,14	1,14	1,14	1,14	1,14	1,14	1,14	1,14	1,14	1,14	1,14	1,14	1,14	1,14
0182591	MARGATE	1,06	1,14	1,14	1,14	1,14	-	-	1,14	1,14	1,14	1,14	1,06	1,06	1,06	1,06	1,06
0184491	KOINGNAAS	1,06	1,06	1,00	1,00	1,00	1,00	1,00	1,00	1,00	1,00	1,00	1,00	1,00	1,06	1,06	1,06
0190868	BRANDVLEI	1,00	1,06	1,14	1,14	1,14	1,06	1,00	1,00	1,00	1,00	1,00	1,00	1,00	1,00	1,00	1,00
0214700	SPRINGBOK WO	-	-	-	-	-	-	-	-	-	-	-	-	-	-	-	-
0224400	PRIESKA	1,06	1,06	1,06	1,14	1,06	1,00	1,00	1,00	1,00	1,00	1,00	-	-	-	1,06	-
0239698	PIETERMARITZBURG	-	-	-	-	-	-	-	-	1,14	1,14	1,14	1,43	1,43	1,43	1,43	1,43
0239699	ORIBI AIRPORT	1,14	1,14	1,29	1,14	1,14	1,14	1,06	1,06	1,06	1,14	1,14	1,14	1,14	1,14	1,14	1,14
0240808	DURBAN WO	1,14	1,14	1,14	1,14	1,14	1,14	1,14	1,06	1,06	1,00	1,14	1,06	1,14	1,14	1,14	1,14
0241072	MOUNT EDGECOMBE	-	-	-	-	1,06	1,06	1,14	1,14	-	1,14	1,14	1,47	1,47	-	-	-
0241076	VIRGINIA	1,14	1,06	1,00	0,89	0,89	0,89	0,89	0,89	0,89	0,89	1,00	1,06	1,14	1,14	1,14	1,14
0261516	BLOEMFONTEIN WO	1,00	1,00	1,00	1,06	1,06	1,06	1,00	1,00	1,00	1,00	1,06	1,00	1,00	1,00	1,00	1,00
0268016	GAINTS CASTLE AWS	-	-	-	-	-	-	-	-	-	-	-	-	-	-	-	-

Station Number	0270155	0274034	0290468	0300454	0304357	0317475	0321110	0331585	0333682	0337738	0339732	0356880	0360453	0362189
Station Name	GREYTOWN	ALEXANDERBAAI	KIMBERLEY WO	LADYSMITH	MTUNZINI	UPINGTON WO	POSTMASBURG	BETHLEHEM WO	VAN REENEN	ULUNDI	CHARTERS CREEK	KATHU	TAUNG	BLOEMHOF
N	1,14	0,94	1,00	1,06	1,19	1,00	1,14	1,06	1,06	1,14	1,21	1,00	1,06	-
NNE	1,14	0,94	1,00	1,06	1,19	1,00	1,14	1,00	1,06	1,14	1,21	1,00	-	-
NE	1,14	0,94	1,06	1,06	1,19	1,00	1,14	1,00	1,06	1,14	1,21	1,00	-	-
ENE	1,14	0,94	1,00	1,06	1,19	1,00	1,06	1,00	-	1,06	0,89	1,00	-	-
E	1,06	0,94	1,00	1,06	1,19	1,00	1,00	1,00	-	1,14	0,89	1,00	1,06	-
ESE	1,06	0,94	1,00	1,06	1,19	1,00	1,00	1,00	1,06	1,14	0,89	1,00	1,06	1,00
SE	1,06	0,94	1,00	1,00	1,19	1,00	1,00	1,06	1,06	1,14	0,89	1,00	1,06	1,00
SSE	1,06	0,94	1,00	1,00	1,19	1,00	1,00	1,06	-	1,14	1,00	1,00	1,06	1,00
S	1,06	1,00	1,00	1,00	1,19	1,00	1,00	1,06	-	1,14	1,21	1,00	1,06	1,00
SSW	1,21	1,00	1,00	1,00	1,19	1,00	1,00	1,06	-	1,00	1,21	1,00	1,06	1,00
SW	-	1,00	1,00	1,00	1,19	1,06	1,00	1,06	-	1,00	1,21	1,00	1,06	1,00
WSW	-	1,00	1,00	1,00	1,19	1,06	1,00	1,06	-	1,00	1,21	1,00	1,06	1,00
W	-	0,94	1,00	1,00	1,19	1,00	1,00	1,14	-	1,00	1,21	1,00	1,06	1,06
WNW	-	0,94	1,00	1,00	1,19	1,00	1,00	1,14	1,06	1,14	1,21	1,00	1,06	1,14
NW	-	0,94	1,00	1,06	1,19	1,00	1,00	1,14	1,06	1,14	1,21	1,00	1,06	1,06
NNW	-	0,94	1,00	1,06	1,19	1,00	1,06	1,14	1,06	1,14	1,21	1,00	1,06	1,06

Station Number	0364300	0365398	0370856	0410175	0427083	0438784	0441416	0472278	0475879	0476399	0479870	0508047	0511399	0513346
Station Name	WELKOM	KROONSTAD	NEWCASTLE	PONGOLA	VAN ZYLSRUS	VEREENIGING	STANDERTON	LICHTENBURG	JHB BOT TUINE	JOHANNESBURG WO	ERMELO WO	MAFIKENG WO	RUSTENBURG	PRETORIA UNISA
N	1,00	-	1,14	1,06	-	1,00	-	1,00	1,67	1,06	1,00	1,00	1,67	-
NNE	1,00	-	1,14	1,06	-	1,00	1,67	1,00	1,14	1,00	1,00	1,00	1,67	-
NE	1,00	-	1,06	1,06	-	1,00	1,67	1,00	1,43	1,00	1,00	1,00	1,67	-
ENE	1,00	-	1,00	1,06	-	1,00	1,67	1,00	1,67	1,00	1,00	1,00	1,43	-
E	1,00	-	1,00	1,06	-	1,00	1,67	1,00	1,67	1,00	1,06	1,00	1,43	-
ESE	1,00	-	1,00	1,06	-	1,00	1,67	1,00	1,67	1,00	1,14	1,00	1,75	-
SE	1,00	-	1,00	1,06	-	1,00	1,67	1,00	1,67	1,00	1,14	1,00	1,75	-
SSE	1,00	-	1,00	1,06	-	1,00	1,67	1,00	-	1,00	1,06	1,00	1,67	-
S	1,00	-	1,00	1,06	-	1,06	1,67	1,00	1,14	1,00	1,14	1,00	1,67	-
SSW	1,00	-	1,06	1,06	-	1,29	1,67	1,00	-	1,06	1,14	1,00	1,43	-
SW	1,00	-	1,00	1,06	-	1,14	1,14	1,00	-	1,14	1,14	1,00	1,14	-
WSW	1,00	-	1,00	1,06	-	1,14	1,06	1,00	1,14	1,59	1,14	1,00	1,14	-
W	1,00	-	1,00	1,06	-	1,06	1,00	1,00	1,14	2,64	1,06	1,06	1,43	-
WNW	1,00	-	1,00	1,06	-	1,14	1,00	1,00	1,67	2,64	1,00	1,06	1,67	-
NW	1,00	-	1,00	1,06	-	1,00	1,06	1,00	1,67	1,14	1,00	1,00	1,67	-
NNW	1,00	-	1,06	1,06	-	1,00	-	1,00	1,67	2,64	1,00	1,00	1,67	-

Station Number	Station Name	N	NNE	NE	ENE	E	ESE	SE	SSE	S	SSW	SW	WSW	W	WNW	NW	NNW
0513385	IRENE WO	1,06	1,06	1,06	1,00	1,00	1,06	1,06	1,06	1,06	1,06	1,29	1,29	1,29	1,06	1,06	1,06
0515320	WITBANK	1,00	1,00	1,06	1,06	1,06	1,06	1,14	1,06	1,06	1,06	1,06	1,06	1,06	1,06	1,14	1,14
0520691	KOMATIDRAAI	1,19	1,19	1,19	1,19	1,19	1,19	1,19	1,19	1,19	1,19	1,19	1,19	1,19	1,19	1,19	1,06
0548375	PILANESBERG	1,06	1,06	1,14	1,29	1,36	1,06	1,00	1,00	1,06	1,06	1,06	1,06	1,06	1,00	1,06	
0587725	THABAZIMBI	1,14	1,14	1,14	1,14	1,14	1,29	1,29	-	-	-	-	-	-	-	1,06	-
0594626	GRASKOP AWS	1,29	1,29	1,14	1,14	1,14	1,14	1,14	1,14	1,14	1,29	1,29	1,29	1,29	1,14	1,14	1,14
0638081	HOEDSPRUIT	1,00	1,00	1,00	1,00	1,00	1,00	1,00	1,00	1,00	1,00	1,00	1,00	1,00	1,00	1,00	1,00
0674341	ELLISRAS	1,06	1,06	1,06	1,06	1,06	1,06	1,06	1,06	1,06	1,14	1,14	1,14	1,14	1,06	1,06	1,06
0675666	MARKEN	1,14	1,14	1,14	1,14	1,14	1,14	1,14	1,14	1,14	1,14	1,14	1,14	1,14	1,14	1,14	1,14
0677802	PIETERSBURG WO	1,00	1,00	1,00	1,06	1,14	1,14	1,14	1,14	1,14	1,14	1,06	1,06	1,00	1,00	1,00	1,00
0723664	THOHOYANDOU WO	1,00	1,00	1,00	1,06	1,06	1,06	1,06	1,06	1,06	1,00	1,00	1,00	1,00	1,06	1,06	1,00

Empty cells indicate that it was impossible to estimate ECF due to complex topography, or the sheltering by close-by obstacles.

The accuracy of correction factors outside the range 0,8<ECF<1,2 is likely to be poor. While for 14 weather stations eventually utilised this such ECF were applied, it was only for a few strong wind values per station.

6.5.3. Correction factors from building design standards

The correction factors for mean wind speeds can also be deduced from the procedures for exposure correction prescribed by the various building design standards. For example, in the exposure procedures discussed in EN 1991-1-4, the mean wind velocity v_m at height z is given by

$$v_m(z) = c_r(z)c_o(z)v_b \tag{6.5}$$

where $c_r(z)$ is the roughness factor, and $c_o(z)$ is the orography factor (taken as 1 for flat terrain), and v_b is the wind speed that would be measured in Terrain Category II. It follows then that

$$v_b = v_m(z)/c_r(z) \tag{6.6}$$

$c_r(z)$ accounts for the ground roughness of the terrain upwind of the point of interest and is defined by

$$c_r(z) = k_r ln(z/z_0) \qquad 10 \text{ m} < z < 200 \text{ m} \tag{6.7}$$

where z_0 is the roughness length. The variable k_r is called the terrain factor, which depends on z_0:

$$k_r = 0.19\left(z_0/z_{0,II}\right)^{0.07} \tag{6.8}$$

where $z_{0,II}$ is equal to 0,05 m, corresponding to Terrain Category II. From the above discussion it follows that the measured wind speed can be adjusted to that of a wind blowing over Terrain Category II, by employing the local roughness factor. For cases where the anemometer is at height 10 m, it follows then that

$$c_r(10) = 0.19(z_0/0.05)^{0.07} ln(10/z_0) \tag{6.9}$$

where z_0 is the roughness length, that can be obtained from Table 6.1 or 6.3. Then

$$v_{II}(10) = v_m(10)/c_r(10) \tag{6.10}$$

which is the mean wind speed adjusted to a terrain with z_0 = 0,05, at a height of 10 m.

Due to the conservatism of the building design standard, the approach in EN 1991-1-4 is to use the lowest observed roughness length that appears in a particular angular sector under consideration. As this exercise is essentially a reversal of the calculations in EN 1991-1-4, it is suggested here that the roughness length of a given wind direction is determined by the terrain category that covers the largest area within a 30° angular sector from that wind direction, over a distance of 2 km, which is sufficient (Hansen, pers. comm.). As an example, consider an anemometer which is surrounded by the Terrain Category III in Table 6.1. The value of z_0 is then estimated as 0,3 m. To compare the values obtained in section 6.5.2 with equation 6.9, the roughness factor for Terrain Category II in Table 6.1 is changed to 0,03 in equation 6.9. The value of $c_r(10)$ is then found to be equal to 0,78. The correction factor with which the measured wind speed should therefore be multiplied is 1/0,78, which is equal to 1,28. This value is substantially higher than if the methodology in section 6.5.2 is applied, which will for the same z_0 give an ECF of 1,15.

Other comparisons of estimated correction factors are presented in Table 6.6, where the ECF for the terrain categories in Table 6.1 is compared to the correction factors deduced from some of the available building design standards.

Table 6.6. The ECF for Terrain Categories I to IV in Table 6.1, compared to correction factors deduced from the building design standards.

Terrain category	ECF	EN 1991-1-4	AS 1170.2	ASCE 7-98	SANS 10160-1989	GBJ 9-87	SANS 10160-3
I	0,96	0,82	0,89	0,90	0,91	0,72	0,92
II	1,02	0,96	1,00	1,01	1,00	1,00	1,02
III	1,15	1,28	1,20	1,26	1,35	-	1,18
IV	1,36	1,79	1,33	2,29	1,54	1,41	1,41

EN 1991-1-4 (2005) (European Standard), AS 1170.2 (1989) (Australian Standard), ASCE 7-98 (1998) (American Standard), SANS 10160-1989 (1989) (South African Standard), GBJ 9-87 (1994) (Chinese Standard) and SANS 10160-3 (2010) (new proposed South African Standard).

For Terrain Category I the ECF gives the smallest correction, i.e. the closest to 1, to be made to the measured wind speed. The correction factors for Terrain Category II should be close to 1. For Terrain Category III the ECF also gives the smallest correction to be applied, while for Terrain Category IV it is the second lowest of the corrections tabulated.

In the calculation of the ECF, as presented in Table 6.5, the separation height z_d is in the majority of cases taken into account whenever z_0 is equal or greater than 0,25 m. The incorporation of z_d tends to produce a larger correction factor, if compared to the correction factor determined without z_d. Table 6.7 presents the correction factor for various roughness lengths equal and above 0,25, and separation heights z_d equal and above 0 m. From the results it can be concluded that for the larger values of z_0, in most instances the magnitude of the ECF will compare well with the correction factors deduced from the building standards in Table 6.6, due to the incorporation of z_d in the calculation of the ECF. Therefore the application of the ECF's, as estimated in section 6.5.2, can be regarded to be an acceptable method to correct the measured wind speeds, to obtain estimates of the basic mean wind speed.

Table 6.7. The ECF for various roughness lengths z_0 equal and above 0,25 m, and separation height z_d equal and above 0 m.

z_0	z_d					
	0	**1**	**1,5**	**2**	**2,5**	**3**
0,25	1,14	1,17	1,19	1,21	1,23	1,26
0,5	1,22	1,27	1,29	1,32	1,35	1,39
1	1,36	1,42	1,46	1,50	1,55	1,61
1,5	1,49	1,57	1,63	1,68	1,75	1,83

6.5.4. Other distortions to wind flow

Where there are obstacles close to the anemometer which will distort the wind flow, the best way to obtain correction factors to the wind measurements is by full-scale testing or by a wind tunnel study, but also by the application of software which are specifically designed to address these problems. The same applies for topography which does not conform to the ideally flat terrain required for the calculation of the design wind speeds. However, the applications of these methods fall beyond the scope of this study. Therefore, wind analysis results of the weather stations with major obstacle, terrain or topography problems are not included in the data sets that can be used in the development of the proposed design wind speed maps.

6.5.5. Correction factors for wind gust data

The correction factors discussed so far in this chapter apply, in a strict sense, to mean wind speeds, measured over periods of 10 minutes or longer. There has been considerable debate on the application of correction factors to wind gusts, and it mostly revolves around the uncertainty of the origin of particular wind gusts. Because correction factors take into consideration the surface roughness over long distances, such correction factors should ideally not be applied to wind gusts which originate in the very close vicinity of an anemometer, e.g. if caused by the outflow from a local thunderstorm. However, it can be argued that some wind gusts originate further away, so that the surface roughness can affect the strength of the wind gusts. While it is impossible to make such distinctions from the available information, it is attempted here to make a broad assessment on the desirability of applying correction factors to the 2-3 second wind gusts.

ISO 4354: 2009, the International Standard on Wind Action and Structures, supply typical correction factors applicable to wind gust speeds for reference conditions, in relation to the terrain category. For synoptic storms, the correction factors for the 3 s

wind gusts at a height 0f 10 m are presented in Table 6.8, for the different terrain categories. These correction factors are deduced from Table C1 in ISO 4354: 2009.

Table 6.8. Correction factors for the 3 s wind gusts deduced from ISO 4354: 2009, at a height of 10 m for the different terrain categories.

Terrain roughness category	Roughness length (m)	Correction factor
I. Open sea/flat surface	z_0 = 0,003	0,90
II. Open country	z_0 = 0,03	1,00
III. Suburban	z_0 = 0,3	1,19

For thunderstorm gusts the correction factor is assumed to be 1,0 at a height of 10 m, for all the terrain categories. This decision is guided by Table C2 in ISO 4354: 2009. Therefore no corrections are applied to the wind gust values which originated from thunderstorms.

Due to the differential application of correction factors for synoptic storms and thunderstorms respectively, the annual maximum wind gusts utilised in the Gumbel and mixed strong wind climate analyses were first corrected. These analyses were investigated and a decision was then taken of the most likely causes of the 1:50 year annual maximum wind gusts at particular weather stations. This was done to decide on whether to apply correction factors to the wind gust values in the POT analysis.

The following decision was taken: If the 1:50 year annual maximum wind gust is most likely produced by a thunderstorm, no correction factors are applied to the wind gust values utilised. However, if the most probable cause of the 1:50 year annual maximum wind gust is synoptic in origin, the correction factors presented in Table 6.8 are applied to the wind gust values.

Chapter 7

Design Wind Speed Values for South Africa

7.1. General

The Institute of Structural Engineering at Stellenbosch University and the CSIR are currently involved in the process of developing a set of new generation building design codes for South Africa. The wind-loading procedure of the current code is based on the extreme wind analysis by Milford (1985a and b) which utilised the data of only 15 weather stations. In Chapter 6 it was shown that the number of weather stations which have suitable data available for a present extreme wind analysis for South Africa is 76, which is about five-fold if compared to the previous analysis. Due to the climatological diversity of South Africa, such an increase in the spatial coverage of extreme values promises to make a significant improvement on the maps in Figure 2.8, if updated design wind speed maps were to be developed for the country.

7.2. Statistical estimation methods and selected quantiles

It was shown in Chapter 5 that the choice of the best approach to statistically estimate extreme wind values ultimately depend on various factors, which are:

- The period of record;
- The averaging period of the measured wind speed values;
- The strong-wind producing mechanisms involved; and
- The temporal spacing of the strong wind values to be utilised.

Of these factors the period of record seems to be the most critical in the selection of an appropriate statistical approach. Due to the fact that the data series of all the weather stations are between 10 and 20 years long, approaches based on the annual extreme

wind speed values are acceptable but not ideal. This was shown to be especially true for the more general GEV approach, where the values of the shape parameter κ are not restricted to zero as is the case with the Gumbel approach. It was found that the non-zero estimations for κ cannot be reliably considered when short time series are analysed, and that in such cases it is better to use the Gumbel method. Even with the POT approach, where it was possible to use many more strong wind values, similar dubious values for κ were obtained as with the GPD method. More realistic results were obtained with the EXP method, where the value of κ is assumed to be zero.

Regarding the different averaging periods of the wind data series, it was found that the POT approach is not compatible with the hourly mean wind speeds. Therefore only annual extreme methods can be used in estimating extreme hourly mean wind speeds, while both the annual extreme and POT approaches are compatible with the estimation of the extreme 2-3 second wind gusts.

Where there is more than one strong wind producing mechanism involved in producing annual extreme winds, which is the case for a large part of South Africa as shown in Chapter 4, it is advisable to use a mixed distribution approach as demonstrated in section 5.5.

The temporal spacing of strong wind values has a bearing on the number of data values that can be utilised in the POT method. In time series where many consecutive values are relatively high, an unacceptably high percentage of strong wind values can be statistically dependent, even when a very high threshold value is selected. For some weather stations the POT method could not be applied due to this effect. The optimum statistical method to estimate extreme wind values should therefore be selected on a station-by-station basis, by taking all of the above factors into account.

Following are the selection criteria for the most realistic, but also conservative, extreme wind values for the maps of the 1:50 year hourly mean wind speed values and the 1:50 year extreme wind gusts:

- For hourly mean wind speeds the result from the Gumbel distribution was used, except where the strong winds were forthcoming from more than one strong wind producing mechanism. Then the results from the mixed distribution method were used.
- For wind gusts a choice had to be made between the results of the Gumbel, mixed distribution, and the EXP methods. Where strong gusts were forthcoming only from one strong wind producing mechanism, results from the EXP or Gumbel methods were used. In cases of more than one strong wind producing mechanism, the estimated values of the mixed distribution and EXP methods were selected. For conservativeness, where a choice had to be made between the results of different methodologies (e.g. Gumbel and EXP), the higher quantile value was then selected.

In Chapter 6 it was shown that the surroundings of most weather stations do not conform to the prescribed terrain, which is described by Terrain Category II in Table 6.1. A Terrain Category II is required for the direct and consistent estimation of extreme wind speeds for design purposes. Therefore, for the development of maps of the 1:50 year wind speeds, only those weather stations were selected of which the surroundings conform to terrain Category II, or where the exposure could realistically be corrected to conform to Terrain Category II, as discussed in Chapter 6. Table 7.1 presents the resultant list of 76 weather stations that were utilised for the development of the 1:50 year maps. Also presented are the selected statistical methods for the estimation of the extreme values, i.e. the 1:50 year wind gust and hourly mean wind speed quantiles, and the nature of exposure corrections where applicable.

Table 7.1. Selected statistical methods and values of the 1:50 year quantiles of annual maximum wind gusts and annual maximum hourly mean wind speeds.

Station Number	Station Name	Wind gust			Hourly mean wind speed		
		Method	X_{50}	Exposure correction	Method	X_{50}	Exposure correction
0003108	STRUISBAAI	EXP	41,3	Table 6.8	Mixed	23,6	ECF
0005609	STRAND	Mixed	43,9	Table 6.8	Mixed	23,2	ECF
0006386	HERMANUS	EXP	43,5	Table 6.8	Mixed	24,6	ECF
0007699	TYGERHOEK	EXP	37,3	Table 6.8	Gumbel	18,5	ECF
0010682	STILBAAI	EXP	30,3	Table 6.8	Gumbel	16,2	ECF
0012661	GEORGE WO	EXP	33,3	Table 6.8	Gumbel	21,4	ECF
0014123	KNYSNA	Gumbel	33,5	Table 6.8	Gumbel	20,8	ECF
0014545	PLETTENBERGBAAI	Gumbel	31,1	Table 6.8	Mixed	15,9	ECF
0015692	TSITSIKAMMA	EXP	28,0	Table 6.8	Gumbel	14,5	ECF
0020618	ROBBENEILAND	EXP	28,7	Table 6.8	Mixed	14,4	ECF
0021178	CAPE TOWN WO	Mixed	38,3	Table 6.8	Mixed	22,7	ECF
0021823	PAARL	Mixed	31,1	Table 6.8	Mixed	18,4	ECF
0022729	WORCESTER	EXP	41,5		Gumbel	21,5	
0033556	PATENSIE	Mixed	33,1	Table 6.8	Mixed	15,4	ECF
0034763	UITENHAGE	Mixed	39,3	Table 6.8	Gumbel	21,3	ECF
0035209	PORT ELIZABETH	EXP	40,4	Table 6.8	Gumbel	24,7	ECF
0040192	GEELBEK	EXP	28,8		Mixed	15,9	
0041388	MALMESBURY	Mixed	33,2	Table 6.8	Mixed	16,6	ECF
0041841	PORTERVILLE	EXP	39,2	Table 6.8	Mixed	18,1	ECF
0056917	GRAHAMSTOWN	Mixed	32,2	Table 6.8	Gumbel	17,2	ECF
0059572	EAST LONDON WO	EXP	36,1	Table 6.8	Gumbel	19,2	ECF
0061298	LANGEBAANWEG	Mixed	33,2	Table 6.8	Mixed	21,0	ECF
0078227	FORT BEAUFORT	Mixed	38,4	Table 6.8	Gumbel	18,4	ECF

Station Number	Station Name	Wind gust			Hourly mean wind speed		
		Method	X_{50}	Exposure correction	Method	X_{50}	Exposure correction
0083572	LAMBERTSBAAI	EXP	27,9	Table 6.8	Mixed	16,0	ECF
0092081	BEAUFORT-WES	EXP	39,0		Gumbel	25,5	ECF
0096072	GRAAFF - REINET	Mixed	31,2		Mixed	14,8	
0123685	QUEENSTOWN	EXP	44,1	Table 6.8	Gumbel	18,3	ECF
0127272	UMTATA WO	Mixed	40,5	Table 6.8	Gumbel	22,9	ECF
0134479	CALVINIA WO	EXP	33,4	Table 6.8	Mixed	17,3	ECF
0144791	NOUPOORT	EXP	37,4		Mixed	19,3	ECF
0148517	JAMESTOWN	EXP	38,0		Gumbel	16,4	ECF
0150620	ELLIOT	EXP	44,2		Gumbel	18,2	ECF
0155394	PORT EDWARD	EXP	32,6	Table 6.8	Gumbel	19,1	ECF
0169880	DE AAR WO	EXP	42,3		Mixed	16,9	ECF
0182465	PADDOCK	Mixed	36,3	Table 6.8	Mixed	19,6	ECF
0182591	MARGATE	Gumbel	34,8	Table 6.8	Gumbel	18,0	ECF
0184491	KOINGNAAS	Mixed	26,6	Table 6.8	Mixed	16,1	ECF
0190868	BRANDVLEI	EXP	35,2	Table 6.8	Mixed	16,2	ECF
0224400	PRIESKA	EXP	33,9		Mixed	17,5	ECF
0239698	PIETERMARITZBURG	EXP	34,6		Mixed	14,7	ECF
0239699	ORIBI AIRPORT	Mixed	36,6	Table 6.8	Mixed	16,3	ECF
0240808	DURBAN WO	Gumbel	33,3	Table 6.8	Gumbel	19,4	ECF
0241076	VIRGINIA	Gumbel	31,1	Table 6.8	Mixed	13,3	ECF
0261516	BLOEMFONTEIN WO	EXP	36,3		Mixed	14,2	ECF
0274034	ALEXANDERBAAI	EXP	32,1	Table 6.8	Gumbel	22,3	ECF
0290468	KIMBERLEY WO	EXP	37,7		Mixed	16,8	ECF
0300454	LADYSMITH	Mixed	37,4	Table 6.8	Gumbel	15,9	ECF

Station Number	Station Name	Wind gust			Hourly mean wind speed		
		Method	X_{50}	Exposure correction	Method	X_{50}	Exposure correction
0304357	MTUNZINI	Mixed	34,1	Table 6.8	Gumbel	20,1	ECF
0317475	UPINGTON WO	Gumbel	37,5		Mixed	16,6	ECF
0321110	POSTMASBURG	EXP	32,7		Mixed	18,2	ECF
0331585	BETHLEHEM WO	Mixed	35,8	Table 6.8	Mixed	17,4	ECF
0337738	ULUNDI	EXP	32,9		Gumbel	17,5	ECF
0339732	CHARTERS CREEK	Mixed	28,4	Table 6.8	Mixed	18,0	ECF
0356880	KATHU	EXP	33,3		Mixed	13,4	ECF
0360453	TAUNG	EXP	36,9		Mixed	13,5	ECF
0362189	BLOEMHOF	Mixed	36,7	Table 6.8	Gumbel	13,5	ECF
0364300	WELKOM	EXP	40,0		Mixed	12,4	
0370856	NEWCASTLE	EXP	38,2		Gumbel	17,9	ECF
0410175	PONGOLA	EXP	31,2		Gumbel	12,4	ECF
0438784	VEREENIGING	EXP	33,4		Mixed	15,1	ECF
0441416	STANDERTON	Gumbel	34,4		Mixed	18,5	ECF
0472278	LICHTENBURG	Gumbel	33,1		Gumbel	14,7	
0476399	JOHANNESBURG	Gumbel	34,0		Mixed	18,6	ECF
0479870	ERMELO WO	EXP	32,1		Gumbel	18,6	ECF
0508047	MAFIKENG WO	EXP	33,0		Gumbel	19,0	ECF
0511399	RUSTENBURG	Gumbel	29,2		Gumbel	16,1	ECF
0513385	IRENE WO	EXP	33,6		Mixed	19,8	ECF
0515320	WITBANK	EXP	31,5		Gumbel	15,2	ECF
0520691	KOMATIDRAAI	Gumbel	31,0		Gumbel	13,8	ECF
0548375	PILANESBERG	EXP	32,4		Gumbel	12,3	ECF
0594626	GRASKOP	Gumbel	31,2		Gumbel	18,4	ECF

Station Number	Station Name	Wind gust			Hourly mean wind speed		
		Method	X_{50}	Exposure correction	Method	X_{50}	Exposure correction
0638081	HOEDSPRUIT	Mixed	30,9		Gumbel	16,3	
0674341	ELLISRAS	Mixed	28,6	Table 6.8	Mixed	9,7	ECF
0675666	MARKEN	Mixed	29,5	Table 6.8	Gumbel	12,0	ECF
0677802	PIETERSBURG WO	EXP	35,0		Mixed	17,2	ECF
0723664	THOHOYANDOU WO	EXP	29,0		Mixed	13,8	ECF

"Exponential" indicates the POT with EXP distribution and "Mixed" indicates the mixed distribution approach. The nature of the exposure corrections are also indicated where applicable: ECF indicates the environmental correction factor discussed in section 6.5.2.

7.3. Spatial interpolation of the 1:50 year quantiles

In the development of maps of extreme wind speeds, it is essential that some objective method be applied to spatially interpolate the extreme wind data. This basically implies the estimation of the extreme wind values at places where no wind measurements were made. For South Africa this would mean that these interpolations should in many cases be done over long distances, and most often over heterogeneous terrain.

7.3.1. Hourly mean wind speeds

7.3.1.1. Height above sea level

Several extreme wind analyses use the height above sea level of the weather stations to interpolate the quantile values between the weather stations, which will then assist in the drawing of lines of equal quantiles on a map (e.g. Ballio *et al.*, 1999). The assumption over the region of concern will generally be that, because the wind speed increases with height, ignoring other factors, the same applies to the extreme wind speeds. The relationship between height above sea level and the extreme wind speed is then assumed to be linear. However, it is argued that such a simple relationship

between wind speed and height can only be made for an area with a homogeneous strong wind climate and a simple topography, which is not the case for South Africa. Figure 7.1 presents the test of a possible linear relationship between height above sea level and the 50-year quantile of hourly mean wind speed, which seems to indicate a negative correlation (although not statistically significant at the 5% level). This result suggests that if the whole area of South Africa is taken into consideration, the wind speeds tend to be stronger at lower elevations. This apparent negative relationship between height above sea level and the 50-year quantile of hourly mean wind speed is due to the stronger winds at the coastal regions, which are subject to a different strong wind regime than the interior.

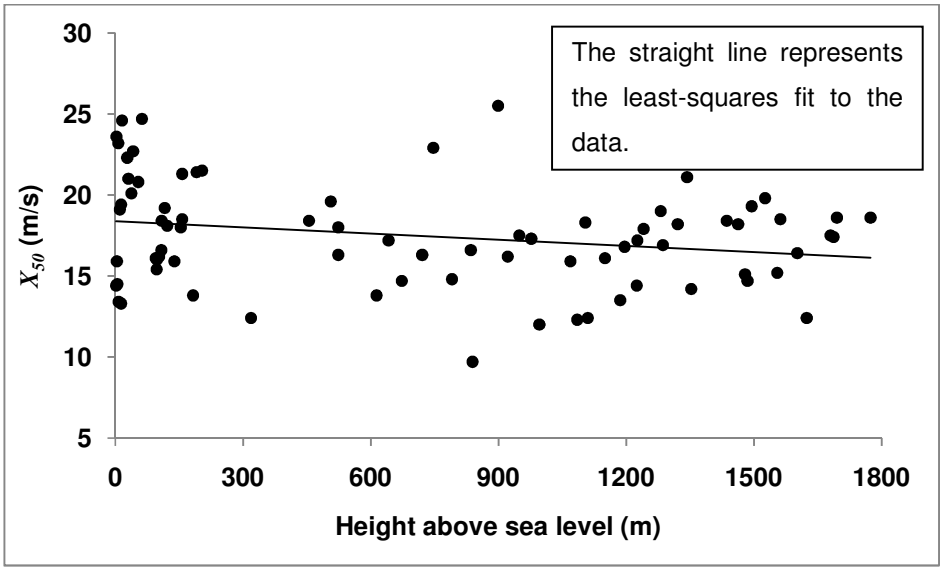

Figure 7.1. Relationship between the height above sea level and the 50-year quantile of hourly mean wind speed.

7.3.1.2. Latitude

Inspecting the quantile data in Table 7.1, it is also apparent that there is a tendency of the quantiles to be stronger in the south than in the north of South Africa. Figure 7.2 presents the relationship between the latitude of the weather station and the 50-year quantile of the hourly mean wind speed, due to the predominance of synoptic-scale

extreme winds at higher latitudes. This relationship renders a positive correlation which is statistically significant at the 5% level.

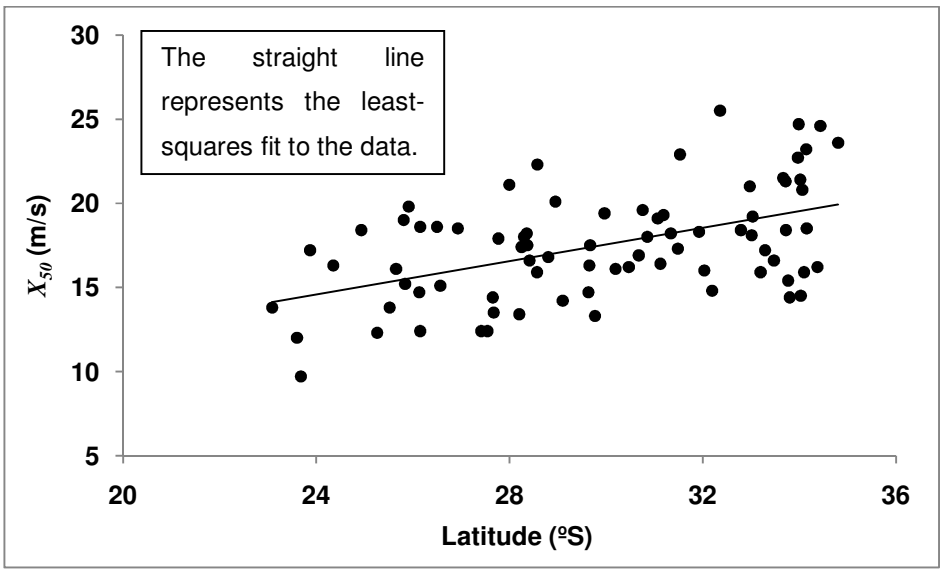

Figure 7.2. Relationship between the latitude and the 50-year quantile of hourly mean wind speed.

7.3.1.3. Zoning of quantiles

From section 7.3.1.1 it is clear that, although it is often assumed that there is a relationship between the height above sea level and the extreme wind quantiles, it cannot be generalized for South Africa taken as a whole. Also, one can see, from the analysis in section 7.3.1.2, that there is a general tendency for extreme wind quantiles to be stronger in the south. The relationships between extreme wind quantiles were therefore investigated on regional bases.

In their study of extreme winds in Italy, Ballio *et al.* (1999) subdivided the weather stations into two classes; the weather stations near sea level (close to the coast) and those at higher altitudes (interior). These two classes were then subdivided further into areas or regions, where the 10-minute wind speed quantiles showed similar magnitudes and/or characteristics. Different inland areas or zones were characterised by different

slopes of increase of the 10-minute wind speed quantiles with the height above sea level. The areas along the coast were characterised mainly by the average values of the 50-year quantile of the mean 10-minute wind speeds, as it was established there is not a significant increase of extreme wind quantiles with height above sea level along, and adjacent to, the coast.

An attempt was made to conduct a similar exercise for South Africa, to demarcate the country into zones of similar characteristics of the maximum hourly mean wind quantiles. South Africa would then be zoned according to the relationships between the height above sea level and the 50-year hourly mean wind speed quantile. These zones would then exhibit unique slopes of increase in the quantile wind speeds with height above sea level. To formalise the process, the zones had to fulfil the following criteria:

- A linear relationship between heights above sea level and the 50-year hourly mean wind speed quantiles should exist, which is statistically significant at the 5% level;
- The region should, as far as possible, be spatially coherent; and
- The weather stations within a region should have the same causes of extreme hourly mean wind speeds (this information could be obtained from the work discussed in Chapters 3 and 4).

Almost all of the weather stations could be grouped according to their relationships between the 50-year maximum hourly mean wind speed and the height above sea level. The analyses of the weather station into groups A to N (mostly according to their proximity to each other) are presented in Figure 7.3, from which the clear gap between the quantile/height relationships close to the coast and those in the interior is noticeable. Different slopes of increase of quantiles with height are apparent, with very steep trends observed for the regions close to the coast in contrast to those in the interior.

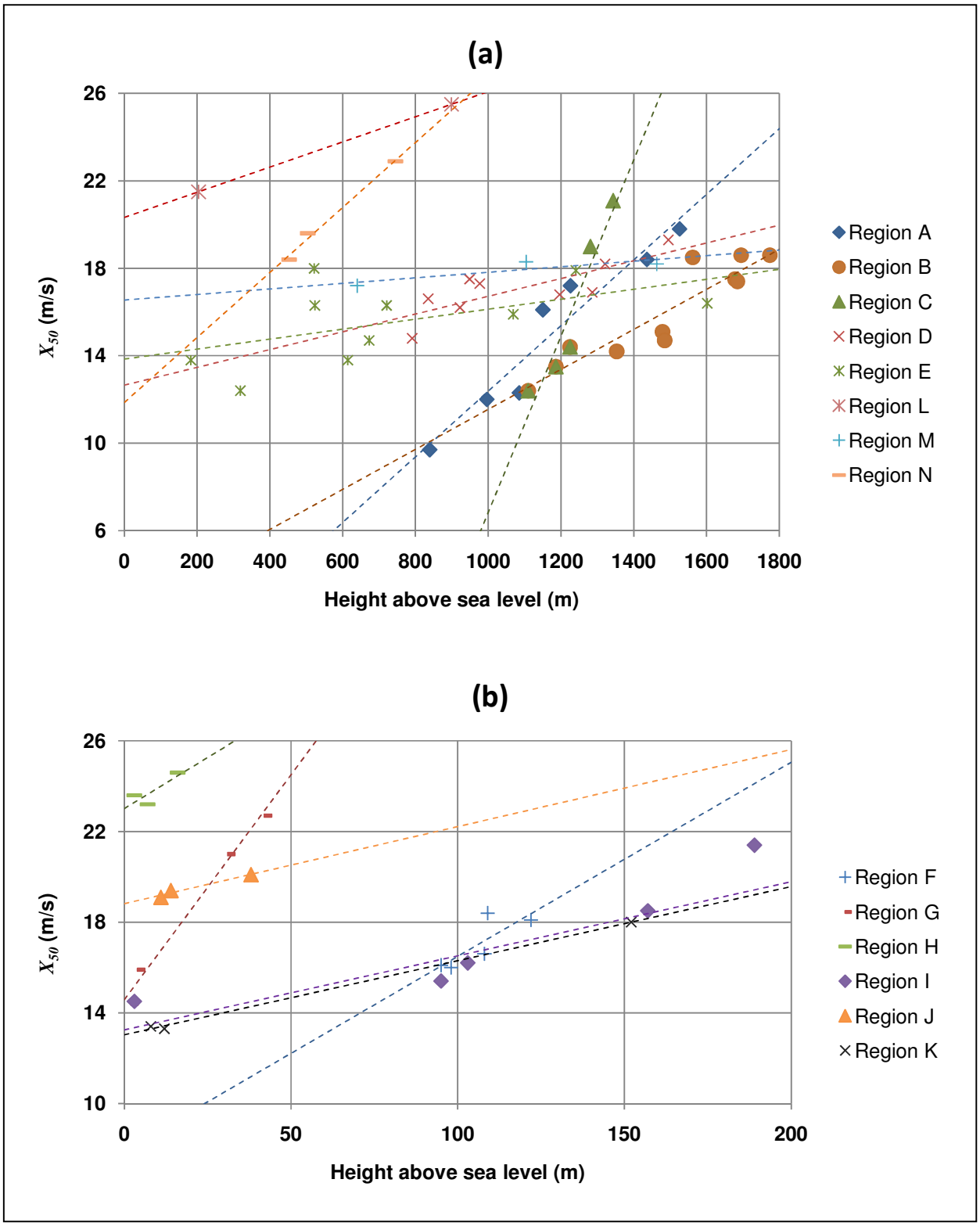

Figure 7.3. Analysis of the regionalised 1:50 year annual maximum hourly mean wind speed quantiles for (a) interior regions and (b) coastal regions.

Four weather stations, i.e. three along the coast and one station in the interior, could not be assigned to any particular groups. These are Alexander Bay on the far north-west coast, Port Elizabeth and East London on the south-east coast, and Johannesburg Botanical Gardens in the Gauteng province. The latter weather station, even after correction for inadequate exposure, still show anomalously low quantile values if compared to the quantiles of the surrounding weather stations. Therefore it was decided to exclude the Johannesburg Botanical Gardens weather station from further analyses. In the case of Alexander Bay its 50-year quantile value is much higher than that of its closest neighbouring station, Koingnaas, which also lies close to the coastline but about 200 km to the south-south-east. The strong winds at both Alexander Bay and Koingnaas tend to be southerly to south-easterly, due to ridging of the Atlantic Ocean High, but the transition to the plateau is much more prominent to the east of Alexander Bay than at Koingnaas. It is argued that the steeper topography in the adjacent interior of Alexander Bay causes an increase in the horizontal pressure gradient, which has the effect of accelerating the wind flow when ridging occurs. At Port Elizabeth the quantile value is also much higher than those for the neighbouring weather stations. The closest other coastal weather station to Port Elizabeth is Tsitsikamma, about 120 km to the west, with a quantile value which is about 10 m/s lower. At both weather stations the strong winds tend to be south-westerly. A possible physical explanation for the discrepancy between these quantile values could not be found. In the case of East London there is no other weather stations close by with a comparative quantile value.

The positions of the weather stations, showing their allocations to the groups A to N, as well as the individual unallocated weather stations, which are indicated with X, are presented in Figure 7.4. Through close inspection of Figures 7.3 and 7.4, the groups and the individual station areas can be summarised as in Table 7.2. It is recognized that the grouping of the weather stations in this manner is liable to some amount of subjectivity. However, this method is still deemed to be the most reasonable method in the interpolation of the quantile values, when only the quantiles estimated from observed values are available. Comparing the spatial distribution of the groups in Figure 7.4 with the strong wind zones developed in Chapter 4, and presented in Figure 4.6,

some correlations between the figures can be identified: Figure 4(a): A to E and M to N, 4(b): A to B and D to N, 4(c): A to B and E to H, 4(d): B to D, 4(e): A, E and L to N and 4(f): F.

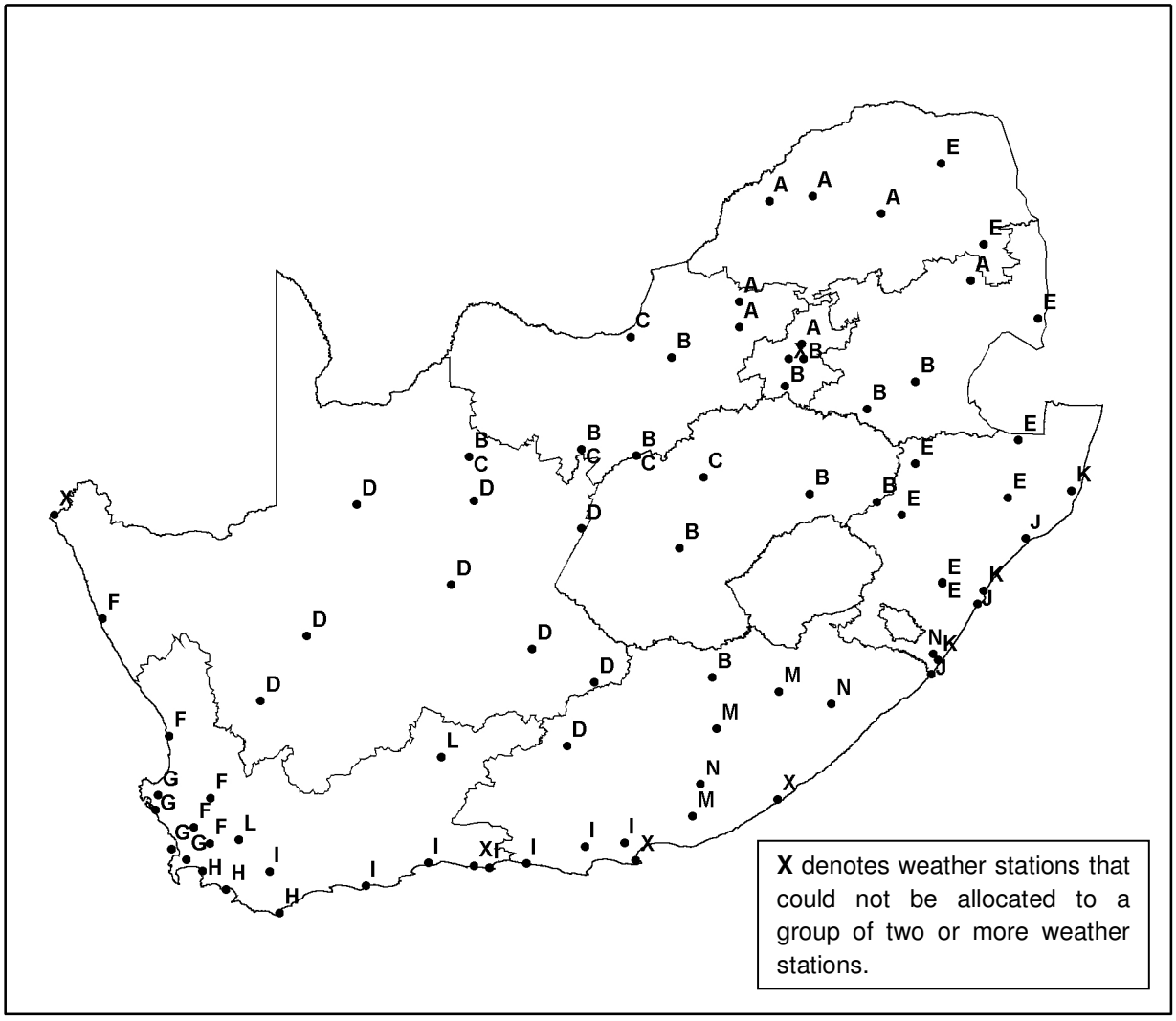

Figure 7.4. Allocations of the weather stations to groups A to N with similar relationships between height above sea level and the 50-year maximum hourly mean wind speed.

Table 7.2. Summary of the extreme wind zones for the annual maximum hourly mean wind speed, as well as individual weather stations that could not be grouped.

Region	Locality	Causes of strong hourly mean wind speeds	Slopes of increase (m/s per 100m)	Approximate borderlines with adjacent regions	Number of stations
A	The northern parts of Limpopo, North-West, Gauteng and Mpumalanga provinces, but west of the escarpment	Mainly the ridging of the Indian Ocean High from the east, but also the occasional passage of frontal systems from the south or south-west.	1,50	B: 1500m C: 1200m E: Along the west of the eastern escarpment at +/- 1500 m	7
B	Southern Gauteng and Mpumalanga, central and southern North-West, southern and eastern Free State and northern Eastern Cape.	Mainly the passage of cold fronts, but also ridging from the east and surface troughs to the west.	0,92	A: 1500m C: 1500m D: Approximately the Free State border on the west E: The eastern escarpment M: The south-eastern escarpment	11
C	This region shares some territory with region B. It covers the west of North-West, north-western Free State and a small part of the north of the Northern Cape.	Mainly the passage of cold fronts, but also surface troughs to the west. Very strong winds are frequent.	4,03	A: 1200m B: +/- 1200m	5

Region	Locality	Causes of strong hourly mean wind speeds	Slopes of increase (m/s per 100m)	Approximate borderlines with adjacent regions	Number of stations
D	The Northern Cape excluding the coastal region, as well as the north-west of the Eastern Cape	Mainly the passage of cold fronts, but also surface troughs to the west.	0,41	B/C: 28ºS in the north and the Northern Cape border in the east F: The western escarpment at +-/ 500m L: The southern escarpment at +/- 1500m M: The south-eastern escarpment at +/- 1500m	9
E	East of the eastern escarpment	Ridging of Indian Ocean High in the north and strong winds behind a coastal low and ahead of a cold front in the south	0,23	A: The eastern escarpment at +/- 1500m. B: The eastern escarpment at +/- 1500m J/K: 100m M: The KwaZulu-Natal border in the south-west N: 1000m in the south and south-east.	10
F	The West Coast from the north south-eastwards into the adjacent interior of the south-western Cape coast	Cold fronts and strong coastal lows	8,57	29ºS in the north D: The western escarpment at +/- 500m. G: 100m L: 100m	5

Region	Locality	Causes of strong hourly mean wind speeds	Slopes of increase (m/s per 100m)	Approximate borderlines with adjacent regions	Number of stations
G	The western part of the south-western Cape coast	Ridging of the Atlantic Ocean High and the passage of cold fronts	19,86	F: 100m H: 18.7ºE	4
H	The southern and eastern part of the south-western Cape coast	Ridging of the Atlantic Ocean High and the passage of cold fronts	9,02	F: 100m G: 18.7ºE I: 100m to the north and 20.5ºE to the east	3
I	The southern Cape coast and adjacent interior	Passage of cold fronts	3,27	H: 100m to the south in the west and 20.5ºE at the coast L: 100m M: 100m	7
J/K	The KwaZulu-Natal coast	South-westerly busters behind coastal lows, as well as ridging in the north	3,30	The KwaZulu-Natal border in the south E: 100m N: 100m	3/3
L	The interior of the south-western Cape north-eastwards up to the southern escarpment	Passage of cold fronts	0,58	D: The southern escarpment at +/- 1500m F: 100m I: 100m M: The Western Cape border	2
M	The interior of the Eastern Cape, just south east of the escarpment	Strong winds behind a coastal low and ahead of a cold front	0,13	I: 100m J/K: +/- 100m N: +/-700m	3

Region	Locality	Causes of strong hourly mean wind speeds	Slopes of increase (m/s per 100m)	Approximate borderlines with adjacent regions	Number of stations
N	The interior of the Eastern Cape, mostly south- east of the 700m contour	Strong winds behind a coastal low and ahead of a cold front	1,49	J/K: +/- 100m M: +/- 700m	3
X	Alexander Bay area	-	-	M: 29°S in the south D: The escarpment in the west	-
X	Port Elizabeth area	-	-	Confined to the Port Elizabeth metropole	-
X	East London area	-	-	The south-eastern coastline from the PE metropole to the KwaZulu-Natal border. M: +/- 100m N: +/- 100m	-

7.3.1.4. Mapping of quantiles

Figure 7.5 presents a mechanistically interpolated map of the 1:50 year hourly mean wind quantiles presented in Table 7.1, developed with the inverse distance method contained in the GIS Spatial Analyst software. From the map one can notice the general tendency, with some exceptions, of quantiles to be stronger in the south and weaker in the north. Due to the mathematical method of interpolation, the spatial distribution of data points, and the fact that the forcing effect of topography on wind flow is not taken into consideration, the isolines on the map does not always make physical sense. This illustrates that the approach of simple interpolation of the quantile values is not the ideal approach in the development of the quantile map.

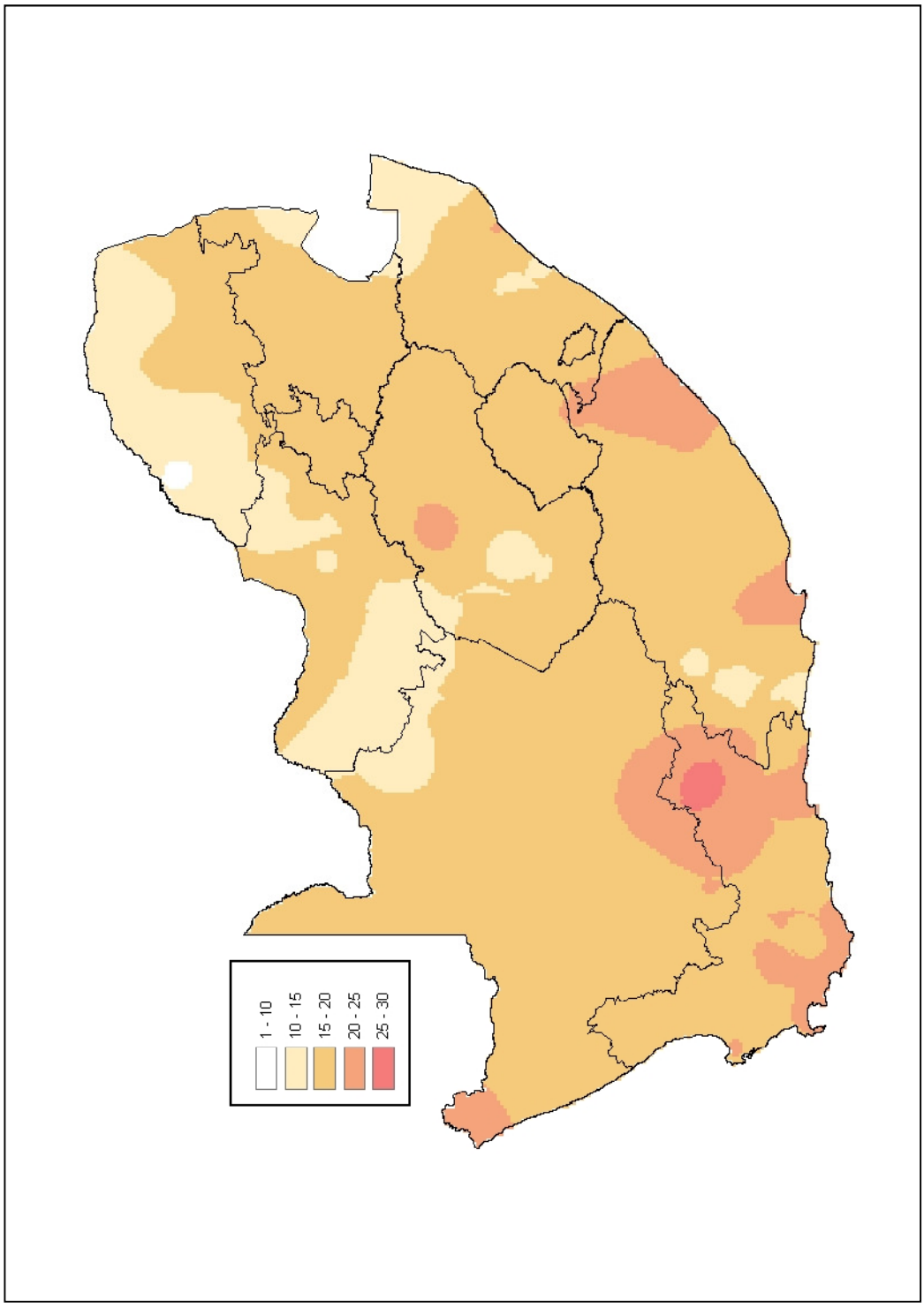

Figure 7.5. Interpolated map of the 1:50 year hourly mean wind quantiles (m/s) in Table 7.1, developed with the inverse distance method.

As shown in section 7.3.1.3 the 1:50 year hourly mean wind speeds could be zoned, albeit somewhat subjectively, according to the common correlation between the wind speed values and the heights above sea level among the weather stations. The aim of the zoning is to assist in the mapping of the extreme wind speeds. With the aid of GIS and Google Earth a 15' x 15' resolution grid of the height above sea level was developed. For each of these grid points the 1:50 year maximum hourly mean wind speeds could then be estimated according to the unique linear relationship between the quantiles and the height above sea level for the specific zone, described in Table 7.2.

From the above exercise, the contour map for the1:50 year hourly mean wind speed is presented in Figure 7.6, in 5 m/s increments. This map gives a more realistic picture of the spatial distribution of the quantile values than the map presented in Figure 7.5. Some of the noteworthy differences between the map in Figure 7.6, and the mechanistically interpolated map in Figure 7.5 are:

- Areas in the 25-30 m/s category are spread along the south of the escarpment in the Western Cape, instead of only the small circular area around Beaufort West.
- The 20-25 m/s category in the south is confined to the south of the escarpment, and covers a greater portion of the Western Cape Province. However, in Figure 7.5 this area is smaller and stretches over the escarpment to the north. This category is also present in isolated patches in the Eastern Cape, while a big part of the north-east of the Eastern Cape falls into this category in the map in Figure 7.5. The same applies to this category in the Free State. Around the Alexander Bay area this category is confined to the west of the escarpment, while this is not the case in Figure 7.5.
- The 10-15 m/s category covers a substantial part of the Western Cape, while this is not the case in Figure 7.5. It also covers the Limpopo and Mpumalanga provinces to the east of the escarpment, while the isolines do not follow the topography so closely in Figure 7.5.

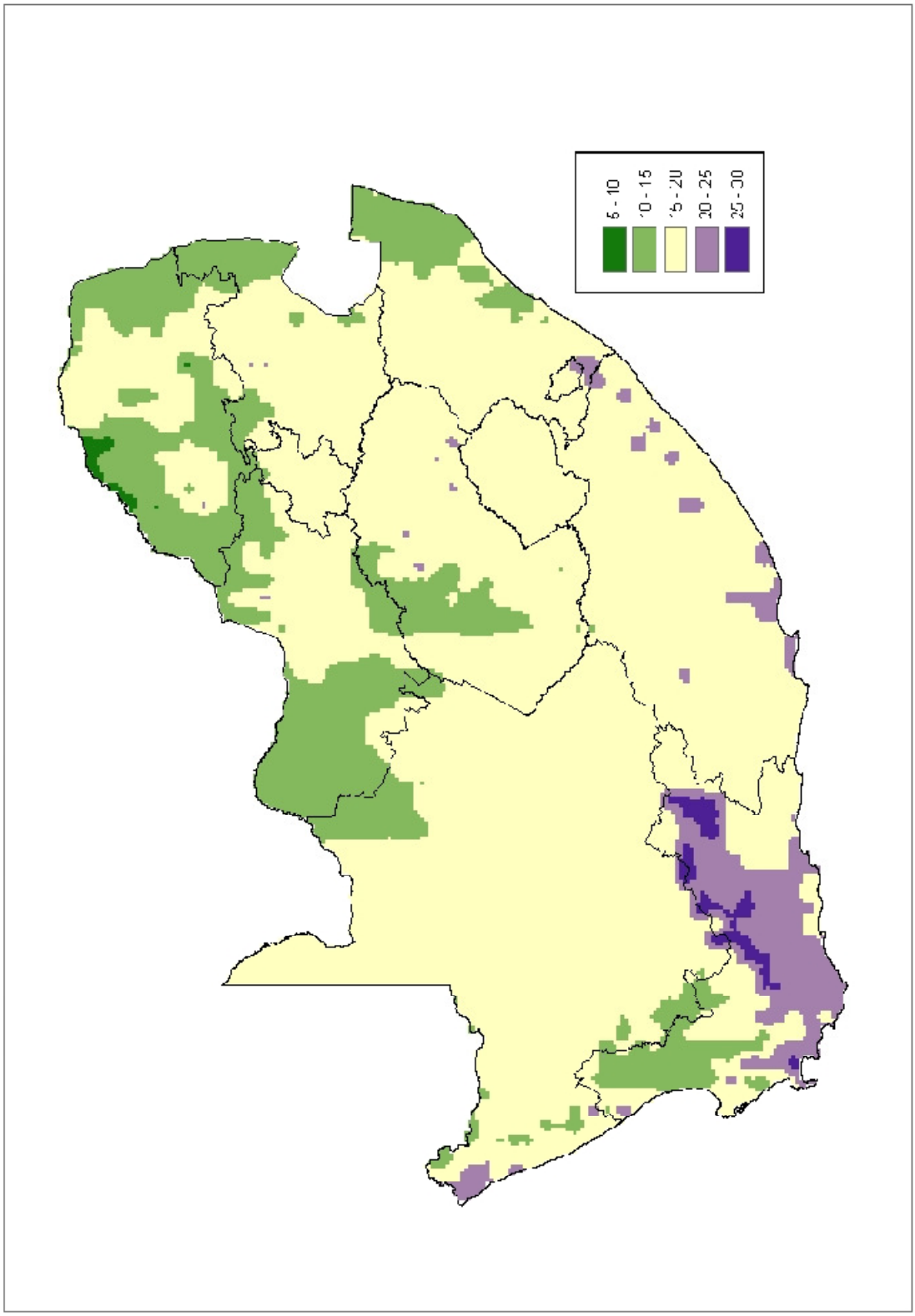

Figure 7.6. The 1:50 year maximum hourly mean wind speed (m/s).

- Observations regarding the metropolitan areas:
  - Cape Town: The metropolitan area mostly falls into the 20-25 m/s category, with a small area of 25-30 m/s just west of the Somerset-West region, and 15-20 m/s from Hout Bay northwards along the coast across the Cape Town CBD. In Figure 7.5 the whole metropole falls into the 20-25 m/s category.
  - Port Elizabeth: This area falls into the 20-25 m/s category, also in Figure 7.5.
  - Durban: Falls into the 15-20 m/s category, but 10-15 m/s to the north of the CBD. The same pattern is evident from Figure 7.5.
  - Bloemfontein: Falls into 10-15 m/s in the west and 15-20 m/s in the east. In Figure 7.5 it falls into the 10-15 m/s category, but closely surrounded by 15-20 m/s.
  - Johannesburg/Pretoria: Categorized as 15-20 m/s, also in Figure 7.5.

7.3.2. Extreme wind gust values

The origins of strong wind gusts, especially those forthcoming from thunderstorms, are usually very local in origin. Therefore it is argued that the approach taken in section 7.3.1.3, to zone the gust quantiles according to their relationships with height above sea level, would not make physical sense. In Figure 7.7 a mechanistically interpolated map of the 1:50 year gust quantiles, included in Table 7.1, is presented, developed with the inverse distance method (As was the case for Figure 7.5, the spacing of the isolines on the map does not take the topography or any other physical factors into account). Another important feature of the map in Figure 7.7, if compared with the maps in Figures 7.5 and 7.6, is that the relative strengths of the gust quantiles do not necessarily coincide with those of the hourly mean wind quantiles.

7.3.2.1. Ratios between gust- and hourly mean wind quantiles

The ratio between the gust quantiles and the hourly mean wind speed quantiles, which could be referred to as the Quantile Gust Factor, will be dependent on the most probable causes of the strong wind gusts in a particular region, whether of thunderstorm

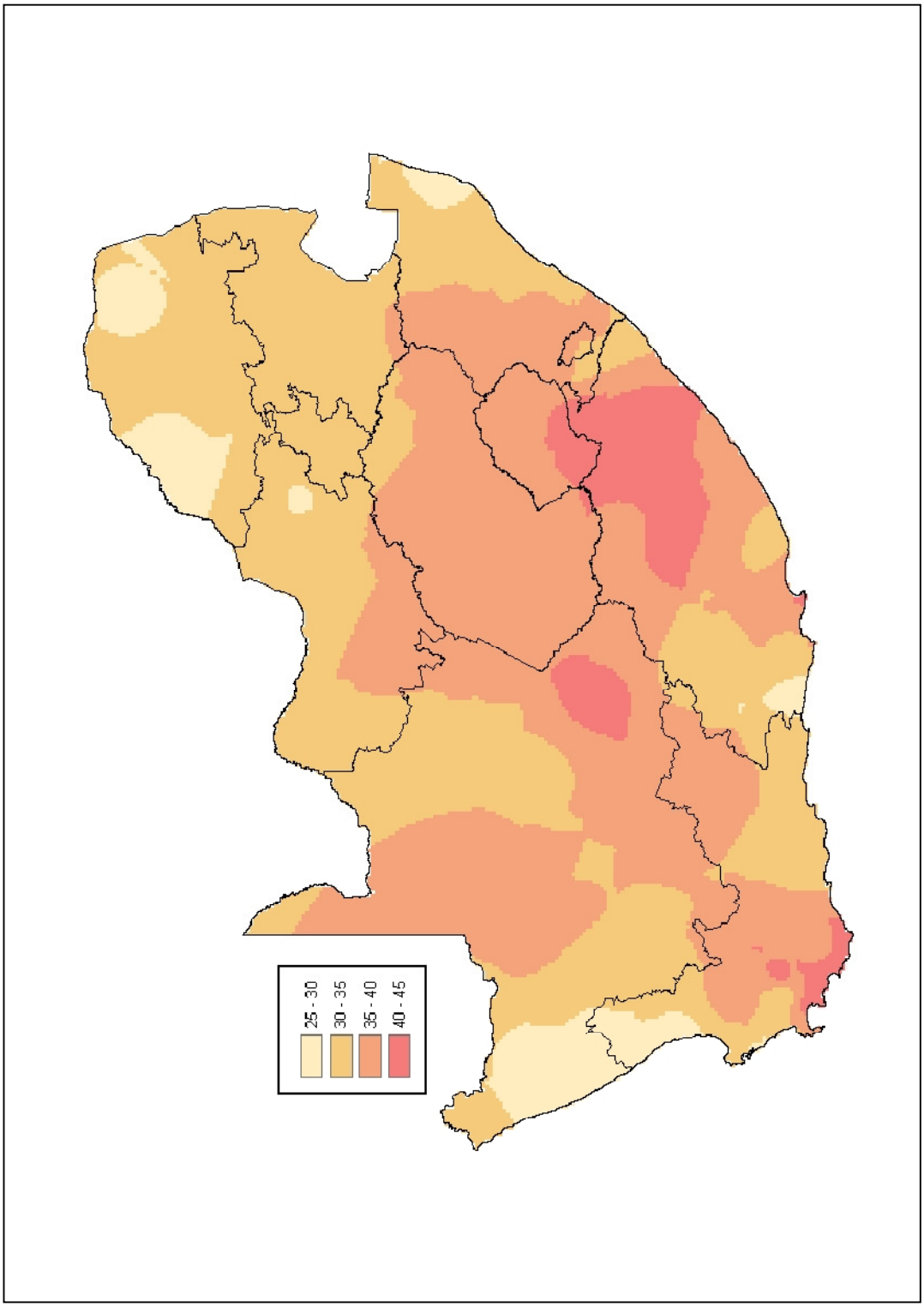

Figure 7.7. Interpolated map of the 1:50 year gust quantiles (m/s) in Table 7.1.

or synoptic origin, as discussed in section 2.1.1. These ratios, between the 1:50 year gust quantiles and the 1:50 year hourly mean wind quantiles from Table 7.1, are presented in the interpolated map in Figure 7.8. The most noteworthy characteristics of the ratios depicted on the map are the following:

- Low ratios are evident in the west and south and further along the coast in the east. The strong mean winds and gusts are both produced by cold fronts, which are characterised by relatively well-correlated flow
- Strong hourly mean wind speeds in the north-east, specifically the Mpumalanga province and parts of the Limpopo and Gauteng provinces, are most often produced by the strong ridging of the Indian Ocean high-pressure system from the east. The strongest gusts in these regions are usually produced by thunderstorms, but these are in general not as strong as elsewhere in the country. The effect is that the ratios here are low.
- The highest ratios are found in parts of the interior of the country. The strong mean wind speeds are produced by cold fronts, or the ridging of the Indian Ocean high-pressure system from the east, although the strengths of these systems have usually diminished somewhat. Intense thunderstorms are however possible over parts of this region, which in turn can produce very strong short duration wind gusts, which cannot be reflected by data in terms of large averaging periods.

7.3.2.2. Mapping of quantiles

The maps presented in Figures 7.6 and 7.8 (i.e. maximum hourly mean wind speed and Quantile Gust Factor), could be used as the basis for the development of a 1:50 year gust map. The 15' x 15' grid of 1:50 year hourly mean wind speed values, determined to develop the map in Figure 7.6, were multiplied with the ratios included in the map in Figure 7.8. The utilisation of these high resolution hourly mean wind speed values in the development of the gust map was the only method available to ensure that the gust map will have a high resolution exhibiting isolines that are physically plausible. For the purpose of the exercise the ratio map in Figure 7.8 was refined to 1 m/s increments.

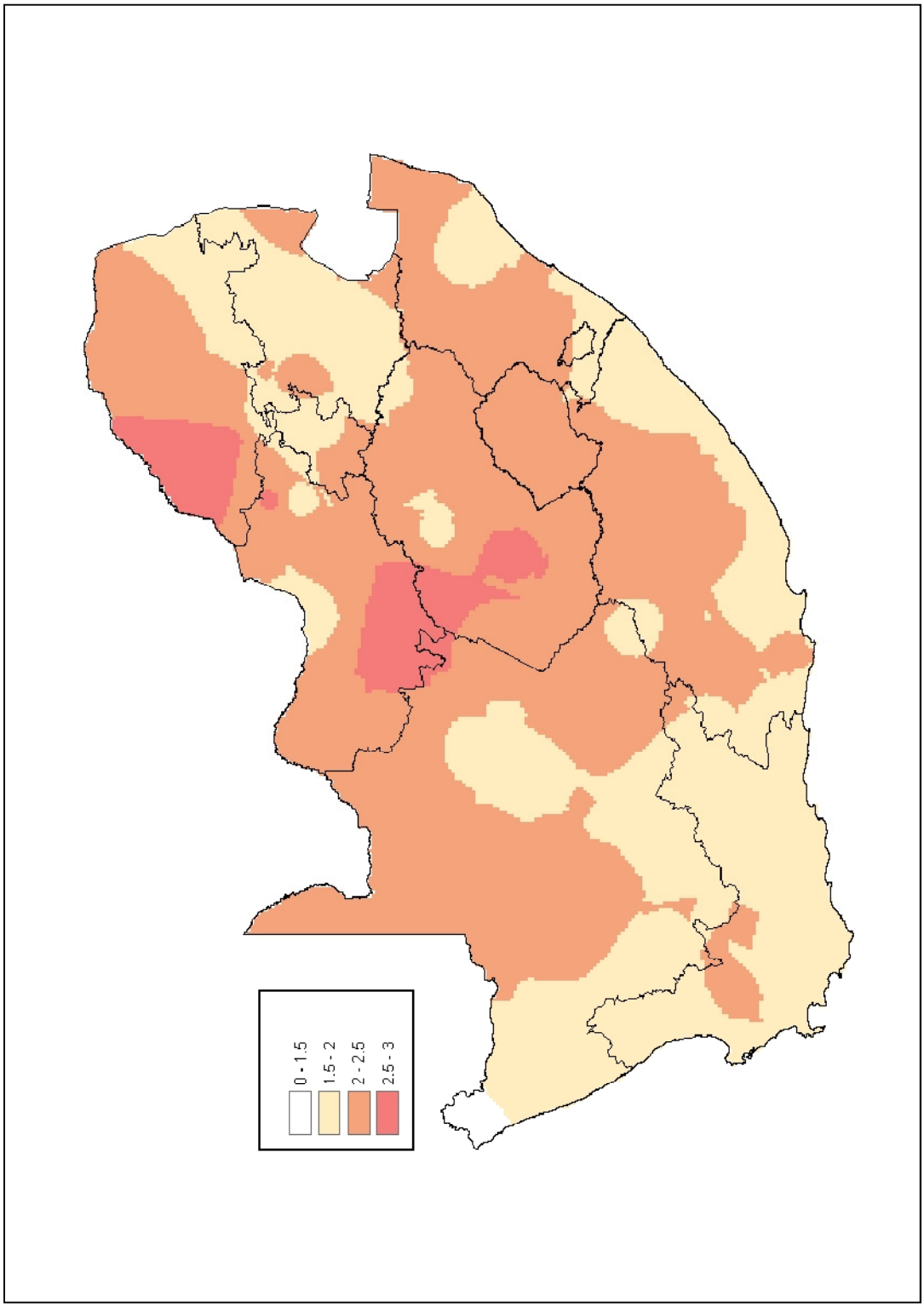

Figure 7.8. The ratios between the gust quantiles and the hourly mean wind quantiles, presented in Table 7.1.

The 1:50 year gust map developed from this procedure is presented in Figure 7.9. If to compare the map in Figure 7.9 with the map in Figure 7.7, the following can be observed:

- The area in the Western Cape, which falls in the 40-45 m/s category, is much larger than in Figure 7.7, and coincides with the area of highest hourly mean wind quantiles. Some isolated areas in the Free State and KwaZulu-Natal also falls into this category, while it is not the case in Figure 7.7. In the Eastern Cape this category is mostly confined to the interior, while it stretches all the way to the coast in Figure 7.7.
- The 35-40 m/s category covers mostly the same regions in both maps, but in Figure 7.9 it covers larger areas to the north, and less of the Northern Cape, if compared to Figure 7.7.
- The 30-35 m/s category covers the largest part of the north of the country in Figure 7.7. However, the same region is divided almost equally between the 25-30 and 30-35 m/s categories in Figure 7.9. This is mainly because lower 1:50 year gusts are expected to the east of the escarpment.
- Metropolitan areas:
    - Cape Town: The metropolitan area is mostly 35-40 m/s, but as with the hourly mean map in Figure 7.6, a higher category exists over a small area to the west of the town of Somerset-West, of 40-45 m/s. An even higher category of 45-50 m/s exists, but very small and isolated in the last-mentioned area, and also around the Cape Point area. The map in Figure 7.7 also shows that the area falls mostly in the 35-40 m/s category, but 30-35 m/s towards the north and 40-45 m/s in the east.
    - Port Elizabeth: The major part of the area is 35-40 m/s, while the area close to the coast is 40-45 m/s. The same pattern is evident from the map in Figure 7.7.

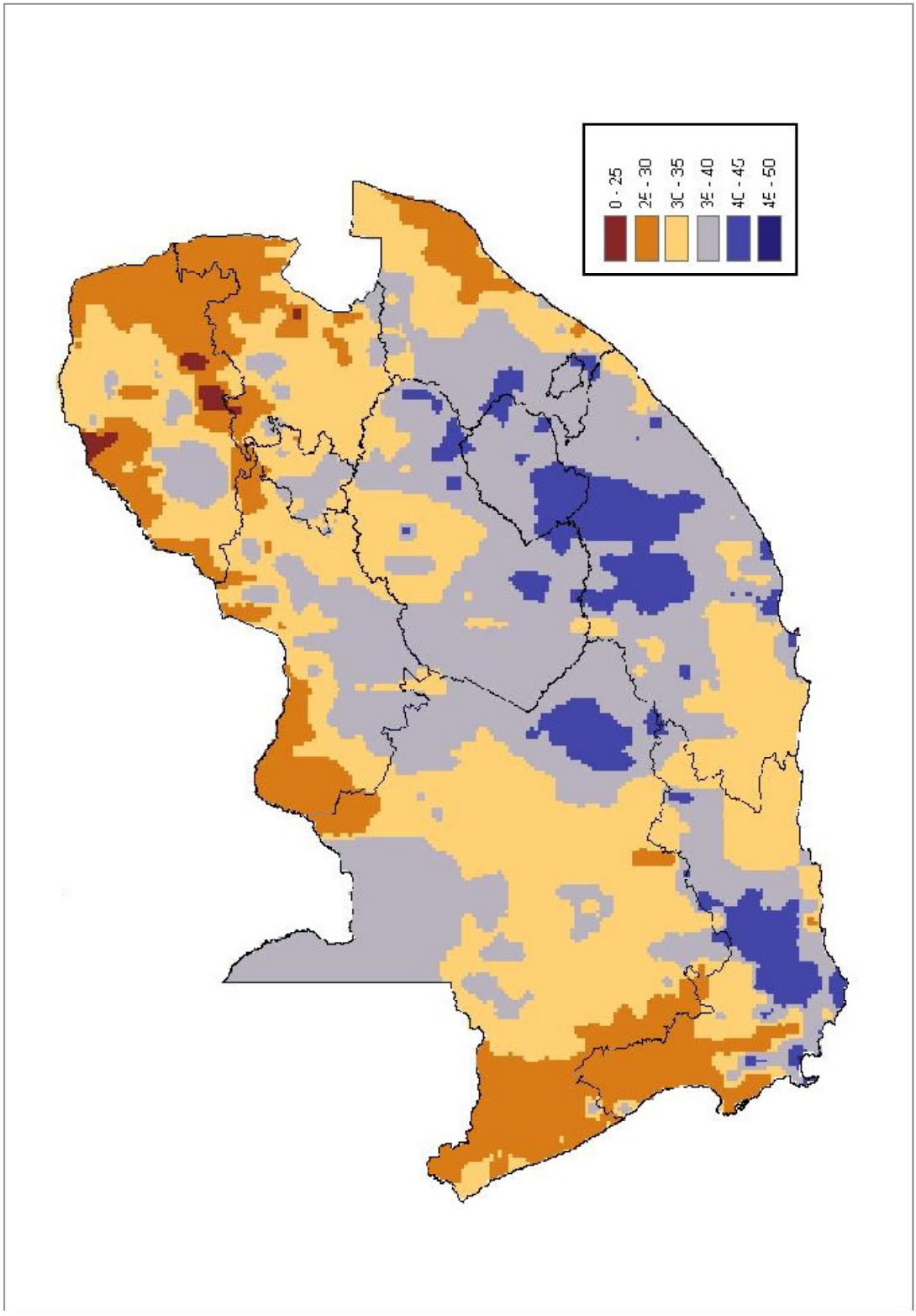

Figure 7.9. The 1:50 year extreme wind gusts (m/s).

- Durban: Most of the area close to the coast is in the 35-40 m/s category, while the area around the CBD is in the 30-35 m/s category. The map in Figure 7.7 shows the whole metropole to all into the 30-35 m/s category.
- Bloemfontein: In the 35-40 m/s category, for both the maps in Figures 7.7 and 7.9.
- Johannesburg/Pretoria: The southern part (mostly Johannesburg) is in the 35-40 m/s category, while the north (mostly Pretoria) is in the 30-35 m/s category. In Figure 7.7 the whole metropole is in the 30-35 m/s category.

It is acknowledged here that, because the ratio values used in the development of the map in Figure 7.9 does not take the topography into account, there would be areas which show possible unrealistic quantile patterns. Some of these areas are:

- The isolated areas in the north, which falls under the 0-25 m/s category, due to their low elevations.
- The almost abrupt change from the 35-40 m/s to the 25-30 m/s category to the west of the North-West province.
- Some of the very high quantile values shown along the escarpment in the east and south-east might not necessarily be realistic, and only be a result of the very high elevations used in their estimations.

Apart from the above possibly unrealistic patterns, there can possibly be more of such detected by closer inspection of Figure 7.9. Notwithstanding these shortcomings, it is argued that the map can still fulfil its purpose, which is to give a general impression of the areas of higher and lower quantile values.

7.4. Proposed design wind speed maps

Arguably the most important characteristics that design wind speed maps should comply with are the conservativeness of the quantile values, and an overall simplicity of the contours for the ease of reference.

7.4.1. Adjustments for uncertainties of quantile values

Uncertainties of the estimated values of the extreme wind quantiles mainly revolve around the estimated values of the parameters of the extreme wind distributions fitted to the observed wind data. These uncertainties, in turn, are due to the uncertainties in whether the sample of values used in the calculation of the distribution parameters is representative of the population. Regarding conservativeness, it is important that the estimated design values should rather err on the higher than on the lower side.

The quantities utilised in the calculation of the parameters of the extreme value distributions are the mean and the standard deviation. In Ang and Tang (1978) the upper confidence limit of the mean is given as

$$UCL(mean) = \bar{x} + t_{\alpha,n-1}\,(s/\sqrt{n}) \tag{7.1}$$

Where t is the Student's t-distribution, α is the upper confidence level, $\bar{x}$ is the sample mean, s is the sample standard deviation and n is the sample size. The confidence limit is exact if the underlying population is Gaussian. However, the results are applicable to non-Gaussian populations if the sample size is greater than 10. Therefore equation 7.1 can be used to determine approximate confidence limits of μ irrespective of the distribution of the underlying population. Also from Ang and Tang (1978), the upper confidence limit of the variance of the population can be deduced as

$$UCL(variance) = s^2/[1 - k_\alpha\sqrt{2/(n-1)}] \tag{7.2}$$

where k_α is the z value of the normal distribution for the appropriate confidence level α, and the other symbols have the same meaning as in equation 7.1. From equations 7.1 and 7.2 adjustments were made to the estimates of the mean and standard deviation as calculated from the sample of n observations. This was done by adding the confidence limits estimated with equations 7.1 and 7.2, at the 75% confidence level (which is accepted practice or convention in the built environment), to the sample mean and variance. This procedure is fundamentally different from the procedures given by equations 5.1 and 5.2, as the last-mentioned is based on the numerical solution of the dispersion matrixes of the distribution parameters. No correlation could be found

between the magnitudes of the adjustments/confidence levels between the two procedures.

After adjustments of the means and variance values of the samples, the parameters for the Gumbel distribution were recalculated, and the adjusted 1:50 year quantiles determined. This procedure was applied to both the Gumbel and mixed distribution methods.

For the cases where the POT method with the EXP approach was selected, as indicated in Table 7.1, the only distribution parameter is α, which is simply the mean of the exceedances of the threshold value β of the values in the sample utilized (see equation 2.25(b)). Therefore the value of α was adjusted by addition of the 75% confidence limit to the mean of the exceedances, calculated with equation 7.1.

Table 7.3 presents the adjusted values of the 1:50 year quantiles of the annual maximum wind gusts and the annual maximum hourly mean wind speeds, to be utilised in the development of the final proposed design wind speed maps. The original values in Table 7.1 are included for comparative purposes.

Table 7.3. Adjusted values of the 1:50 year quantiles of the annual maximum wind gusts and the annual maximum hourly mean wind speeds.

Station Number	Station Name	Original 1:50 year wind gust	Adjusted 1:50 year wind gust	Original 1:50 year hourly mean wind speed	Adjusted 1:50 year hourly mean wind speed
0003108	STRUISBAAI	41,3	43,9	23,6	24,6
0005609	STRAND	43,9	46,7	23,2	24,7
0006386	HERMANUS	43,5	44,2	24,6	26,1
0007699	TYGERHOEK	37,3	38,7	18,5	18,9
0010682	STILBAAI	30,3	31,1	16,2	16,8

Station Number	Station Name	Original 1:50 year wind gust	Adjusted 1:50 year wind gust	Original 1:50 year hourly mean wind speed	Adjusted 1:50 year hourly mean wind speed
0012661	GEORGE WO	33,3	34,0	21,4	22,1
0014123	KNYSNA	33,5	35,7	20,8	24,2
0014545	PLETTENBERGBAAI	31,1	32,6	15,9	17,4
0015692	TSITSIKAMMA	28,0	29,2	14,5	14,6
0020618	ROBBENEILAND	28,7	29,4	14,4	15,3
0021178	CAPE TOWN WO	38,3	39,5	22,7	24,1
0021823	PAARL	31,1	32,6	18,4	19,7
0022729	WORCESTER	41,5	42,6	21,5	22,1
0033556	PATENSIE	33,1	35,4	15,4	16,1
0034763	UITENHAGE	39,3	42,5	21,3	22,6
0035209	PORT ELIZABETH	40,4	41,1	24,7	25,9
0040192	GEELBEK	28,8	29,8	15,9	16,9
0041388	MALMESBURY	33,2	35,2	16,6	18,0
0041841	PORTERVILLE	39,2	41,0	18,1	19,7
0056917	GRAHAMSTOWN	32,2	36,8	17,2	18,1
0059572	EAST LONDON WO	36,1	36,7	19,2	19,9
0061298	LANGEBAANWEG	33,2	36,2	21,0	22,3
0078227	FORT BEAUFORT	38,4	41,4	18,4	19,4
0083572	LAMBERTSBAAI	27,9	28,7	16,0	16,7
0092081	BEAUFORT-WES	39,0	40,3	25,5	27,3
0096072	GRAAFF - REINET	31,2	33,7	14,8	15,8
0123685	QUEENSTOWN	44,1	44,5	18,3	18,9
0127272	UMTATA WO	40,5	45,0	22,9	24,7
0134479	CALVINIA WO	33,4	34,3	17,3	18,1

Station Number	Station Name	Original 1:50 year wind gust	Adjusted 1:50 year wind gust	Original 1:50 year hourly mean wind speed	Adjusted 1:50 year hourly mean wind speed
0144791	NOUPOORT	37,4	38,6	19,3	20,2
0148517	JAMESTOWN	38,0	39,2	16,4	17,1
0150620	ELLIOT	44,2	46,0	18,2	19,4
0155394	PORT EDWARD	32,6	33,8	19,1	20,6
0169880	DE AAR WO	42,3	43,8	16,9	17,8
0182465	PADDOCK	36,3	38,4	19,6	20,5
0182591	MARGATE	34,8	36,6	18,0	18,3
0184491	KOINGNAAS	26,6	29,1	16,1	17,4
0190868	BRANDVLEI	35,2	36,6	16,2	17,2
0224400	PRIESKA	33,9	35,0	17,5	18,4
0239698	PIETERMARITZBURG	34,6	35,2	14,7	15,8
0239699	ORIBI AIRPORT	36,6	40,0	16,3	17,3
0240808	DURBAN WO	33,3	34,9	19,4	19,6
0241076	VIRGINIA	31,1	33,0	13,3	14,1
0261516	BLOEMFONTEIN WO	36,3	37,3	14,2	15,1
0274034	ALEXANDERBAAI	32,1	32,5	22,3	22,9
0290468	KIMBERLEY WO	37,7	38,8	16,8	17,7
0300454	LADYSMITH	37,4	39,4	15,9	16,5
0304357	MTUNZINI	34,1	36,1	20,1	21,1
0317475	UPINGTON WO	37,5	39,8	16,6	17,7
0321110	POSTMASBURG	32,7	34,0	18,2	19,9
0331585	BETHLEHEM WO	35,8	38,2	17,4	18,0
0337738	ULUNDI	32,9	33,9	17,5	19,2
0339732	CHARTERS CREEK	28,4	30,4	18,0	14,4

Station Number	Station Name	Original 1:50 year wind gust	Adjusted 1:50 year wind gust	Original 1:50 year hourly mean wind speed	Adjusted 1:50 year hourly mean wind speed
0356880	KATHU	33,3	34,3	13,4	14,1
0360453	TAUNG	36,9	38,0	13,5	12,8
0362189	BLOEMHOF	36,7	38,8	13,5	14,9
0364300	WELKOM	40,0	40,9	12,4	22,4
0370856	NEWCASTLE	38,2	39,3	17,9	19,2
0410175	PONGOLA	31,2	32,0	12,4	13,2
0438784	VEREENIGING	33,4	34,3	15,1	16,6
0441416	STANDERTON	34,4	37,0	18,5	19,4
0472278	LICHTENBURG	33,1	35,0	14,7	15,5
0476399	JOHANNESBURG	34,0	36,3	18,6	19,8
0479870	ERMELO WO	32,1	32,8	18,6	19,4
0508047	MAFIKENG WO	33,0	34,1	19,0	20,1
0511399	RUSTENBURG	29,2	31,0	16,1	17,2
0513385	IRENE WO	33,6	34,7	19,8	21,2
0515320	WITBANK	31,5	32,4	15,2	16,1
0520691	KOMATIDRAAI	31,0	32,6	13,8	14,2
0548375	PILANESBERG	32,4	33,8	12,3	13,0
0594626	GRASKOP	31,2	33,9	18,4	20,2
0638081	HOEDSPRUIT	30,9	34,3	16,3	17,1
0674341	ELLISRAS	28,6	30,5	9,7	10,3
0675666	MARKEN	29,5	32,7	12,0	11,0
0677802	PIETERSBURG WO	35,0	36,4	17,2	18,4
0723664	THOHOYANDOU WO	29,0	29,3	13,8	14,9

The original values in Table 7.1 are included for comparative purposes.

The quantile values included in Table 7.3, presented in Figures 7.10 and 7.11, were adopted as the final values to be used in the development of the wind speed maps.

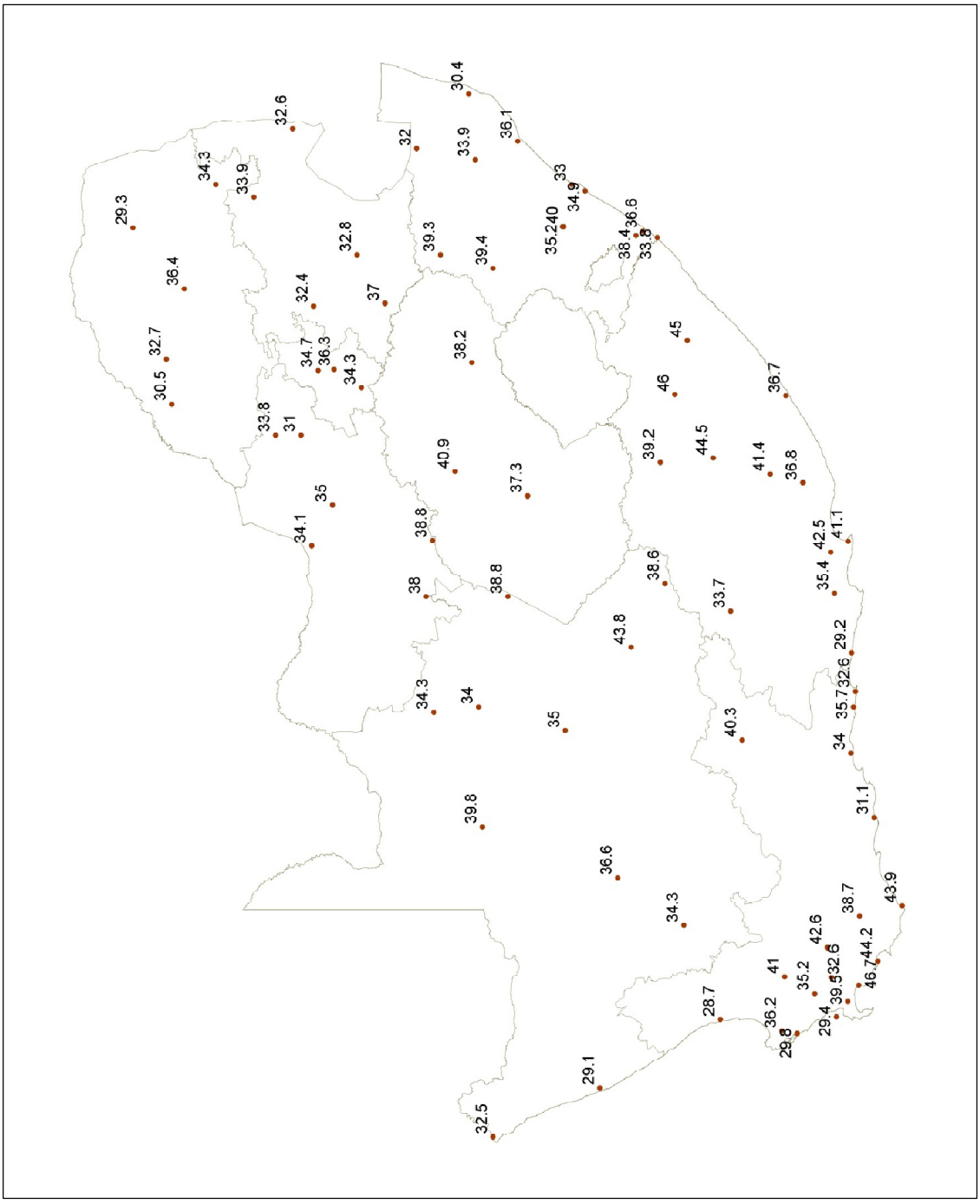

Figure 7.10. Adjusted values of the 1:50 year quantiles of the annual maximum wind gusts (m/s), as presented in Table 7.3.

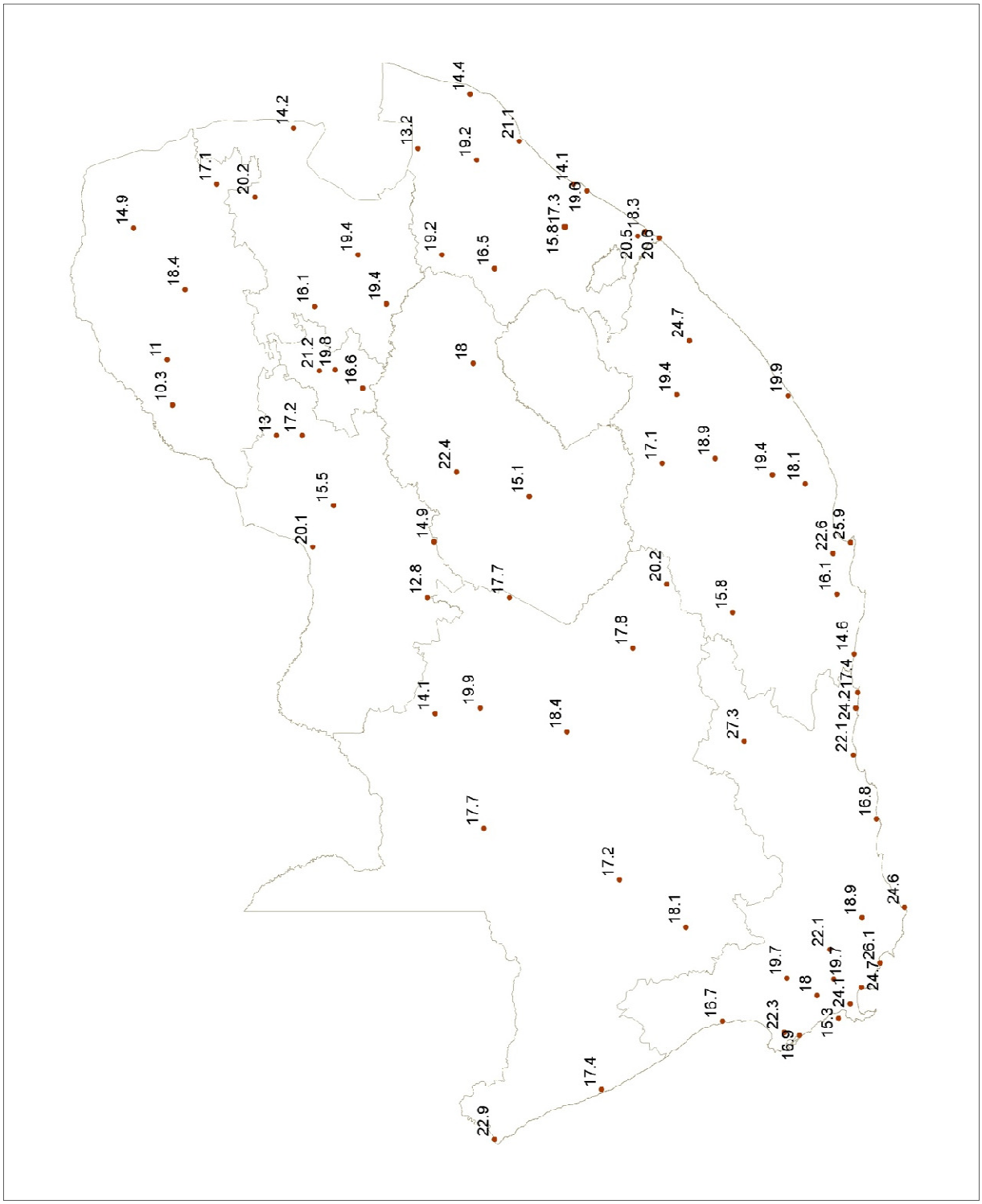

Figure 7.11. Adjusted values of the 1:50 year quantiles of the annual maximum hourly mean wind speeds (m/s), as presented in Table 7.3.

7.4.2. Development of design wind speed maps

The quantile values in Figures 7.10 and 7.11 were used as the basis to draw updated gust and hourly mean wind speed maps. In addition, the maps presented in *Figures 7.6 and 7.9 were used as guidelines* to indicate regions of relatively higher and lower quantile values. Noted here is that Figures 7.6 and 7.9 are based on figures not adjusted for small n. It is also prudent to *take the assessment and integration of the extreme wind estimations, conducted in Chapter 8, into account*, particularly for regions where relatively high quantiles are predicted due to the grouping of similar distribution parameters with cluster analysis.

Apart from the establishment of regions of relatively higher and lower quantiles, another important aspect to take into consideration is the interval of the contours. Milford (1985 a and b) used 5 m/s intervals for both the hourly mean wind speed map and the gust map. In these maps the areas of equal quantile values were simplified, apparently because of the small number of stations utilised. Another factor could have been the low data resolution, making it impossible to confidently identify areas of higher or lower quantiles according to physical considerations, e.g. topography and prevalent strong wind mechanisms.

Figures 7.6 and 7.9 enable the drawing of contour lines which takes the topography, and to a lesser degree the nature of the strong wind mechanisms, into account. However, these maps were developed with intervals of 5 m/s, as it was not feasible to increase the resolution; mainly due to the trustworthiness one would attach to such high resolution maps, which were developed with an *appreciable measure of subjectivity*. Maps with resolutions higher than 5 m/s created isolated areas of very high or low quantile values, which were not always possible to explain. Another factor taken into consideration was the requirement of simplicity of the contours, for subsequent ease of reference.

Figure 7.12 presents the proposed 1:50 year maximum wind gust map. Some noteworthy features of the map are:

- The general decrease in quantile values from south to north;
- An area of relatively high values in the north of the Eastern Cape province, due to very intense thunderstorms that occur there from time to time;
- The extension of the 40-45 m/s region up to North-West province and incorporating the eastern Free State , to include the regions of relatively strong gusts presented in Figures 8.1 and 8.5. Without this extension the 40-45 m/s region will follow more or less the dashed lines depicted on the map;
- The close spacing of the contours in the Cape Peninsula, due to the complex topography; and
- Two linear features in a SW-NE direction, from the south-western Cape through to Limpopo province. These patterns in the map do not coincide with a single topographical feature, neither with patterns caused by a specific strong wind mechanism (thunderstorms dominate in the north and cold fronts in the south), but are due to the coincidence of prominent topographical features and high gust factors across the country.

Figure 7.13 presents the proposed 1:50 year maximum hourly mean wind speed map. Some noteworthy features are:

- As is the case with the gust map, a general decrease in quantile values from south to north;
- Areas of highest quantiles are the southern part of the Cape Peninsula westwards to include the southern part of the Overberg region, the coast and adjacent interior around Algoa Bay, and an area in the southern interior from the eastern side of the Hex River mountains up to Beaufort-West.

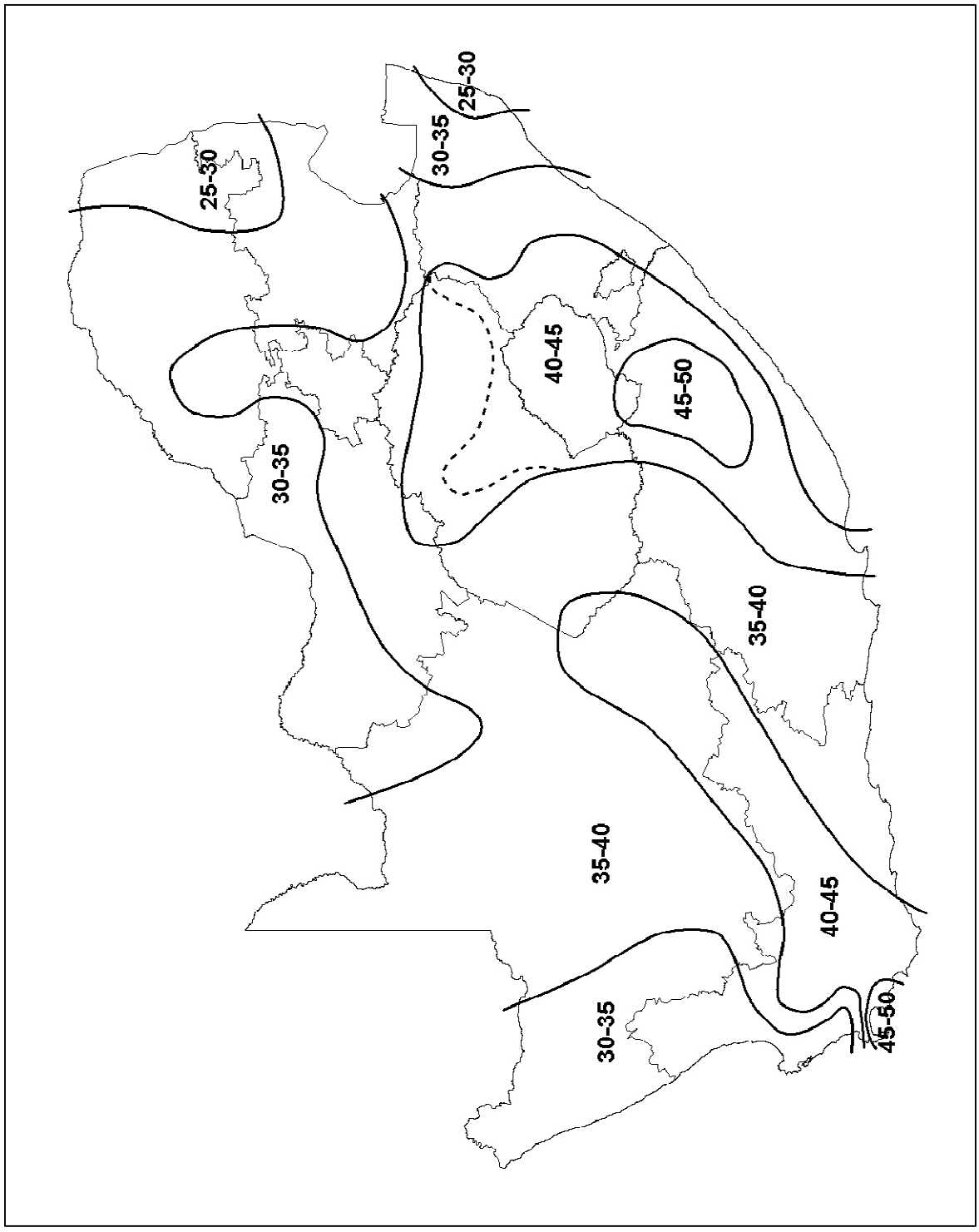

Figure 7.12. Proposed 1:50 year quantiles of the annual maximum gusts (m/s).

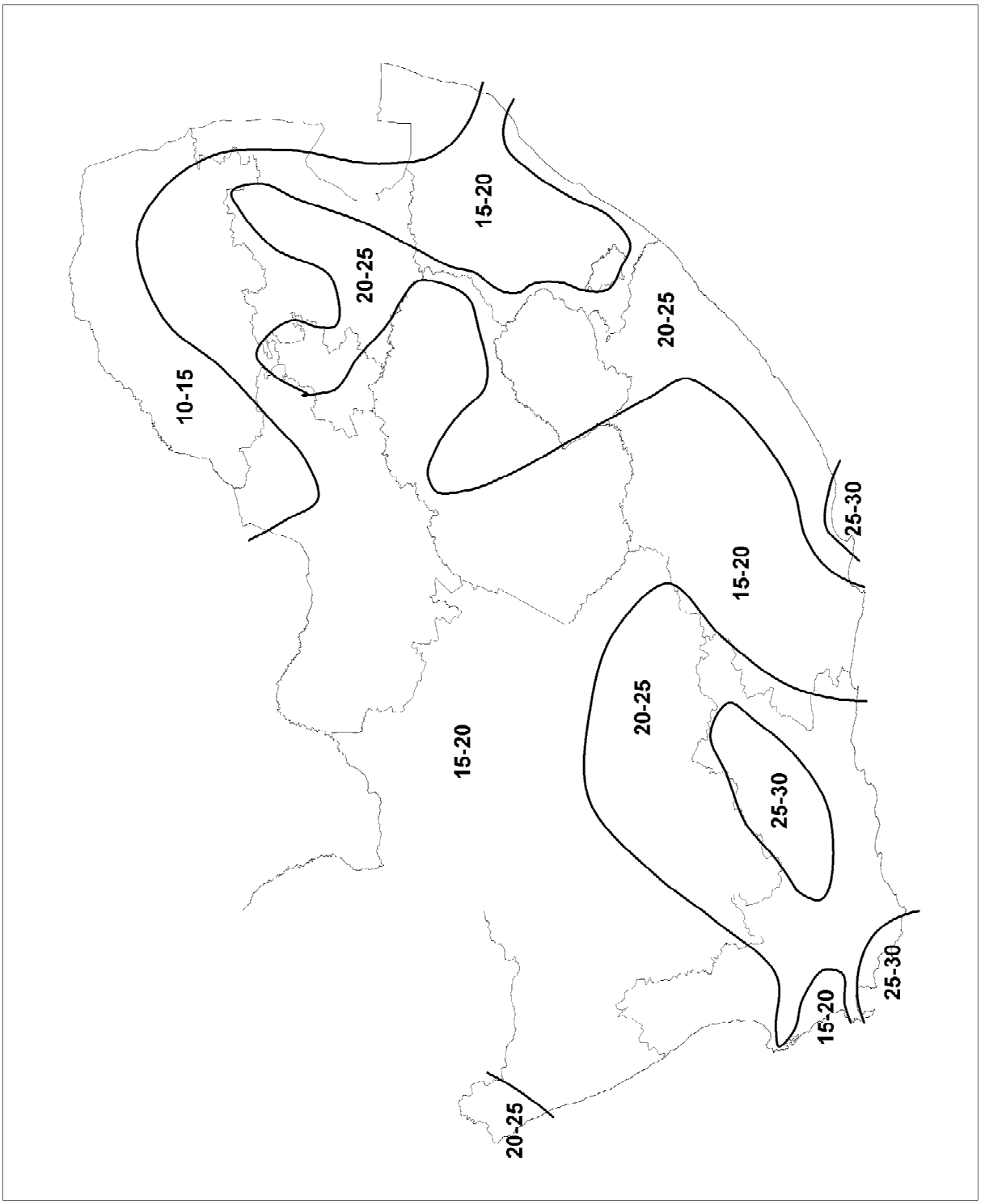

Figure 7.13. Proposed 1:50 year quantiles of the annual maximum hourly mean wind speeds (m/s).

Chapter 8

Assessment and Integration of Extreme Wind Estimations

8.1. Motivation

The development of extreme wind quantiles in Chapter 5, together with the results obtained from the development of the quantile maps in Chapter 7, produced a wealth of new information regarding the characteristics of strong winds in South Africa. However, to obtain a characterisation of these aspects of the strong wind climate, the results need to be integrated to obtain a condensed view of the relationships between strong winds and the mechanisms from which they derive.

In Chapter 6 correction factors to compensate for inadequate exposure of the anemometers were developed. The application of the correction factors made it possible to spatially compare some of the wind characteristics of weather stations with one another. Apart from the intercomparison of extreme wind quantiles, to develop the quantile maps in Chapter 7, other characteristics of the wind can be compared between weather stations on a quantitative basis.

8.2. The mixed climate effect on quantile estimations

In Chapter 5 various statistical extreme value distributions were fitted to samples of the strong wind values. After correction for inadequate exposure, the distribution parameters can be compared to obtain some characterisation of the strong winds.

Of particular importance is the assessment of the distribution of strong wind values forthcoming from the various strong wind producing mechanisms, identified in Chapter 4

and analysed in Chapter 5, to characterise the effect of the mixed strong wind climate on the estimation of quantiles. As shown in section 5.5.2.2, *quantile estimations from the mixed distribution method almost always produce higher quantile values than estimations with the traditional Gumbel method*. The magnitudes of these differences will depend on the estimated values of the distribution parameters of the various strong wind mechanisms involved.

For each weather station and for each relevant strong wind mechanism, the Gumbel distribution parameters have been estimated; i.e. α, the scale or dispersion parameter, and β, the mode. The value of α is mostly influenced by the variance between the annual extreme values in the sample, while the mode is mostly dependent on the mean (see equations 2.6 and 2.7). The values of the quantiles estimated by the mixed distribution method are determined by the values of the distribution parameters of each relevant mechanism, and the resulting contributions of these parameters to the mixed distribution in equation 2.19. Many combinations of parameter values exist in the data set used for analysis.

There are cases where the values of the distribution parameters of one strong wind mechanism are such that the contribution of the particular mechanism tends to dominate the estimation of the quantiles relevant to the built environment, i.e. those of 50 years or longer. Such cases usually occur where the value of α for one mechanism is considerably larger than for the other contributing mechanism(s). However, the value of β can also play a significant role.

The identification of zones of similar values of the distribution parameters requires the application of an objective analysis method. Cluster analysis is often used in climatological studies to define regions with similar climatological characteristics. This type of analysis was applied to group weather stations according to similar values of distribution parameters. Of the different cluster analysis techniques, the most widely applied method is the K-means method, as it is relatively simple to use and also allows reassignment of observations as the analysis proceeds from one iteration to the next.

The K refers to the number of groups or clusters, which is specified in advance of the analysis. The K-means algorithm usually begins with a random partition of the n data vectors into the pre-specified number of groups. The algorithm proceeds then as follows:

1. Compute the vector means, i.e. $\bar{x}_k$, k = 1,…., K; for each cluster.
2. Calculate the Euclidian distances between the current data vector x_i and each of the K $\bar{x}_k$'s.
3. If necessary the x_i is reassigned to the group whose mean is closest. Repeat for all x_i, i = 1...n. Return to step 1.

The algorithm is iterated until a full cycle through all the data vectors produces no reassignments (Wilks, 2006).

For the analysis of the distribution parameters of single climates, cluster analysis could only be performed on thunderstorms and cold fronts in a meaningful manner, mostly due to the limited spatial extent of the other secondary strong wind mechanisms. For the single climate analyses the data from mixed climate cases were also utilised. Where strong wind mechanisms were combined, the combination of thunderstorms and cold fronts, as well as combinations of these two dominant mechanisms with the other secondary mechanisms, could be analysed.

8.2.1. Thunderstorms gusts

Figure 8.1 presents the results of cluster analysis on the distribution parameters of the thunderstorm gusts. Three clusters could be resolved, of which the number of stations, ranges and standard deviations of the values of the distribution parameters are presented in Table 8.1. The weather stations grouped into each zone are also shown. In this regard one should note that the zones presented in the figure and those further on only indicate same strong wind characteristics for the weather stations depicted. Examples where one could erroneously interpolate or extrapolate the results are the Western Cape and Lesotho in Figure 8.1.

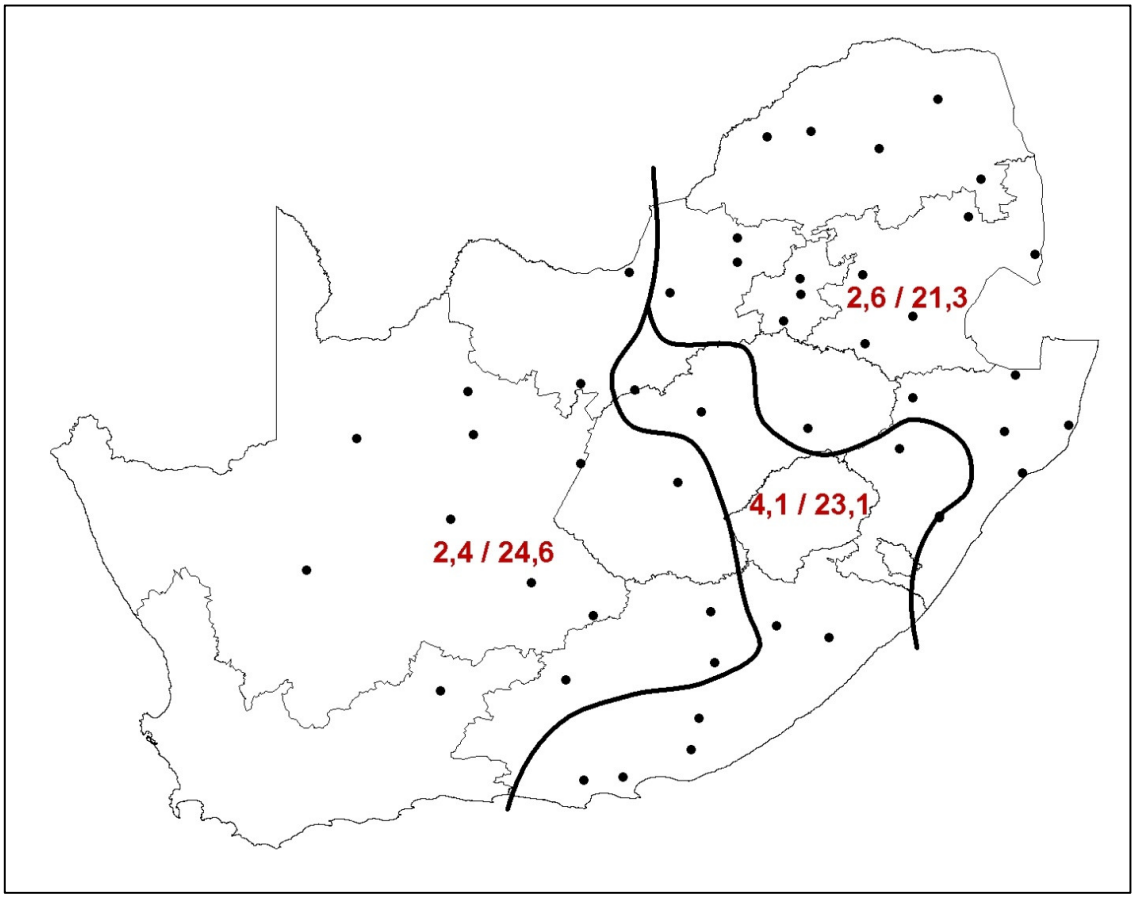

Figure 8.1. Cluster analysis of distribution parameters of thunderstorm gusts, with $\bar{\alpha}/\bar{\beta}$ for each cluster.

Table 8.1. Ranges and standard deviations of estimated values of distribution parameters for weather stations in clusters presented in Figure 8.1.

Cluster $\bar{\alpha}/\bar{\beta}$	Number of stations	α		β	
		Range	σ	Range	σ
2,4 / 24,6	15	2,0 – 3,5	0,5	16,6 – 25,9	2,1
4,1 / 23,1	10	3,8 – 5,1	0,5	17,5 – 26,6	2,9
2,6 / 21,3	23	1,7 – 3,6	0,5	20,6 – 30,0	2,1

The average value of α ranges from 2,4 to 4,1 for each cluster, with the region of highest α covering the larger part of the Eastern Cape province, south-western KwaZulu-Natal and the central Free State provinces, into the North-West province. The

average values of β show a general increase from 21,3 to 24,6, from north-east to south-west. In Table 8.1 it is noticeable that the ranges of the average distribution parameters are comparable, except for the cluster covering the south-east of the country. The high α value is reflected in the relatively bigger range of values of β, which reflects the high interannual variability of the annual maximum gust values in the region.

The region of highest α coincides with the areas of highest quantile values in the east of the country in Figure 7.12. This illustrates the *significant role that the interannual variability of the annual maximum gusts from thunderstorms plays in the estimation of high gust quantiles in the east*. Figure 8.2 graphically illustrates the effect of the different mean distribution parameters, particularly α, on the estimation of the quantiles, in which it can be seen that the regions with similar α show almost the same slope, while the slope for the higher α value presents a much flatter slope with a consequent rapid increase of quantile values with return period.

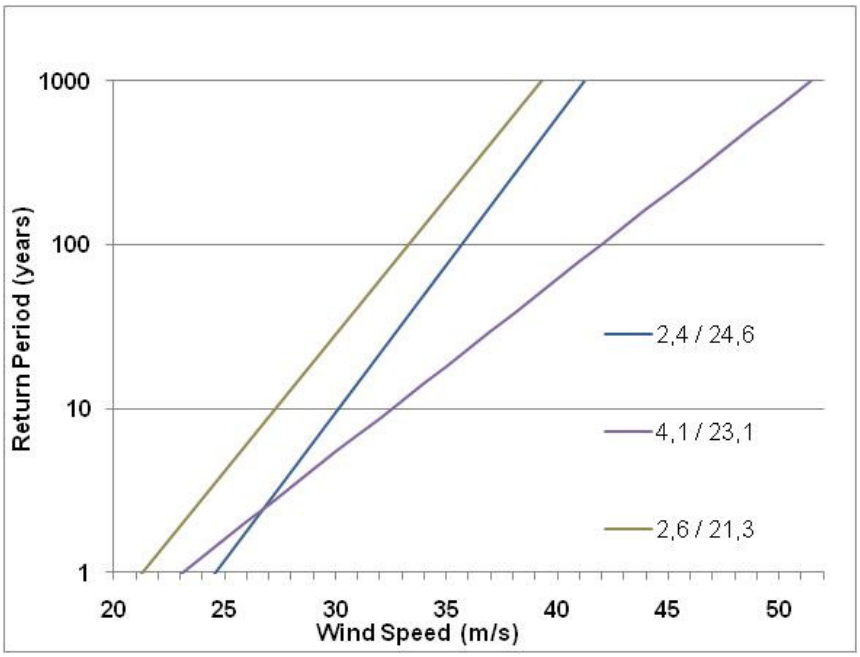

Figure 8.2. Annual maximum wind gust distributions for the clusters presented in Figure 8.1.

8.2.2. Cold front gusts and hourly mean wind speeds

High hourly mean and gust quantiles in the west of the country are mostly due to the frequent occurrence of strong cold fronts, but also the interaction of these fronts with the topography. As cold fronts produce strong winds on the synoptic scale, the relative strength of the winds will also be determined by the height above sea level, as shown in section 7.3.1.3. Apart from the topography, the winds from the cold fronts also tend to be stronger closer to the coastline.

The zoning of similar distribution parameters of wind gusts produced by cold fronts were not satisfactorily resolved by the cluster analysis. The reasons for this seem to be the complex topography, as well as the spatial variability of the gust factor. It is thought that a denser network of weather stations could have produced a result that is spatially more coherent.

However, four spatially coherent zones of similar distribution parameters could be resolved for the hourly mean wind speeds, which are presented in Figure 8.3. The number of stations and ranges of the distribution parameters values for each cluster are presented in Table 8.2. The numbers of stations in each cluster are a function of the spatial distribution of the weather stations influenced by cold fronts, as well as the relative sizes of the zones, e.g. the zone in the south has the smallest number of stations as it mainly covers only the coastal region in the south and parts of the adjacent interior. The ranges and standard deviations of α are comparable. However, the zones in the south exhibit higher ranges and standard deviations of β, which indicates relatively high spatial variability of β values between stations in the south and west of the country. This is probably a reflection of the complex topography of the region.

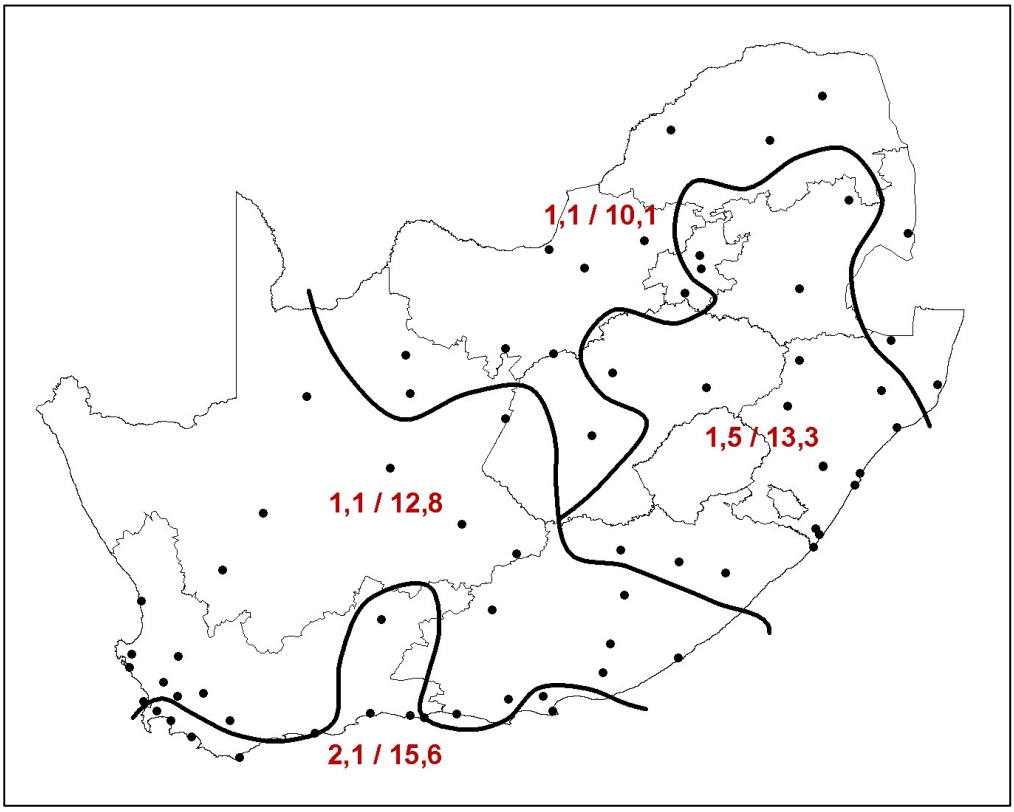

Figure 8.3. Cluster analysis of distribution parameters of hourly mean wind speeds produced by cold fronts, with $\bar{\alpha}/\bar{\beta}$ for each cluster.

Table 8.2. Ranges and standard deviations of estimated values of distribution parameters for weather stations in clusters presented in Figure 8.3.

Cluster $\bar{\alpha}/\bar{\beta}$	Number of stations	α		β	
		Range	σ	Range	σ
2,1 / 15,6	11	1,5 – 2,8	0,4	12,0 – 18,9	2,3
1,1 / 12,8	22	0,7 – 1,6	0,3	8,8 – 18,6	2,1
1,1 / 10,1	15	0,6 – 1,8	0,3	7,0 – 11,9	1,3
1,5 / 13,3	19	0,8 – 2,4	0,4	10,6 – 15,2	1,3

The results for the hourly mean wind speed indicate a general decrease in the mean value of α from south to north, which illustrates the relative strength of the cold fronts as they move over the country. The zone in the east of the country, with a high mean value for α of 1,5, coincides with those annual maximum wind speeds that were caused by

strong winds developed by deep coastal lows to the east, in conjunction with cold fronts to the west. The zone in the south of the country shows the highest mean value for α of 2,1. This region will not only experiences the highest annual hourly mean wind speeds from cold fronts, but also the highest interannual variability, both contributing to the estimation of relatively high quantiles.

Figure 8.4 illustrates the effect of the different mean distribution parameters of the clusters on the estimation of the quantiles. In the south the combination of high α and β values leads to a relatively rapid increase of quantile value with increase in return period, but also to a lesser degree in the east.

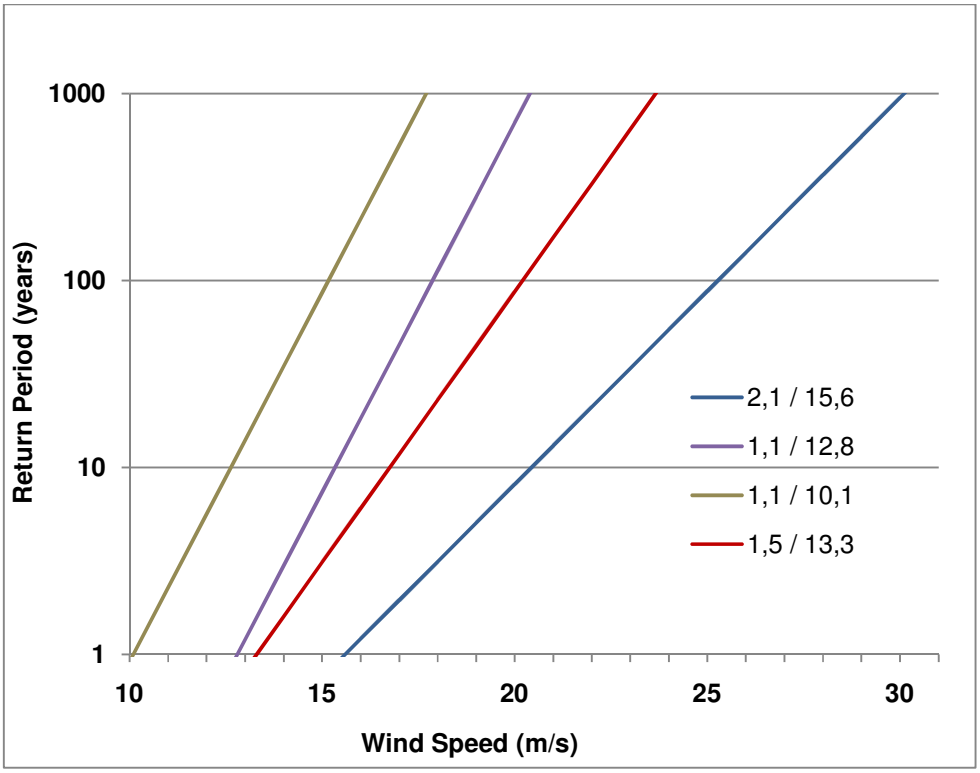

Figure 8.4. Annual maximum hourly mean wind speed distributions for the clusters presented in Figure 8.3.

8.2.3. Combination of thunderstorms and cold front gusts

Cluster analysis was performed on combinations of distribution parameters of different strong wind mechanisms, to investigate the dominance of the particular mechanisms on the estimation of quantiles at different return periods. Figure 8.5 presents the cluster analysis performed on the distribution parameters of the gusts at weather stations where the annual maxima are caused by both the two dominant strong wind mechanisms, i.e. thunderstorms and cold fronts.

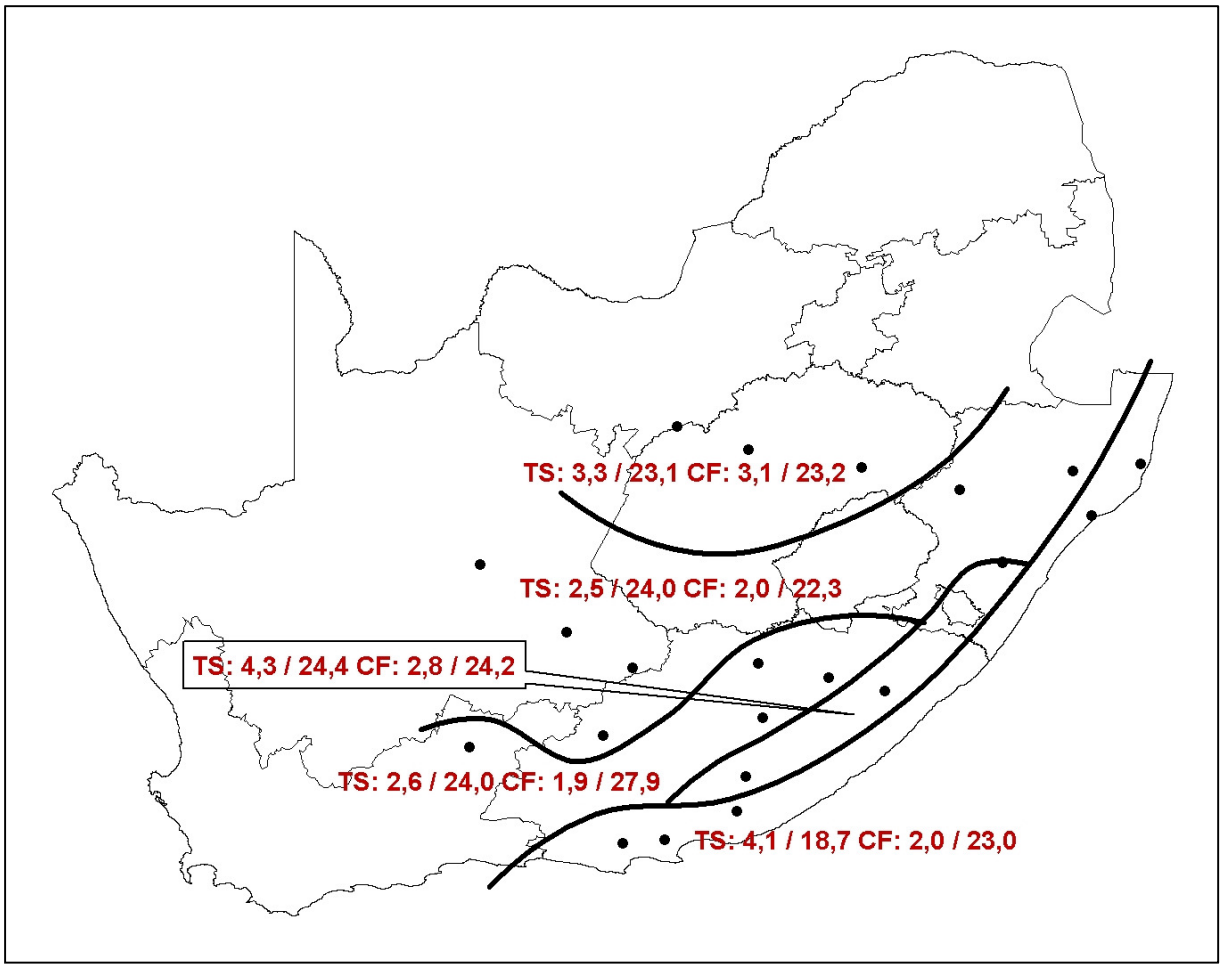

Figure 8.5. Cluster analysis of distribution parameters of gusts produced by thunderstorms (TS) and cold fronts (CF) combined. TS: $\bar{\alpha}/\bar{\beta}$ CF: $\bar{\alpha}/\bar{\beta}$ is shown for each cluster.

The number of stations and ranges of the values of the distribution parameters for each cluster are presented in Table 8.3. For all five clusters the mean value of α is higher for thunderstorms, which indicate larger interannual variability of the maximum gusts from thunderstorms compared to cold fronts. This is especially true for the clusters in the east and south-east of the country, where thunderstorms tend to dominate the estimation of quantiles at longer return periods, such as the weather station of Uitenhage described in section 5.5.2.2. The zones toward the north indicate less dominance from thunderstorms for the weather stations where thunderstorms and cold fronts are the main sources of a mixed strong wind climate. Also notable are two of the zones in the south which show the mean β value for cold fronts to be higher than for thunderstorms. The effect of this is for cold fronts to dominate the estimations of quantiles at shorter return periods, but eventually the thunderstorms will still dominate for the longer return periods.

Table 8.3. Ranges and standard deviations of estimated values of distribution parameters for weather stations in clusters presented in Figure 8.5.

Cluster TS: $\bar{\alpha}/\bar{\beta}$; CF: $\bar{\alpha}/\bar{\beta}$	**Total**	**TS**				**CF**			
		α		β		α		β	
		Range	σ	**Range**	σ	**Range**	σ	**Range**	σ
4,1 / 18,7; 2,0 / 23,0	4	3,0-5,1	0,8	16,6-21,5	1,9	1,8-2,3	0,2	21,6-24,1	0,9
4,3 / 24,4; 2,8 / 24,2	3	3,1-4,9	0,7	20,1-29,2	2,3	2,6-3,1	0,2	21,4-26,8	2,0
2,6 / 24,0; 1,9 / 27,9	5	1,7- 3,9	0,9	20,6-26,6	2,4	1,5-2,0	0,3	25,7-31,5	2,1
2,5 / 24,0; 2,0 / 22,3	7	2,0-3,5	0,5	19,4-30,0	3,0	1,6-2,5	0,3	19,9-24,6	1,7
3,3 / 23,1; 3,1 / 23,2	3	2,3-4,1	0,7	22,3-24,8	1,2	2,8-3,4	0,2	20,5-24,7	1,9

Figure 8.6 illustrates the effect of the different mean distribution parameters of the clusters on the estimation of the quantiles. *For most clusters the estimations of relevant quantiles are almost solely determined by thunderstorms*, except for the north where the mean distribution parameters of thunderstorms and cold fronts are comparable, and a region in the south that are prone to relatively strong gusts from cold fronts.

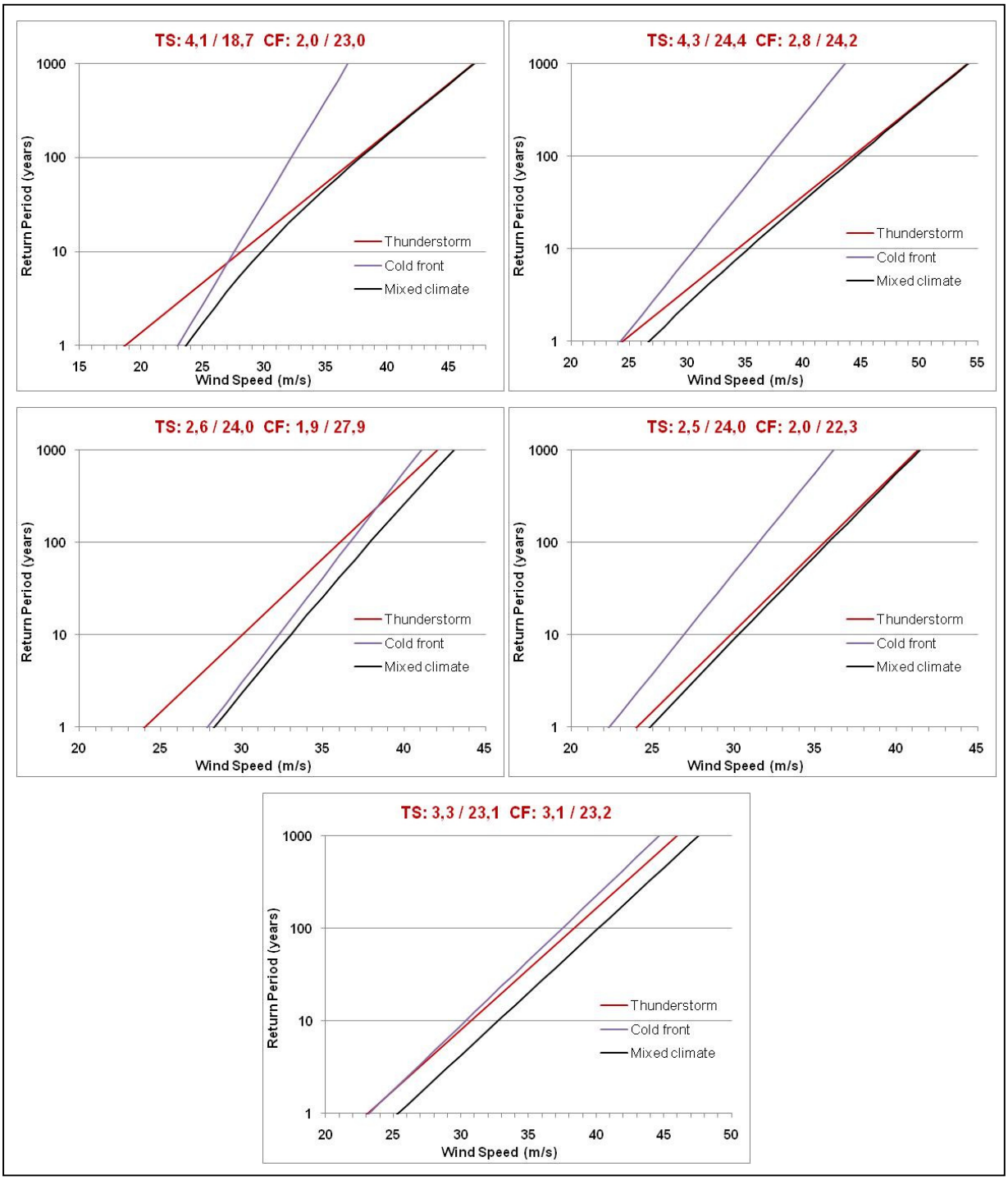

Figure 8.6. Annual maximum gust distributions for the clusters presented in Figure 8.5.

8.2.4. Thunderstorms or cold fronts combined with other strong wind mechanisms

8.2.4.1. Wind gusts

Similar analysis to that performed in the previous section was done for combinations of cold fronts or thunderstorms with other strong wind mechanisms. For only three stations there was a combination of thunderstorms and the other mechanisms for the wind gusts; one station in the western interior where isolated lows play a secondary role in the mixed distribution, and two stations in the north-east where the ridging of the Indian Ocean high-pressure system plays the secondary role.

There were 15 weather stations where the cold front gusts were combined with another mechanism apart from thunderstorms, mostly situated in the west and south of the country. Three clusters could be resolved, as presented in Figure 8.7. The numbers of stations, and ranges and standard deviations of the values of the distribution parameters for each cluster, are presented in Table 8.4. Because of the small number of weather stations that could be analysed the numbers of stations in each cluster are very small, with only three stations in one of the clusters in the south-west. This is also the cluster with the *highest mean value in α for cold fronts*, indicating a relatively larger *diversity in annual maximum wind gusts* compared to the other clusters. This is probably an indication of the *complex topography* of the particular zone. On the other hand the large range in the β values, as well as a high mean α value for cold fronts in the *eastern cluster*, reflects the *climatic diversity of this zone*.

The analysis shows that where cold fronts are combined with other mechanisms, apart from thunderstorms, they tend to dominate the estimation of quantiles for longer return periods in the west and south-west. However, from the eastern side of the south-western Cape and further eastwards, other synoptic-scale mechanisms tend to dominate, particularly the ridging of the Atlantic Ocean high-pressure system in the west, and convergence towards isolated low-pressure systems close to the coast elsewhere.

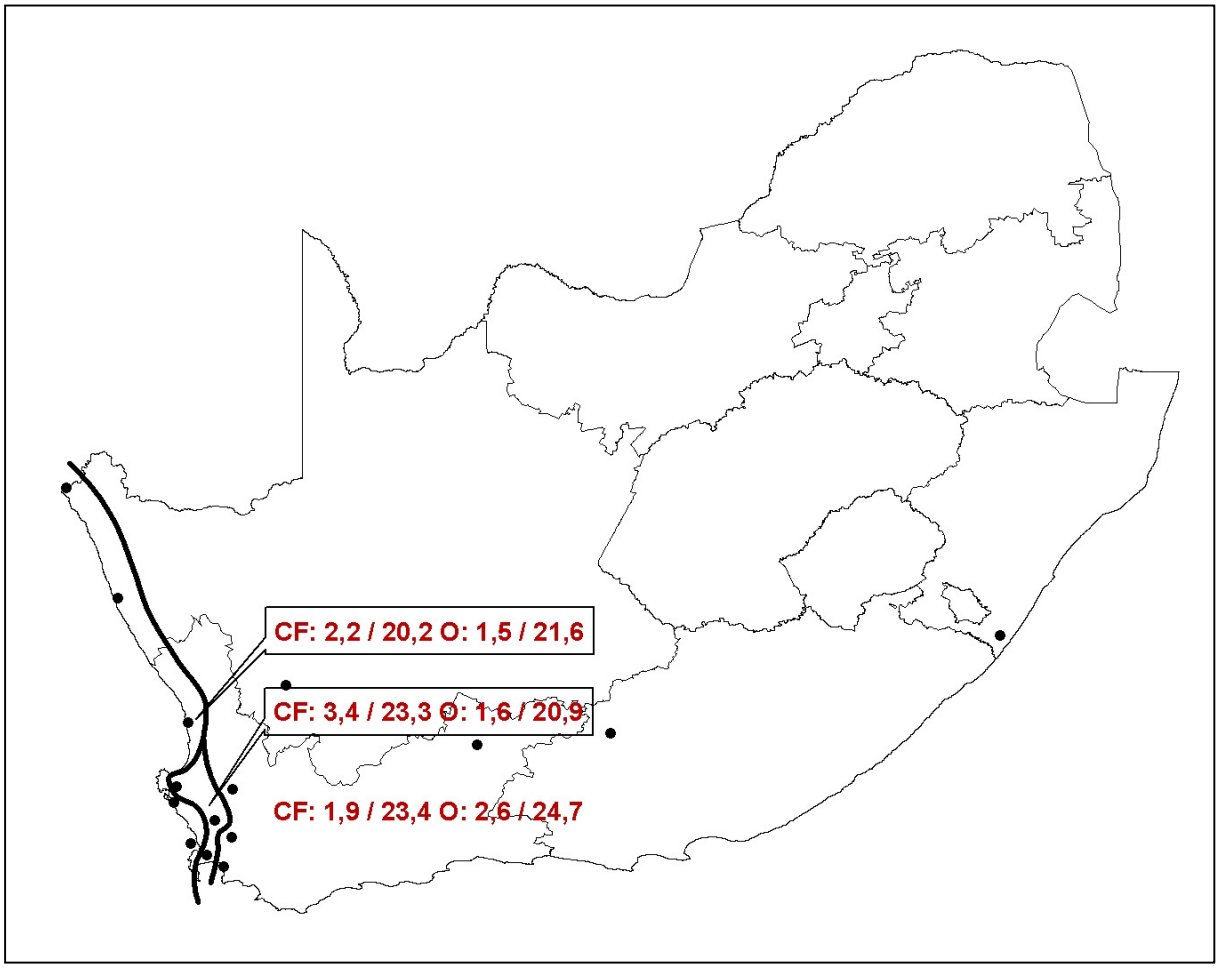

Figure 8.7. Cluster analysis of distribution parameters of gusts produced by cold fronts (CF) and other mechanisms (O) combined. CF: $\bar{\alpha}/\bar{\beta}$ O: $\bar{\alpha}/\bar{\beta}$ is shown for each cluster.

Table 8.4. Ranges and standard deviations of estimated values of distribution parameters for weather stations in the clusters presented in Figure 8.7.

Cluster CF: $\bar{\alpha}/\bar{\beta}$; O: $\bar{\alpha}/\bar{\beta}$	Total	CF				O			
		α		β		α		β	
		Range	σ	Range	σ	Range	σ	Range	σ
2,2 / 20,2; 1,5 / 21,6	6	1,4-2,6	0,4	18,5-22,0	1,1	1,1-1,7	0,2	19,8-23,5	1,2
3,4 / 23,3; 1,6 / 20,9	3	2,7-3,8	0,5	21,2-25,1	1,6	1,1-1,9	0,4	19,1-22,8	1,5
1,9 / 23,4; 2,6 / 24,7	6	1,7- 2,3	0,2	17,4-29,2	3,9	1,9-3,7	0,7	22,5-27,4	1,6

Figure 8.8 illustrates the effect of the different mean distribution parameters of the clusters on the estimation of the quantiles. For all relevant return periods, cold fronts tend to dominate the estimation of quantiles, except for the eastern zone.

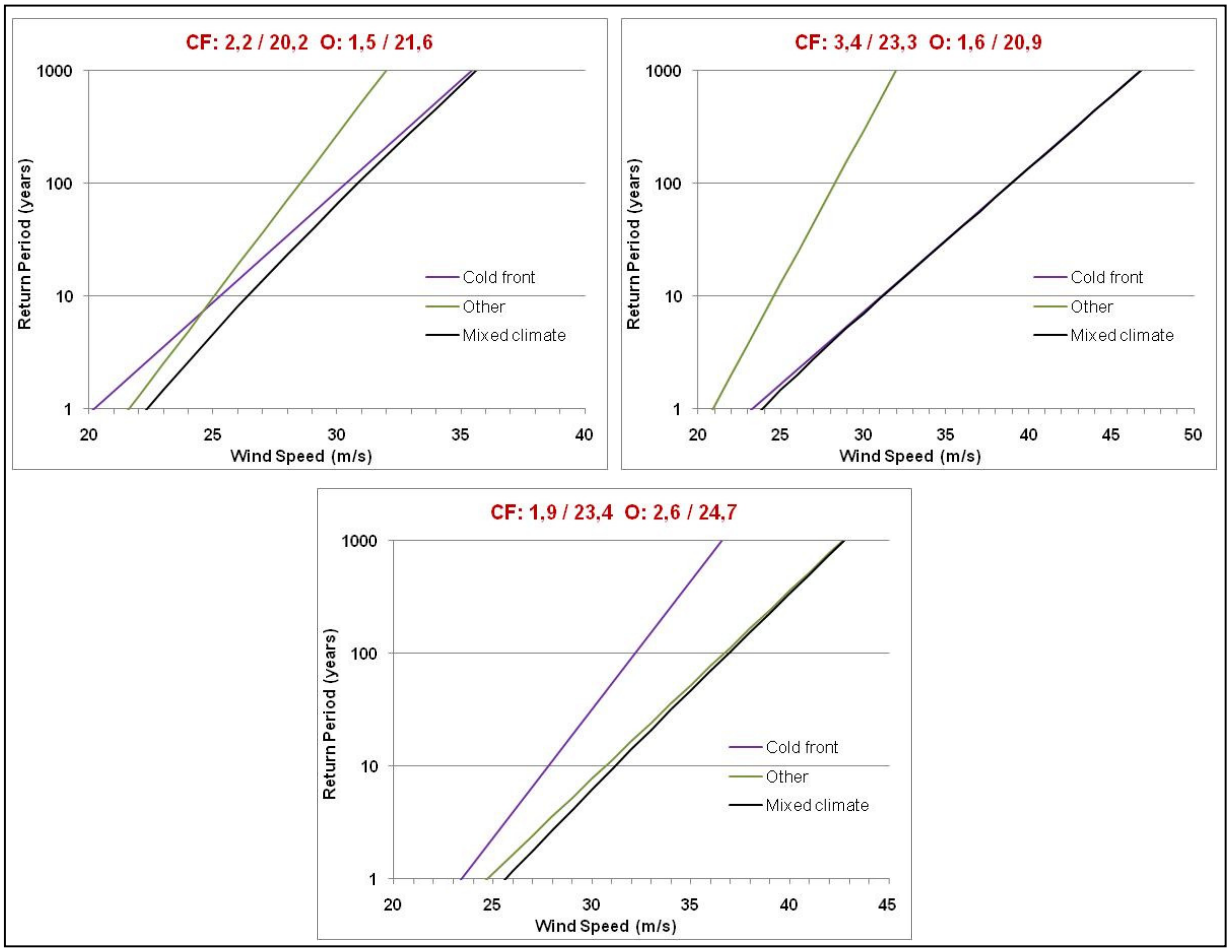

Figure 8.8. Annual maximum gust distributions for the clusters presented in Figure 8.7.

8.2.4.2. Hourly mean wind speed

There were 34 weather stations where the hourly mean wind speeds from cold fronts were combined with other synoptic-scale mechanisms. From the distribution parameters of these stations five clusters could be resolved, which are presented in Figure 8.9. The numbers of stations, and ranges and standard deviations of the distribution parameter values for each cluster, are presented in Table 8.5. The numbers of stations in each

cluster are comparatively small, except for the cluster mostly covering the central and western interior, which covers a much larger area than any of the other clusters. The mean value of α in the southern zone is much larger than in the remainder of the country. The range and standard deviation of the β values for other mechanisms in the south is much larger than elsewhere. This would indicate a tendency in the south for other mechanisms to dominate at short return periods.

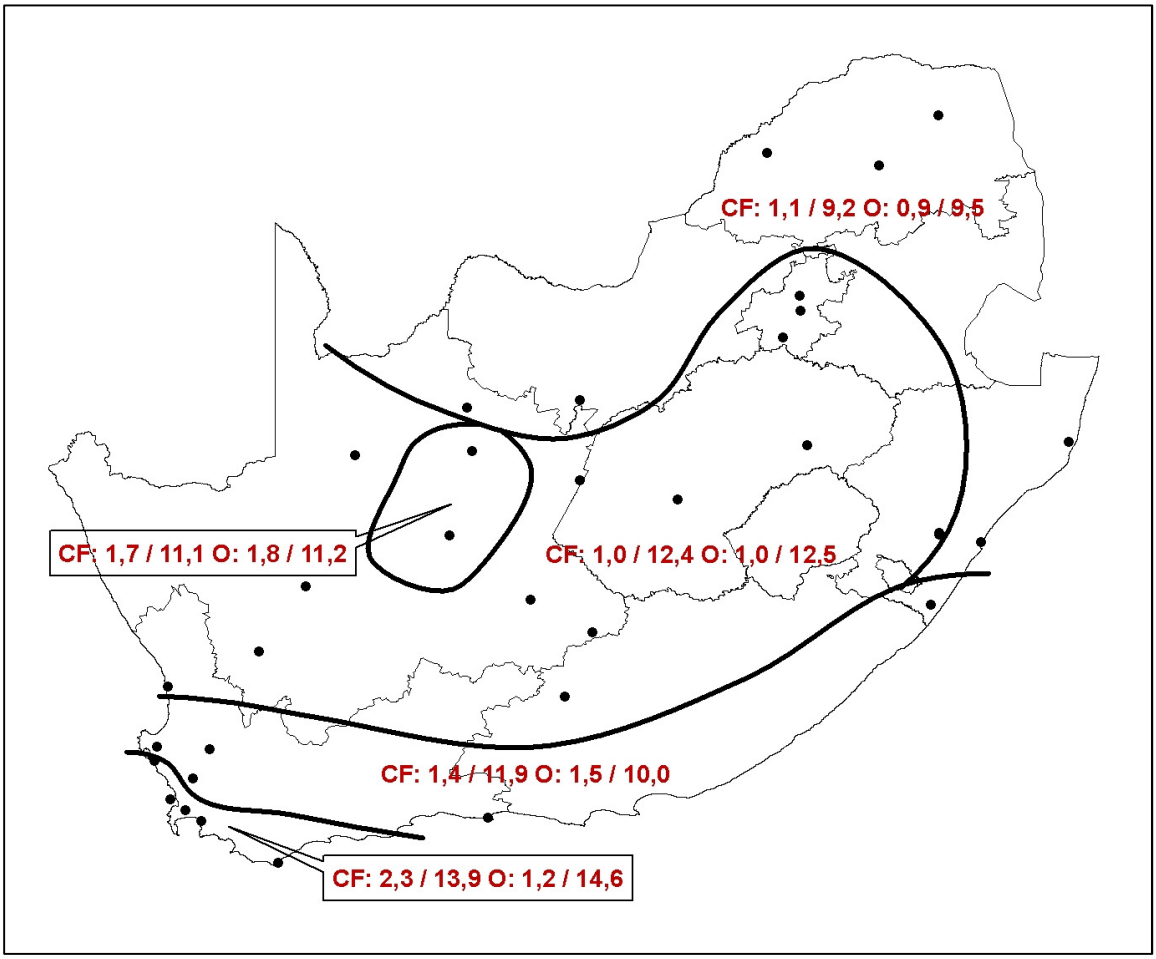

Figure 8.9. Cluster analysis of distribution parameters of hourly mean wind speeds produced by cold fronts (CF) and other mechanisms (O) combined. CF: $\bar{\alpha}/\bar{\beta}$ O: $\bar{\alpha}/\bar{\beta}$ is shown for each cluster.

Table 8.5. Ranges and standard deviations of estimated values of distribution parameters for weather stations in clusters presented in Figure 8.9.

Cluster CF: $\overline{\alpha}/\overline{\beta}$; O: $\overline{\alpha}/\overline{\beta}$	Total	CF				O			
		α		β		α		β	
		Range	σ	Range	σ	Range	σ	Range	σ
2,3 / 13,9; 1,2 / 14,6	5	2,0-2,8	0,3	13,2-15,6	1,0	0,5-1,9	0,5	12,7-16,8	1,7
1,4 / 11,9; 1,5 / 10,0	5	1,0-1,6	0,2	10,6-14,2	1,4	1,1-2,2	0,4	9,1-10,8	0,7
1,0 / 12,4; 1,0 / 12,5	15	0,8-1,3	0,2	10,1-15,9	1,4	0,5-1,6	0,3	10,8-15,4	1,2
1,7 / 11,1; 1,8 / 11,2	2	1,3-2,0	0,4	10,6-11,5	0,5	1,7-1,9	0,1	11,2-11,2	0
1,1 / 9,2; 0,9 / 9,5	7	0,6-1,6	0,3	7,0-10,0	0,9	0,5-1,2	0,2	7,0-11,0	1,1

The zone in the extreme south-west indicates that cold fronts tend to dominate the quantile estimations, indicated by the relatively high mean value of α. The other zones show the distribution parameters of the cold fronts and other mechanisms to be comparable, so that no mechanism will totally dominate the other in the estimation of quantiles over the relevant time scales. Figure 8.10 illustrates the effect of the different mean distribution parameters of the clusters on the estimation of the quantiles. It is only in the south-west of the country where cold fronts totally dominate the estimations of quantiles at relevant time scales.

8.2.5. Combinations of secondary strong wind mechanisms

For the annual maximum wind gusts there are no weather stations with mixed strong wind climates that exclude both thunderstorms and cold fronts. For hourly mean wind speeds there are only two such weather stations, both situated in the extreme west of the country. For these stations the hourly mean wind speed quantiles for longer return periods are dominated by the ridging of the Atlantic Ocean high-pressure system at the one station, while a trough or coastal low-pressure system situated on the West Coast dominates the other.

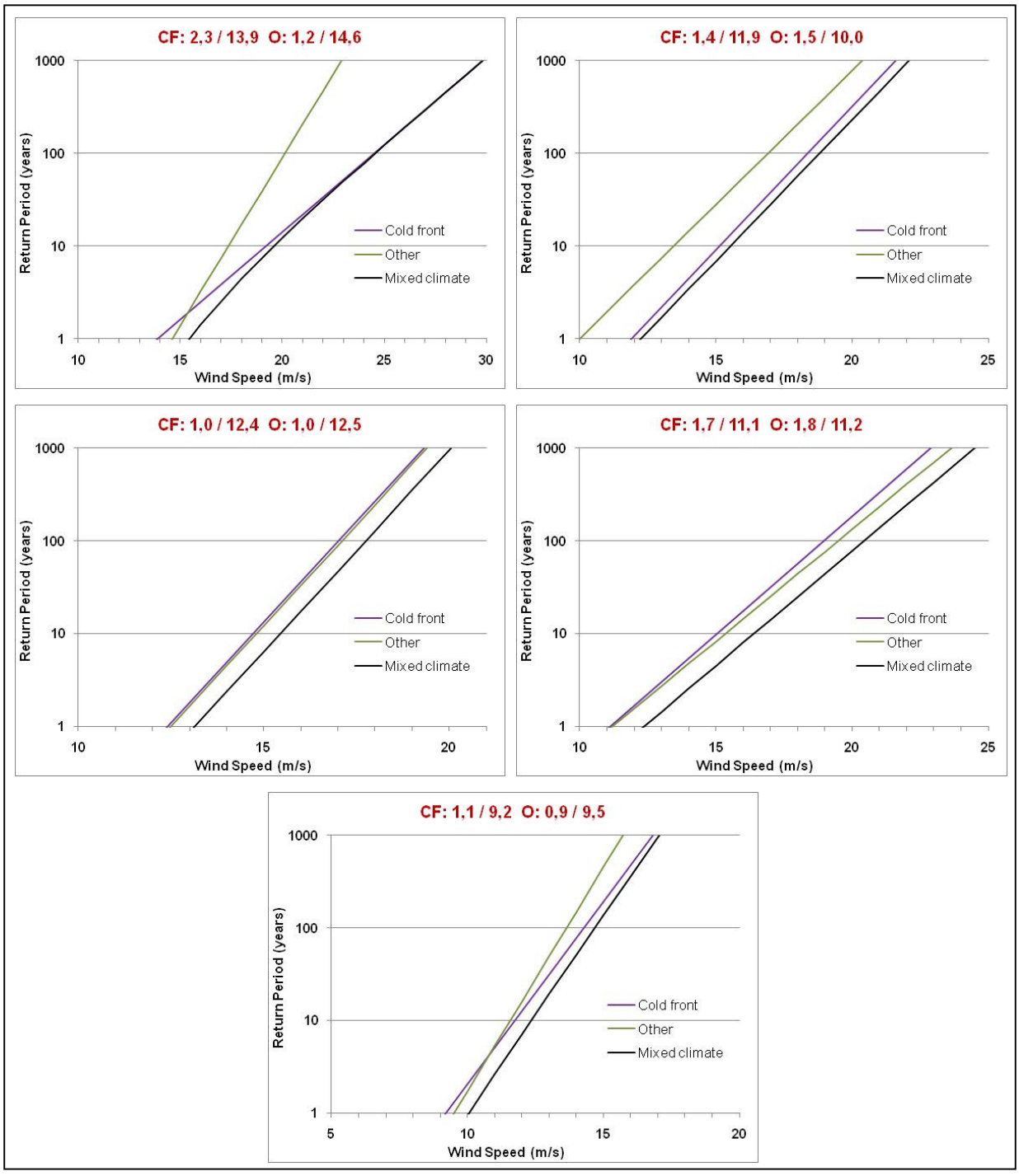

Figure 8.10. Annual maximum hourly mean wind speed distributions for the clusters presented in Figure 8.9.

8.3. Strong wind climatology according to statistical characteristics of mixed strong wind climate

In Chapter 4 South Africa was zoned into geographical regions that indicate the most likely sources of strong winds, particularly the annual maxima of the 2-3 second wind gusts, with the results presented in Figure 4.7. The aim in this section is to identify and characterise strong wind climate regions from the results of the analyses in section 8.2, and, in the case of the 2-3 second wind gusts, to compare these regions with those developed in Chapter 4.

8.3.1. Wind gusts

In section 8.2.1 it was shown that the relatively high gust quantiles in parts of the east and south-east of the country are mainly due to the *high interannual variability of the annual maximum wind gusts from thunderstorms*. This feature of the strong wind climate also plays a role in the estimation of the gust quantiles in a mixed strong wind climate with thunderstorms and cold fronts, as discussed in section 8.2.3. It is shown in Figures 8.5 and 8.6, that in a large part of the south-east of the country thunderstorms tend to dominate the estimation of relevant quantiles, but with their dominance generally decreasing in a north-westerly direction.

It was mentioned that, regarding cold fronts, cluster analysis could not satisfactorily resolve clusters of weather stations with similar distribution parameters for wind gusts.

The combination of cold fronts and thunderstorms was analysed in section 8.2.3, with thunderstorms dominating cold fronts in the south-east, but not so elsewhere. The combination of cold fronts and other mechanisms, discussed in section 8.2.4.1, indicates dominance of cold fronts in the extreme west and south-west, while other mechanisms, such as ridging and isolated low pressure systems play a larger role elsewhere. These results can be summarised on a map as presented in Figure 8.11, which represents a broad characterisation of the relative dominance of the different

strong wind mechanisms, what the statistical estimations of relevant quantiles are concerned. Lesotho has been blocked out due to lack of information.

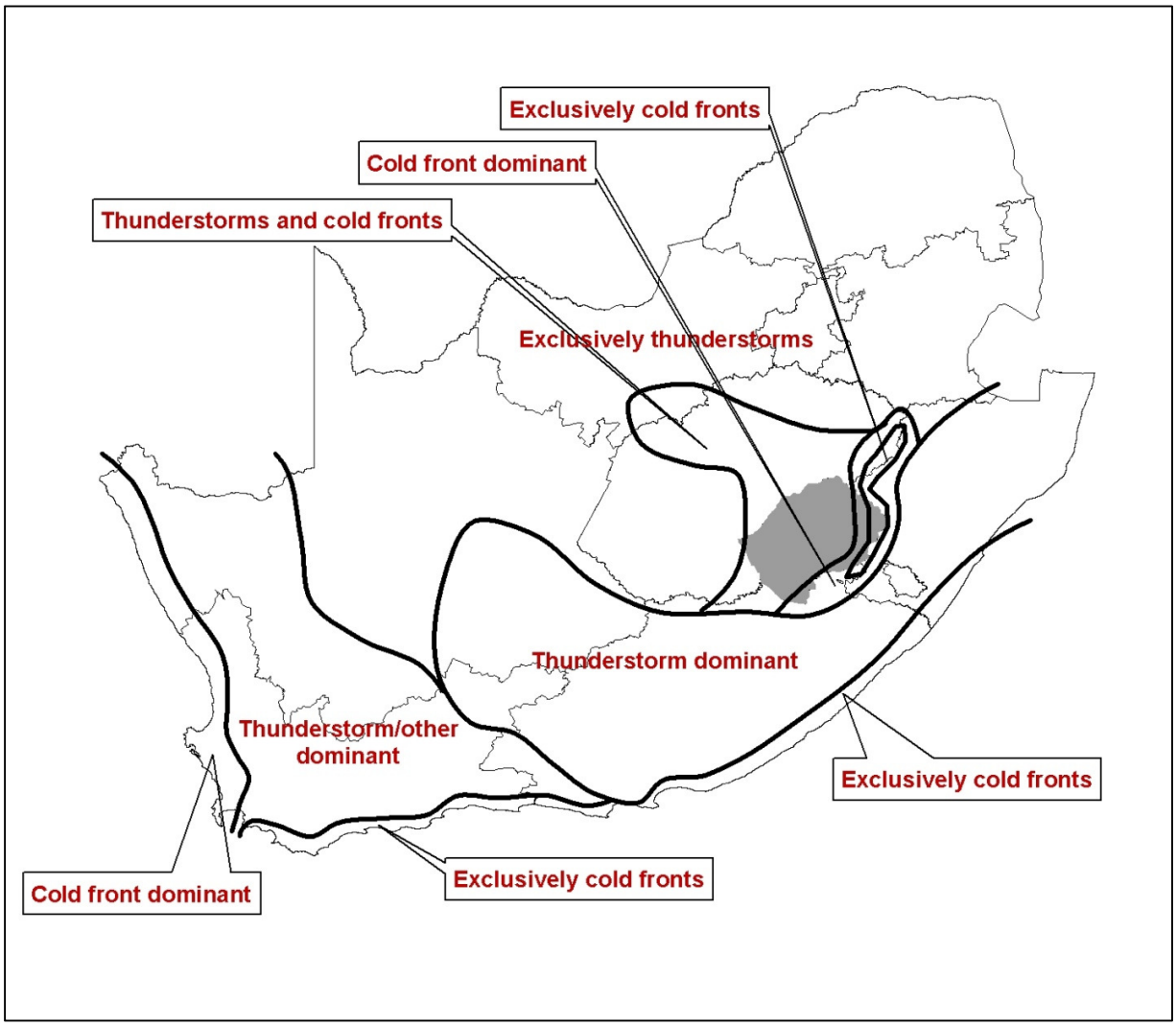

Figure 8.11. Relative dominance of the different strong wind mechanisms for wind gusts.

This map can be deemed to be more informative for some uses than Figure 4.7, which does not provide information on the dominance of the different strong wind mechanisms where they overlap. Over the coastal and higher-lying areas cold fronts tend to dominate. This is probably due to the relationship between the strength of synoptic-scale winds and elevation, as discussed in section 7.3.1.3. Over the lower-lying areas,

even in the south, other mechanisms, especially thunderstorms, dominate the cold fronts. Towards the north the strengths of cold fronts decrease, to such a degree that in most of the northern and north-western interior the annual maximum gusts originate exclusively from thunderstorms

8.3.2. Hourly mean wind speed

It is noted here, as was decided in Chapter 5, that thunderstorms are not considered to be a strong wind mechanism for time-scales longer than a few seconds, due to the very short duration of strong winds from thunderstorms, usually in the form of gust fronts. Therefore a map of the relative dominance of the strong wind mechanisms in the estimation of quantiles on the hourly scale only take synoptic scale mechanisms into consideration.

In section 8.2.2 the relative strengths of cold fronts in the south, in comparison with elsewhere in the country, was discussed. Also, in section 8.2.4.2, as presented in Figure 8.9, the dominance of cold fronts is shown for the weather stations where the strong-wind mechanisms are cold fronts and other synoptic-scale mechanisms. Figure 8.12 presents a map which indicates the relative dominance of the strong wind mechanisms for the hourly mean wind speeds. In the south-west, cold fronts are dominant, with the ridging of the Atlantic Ocean high-pressure system the secondary mechanism. Towards the north along the West Coast annual maximum hourly mean wind speeds are exclusively due to ridging in the south, or the presence of a deep trough or coastal low pressure system more to the north. In the south and east of the country the vast majority of weather stations show annual maximum wind speeds exclusively caused by cold fronts. However, for a small number of stations other mechanisms also play a role, such as ridging or isolated low pressure systems close to the coast. In the region situated mostly in the interior of the country, indicated by “Cold fronts and other”, the cold fronts share their influence with other mechanisms. In the west it is mostly deep surface troughs, while in the north-east it tends to be the

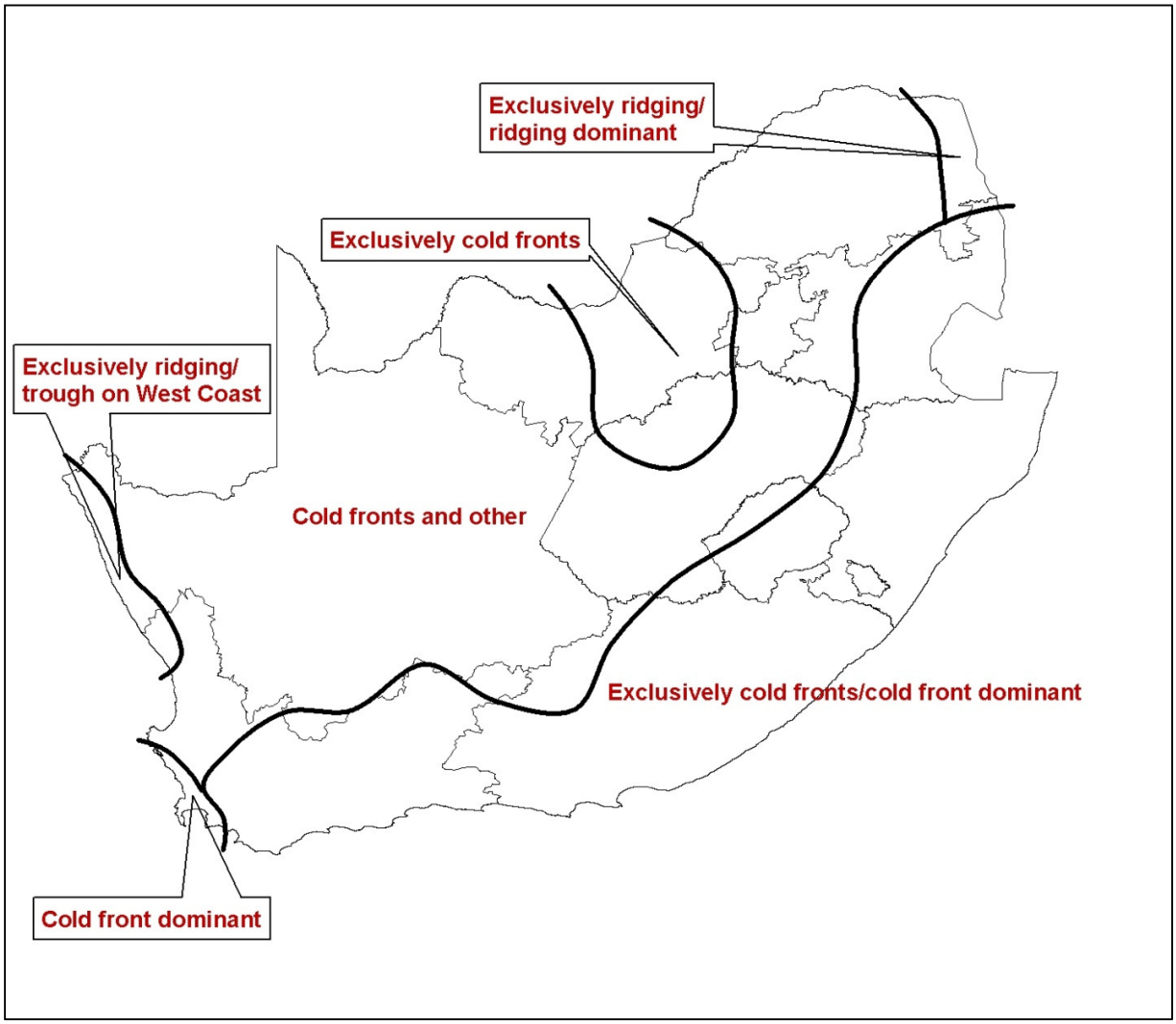

Figure 8.12. Relative dominance of the different strong wind mechanisms for hourly mean wind speeds.

ridging of the Indian Ocean high-pressure system. An area covering most of the North-West province falls beyond the influence areas of these two mechanisms, with the effect that all annual maximum hourly mean wind speeds are caused by cold fronts. In the Lowveld in the far north-east, ridging of the Indian Ocean high-pressure system tends to dominate due to the diminished strength of the cold fronts reaching the area, but also the relative proximity of the area to the quasi-stationary Indian Ocean high-pressure cell.

Chapter 9

Comparison of Extreme Wind Estimations with Previous Analysis

9.1. General

It is important to make a comparison between the design wind speed maps created in the current research, as presented in section 7.4, with those developed in the analysis of Milford (1985a and b), which were introduced in section 2.5. The maps obtained from that study were presented in Figure 2.8, and essentially form the basis of the design wind speeds of the current building standards (SANS 10160-1989, 1989). It is understandable that there will be differences in the maps developed in both studies, due to differences in instrumentations, the related data storage and processing technologies, as well as the analysis methods. The aim of this chapter is to investigate these differences, but also the consequent discrepancies in the quantile estimations.

9.2. Factors influencing the estimation of wind quantiles

9.2.1. Instrumentation

The wind data utilised in the analysis by Milford (1985a and b) were all forthcoming from measurements made with the Dines anemograph, described in section 3.2. At the time AWS technology was non-existent or not mature enough to be used by weather services for routine weather measurements. In contrast, in the present study the data that were used was only that measured by the RM Young sensors, which are incorporated in AWSs.

Table 9.1 presents a list of the national weather stations, as well as their periods of record, of which the wind data was utilised by Milford (1985a and b). From the last column, which indicates the measuring height of the wind instrumentation, one can see that all of these anemometers, except the one at Grootfontein in the Eastern Cape, measured the wind speed at non-standard heights. While most of the measurements were done close to the required standard height of 10 m, some of the weather stations measured at heights significantly different from 10 m, e.g. George (15 m), Port Elizabeth (15 m) and Pretoria (32 m). The latter anemometer measured wind speeds on the roof of a tall building in the Pretoria CBD, where the head office of the SAWS (previously SAWB) was located at the time. The positioning of this weather station makes the wind data from this anemometer unusable for any wind analysis. In the current study all the anemometers measure wind speeds at the standard height of 10 m.

Table 9.1. Wind data utilised in Milford (1985a and b).

Weather station	Station number	Period of record	Anemometer height (m)
Alexander Bay	0274034	1952-82	12
Beaufort West	0092288	1948-63	12
Bloemfontein (Tempe)	0261307	1948-60	12
Bloemfontein (JMBH)	0261516	1962-83	12
Cape Town	0021178	1956-81	12
Durban	0240808	1957-71	13
East London	0059572	1948-83	13
George	0028748	1948-76	15
Grootfontein	0145059	1961-82	10
Johannesburg	0476398	1954-83	13
Kimberley	0290468	1941-83	12
Pietersburg	0677802	1951-83	12
Port Elizabeth	0035179	1949-83	15
Pretoria	0513314	1965-83	32
Upington	0317474	1970-83	12

In Chapter 3 the motivations are outlined why the data from the Dines anemograph were not utilised in the estimations of the wind quantiles in the present study. In essence it was concluded that, due to systematic differences in measurements of mean

wind speeds, the data forthcoming from the Dines anemographs were not compatible with those from the RM Young anemometer.

As shown by other research, this discrepancy between the measurements seems to be especially true during strong wind speeds. Comparing the peak velocities recorded by Dines, cup and sonic anemometers, Holmes and Henderson (2010) found that, for a time history of turbulence used for comparison, the Dines anemograph would have recorded peak gusts about 3% higher than the cup anemometer, which is predominantly used with AWSs in Australia. Additional analysis revealed that the average peak ratio of Dines to cup is about 1,05, but for some peaks the ratio approached 1,1. A companion study by Henderson *et al.* (2010) shows the Dines anemograph to miss large peak gusts (but only for very high frequencies), but amplifying broader peaks from air pressure applied to the Dines pressure-tube. Therefore, the results from both these studies indicate a tendency of the Dines to recorded higher gust values than the AWS. Due to both technologies being of a modern standard, it can be assumed that the response to wind speeds of the cup anemometers utilised in Australia and the RM Young anemometer used in South Africa is about the same. The studies by Holmes and Henderson (2010) and Henderson *et al.* (2010) suggest that correction factors would have to be developed for the Dines measurements, to be compatible with those from present AWS technology.

To illustrate some of the possible discrepancies between the Dines and AWS measurements, the annual maximum gusts speeds recorded at two weather stations are investigated, presented in Figure 9.1 (a) for Alexander Bay and (b) for Cape Town. Both of these stations are located at airports, where the exposure is assumed to be good in the direction of the prevailing strong wind directions. Of relevance are the mean values, but also the standard deviations, during the different recording periods.

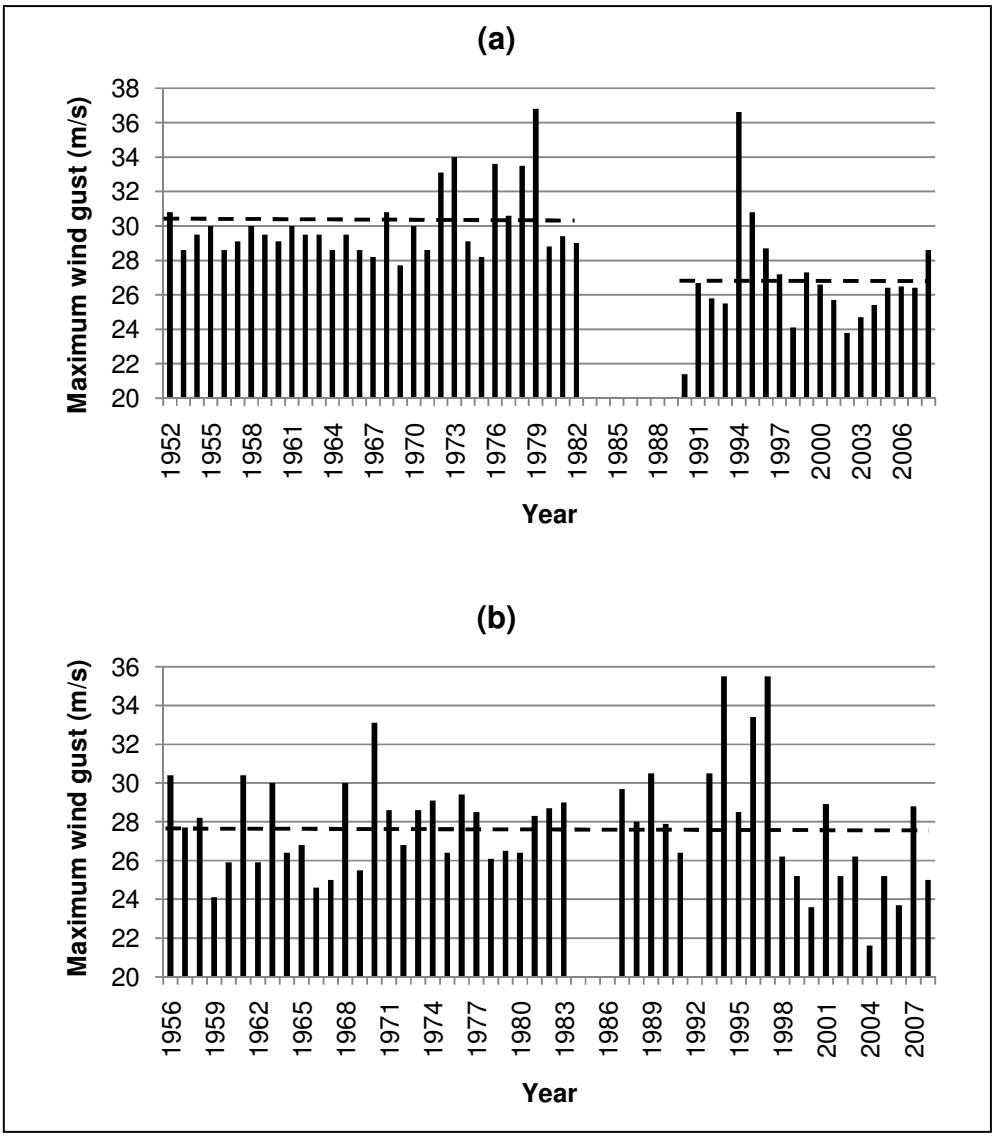

Figure 9.1. Annual maximum wind gust recorded at (a) Alexander Bay and (b) Cape Town. Red lines indicate the mean values over the recording periods.

For Alexander Bay the mean values of the Dines period is 30,1 m/s, while for the AWS period it is 26,7 m/s. The standard deviation for the different recording periods are 2,0 and 3,0 respectively. Both the differences in the mean and standard deviations are statistically different at the 5% level. For Cape Town the mean of the values is almost the same at 27,6 m/s and 27,7 m/s respectively. However, there is a large, statistically significant, difference in the standard deviations, which are 2,0 and 4,1 for the different recording periods. From these results one can conclude that for Alexander Bay there

was a systematic over-estimation of wind gusts, while at both of the weather stations the Dines anemographs seem to have failed to reflect the interannual variation of the wind gusts.

In section 9.3 the values of the 1:50 year wind gusts and hourly mean wind speeds determined by Milford (1985a and b), in comparison to the values used in the present research, for the same weather stations are further investigated.

9.2.2. Spatial coverage of data sets

The periods of data that were utilised in Milford (1985a and b) are presented in Table 9.1. All of the weather stations in Table 9.1 are still operating, except for Bloemfontein (Tempe) and Grootfontein. In the present study a total of 75 weather stations were utilised. This improved coverage of data made it possible to improve on the spatial interpolation of the estimated quantiles, as discussed in section 7.3, which would make the present quantile maps more realistic in terms of the variation of wind speeds with elevation and distance from the coastline.

9.2.3. Exposure of weather stations

For the weather stations which coincide between the study by Milford (1985a and b) and the current study, there were inevitable movement of instrumentation, as they underwent changes in their instrumentation from manual instrumentation to AWS, most of them during 1992. Therefore, while the exact positions of the old Dines anemographs cannot be readily established at present, it is imperative that the new RM Young anemometers would be set up in a different position. The large size requirement of the old Dines anemograph installation (essentially to be housed in a small building) also required the manual observations of wind readings. For this reason the old anemometers were usually situated close to the weather offices for ease of access. With the new AWS technology this requirement was not necessary anymore, with the effect that the new instrumentations could be placed very close or in between runways

in the case of airports, with consequent improvement in exposure. It is argued then that for weather stations located at airports, the exposure of the present instrumentation would in most cases be better than what was the case for the old instrumentation.

However, it is noted here that for many weather stations in the current study, which are not located at airports, the exposure is inadequate. This fact made the development of correction factors for exposure, as discussed in Chapter 6, necessary. In the study by Milford the development of such correction factors would, perhaps in most cases, not have been such a critical factor in the reasonable estimation of quantiles, due to the positioning of most anemometers at airports.

9.2.4. Duration of wind time series

The periods of data for the weather stations utilised by Milford (1985a and b) are also presented in Table 9.1. These periods of wind speed records varied considerably in length between the weather stations; from 13 years for Bloemfontein (Tempe) to 43 years for Kimberley. The average length of record is about 26 years. The lengths of record utilised in the present research varies from 10 to 19 years, as it only utilised data from the AWSs and not the Dines anemographs as was the case in the previous study. If only the lengths of record are taken into consideration, the previous study should provide better estimates of the extreme wind speeds, at these specific locations, than the current analysis.

9.2.5. Data capturing and storage

In the case of the Dines anemographs, the wind speed was recorded with an ink pen on graph paper, which was exchanged on a daily basis. The hourly mean wind speeds were estimated with a scale-ruler by eye. Because the wind speeds measured by the Dines anemograph rest upon the deduction of the wind speed from the air pressure exerted by the wind in a tube, scale-rulers were used to incorporate correction factors to the mean wind speed, to compensate for the variation of the air pressure with height

above sea level. These corrections were standard and used at all weather stations considered to be in the interior of the country, regardless of the variation in height above sea level (and therefore mean air pressure). The daily maximum wind gust were directly read off the graph and digitized, with no correction factor applied. The above factors, as well as the possible human bias or error in the manual digitization of the wind data, obviously could have caused systematic over- or underestimations in the Dines anemograph wind data stored in the climate database.

In contrast to the old technology, wind measurements from the AWSs are digitally stored and electronically transferred to the climate database. Presently the only human intervention is the eventual quality control of the data, e.g. the removal of spikes, which would make the AWS data in general more reliable than the wind data that were forthcoming from the Dines anemographs.

9.2.6. Statistical approaches of strong wind speed estimations

The strong wind speed estimations by Milford (1985 a and b) are based on the average of a number of statistical methods. In the case of the hourly mean wind speed, the 1:50 year quantiles were obtained by the results of the applications of the Type I, II and III GEV distributions, as well as those obtained directly from the parent distribution. For the wind gusts, the 1:50 year estimations were based on fitting the Type I distribution to the square of the gust speed. It is shown in Milford (1985b) that the fitting of the Type I distribution to the square of the wind gusts instead of the wind gust values themselves render slightly reduced values, usually in the region of 0,5 to 1 m/s in the case of the 1:50 year wind gust.

In the present research the statistical method to estimate the maximum hourly mean wind speed estimations depended on the type of strong wind climate at the location of a specific weather station. Where the strong winds had a single cause, the 1:50 year maximum wind speeds were estimated with the Type I distribution, while in the case of a mixed strong wind climate the mixed strong wind distribution approach was followed.

Milford (1985a) found apparent mixed climatic conditions in the parent distribution, and considered the necessity of the separation of each climatic condition. This was however not done, as the extreme value distributions obtained directly from the annual maxima did not show this trend. Following the findings of the research by Milford, it was shown that on most occasions the mixed climate approach renders quantile values which are significantly higher than when a single strong wind climate is assumed.

For the extreme wind gust the approach in the present study is to use the values of either the POT method with the EXP distribution, or the method for mixed climates. In the case of a mixed strong wind climate the preferred method depends on which estimated extreme value is the largest, which contributes to the conservativeness of the current estimations. In the case of a single strong wind climate only the results from the POT method was used. It was mentioned in Chapter 2 that the Gumbel approach is not the preferred method for shorter time series, especially those shorter than 20 years (Palutikof *et al.*, 1999). The present approach, which uses the POT method, is therefore preferable above the Gumbel, due to the short data records. Considering only the differences in analysis methods, the present research should produce somewhat higher, i.e. more conservative quantile values, than those reported by Milford.

9.3. Comparisons of specific results

In Table 7.3 the final 1:50 year wind gusts and hourly mean wind speeds were presented which were used in the development of the maps presented in Figures 7.12 and 7.13. Table 9.2 presents the values of the 1:50 year wind gusts and hourly mean wind speeds determined by Milford (1985a and b), in comparison to the values used in the present research, for the same weather stations. It can be seen that for most stations the differences in the estimates quantiles will have an influence on the design of the built environment.

Table 9.2. Comparison between the 1:50 year maximum wind gusts and maximum hourly mean wind speeds as determined by Milford (1985a and b), and those in the present study (m/s).

Weather station	1:50 year wind gust speed			1:50 year hourly mean wind speed		
	Milford (1985b)	Table 7.3	Difference in values	Milford (1985a)	Table 7.3	Difference in values
Alexander Bay	41	32,5	-8,5	25	22,9	-2,1
Beaufort West	51	40,3	-10,7	30	27,3	-2,7
Bloemfontein (JMBH)	41	37,3	-3,7	21	15,1	-5,9
Cape Town	34	39,5	+5,5	22	24,1	+2,1
Durban	37	34,9	-2,1	23	19,6	-3,4
East London	38	36,7	-1,3	23	19,9	-3,1
George	37	34,0	-3,0	22	22,1	+0,1
Johannesburg	39	36,3	-2,7	19	19,8	+0,8
Kimberley	40	38,8	-1,2	19	17,7	-1,3
Pietersburg/Polokwane	34	36,4	+2,4	17	18,4	+1,4
Port Elizabeth	40	41,1	+1,1	23	25,9	+2,9
Upington	40	39,8	-0,2	21	17,7	-3,3

9.3.1. Wind gusts

For the 1:50 year maximum wind gusts, the values included in Milford (1985b) are generally higher than those from the present study. This is the case for nine out of the 12 coinciding weather stations. The mean difference between the values is 2,0 m/s. These differences cannot be solely attributed to the higher elevations of the old instrumentation, as according to the logarithmic profile the difference in wind speed between e.g. heights of 10 m and 12 m should typically be around 1 m/s for the magnitudes of the wind speeds concerned. The differences in wind gusts are also not spatially correlated. Examples are the weather stations at Cape Town and George in the south, with +5,5 m/s and -3,0 m/s respectively, and Polokwane and Johannesburg, with +2,4 m/s and -2,7 m/s respectively.

The largest difference in the estimated 1:50 year gusts is for Beaufort West, where the Milford study indicates a value 10,7 m/s higher than in the present study. Actually, the value for Beaufort West of 51 m/s is significantly higher than any other 1:50 year gust value determined in the Milford as well as present study. The present value of 40,3 m/s estimated for Beaufort West is more comparable to those of the surrounding weather stations (see Figure 7.10). While 16 years were utilised in the Milford study, a comparable 13 years were utilised in the present study. Therefore the difference in the number of years utilised should not play a significant role in the large discrepancies in the estimated quantiles. On closer inspection of the data sets, the data set used by Milford indicates annual maximum gust speeds higher than 40 m/s for 7 of the 16 years utilised. The current AWS has not once measured gust speeds above 40 m/s, the highest being 38,7 m/s. While it is currently not possible to establish the specific reason for the differences in these wind gust strengths measured, it seems a possibility that the older instrument experienced calibration problems. Operational experience of ESKOM suggests that the magnitude of the 3s gusts over the central parts of South Africa is less extreme and more evenly distributed than suggested by the previous wind speed maps (Marais, pers. comm.), which were dominated by the high quantile value estimated for Beaufort West. Therefore, it is reasonable to assume that the quantile value of 51 m/s for Beaufort West is unrealistic; possibly due to incorrect location or calibration of the anemometer.

Another large difference is for Cape Town weather office. The study reported by Milford estimates a 1:50 year gust quantile of 34 m/s, while in the present study the 1:50 year gust is estimated as 39,5 m/s. The Cape Peninsula is well known for stronger winds than its surrounding areas. It therefore seems unlikely that the closest weather station to Cape Town in the study by Milford, which is George, would have a 1:50 year gust value 3 m/s higher than Cape Town. Visual inspection of the 1:50 year gust values in and around the Cape Peninsula estimated in the present study would indicate that a 1:50 year gust value of 39,5 m/s might be a more accurate estimation than 34 m/s.

9.3.2. Hourly mean wind speed

For the 1:50 year hourly mean quantiles the values obtained by Milford (1985a) are also generally higher than those in the present study. However, this is the case for seven out of the 12 weather stations, which is fewer weather stations than for the gusts. The mean difference between the values is 1,2 m/s. One can also note that for the weather stations for which the quantiles were estimated higher by Milford, it was usually also the case for the gust values, and vice versa. Also, as was the case for the gust values, the differences are not spatially correlated. This is important to note, as it eliminates the possibility that the differences in values can be attributed to a gradual change in the strong wind climate over specific regions in South Africa.

Some of the largest differences between those obtained by Milford and the present study are for Bloemfontein (5,9 m/s), Durban (3,4 m/s) and Upington (3,3 m/s), where the older study estimated higher values for all these weather stations. The number of years utilised in the estimations of the quantiles for the older study, compared to the present study, were Bloemfontein: 22 years and 16 years, Durban: 27 years and 15 years, and Upington: 14 years and 16 years. The argument can therefore be that because the Milford study utilised a larger number of years for most of these estimations, the results should be more accurate. However, this would not explain why all of these quantile estimates were higher in the older study, even with the very conservative approach in estimations of the current study.

9.4. Combinations of old and new time series

In section 9.2.1 the discrepancies in the annual maximum wind gust readings between the Dines and AWS periods were highlighted for two weather stations, namely Alexander Bay and Cape Town. However, the argument exists that the combination of all recording periods will produce quantile estimates that are more reliable, due to the use of very long time series. Figure 9.2 presents the gust distributions estimated with the old, new as well as combined data sets for Alexander Bay and Cape Town.

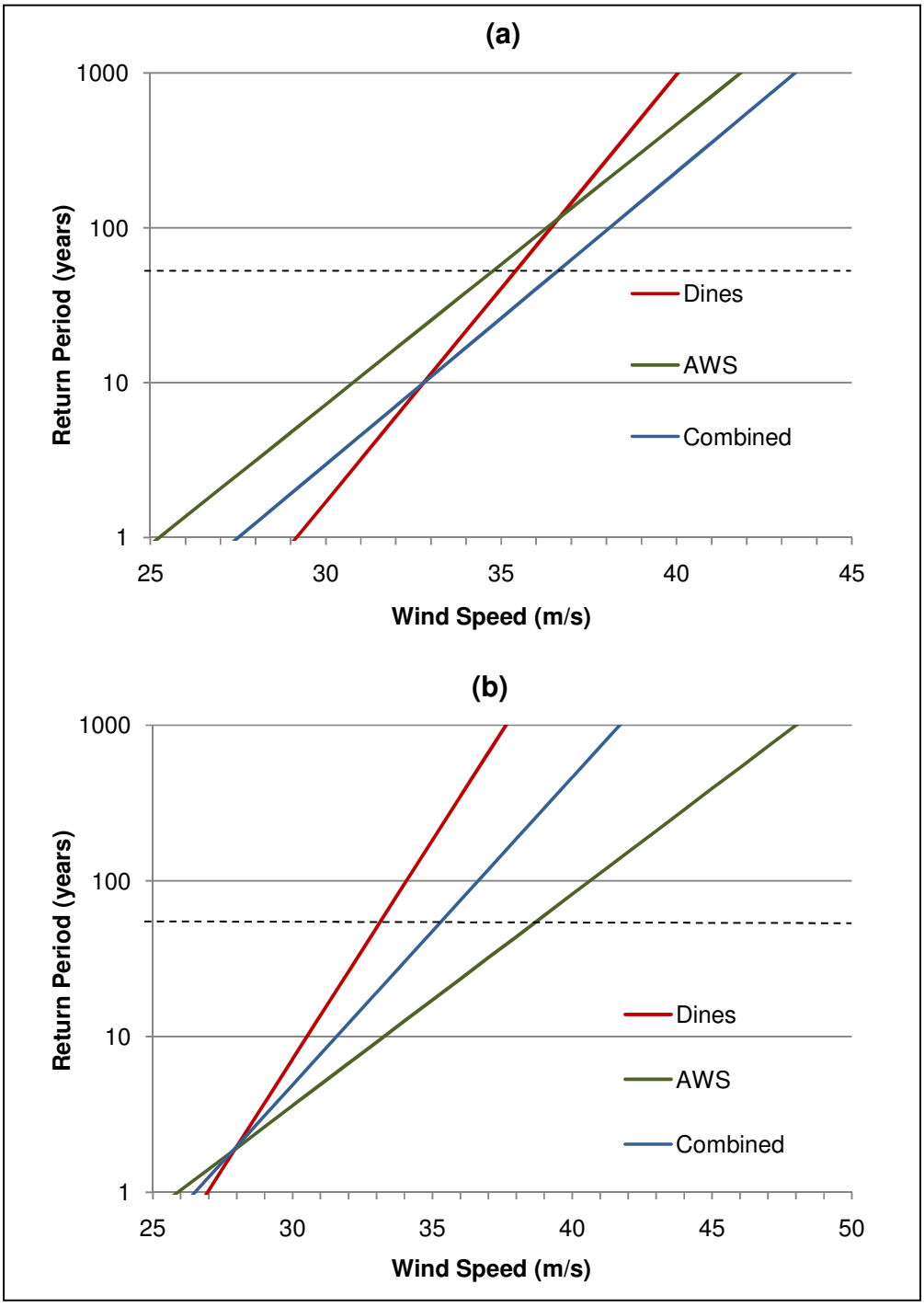

Figure 9.2. Wind gust distributions for different periods of data for (a) Alexander Bay and (b) Cape Town.

Table 9.3 summarises, for the different recording periods, the statistical differences in the data sets, distribution parameters and quantile estimates for different return periods. For Alexander Bay one can see that for all relevant return periods, *the combined data set produces the highest quantile estimates*. Comparing the Dines and AWS data sets, the AWS data produces lower quantiles up to a return period of about 100 years, after which, due its higher interannual variability and therefore α parameter, the AWS data produces higher quantiles. For Cape Town the *AWS data produces the highest quantile estimates for all relevant return periods*. This is because, while there is not a systematic change in the mean of the annual maximum wind gusts, the interannual variability, and therefore α parameter, of the maximum wind gusts are much higher in the AWS than for the Dines recording period.

Table 9.3. Mean and standard deviations, distribution parameters and quantile estimations for annual maximum wind gusts for the different recording periods, for (a) Alexander Bay and (b) Cape Town.

(a) Alexander Bay							
Data set	**Mean**	**Standard deviation**	α	β	**Return period (years)**		
					50	**100**	**500**
Dines	30,1	3,0	1,6	29,1	35,5	36,4	39,0
AWS	26,7	2,0	2,4	25,3	34,9	36,6	40,2
Combined	28,8	2,9	2,3	27,5	36,5	38,0	41,5
(b) Cape Town							
Data set	**Mean**	**Standard deviation**	α	β	**Return period (years)**		
					50	**100**	**500**
Dines	27,6	2,0	1,5	27,0	33,0	34,1	36,6
AWS	27,7	4,1	3,2	25,9	38,5	40,6	45,8
Combined	27,7	2,8	2,2	26,5	35,1	36,7	40,2

The above two examples illustrate how the use of different periods of data can significantly affect the quantile estimations. The differences between the quantile estimates for the different recording periods can be assumed to be unique for all the weather stations in Table 9.1. Therefore, before data sets are combined to produce

longer time series, which are ideal, it would be advisable to thoroughly investigate the unique circumstances which prevailed when the Dines anemographs were used. For example, if data sets were combined the 1:50 year quantile for Cape Town will be estimated as 35,1 m/s, which is significantly lower than the 38,5 m/s estimated with the AWS data. *The risk of such underestimations motivates the use of data sets of which a fair assessment of the quality can be made*.

9.5. Conclusions

This chapter compared the differences in the results obtained by the study of Milford (1985a and b) and the present study. It should be acknowledged that even for the same locations, data sets spanning different periods will produce different quantile estimations, as the climate is never constant and often exhibits some kind of cyclic variability. However, in the study by Milford, substantial differences in the quantile values than those in the present study were obtained. *Without any additional information or metadata on the old instrumentation, such as exposure assessments and calibration routines, it is virtually impossible to find the specific reasons for some of the large differences in the quantile values*. Due to these uncertainties, it is therefore concluded that the present study should produce more adequate quantile estimations because of the application and use of:

- Data sets from instrumentation which *responds better* to the measurement of strong winds;
- *More appropriate statistical techniques* for the data at hand, such as the POT and mixed distribution methods;
- Climate data of which the reliability is better known, due to readily available *metadata*;
- The consideration of the *exposure* of the weather stations and application of correction factors; and
- The adjustment of values to compensate for the *number of years* of data utilised in the quantile estimations.

Chapter 10

Conclusions

10.1. Summary of work

This dissertation endeavoured to provide better insight into the strong wind climatology of South Africa, with the main aim an update of the statistical analyses of extreme winds relevant to the design of the built environment.

Figure 10.1 presents a summary of the investigative process which was followed in the development of updated design wind speed maps:

- An initial investigation, from existing literature, into the *prevailing macroclimatic conditions* over South Africa was conducted in section 2.2: Strong winds can be associated with synoptic as well as mesoscale causes, and therefore a mixed strong wind climate prevails over substantial parts of South Africa.
- The various *statistical approaches for the estimation of extreme winds* were investigated in section 2.3. This includes the traditional approaches as well as other approaches that were developed for mixed strong wind climates and short time series.
- After investigation into the occurrence of *infrequent extreme meteorological events*, i.e. tornadoes and tropical cyclones, in section 2.4, it was shown that, for design purposes of single structures, these wind speeds do not need to be taken into consideration due to their low annual probability. However, it is advisable that the probability of tornadic events be taken into account in the design of line structures, such as power transmission lines, which can cover large distances.

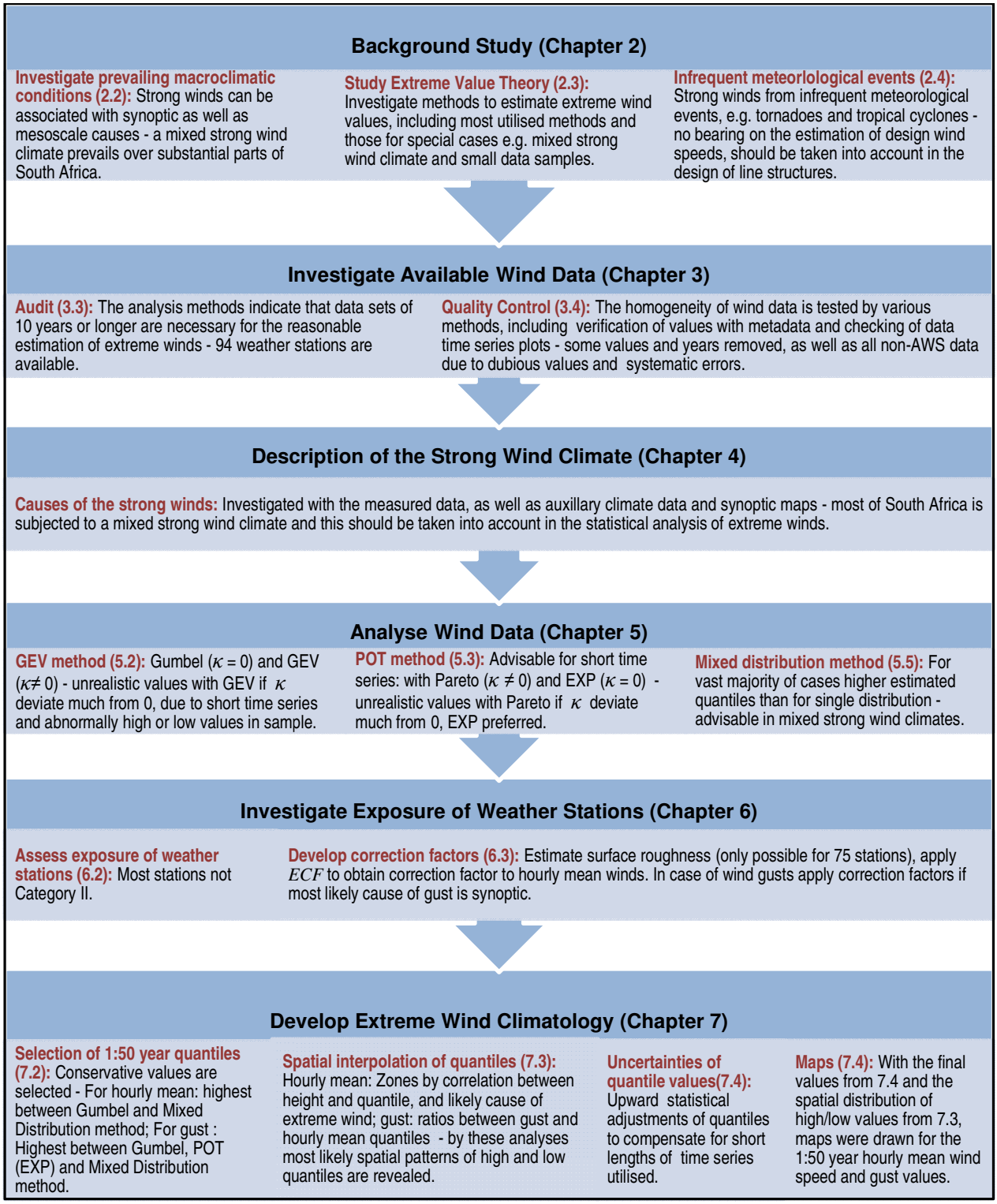

Figure 10.1. General process followed in the development of an extreme wind climatology for South Africa.

- The available *wind data* in the SAWS database, which is suitable for use in the study, were audited and quality controlled, and presented in sections 3.3 and 3.4. An important finding in this regard was that the data from the old Dines instrumentation were not to the same standard as that from the new AWS technology. This older data was therefore excluded from further analysis. A data set consisting of 94 weather stations, with more than 10 years of wind data of acceptable quality were selected for further analysis.
- The *strong wind climatology for South Africa*, presented in the form of detailed maps of zones of strong wind mechanisms, was updated in Chapter 4. These strong wind zones can now be referred to as a reference to the nature of prevailing strong winds over a specific geographical region in South Africa: Strong winds in South Africa are caused by both synoptic- (e.g. cold fronts) and mesoscale phenomena (thunderstorms).
- Chapter 5 discusses the *use of applicable statistical approaches* to estimate the extreme wind speeds: Alternative approaches to the traditional Gumbel method is advisable, firstly because of the mixed strong wind climate prevailing over the larger part of South Africa, but secondly also due to the use of the short time series in the study.
- The *exposure of the weather stations* utilised in the study were investigated in Chapter 6: The surroundings of most weather stations did not conform to Terrain Category II, which necessitated the estimation and incorporation of correction factors to the wind speed, unique for each weather station and every wind sector. Due to inadequate exposure and surrounding complex topography of some weather stations, a reduced number of 75 weather stations, from the 94 weather stations identified for the study, remained to be utilised for the development of the wind speed design maps which would follow.
- The values estimated from the most appropriate statistical methods for design wind speeds, from the various techniques investigated in Chapter 5, were used to develop the *updated maps of the regional design wind speeds* in Chapter 7. For conservativeness the following approach was taken: The highest result from the acceptable analysis methods was used. To compensate for the short lengths

of record the quantile values were adjusted upwards according to their confidence limits at the 75% level, which is common engineering practice. In section 7.3, techniques were developed to guide the spatial interpolation of the quantiles. The final extreme wind speed maps are presented in Figures 7.12 and 7.13, for the 1:50 year maximum wind gusts and hourly mean wind speed respectively.

To obtain a *characterisation of the strong wind climate* of South Africa, specifically with regards to the effect of the mixed strong wind climate on extreme wind estimations, the results of Chapters 5 to 7 were integrated to obtain a condensed view, as it was then possible to compare the characteristics of the strong wind mechanisms between weather stations on a quantitative basis.

Finally, a *critical comparative study* was conducted between the analysis approach and results of this study, and that by Milford (1985a and b). The present maps provide a more detailed representation of extreme winds in South Africa, mainly because of the analysis of many more weather stations, and the integration of topographical features in the interpolation of quantile values, e.g. if a comparison is made between the quantile values around Beaufort West between the previous and present maps. Therefore it could be concluded that the current study produced more reliable results because of the application and use of more appropriate statistical techniques for the data at hand, the use of climate data of which the reliability is better known, the consideration of the exposure of the weather stations, and the adjustment of values to compensate for the limited number of years of data utilised in the quantile estimations.

10.2. Assessment of results

The assessment of the results is based on the degree in which the problems stated in section 1.3 were resolved. Residual issues are indicated and measures are proposed for these to be addressed.

10.2.1. Physical environment

The *diversity of the strong wind climate* of South Africa is characterised by the different mechanisms which produce the strong winds. These are thunderstorms, which are the main producers of strong winds in the interior of the country, and synoptic-scale systems, especially cold fronts, which produce the strongest winds observed along the coast and adjacent interior.

Apart from the different strong wind producing mechanisms, the topography also plays a major role in the magnitude of the strong winds at the synoptic scale. It has been found that, at a regional scale, the quantiles for the hourly mean wind speed tend to be higher at higher altitudes and vice versa. This property of the strong winds assisted in the development of the design wind speed maps.

While the *coverage of the weather stations* utilised in the present study provides an improvement on that in previous studies, some issues still remain which compromise the adequate analysis of the strong wind climate:

- In those regions where strong winds from thunderstorms dominate there might be the risk of underestimation of extreme winds. Thunderstorms, in contrast with synoptic-scale systems, are mesoscale phenomena and therefore occur on a much smaller spatial scale. Smaller areas prone to relatively strong gusts, located in a region dominated by thunderstorms but with a sparse observation network, might therefore not be resolved.
- Other regions as well can be deemed to be insufficiently covered with long-term wind observations to accurately estimate the strong wind climate. Examples of these are the *Drakensberg area along the eastern escarpment*, as well as the *densely populated Gauteng area*. With regards to Gauteng, it will be beneficial for the built environment if the denser populated areas have denser data networks to estimate the extreme winds, especially where thunderstorms are prevalent.

It has been found that, similar to other climatic parameters, *near-decadal cycles in mean wind speeds* exist. Most probably this will have an effect on the estimation of extreme wind speeds, due to the short time series, all shorter than two decades, utilised in the study. If the extreme winds are estimated with a data sample from a period of higher mean wind speeds, higher quantiles may be estimated, and vice versa. This is especially true for synoptic-scale winds.

A follow-up study is proposed to assess the prevalence of cycles in the wind data of South Africa, and to what degree these influence the estimation of wind quantiles.

10.2.2. Interpretation of wind data

The interpretation of the wind data in terms of the strong wind mechanisms, were performed in Chapter 4, the design wind speed maps in Chapter 7 and the synthesis of the results in Chapter 8. The general characteristics of the magnitude of the quantiles could be identified, as well as regions which have significantly higher quantiles than their surroundings.

10.2.2.1. Hourly mean wind speed

For the hourly mean wind speeds, a general decrease in quantile values could be observed from south to north. Strong hourly winds are caused mainly by the passage of cold fronts, which originate in the Southern Ocean. As these fronts move over the southern African subcontinent they tend to lose strength, mainly due to interaction with other weather systems to the north. The regions of highest quantile values are the southern part of the Cape Peninsula eastwards to include the southern part of the Overberg region, the coast and adjacent interior around Algoa Bay, and an area in the southern interior from the eastern side of the Hex River Valley to Beaufort-West. No in-depth study into these regional anomalies was conducted; as such a study will entail the investigation of the variability of wind speeds at a resolution significantly higher than the synoptic scale by climate modelling. However, it is highly possible that in all of the

mentioned regions, *topography* plays a major role in the strength of the wind speeds observed: Significant topographical features, *essentially the escarpment* which form the divide between the coastal regions and the plateau in the interior, are present to the north, while the cold fronts approach the regions from the south. This might result in an increase in pressure gradient, which in turn has the effect of accelerating the wind flow.

10.2.2.2. Gusts

For the gust quantiles, a decrease in quantile values could also be observed from south to north, but less so as is the case for the hourly mean wind speeds, due to the different origins between strong gusts at the coast and in the interior. While the strongest winds in the south of the country, as well as the coastal regions, are caused by the passage of cold fronts, highest gusts in the interior are mainly caused by the gust fronts originating from thunderstorms. The strength of thunderstorm gusts decrease from east to west. Conspicuous is an area of relatively high quantiles in the north of the Eastern Cape Province. This is due to very strong thunderstorms that occur in this region from time to time: In the major part of the interior a mixed strong wind climate exists. In certain parts, such as the Eastern Cape interior, the strengths of the annual maximum wind gusts from thunderstorms vary widely from year to year, with the consequence that the variance used in the estimation of the shape parameter of the Gumbel distribution is very high, which in turn causes an estimation of large quantiles. Other parts where the interannual variability in the strength of the maximum wind gusts are high are central Free State, as well as the east of the Northern Cape province. The close spacing of the contours in the Cape Peninsula, with anomalously high quantile values to the south, is probably due to the complex topography as is the case for the hourly mean wind speed quantiles.

10.2.2.3. Strong wind climate

The differences in the dominance of the different strong wind mechanisms on the hourly and 2-3 s gust time scales were shown in Figures 8.11 and 8.12. A combination of

these figures, as illustrated in Figure 10.2, indicates the *complexity of the South African strong wind climate* in the sense that, except for the larger part of the coastal region and the eastern escarpment, it is impossible to use established conversion factors between different averaging time scales.

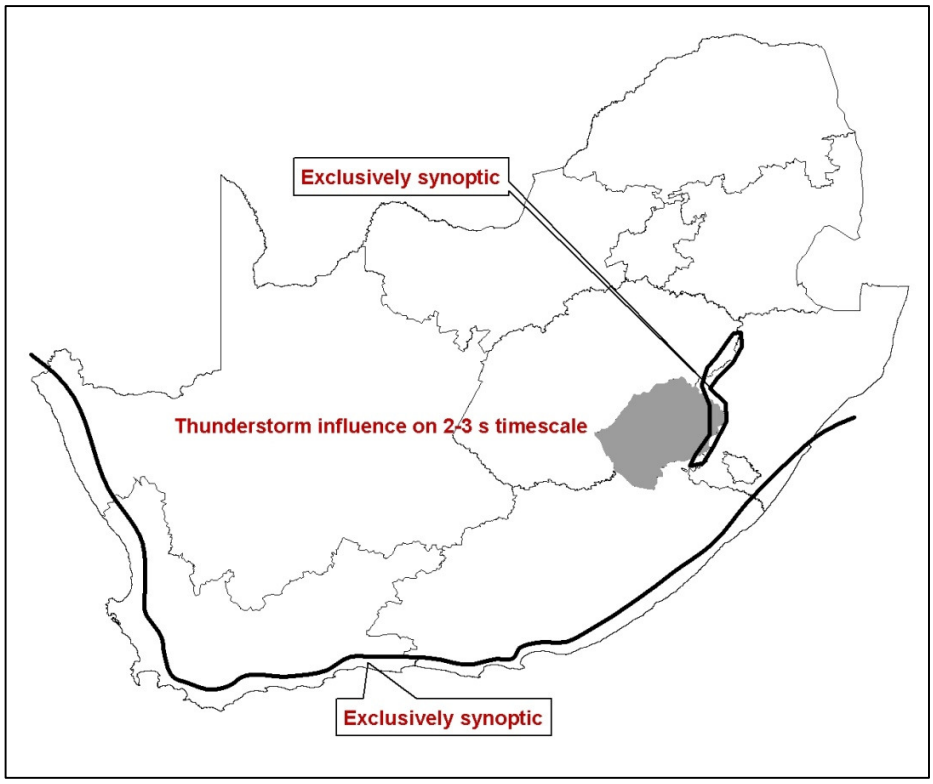

Figure 10.2. Combination of Figures 8.11.and 8.12, illustrating the synoptic and thunderstorm influences on the hourly and 2-3 s gust time scales.

- It was found that even in regions where same mechanisms are responsible for the strong winds on hourly and gust time scales, other factors play a role in the complexity of the strong wind climate. Examples of these are the south-western Cape and the Drakensberg, where the topography increases the spatial variability of the quantiles.
- Important regions, in terms of population density and economy, are not excluded from the complexity of the strong wind climate. In Gauteng and to a lesser degree the Durban area, it is mainly because of the spatial variability of the gust factor, while

in the south-western Cape and possibly also the Port Elizabeth area, the topography seems to be the main factor.

- Other factors that add to the uncertainty and complexity of quantile estimations are the occurrence of thunderstorms, embedded in cold fronts, which in many cases are the cause of the annual maximum wind gusts along the south-eastern and eastern coastlines, the low resolution of weather stations in regions where thunderstorms are dominant, e.g. Gauteng, as well as the estimation of quantiles in regions of complex topography such as the escarpment and the regions around Lesotho.

10.2.3. Strong wind data

In section 3.3 and audit was made of the available climate data. The wind data can be divided into two distinct periods. These are the period of manual observations with the Dines anemograph, and the AWS period, mostly since 1992. It was found that significant discrepancies exist between the two recording periods for relevant weather stations in terms of the mean wind speed. The measurements made by these two types of instrumentation differ in the sense that the Dines in most cases probably overestimated the magnitudes of strong wind gusts, while not detecting some gusts of very short duration. Research into the Dines anemograph by Holmes and Henderson (2010) and Henderson *et al.* (2010) confirmed initial suspicions, and suggest that correction factors would have to be developed for the Dines measurements, to be compatible with those from present AWS technology. In the light of these findings a decision was made that, due to the present incompatibility of the measurements, only data from the AWSs would be utilised in the study. This decision compromised the lengths of record that could be utilised for 13 weather stations, which in turn would compromise the suitability of some statistical methods for the estimations of quantiles.

While a total of 93 weather stations with more than 10 years of AWS data were initially identified for use, the eventual number suitable for the development of design wind speed maps was limited to 75 stations, due to inadequate exposure of the anemometers. For most weather stations correction factors for exposure had to be

applied, while for a significant proportion the exposure was so compromised that, for the data to be usable, wind tunnel studies are suggested to develop reasonable correction factors to their data. The sitings of weather stations are critical, and in this regard the cooperation between the built environment, which can provide advice on the optimal positioning of wind recording facilities, and meteorological services are critical. *Adequate exposure of all the weather stations which were potentially available would have made a significant difference in the shortcomings in the coverage of the wind data, highlighted in 10.2.1.*

Apart from the inadequate exposure, other quality issues regarding the climate data were found. These are mainly gaps in the data records, spikes and calibration issues. An effort was made to detect these problems and remove erroneous values from the data sets eventually utilised. In this regard no stations were omitted due to these quality issues. However, calibration problems caused some years to be excluded from further analyses; but this was not a widespread issue. *The wind data itself was therefore in general of good quality.*

The duration of the wind records was a challenge, and limited the choice of appropriate statistical analyses that could be applied. Examples of these limitations are the compromise in the applications of the GEV and POT methods to estimate quantiles, where the κ parameter was set to zero to avoid the estimations of unrealistically high or low quantile values due to *anomalously high or low values* in the short time series.

Also, the consideration of a mixed strong wind climate is essential for South Africa. The mixed climate approach is based on the Gumbel distribution, and therefore in the application of this method only a limited number of observations (one per year for each strong wind mechanism) could be utilised. Steps to resolve this issue were the application of appropriate statistical methods, which took the short time series and mixed strong wind climate into account, and the upward adjustments of the sample parameters at the 75% confidence limit. Thereafter, for conservativeness, the highest

estimated quantiles between the different approaches were proposed as design wind speed values.

The challenge of short duration records are more acute for certain parts of the country, specifically those regions which are prone to strong thunderstorms such as the south-eastern interior. It is especially for weather stations in these regions where variable κ parameters produced unrealistic quantile estimates, due to the presence of *anomalously high values* in the data samples. The likelihood exists that the setting of the κ parameter to zero for these stations will produce a stronger likelihood for the underestimation of quantile values, for a region where the quantile estimates are already relatively high.

As mentioned in Chapter 2, the Weather Service is continually enhancing its observation network in terms of increasing the number of AWSs, as well as improving the existing instrumentation. Due to the complex nature of the strong wind climate of South Africa, it is obvious that an accurate representation of the extreme wind climate requires a dense spatial distribution of long-term observed data. In this context it is recommended that this study be updated on a regular basis, of which the frequency will depend on the increase in data availability, as well as the enhanced spatial distribution of results that the updated data sets would produce. One should keep in mind that this analysis utilised the available data only up to 2008. Therefore, if an updated study should be conducted as early as 2011, already two more years of data will be available. For a weather station which had 10 years of data available for this study it equates to an increase of more than 25% of observed information.

Recently the extension of the SAWS observation network has been accelerating, with the conversion of all manual stations to automatic stations. In the 2010/11 financial year alone, it is envisaged that 20 more AWSs will come into operation. In light of the limited lengths of the data sets utilised in this study, as well as the continuous increase in the number of suitable weather stations, every update of this analysis in the medium term, i.e. the next two to 10 years, will produce results with a notable increase in perceived

reliability. The wind data of the weather stations utilised in the present study has been quality controlled up to 2008, and the methodologies for the data analysis have been established. Therefore an update of the present study will be based more on routine analysis than investigative research. However, the data of any additional stations that reach the minimum length of time series, i.e. 10 years, will have to be quality controlled and analysed from scratch. After the updating of the analysis, the results will have to be reinterpreted through comparison with the present results.

10.2.4. Analysis methods

The conclusions made from the statistical analysis of the extreme winds in Chapter 5 can be summarised as follows, coupled with recommendations regarding the approaches of extreme wind estimations in the South African context:

- While the Gumbel method is the most widely used and recognised in the estimation of extreme winds, two important factors have an influence on the appropriateness of the method, namely the length of the time series analysed and the nature of the local strong wind climate. In the case of time series shorter than 20 years, it is preferable that analysis methods specifically developed for shorter time series be used, such as the POT method. In a mixed strong wind climate, it is advised that a mixed climate approach be taken, especially in cases where the quantiles for periods longer than 50 years need to be estimated.
- Currently it is not advisable to apply the GEV method to estimate extreme winds, as the shape parameter of the distribution is highly sensitive to anomalously high or low values in the usually small data samples available for this study. More realistic estimates of extreme winds are obtained if the shape parameter is assumed to be zero, such as is the case for the Gumbel method. For short time series anomalously high or low values in the data samples seem to play the bigger role in the estimation of the sign of the shape parameter, if compared to the nature of the strong wind climate.
- Even in cases where the time series is short and a method such as the POT method is applied, it is still preferable that the value of the shape parameter of

the distribution applied to the data set be set to zero. Statistically, the degrees of freedom of a small dataset is reduced even further by the additional parameter κ. Large absolute values of κ produces unrealistically high or low values for especially the longer return periods. With κ set to zero, it "dampens out" instabilities, i.e. anomalously higher and lower values that were observed. It is therefore advisable to use the EXP distribution instead of the Pareto distribution to estimate the extreme wind quantiles with the POT method.

The building design standard EN 1991-1-4 (2005) or Eurocode is used as basis for the development of the new building design standard for South Africa (Retief and Dunaiski, 2009). The Eurocode specifies the use of the Gumbel distribution in the estimation of the extreme wind values. However, it was demonstrated in Chapter 5 that the Gumbel distribution is not always the best method to estimate extreme winds. If methods other than the Gumbel distribution are used, one should be able to estimate the distribution parameters of the equivalent Gumbel distribution. Such equivalent means and standard deviations can be determined from the solving of two sets of equations, i.e. $F_G(V_T) = F_M(V_T)$ and $f_G(V_T) = f_M(V_T)$, for the wind speed V_T estimated for a specific return period T, where F_G and F_M are the cumulative Gumbel and mixed distributions respectively, and f_G and f_M are the probability density functions of the Gumbel and mixed distributions respectively.

10.2.5. Outputs

The desired outputs should provide a comprehensive description of the strong wind climate of South Africa. These are summarised and assessed below:

10.2.5.1. Identification of causes of strong winds and spatial distribution thereof

In Chapter 3, during the quality control process of the wind data, and expanded in Chapter 4, the causes of annual maximum gusts were identified. A total of six different causes, or strong wind mechanisms, are responsible for the strongest wind gusts

recorded in South Africa. One mechanism is on the mesoscale, the thunderstorms, while the others are on the synoptic scale. It was shown that two mechanisms, thunderstorms and cold fronts, can be considered to be primary, due to their relatively large spatial influence, while the other four are of secondary importance.

This analysis extends the methodology followed in previous studies, locally and elsewhere, in that mechanisms on the synoptic scale were further divided into subgroupings. Also, the analysis method rested on the identification of the strong wind mechanisms through the interrogation of high-resolution time series, weather reports and synoptic maps, which establishes an objective identification of the relationship between strong wind events and the mechanism.

10.2.5.2. Relationships between strong wind mechanisms

While the different strong wind mechanisms and their spatial distributions were identified, the relationships between these mechanisms were investigated in Chapter 8. The results provide new insight in the characteristics of strong winds in the country, which are summarised below:

The investigation focused on the relative contributions of the mechanisms in the estimation of extreme wind quantiles. With the results from the statistical analysis in section 5.5, from which the Gumbel distribution parameter values of the strong wind mechanisms were obtained, and the application of correction factors developed in Chapter 6, these values could be compared on a spatial basis.

As could be deduced from the analysis presented in Chapter 4, quantitative analysis of the distribution parameters showed that in the estimation of gust quantiles, thunderstorms and cold fronts are the primary mechanisms, while others play a secondary role. Thunderstorms tend to dominate in the interior, especially in the north, where for substantial areas the gust quantiles are solely determined by the thunderstorm gust values. In the eastern, south-eastern and southern interior the

dominance of thunderstorms is to a great extent caused by the temporal variability of the annual maximum thunderstorm gusts, especially in the south-east where anomalously high gusts were recorded for some stations for some years.

Along the coastline and the adjacent interior, as well as the south-eastern escarpment, cold fronts dominate the estimation of the gust quantiles. At the coast the gusts are recorded during the passage of the actual front, while along the escarpment the strongest gusts occur due to the acceleration of air towards strong coastal lows on the east and south-east coastline, which precede the fronts. These strong, gusty winds are well known in the KwaZulu-Natal interior, and are locally called “berg winds”. Where the quantiles are determined by both thunderstorms and cold fronts, the resultant mixed distributions vary considerably on a spatial basis. These variations are illustrated in Figure 10.3, in which the combination of mixed distribution curves, as presented in Figure 8.6, is shown.

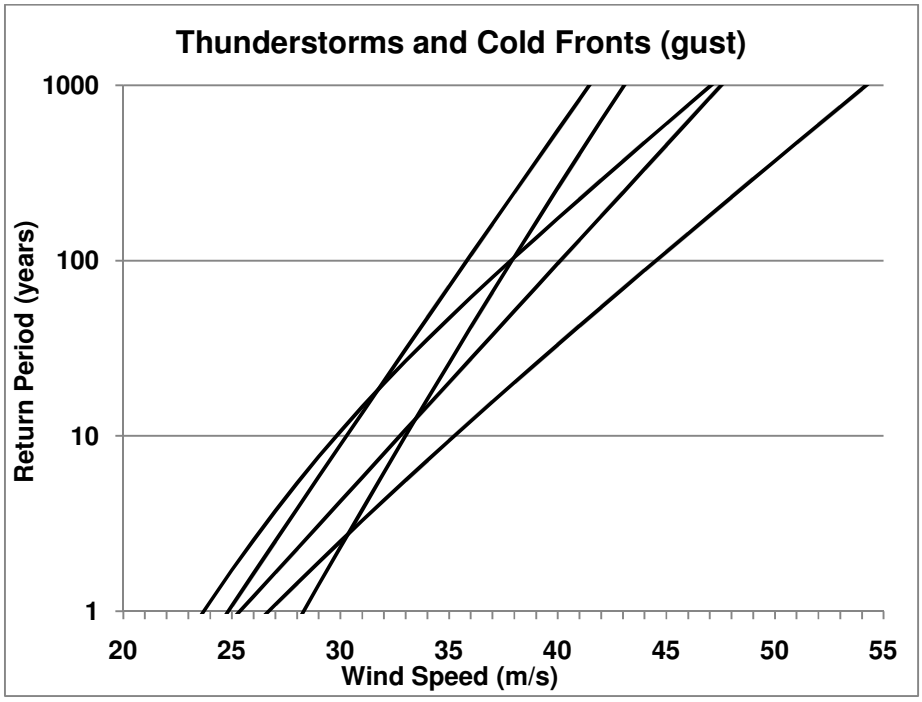

Figure 10.3. Combination of mixed distribution curves of thunderstorms and cold fronts, as presented in Figure 8.6.

Apart from the thunderstorms and cold fronts, secondary strong wind mechanisms on the gust time-scale tend to dominate only over smaller areas. It should however be noted that the occurrence of a secondary mechanism nevertheless results in higher wind predicted as a result of the combined mechanisms.These are for example in the south-west of the country where the ridging of the Atlantic Ocean high-pressure system plays a large role and isolated lows in the southern ocean, which cause relatively strong gusts in the southern interior. Figures 10.4 illustrates the variation in mixed distribution curves, where the gust quantiles are caused by a combination of cold fronts and other secondary mechanisms.

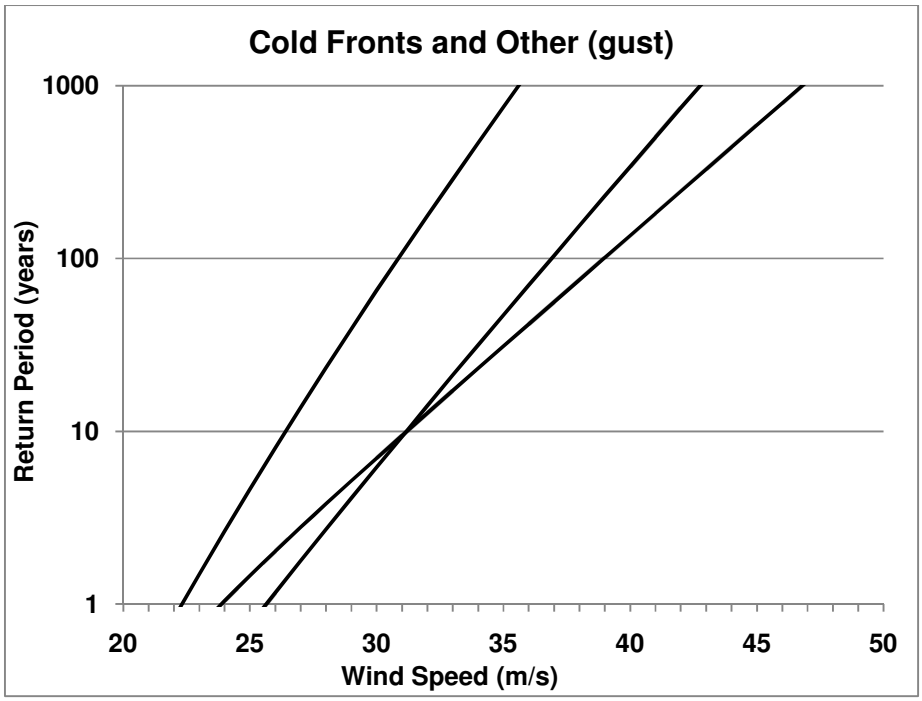

Figure 10.4. Combination of mixed distribution curves of cold fronts and other mechanisms, as presented in Figure 8.8.

For the annual maximum hourly mean wind speeds, cold fronts are the dominant strong wind mechanism, with only relatively small regions on the west coast and the far north-east dominated by other mechanisms. From the south-west through to the east of the country the estimations of relevant quantiles are either dominated or solely determined

by cold fronts. The same applies for a smaller region over the North-West and Free State provinces.

On the west coast the ridging of the Atlantic Ocean high-pressure system or a deep trough or low-pressure system dominate, while in the far north-east it is the ridging of the Indian Ocean high-pressure system from the east. Elsewhere in the country the estimations of hourly quantiles are determined by cold fronts and other secondary mechanisms, but not one of the contributing mechanisms tends to dominate. Figure 10.5 illustrates the variation in the combined distributions of cold fronts and other mechanisms on the hourly time scale, as presented in Figure 8.10.

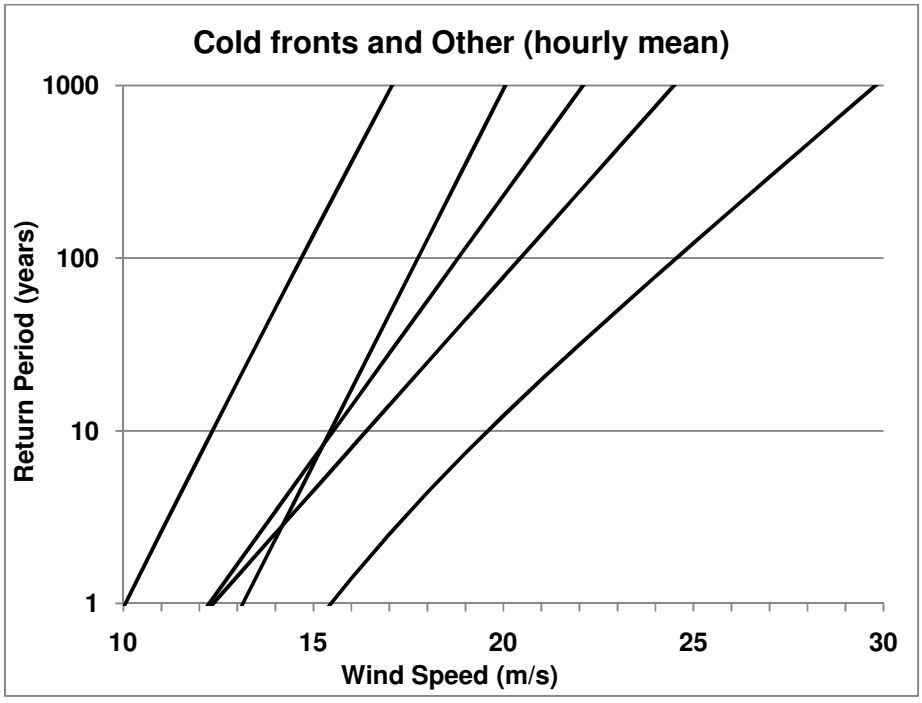

Figure 10.5. Mixed distribution curves of combinations of cold fronts and other mechanisms on the hourly time scale, as presented in Figure 8.10.

10.2.5.3. Statistical development of probability parameters for purposes of design standards

Different factors determine the appropriateness of statistical methods with which probability parameters are estimated. The most important are the length of record, strong wind climate and the temporal distribution of strong values in the time series; all of which have not been taken into consideration in previous analyses for South Africa. It follows that the determination of the optimum statistical methods would be different than before, in the sense that these additional factors have now been considered. The eventual methodologies utilised are summarised in 10.2.3.

Currently in South Africa most of the weather stations that can be used for strong wind analyses have recording periods shorter than 20 years. As a period of at least 30 years is recommended for the accurate estimation of probability parameters, these short periods compromise the reliability of the estimations. To address this problem, the values of the estimated probability parameters were changed, by the upward adjustment of the standard deviations and means of the data samples with their 75% confidence limits. The consideration of the above, as well as:

- Significant improvement of the coverage of quantile values due to increase in number of usable weather stations;
- Application of correction factors for the inadequate exposures of the anemometers;
- Objective interpolation of estimated quantiles;

makes that the design wind speed maps presented in Chapter 7 can be regarded as an improvement on previous versions for South Africa. Figures 10.6 and 10.7 illustrates the differences between the updated 50-year gust quantiles, hourly mean wind speed quantiles, and those which were used for the South African loading code, respectively.

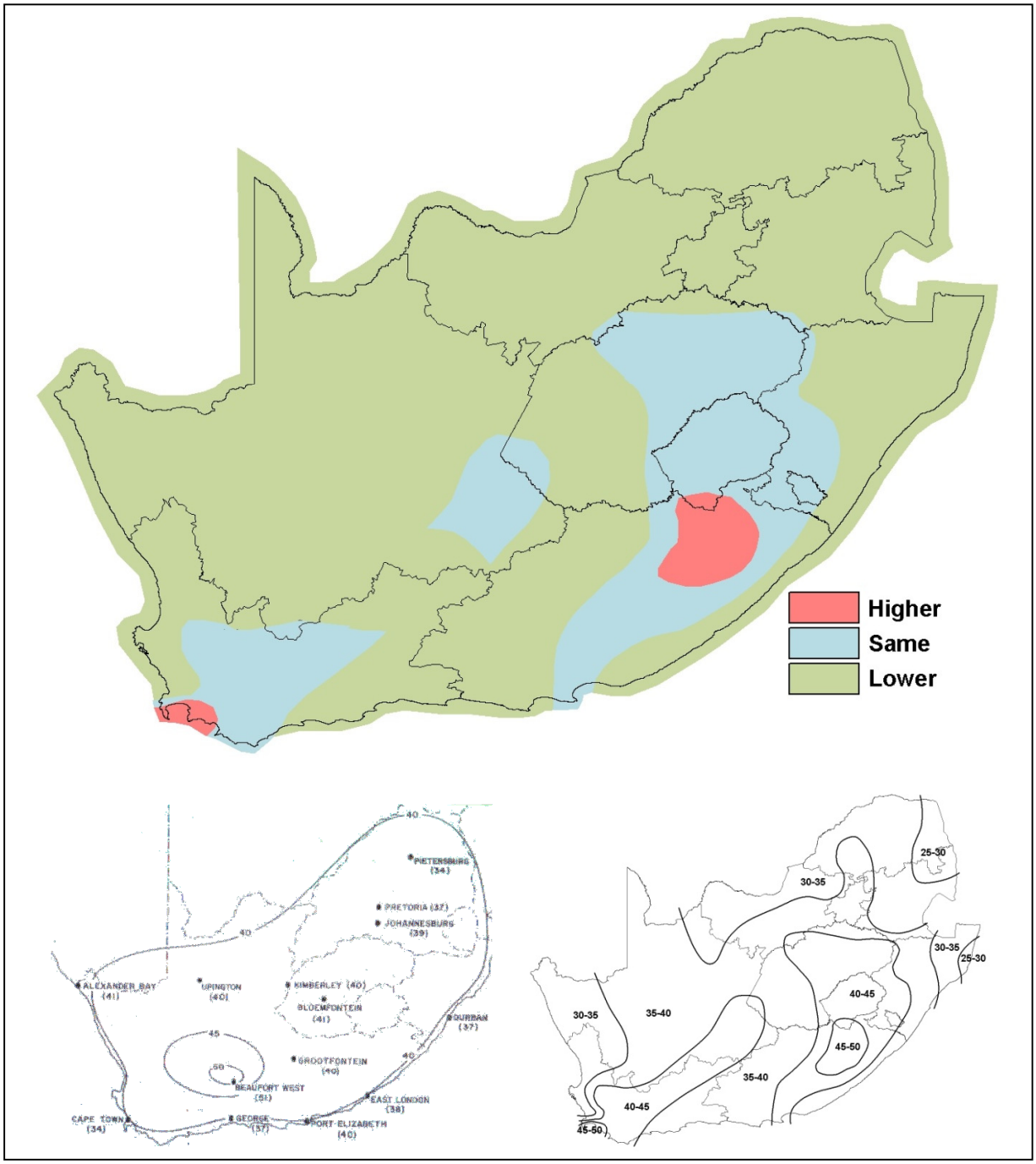

Figure 10.6. Relative differences between the updated 50-year gust quantiles, and those used for the current South African loading code. Maps at the bottom show the previous (left) and new version (right).

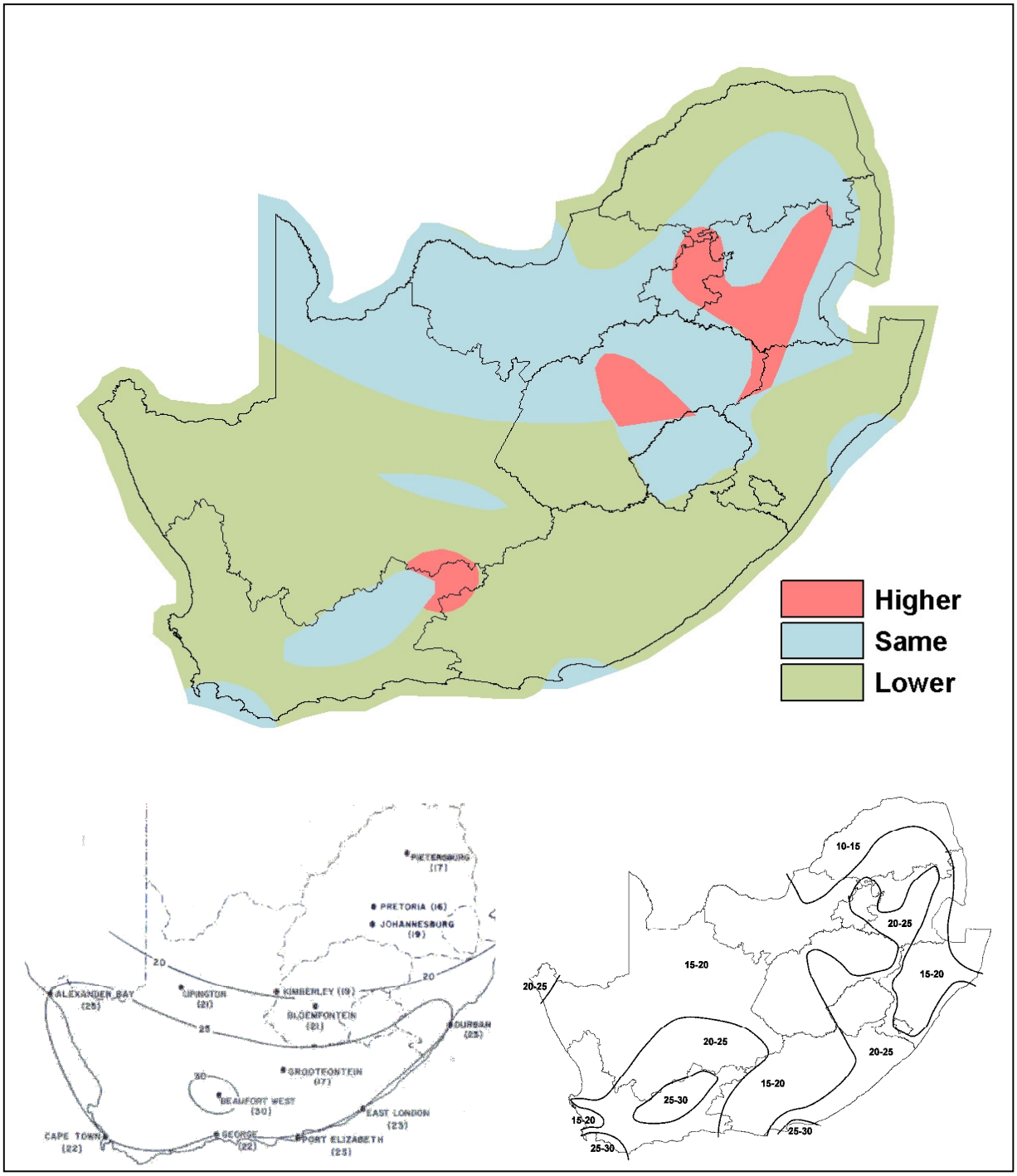

Figure 10.7. Relative differences between the updated 50-year hourly mean wind quantiles, and those used for the current South African loading code. Maps at the bottom show the previous (left) and new version (right).

10.3. Quality of results

In any investigation of this nature it is imperative to make an at least conceptual assessment of the quality of the results obtained. This requires a differentiation between two factors, namely the inherent randomness of the process, and the initial lack of knowledge.

The randomness of the process mostly comprises the imperative use of the available data at hand, in which the quality of the results could be compromised by factors such as the representativeness of the data of the wind climate of a specific location which can be compromised by the lengths of data record available, the spatial coverage of the data, as well as the quality thereof. The quality of the results will be adversely affected if these issues are not addressed. The issue of short records alone has been largely resolved through the application of appropriate statistical techniques. However, the probable lack of representativeness affected the reliability of quantile estimations; more for those regions that are from time to time affected by severe thunderstorms. Therefore the values for these regions can be deemed to be less reliable than elsewhere. What the spatial coverage of data is concerned, reliability issues will affect the regions prone to thunderstorms more than where strong winds are mostly due to synoptic-scale mechanisms: The spatial analysis of smaller-scale phenomena requires denser distributions of data. Data quality issues were resolved through the assessment of the validity of all strong wind values.

Lack of knowledge inhibits proper prediction, and to address this, a thorough investigation of statistical approaches to estimate probability parameters were conducted, and appropriate methods applied. Effort was made to be as objective as possible in the spatial interpolation of quantile values, but a measure of subjectivity still exists in the applied method.

Summarising the above, the quality of the results of this study are mostly compromised by the short periods of data records, the density of available weather stations in

especially the regions prone to thunderstorms, and to a lesser degree the extent of subjectivity in the spatial interpolation of results. Considering the recent rapid expansion of the AWS observation network, significant improvements can be made to this analysis if updated in the short to medium term.

10.4. Final remark

This research on the strong wind climatology of South Africa, in essence, highlights the challenges and shortcomings inherent in the statistical analysis of observed climate data. In the various aspects of the work the importance of the critical evaluation of the climate data, measuring environment, statistical techniques and the spatial interpolation of results are demonstrated and discussed. The findings emphasise the importance of reliable, high-quality climate data in climatological analyses relevant to the built environment.

References

Abild, J. 1994. *Application of the wind atlas method to extremes of wind climatology. Technical Report Risoe-R-722 (EN).* Risø National Laboratory. Roskilde. Denmark.

Abild, J., E. Y. Andersen and D. Rosbjerg. 1992. The climate of the extreme winds at the Great Belt, Denmark. *J. Wind. Eng. Ind. Aerodyn.*, **41-44**, 521-532.

Aksoy, H., Z. F. Toprak, A. Aytek and N. E. Unal. 2004, Stochastic generation of hourly mean wind speed data. *Renewable Energy*, **29**, 2111-2131.

Ang, A. H. S., and W. H. Tang. 1978. *Probability: Basic Principles v. 1: Concepts in Engineering, Planning and Design.* J. Wiley & Sons, London.

AS 1170.2. 1989. *Australian Standard: SAA Loading code, Part 2: Wind loads.* Standards Australia.

ASCE 7-98. 1998. *ASCE Standard: Minimum design loads for buildings and other structures.* American Society of Civil Engineers.

Ballio, G., S. Lagomarsino, G. Piccardo and G. Solari. 1999. Probabilistic analysis of Italian extreme winds: Reference velocity and return criterion. *Wind and Structures*, **2**, 51-68.

Barthelmie, R. J., J. P. Palutikof and T. D. Davies. 1993. Estimation of sector roughness lengths and the effect on prediction of the vertical wind speed profile. *Bound.-Lay. Meteorol.*, **66**, 19-47.

Brabson, B. B., and J. P. Palutikof. 2000. Tests of the Generalized Pareto Distribution for predicting extreme wind speeds. *J. Appl. Meteorol.*, **39**, 1627-1640.

CAELUM. 1991. A history of notable weather events in South Africa 1500 – 1990. South African Weather Bureau, Department of Environmental Affairs, Pretoria.

Cheng, E. D. H. and A. N. L. Chiu. 1985. Extreme Winds Simulated from Short-Period Records. *J. Struct. Eng.*, **111**, 77-94.

Cheng, E. D. H. and A. N. L. Chiu. 1994. Short-record-based extreme wind simulation. *J. Res. Natl. Inst. Stand. Technol.*, **99**, 391-397.

Cook, N. J. 1982. Towards better estimation of wind speeds. *J. Wind Eng. Ind. Aerodyn.*, **9**, 295-323.

Cook, N. J. 1985. *The Designer's Guide to Wind Loading of Building Structures. Part 1: Background, Damage Survey, Wind Data and Structural Classification.* Building Research Establishment, Garston, and Butterworths, London. 371 pp.

D'Agostino, R. B. and M. A. Stephens. 1986. *Goodness-of-Fit Techniques*. Marcel Dekker. 560 pp.

Davenport, A. G. 1960. Rationale for determining design wind velocities. *J. Struct. Div. Am. Soc. Civ. Eng.*, **86**, 39-68.

Davenport, A. G., C. S. B. Grimmond, T. R. Oke and J Wieringa. 2000. Estimating the roughness of cities and sheltered country. *Proceedings of the 12th AMS Conf. On Applied Climatology*, Asheville, 96-99.

Davison, A. C. 1984. Modelling excesses over high thresholds, with an application. In *Statistical Extremes and Applications* (J. Tiago de Oliveira, editor), 461-482, Reidel, Dordrecht.

Davison, A. C. and R. L. Smith. 1990. Models for exceedances over high thresholds. *J. R. Stat. Soc.*, **52**, 393-442.

Department of Transport. 1981. TMH7: Code of Practice for the Design of Highway Bridges and Culverts in South Africa. Department of Transport, Pretoria, South Africa.

De Rooy, W. C. and K. Kok. 2004. A Combined Physical–Statistical Approach for the Downscaling of Model Wind Speed. *Weather and Forecasting*, **19**, 485-495.

EN 1991-1-4 (2005). Eurocode 1: Actions on Structures, Part 1-4: General Actions – Wind. European Committee for Standardisation (CEN), Brussels.

Fujita, T.T. 1971. *Proposed characterisation of tornadoes and hurricanes by area and intensity.* SMROP Research Paper No 91, University of Chicago, Illinois.

Fujita, T. T. 1973. *Experimental classification of tornadoes in FPP scale.* SMRP Research Paper No 98, University of Chicago, Illinois.

GBJ 9-87. 1994. *National Standard of the People's Republic of China. Load code for the design of building structures.* Former State Capital Construction Commission of the People's Republic of China, Beijing.

Goliger, A. M. 1994. Report on the Utrecht Tornado (Northern Natal): 3 November 1993. Internal report 94/01. BPS, Building Technology, CSIR. Pretoria.

Goliger, A. M. 2007. South African wind loading specifications: The Euro way? *J. Wind Eng. Ind. Aerodyn.*, **95**, 1053-1064.

Goliger, A. M. and R. V. Milford. 1988. An investigation into the effect of topography on the pedestrian level wind environment in the city centre of Pretoria. Internal report 88/02. Aero- & Structural Dynamics Programme, Building Tecnology, CSIR, Pretoria.

Goliger, A. M. and R. V. Milford. 1997. A review of worldwide occurrence of tornadoes. *Proceedings of the 2nd European and African Conference on Wind Engineering*, Genoa, Italy, June 1997.

Goliger, A. M., R. V. Milford, B. F. Adam and M. Edwards. 1997. *Inkanyamba: Tornadoes in South Africa*. Joint Publication of the CSIR and SAWB, Pretoria.

Goliger, A. M. and J. V. Retief. 2002. Identification of zones of strong wind events in South Africa. *J. Wind Eng. Ind. Aerodyn.*, **90**, 1227-1235.

Goliger, A. M., J. V. Retief and P. E. Dunaiski. 2009a. Review of codification of wind-loading for structural design. In *Background to SANS 10160: Basis of Structural Design*

and Actions for Buildings and Industrial Structures Part 3: Wind Actions. Editors: Retief, J. V. and P. E. Dunaiski.

Goliger, A. M., J. V. Retief, P. E. Dunaiski and A. C. Kruger. 2009b. Revised wind-loading design procedures for SANS 10160. In *Background to SANS 10160: Basis of Structural Design and Actions for Buildings and Industrial Structures Part 3: Wind Actions.* Editors: Retief, J. V. and P. E. Dunaiski.

Goliger, A. M., J. L. Waldeck and R. V. Milford. 1990. Wind tunnel investigation of the wind pattern approaching Cape Town city centre. Internal report 90/05. ES, Building Technology, CSIR, Pretoria.

Gomes, L. and B. J. Vickery. 1978. Extreme wind speeds in mixed wind climates. *J. Ind. Aerodyn.*, **2**, 331-344.

Grimmond, C. S. B., and T. Oke. 1999. Aerodynamic properties of urban areas derived from analysis of surface form. *J. Appl. Meteor.*, **38**, 1262-1292.

Gringorten, I. I. 1963. A plotting rule for extreme value probability paper. *J. Geophys. Res.*, **68**, 813-814.

Gusella, V. 1991. Estimation of extreme winds from short-term records. *J. Struct. Eng.*, **117**, 375-390.

Henderson, D. J., M. J. Morrison, J. D. Ginger and C. A. Miller. 2010. Response of Dines Anemometer to simulated winds. *Proceedings of the 14th Australasian Wind Engineering Society (AWES) Workshop – incorporating and preceded by the Southern Hemisphere Extreme Winds Workshop.* August 5th and 6th 2010. Geoscience Australia, Canberra.

Hennessey, J. P. Jr. 1977. Some aspects of wind power statistics. *J. Appl. Meteorol.*, **16**, 119-128.

Holmes, J. D. 2002. A re-analysis of recorded extreme wind speeds in Region A, *Aust. J. Struct. Eng.*, **4**, 29-40.

Holmes, J. D. and D. J. Henderson. 2010. Comparison of peak velocities recorded by Dines, cup and sonic anemometers. *Proceedings of the 14th Australasian Wind Engineering Society (AWES) Workshop – incorporating and preceded by the Southern Hemisphere Extreme Winds Workshop.* August 5th and 6th 2010. Geoscience Australia, Canberra.

Hosking, J. R. M., J. R. Wallis and E. F. Wood. 1985. Estimation of the generalized extreme value distribution by the method of probability-weighted moments. *Technometrics*, **27**, 251-261.

Hurry, L. and Van Heerden, J. 1987. *Southern Africa's Weather Patterns. A guide to the interpretation of synoptic maps*. Via Afrika Ltd., Goodwood, Cape Town, South Africa.

Jackson S.P. 1951. Climates of Southern Africa. *S. Afr. Geogr. J.*, **33**, 17-37.

Jenkinson, A. F. 1955. The frequency distribution of the annual maximum (or minimum) values of meteorological elements. *Q. J. R. Meteorol. Soc.*, **81**, 158-171.

Kruger, AC. 2004. *Climate of South Africa. Climate Regions. WS45.* South African Weather Service. Pretoria. South Africa. 29 pp with appendix.

Larsén, X. G. and J. Mann. 2009. Extreme Winds from the NCEP/NCAR Reanalysis Data. *Wind Energ.*, **12(6)**, 556-573.

Lechner, J. A., S. D. Leigh and E. Simiu. 1992. Recent approaches to extreme value estimation with application to wind speeds. Part 1: The Pickands method. *J. Wind Eng. Ind. Aerodyn.*, **41-44**, 509-519.

Ledermann, W., E. Lloyd, S. Vajda and C. Alexander (editors). 1990. *Handbook of Applicable Mathematics Volume 7: Supplement.* Wiley-Interscience, Chichester, 479 pp.

Lee, L. S. 1996. Identification of Gust Front Cases in Hong Kong using Data from Automatic Weather Station Of The Royal Observatory. Technical Note No. 87, Royal Observatory, Hong Kong, 29 pp.

Lieblein, J. 1974. Efficient methods of extreme-value methodology. *Report NBSIR 74-602*, National Bureau of Standards, Washington, DC, 31 pp.

Louw, W. J. and E. Katsiambirtas. 1974. The Estimation of Extreme Wind Gusts from Inadequate Data. Technical Report, Weather Bureau, South Africa. 26 pp.

May, H. I. 1972. Some wind speed data for estimating wind loads on structures in South Africa. *The Civil Engineer in South Africa*, May 1972, 175-180.

McDonald, J. R. 1983. *A methodology for tornado hazard probability assessment.* Institute for Disaster Research, Texas Tech University, prepared for US Nuclear regulatory Commission, NUREG/CR-3058.

McNaughton, K. G., and P. G. Jarvis. 1984. Using the Penman–Monteith equation predictively. *Agric. Water Manage.,* **8,** 263–246.

Milford, R. V. 1985a. *Extreme-value analysis of South African mean hourly wind speed data.* Unpublished Internal Report 85/1, Structural and Geotechnical Engineering Division, National Building Research Institute, CSIR, Pretoria.

Milford, R. V. 1985b. *Extreme value analysis of South African gust speed data.* Unpublished Internal Report 85/4, Structural and Geotechnical Engineering Division, National Building Research Institute, CSIR, Pretoria.

Milford, R. V. 1987. Annual maximum wind speeds for South Africa. *The Civil Engineer in South Africa*, January 1987.

Milford, R. V. and A. M. Goliger. 1994. Tornado activity in South Africa. *Journal of the South African Institution of Civil Engineers*, **36**, 17-23.

Monin, A. S. and A. M. Obukhov. 1954. Basic laws of turbulent mixing in the ground layer of the atmosphere. *Tr. Geofiz. Inst., Akad. Nauk. SSSR,* **24,** 163–187.

Oliver, S. J., W. W. Moriarty, and J. D. Holmes. 2000. A risk model for design of transmission line systems against thunderstorm downburst winds. *Eng. Struct.*, **22**, 1173-1179.

Palutikof, J. P., B. B. Brabson, D. H. Lister and S. T. Adcock. 1999. A review of methods to calculate extreme wind speeds. *Meteorol. Appl.*, **6**, 119-132.

Perrin, O., Rootzén, H., and R. Taesler. 2006. A discussion of statistical methods for estimation of extreme wind speeds. *Theoretical and Applied Climatology*, **85**, 203-215.

Ponte, J. and J. D. Riera. 2007. Wind velocity field during thunderstorms. *Wind Struct.*, **10**, 287-300.

Press, W. H., S. A. Teukolsky, W. T. Vetterling and B. P. Flannery. 1992. *Numerical recipes in FORTRAN: The Art of Scientific Computing (2nd edition)*. Cambridge University Press. Cambridge. 963 pp.

Retief, J. V. and P. E. Dunaiski (ed.). 2009. *Background to SANS 10160*. SUN PReSS. SUN MeDIA. Stellenbosch. 251 pp.

SANS 10160-1989. 1989. *The general procedures and loadings to be adopted in the design of buildings*. South African National Standard. The Council of the South African Bureau of Standards.

SANS 10160-3. 2010. *South African National Standard. Basis of structural design and actions for buildings and industrial structures.* Part 3 *Wind Actions.* South African Bureau of Standards.

Schulze, B.R. 1947. The climates of South Africa according to the classifications of Köppen and Thornthwaite. *S. Afr. Geogr. J.*, **29**, 32-42.

Schulze, B.R. 1965. *Climate of South Africa. Part 8. General Survey. WB 28*. South African Weather Bureau, Pretoria, South Africa.

Simiu, E., and N. A. Heckert. 1996. Extreme wind distribution tails: A “peak-over-threshold” approach. *J. Struct. Eng.*, **122**, 539-547.

Smith, R. L. 1986. Extreme value theory based on the r largest annual events. *J. Hydrol.*, **86**, 27-43.

South African Weather Bureau. 1974. *Extreme values of rainfall, temperature and wind for selected periods. WB36 Part II. Climate of South Africa.* South African Weather Bureau. Pretoria. South Africa. 36 pp.

South African Weather Bureau. 1975. *Klimaat van Suid-Afrika. Deel 12. Oppervlaktewinde. WB38.* South African Weather Bureau. Pretoria. South Africa. 79 pp.

South African Weather Service. 1992-2008. *Daily Weather Bulletin.* South African Weather Service, Pretoria, South Africa.

Taljaard, J. J. 1995. *Technical Report No 30 - Atmospheric Circulation Systems, Synoptic Climatology and Weather Phenomena of South Africa - Part 4: Surface Pressure and Wind Phenomena in South Africa.* South African Weather Bureau. Pretoria. South Africa. 42 pp.

Twisdale, L. A., and W. L. Dunn. 1983. Probabilistic analysis of tornado wind risks, *ASCE J. Of Structural Engineering*, **109**, 468-488.

Twisdale, L. A., and P. J. Vickery.1992. Research on Thunderstorm Wind Design Parameters. *J. Wind Eng. Ind. Aerodyn.*, **41-44**, 545-556.

Uyeda, H. and D. S. Zrnic. 1986. Automatic Detection of Gust Fronts, *J. Atmos. and Oceanic Tech.*, **3**, 36-50.

Verkaik, J. W. 2000. Evaluation of Two Gustiness Models for Exposure Correction Calculations. *J. Appl. Meteorol.*, **39**, 1613-1626.

Viljoen, F. 1987-1988. Lists of extreme weather events in SAWB newsletters. South African Weather Bureau, Department of Environmental Affairs, Pretoria.

Walshaw, D. 1994. Getting the most from your extreme wind data: A step by step guide. *J. Res. Natl. Inst. Stand. Technol.*, **99**, 399-411.

Weissman, I. 1978. Estimation of parameters and large quantities based on the k largest observations. *J. Am. Stat. Assoc.*, **90**, 812-815.

Wever, N., and G. Groen. 2009. Improving potential wind for extreme wind statistics. KNMI scientific report - wetenschappelijk rapport : WR 2009-02. KNMI. De Bilt. The Netherlands. 114 pp.

Wieringa, J. 1986. Roughness-dependent geographical interpolation of surface wind speed averages. *Quart. J. Roy. Meteor. Soc.,* **112,** 867–889.

Wieringa, J. 1992. Updating the Davenport roughness classification. *J. Wind. Eng. Ind. Aerodyn.*, **41**, 357-368.

Wieringa, J., A. G. Davenport, C. S. B. Grimmond and T. R. Oke. 2001. New Revision of Davenport roughness classification. Proceedings of the 3rd European & African Conference on Wind Engineering, Eindhoven, Netherlands.

Wilks, D. S. 2006. *Statistical Methods in the Atmospheric Sciences*. Elsevier Academic Press. 627 pp.

WMO. 1996. Guide to Meteorological Instruments and Methods of Observation. WMO – No. 8. World Meteorological Organization. Geneva, Switzerland.

Appendix A

Distribution parameters and quantile estimations

A.1. Gumbel method estimations of the quantiles X_T .

Station Number	Station Name	Annual maximum wind gust (m/s)					Annual maximum hourly wind speed (m/s)				
		α	β	X_{50}	X_{100}	X_{500}	α	β	X_{50}	X_{100}	X_{500}
0003108	STRUISBAAI	3,66	26,29	40,6	43,1	49,0	0,80	14,73	17,8	18,4	19,6
0005609	STRAND	2,28	27,53	36,4	38,0	41,7	1,14	14,53	19,0	19,8	21,6
0006386	HERMANUS	1,56	27,52	33,6	34,7	37,2	1,05	13,53	17,6	18,3	20,1
0007699	TYGERHOEK	3,19	24,89	37,3	39,5	44,7	1,21	12,70	17,4	18,2	20,2
0010682	STILBAAI	1,65	23,61	30,1	31,3	33,9	0,82	13,01	16,2	16,8	18,1
0012661	GEORGE WO	1,81	25,16	32,2	33,5	36,4	1,63	14,32	20,9	22,0	24,6
0014123	KNYSNA	1,50	22,62	28,5	29,5	31,9	0,81	10,85	14,0	14,6	15,9
0014545	PLETTENBERGBAAI	1,95	23,49	31,1	32,5	35,6	1,17	11,34	15,9	16,8	18,6
0015692	TSITSIKAMMA	1,72	24,43	31,1	32,3	35,1	0,79	13,20	16,3	16,9	18,1
0020618	ROBBENEILAND	1,62	22,13	28,4	29,6	32,1	0,79	12,05	15,1	15,7	17,0
0021178	CAPE TOWN WO	3,18	25,85	38,3	40,5	45,6	1,64	16,00	22,4	23,5	26,2
0021823	PAARL	0,97	21,25	25,1	25,7	27,3	0,68	8,85	11,5	12,0	13,1
0022729	WORCESTER	1,98	29,91	37,6	39,0	42,2	0,80	18,39	21,5	22,1	23,4
0031650	JOUBERTINA	2,83	21,59	32,2	34,1	38,4	0,40	10,60	12,2	12,4	13,1
0033556	PATENSIE	2,03	20,84	26,0	27,2	29,9	0,74	9,02	12,0	12,4	13,6
0034763	UITENHAGE	1,70	25,07	31,7	32,9	35,5	0,95	12,85	16,5	17,2	18,7
0035209	PORT ELIZABETH	2,09	29,90	38,1	39,5	42,9	1,55	18,68	24,7	25,8	28,3
0040192	GEELBEK	1,63	21,84	28,2	29,3	32,0	0,61	13,50	15,9	16,3	17,3
0041388	MALMESBURY	1,78	21,41	28,4	29,6	32,5	0,68	9,01	11,7	12,1	13,2
0041841	PORTERVILLE	2,96	21,20	32,8	34,8	39,6	1,17	10,89	15,5	16,3	18,2
0045642	LAINGSBURG	1,51	26,51	32,4	33,5	35,9	1,33	13,12	18,3	19,3	21,4
0056917	GRAHAMSTOWN	2,30	23,18	32,2	33,7	37,4	0,98	13,02	17,1	17,8	19,4
0059572	EAST LONDON WO	1,50	25,89	31,8	32,8	35,2	0,80	15,68	18,8	19,4	20,7
0061298	LANGEBAANWEG	3,12	20,85	33,2	35,2	40,2	0,95	13,49	17,2	17,9	19,4
0063807	EXCELSIOR CERES	1,67	20,03	26,5	27,7	30,4	0,94	8,58	12,3	12,9	14,4
0078227	FORT BEAUFORT	2,82	25,37	36,4	38,3	42,9	0,74	13,24	16,1	16,7	17,8
0083572	LAMBERTSBAAI	0,85	21,57	24,9	25,5	26,9	0,83	12,71	16,0	16,5	17,9
0092081	BEAUFORT-WES	2,28	29,65	38,6	40,1	43,8	1,88	18,39	25,8	27,1	30,1
0096072	GRAAFF - REINET	1,65	24,76	31,2	32,4	35,0	0,74	11,92	14,8	15,3	16,5
0123685	QUEENSTOWN	1,12	27,58	31,9	32,7	34,5	0,79	12,96	16,0	16,6	17,8
0127272	UMTATA WO	3,44	27,07	40,5	42,9	48,5	1,50	14,58	20,5	21,5	23,9
0134479	CALVINIA WO	1,95	24,75	32,4	33,7	36,9	0,67	14,00	16,6	17,1	18,1

Station Number	Station Name	Annual maximum wind gust (m/s)					Annual maximum hourly wind speed (m/s)				
		α	β	X_{50}	X_{100}	X_{500}	α	β	X_{50}	X_{100}	X_{500}
0144791	NOUPOORT	2,14	24,82	33,2	34,7	38,1	1,24	13,96	18,8	19,6	21,6
0148517	JAMESTOWN	1,89	22,12	28,2	29,3	31,9	0,81	10,76	14,0	14,5	15,8
0150620	ELLIOT	2,41	29,36	38,8	40,5	44,3	1,09	12,94	17,2	18,0	19,7
0155394	PORT EDWARD	1,89	23,43	30,8	32,1	35,2	1,22	12,64	17,8	18,7	20,7
0169880	DE AAR WO	2,25	30,93	39,7	41,3	44,9	0,93	16,22	19,9	20,5	22,0
0182465	PADDOCK	1,96	23,13	30,8	32,2	35,4	1,22	12,64	17,4	18,2	20,2
0182591	MARGATE	1,63	24,18	30,6	31,7	34,3	0,75	13,67	16,6	17,1	18,3
0184491	KOINGNAAS	1,29	21,54	26,6	27,5	29,6	0,40	14,53	16,1	16,4	17,0
0190868	BRANDVLEI	1,74	25,09	31,9	33,1	35,9	0,93	12,70	16,3	17,0	18,5
0214700	SPRINGBOK WO	1,46	26,37	32,1	33,1	35,4	1,23	15,66	20,5	21,3	23,3
0224400	PRIESKA	2,13	24,72	33,3	34,8	38,4	1,30	11,51	16,6	17,5	19,6
0239698	PIETERMARITZBURG	1,89	19,65	27,0	28,3	31,4	0,87	7,62	11,0	11,6	13,0
0239699	ORIBI AIRPORT	3,08	22,97	35,0	37,1	42,1	0,91	11,15	14,7	15,3	16,8
0240808	DURBAN WO	2,16	24,85	33,3	34,8	38,2	1,21	14,66	19,4	20,2	22,2
0241072	MT EDGECOMBE	0,99	21,03	24,9	25,6	27,2	0,75	9,50	12,4	12,9	14,2
0241076	VIRGINIA	2,42	21,63	31,1	32,8	36,7	0,48	10,55	12,4	12,7	13,5
0261516	BLOEMFONTEIN WO	2,60	24,30	34,5	36,3	40,5	0,72	11,40	14,2	14,7	15,9
0268016	GIANTS CASTLE	2,68	29,34	39,8	41,7	46,0	1,62	12,16	18,5	19,7	22,3
0270155	GREYTOWN	2,21	22,98	31,6	33,2	36,7	0,90	9,98	13,5	14,1	15,6
0274034	ALEXANDERBAAI	1,43	25,76	31,3	32,3	34,6	0,80	19,03	22,2	22,7	24,0
0290468	KIMBERLEY WO	2,37	27,10	36,4	38,0	41,8	0,87	13,36	16,8	17,4	18,8
0300454	LADYSMITH	2,99	25,69	37,4	39,5	44,3	0,96	12,01	15,8	16,4	18,0
0304357	MTUNZINI	1,62	23,48	29,8	30,9	33,5	1,26	11,98	16,9	17,8	19,8
0317475	UPINGTON WO	3,11	25,30	37,5	39,6	44,6	0,75	13,68	16,6	17,1	18,3
0321110	POSTMASBURG	1,92	24,67	32,2	33,5	36,6	1,29	10,76	15,8	16,7	18,8
0331585	BETHLEHEM WO	1,41	23,64	29,2	30,1	32,4	0,89	11,84	15,3	15,9	17,4
0333682	VAN REENEN	2,08	26,42	34,8	36,3	39,8	1,11	13,32	17,6	18,4	20,2
0337738	ULUNDI	1,65	23,65	30,1	31,2	33,9	1,04	11,75	15,8	16,5	18,2
0339732	CHARTERS CREEK	1,82	18,78	25,9	27,2	30,1	0,53	8,28	10,4	10,7	11,6
0356880	KATHU	2,16	23,60	32,1	33,6	37,0	0,92	9,91	13,5	14,1	15,6
0360453	TAUNG	2,17	24,35	32,9	34,4	37,9	0,49	9,64	11,5	11,9	12,7
0362189	BLOEMHOF	3,46	23,14	36,7	39,1	44,6	0,67	10,96	13,6	14,1	15,2
0364300	WELKOM	3,22	26,72	39,3	41,6	46,8	1,66	14,60	21,1	22,2	24,9
0365398	KROONSTAD	1,74	26,51	33,3	34,5	37,3	1,63	14,66	17,1	17,6	18,9

Station Number	Station Name	Annual maximum wind gust (m/s)					Annual maximum hourly wind speed (m/s)				
		α	β	X_{50}	X_{100}	X_{500}	α	β	X_{50}	X_{100}	X_{500}
0370856	NEWCASTLE	2,20	26,38	35,0	36,5	40,1	0,94	13,85	17,5	18,2	19,7
0410175	PONGOLA	1,91	22,18	29,7	31,0	34,1	0,66	9,12	11,7	12,2	13,2
0427083	VAN ZYLSRUS	1,20	21,07	26,0	26,6	28,5	0,97	8,27	12,1	12,8	14,3
0438784	VEREENIGING	2,37	23,89	33,2	34,8	38,6	0,76	12,11	15,1	15,6	16,9
0441416	STANDERTON	2,74	23,72	34,4	36,3	40,7	0,65	9,73	12,3	12,7	13,8
0472278	LICHTENBURG	2,60	22,90	33,1	34,9	39,0	0,99	10,79	14,7	15,3	16,9
0475879	JHB BOT TUINE	2,29	18,44	27,4	29,0	32,7	0,71	5,80	8,6	9,1	10,2
0476399	JOHANNESBURG	2,82	22,96	34,0	35,9	40,5	0,96	11,68	15,4	16,1	17,6
0479870	ERMELO WO	1,22	24,14	28,9	29,8	31,7	1,08	14,40	18,6	19,4	21,1
0508047	MAFIKENG WO	1,99	24,14	31,9	33,3	36,5	1,20	14,26	19,0	19,8	21,7
0511399	RUSTENBURG	2,28	20,24	29,2	30,7	34,4	0,58	7,82	10,1	10,5	11,5
0513346	PRETORIA UNISA	1,42	21,63	27,2	28,2	30,5	0,68	10,37	13,0	13,5	14,6
0513385	IRENE WO	2,48	23,22	32,9	34,6	38,6	0,91	12,42	16,0	16,6	18,1
0515320	WITBANK	2,30	21,66	30,7	32,3	36,0	0,68	10,98	13,7	14,1	15,2
0520691	KOMATIDRAAI	2,67	20,51	31,0	32,8	37,1	0,61	9,24	11,6	12,0	13,0
0548375	PILANESBERG	2,67	21,56	32,0	33,9	38,1	0,67	8,93	11,6	12,0	13,1
0554816	LYDENBURG	3,16	20,36	32,7	34,9	40,0	0,79	7,71	10,8	11,4	12,6
0587725	THABAZIMBI	2,04	21,07	29,1	30,5	33,8	1,05	7,61	11,7	12,4	14,1
0594626	GRASKOP	2,83	20,13	31,2	33,1	37,7	1,36	8,56	13,9	14,8	17,0
0633882	POTGIETERSRUS	3,48	18,47	32,1	34,5	40,1	1,04	7,86	11,9	12,6	14,3
0638081	HOEDSPRUIT	2,16	22,46	30,9	32,4	35,9	0,83	13,01	16,3	16,8	18,2
0674341	ELLISRAS	2,42	19,12	28,6	30,2	34,2	0,44	6,70	8,4	8,7	9,5
0675666	MARKEN	2,43	19,95	29,5	31,1	35,0	0,62	8,14	10,6	11,0	12,0
0677802	PIETERSBURG WO	2,40	22,82	32,4	34,0	37,9	0,90	11,37	14,9	15,5	16,9
0723664	THOHOYANDOU WO	1,64	20,78	27,2	28,3	31,0	0,65	10,41	12,9	13,4	14,5

A.2. GEV distribution estimations of the wind gust quantiles X_T.

Station Number	Station Name	Distribution parameters			Annual maximum wind gust (m/s)		
		κ	α	β	X_{50}	X_{100}	X_{500}
0003108	STRUISBAAI	-0,47	1,72	25,93	45,2	54,0	90,0
0005609	STRAND	+0,08	2,68	27,50	36,5	37,8	40,6
0006386	HERMANUS	+0,50	2,26	27,91	31,8	32,0	32,2
0007699	TYGERHOEK	-0,07	3,20	24,64	39,1	42,1	49,8
0010682	STILBAAI	-0,01	1,72	23,55	30,4	31,7	34,6
0012661	GEORGE WO	+0,23	2,39	25,26	31,4	32,0	33,2
0014123	KNYSNA	+0,26	2,02	22,74	27,7	28,2	29,0
0014545	PLETTENBERGBAAI	+0,65	2,91	24,17	28,3	28,4	28,6
0015692	TSITSIKAMMA	-0,01	1,87	24,33	31,7	33,1	36,2
0020618	ROBBENEILAND	+0,05	1,89	22,07	28,7	29,8	32,1
0021178	CAPE TOWN WO	-0,06	3,25	25,61	39,9	42,8	50,1
0021823	PAARL	+0,22	1,26	21,31	24,6	25,0	25,6
0022729	WORCESTER	-0,15	1,84	29,76	39,5	41,9	48,6
0031650	JOUBERTINA	-0,35	1,87	21,16	36,9	42,8	63,5
0033556	PATENSIE	+0,16	2,57	20,88	28,4	29,3	31,1
0034763	UITENHAGE	+0,05	1,99	25,00	32,1	33,2	35,7
0035209	PORT ELIZABETH	-0,13	1,94	29,69	39,6	42,0	48,3
0040192	GEELBEK	-0,20	1,45	21,60	30,1	32,4	39,2
0041388	MALMESBURY	+0,03	2,02	21,33	28,8	30,0	32,8
0041841	PORTERVILLE	+0,12	3,61	21,32	32,5	34,0	36,9
0045642	LAINGSBURG	+0,09	2,22	26,32	32,3	33,4	35,3
0056917	GRAHAMSTOWN	+0,16	2,90	23,22	31,7	32,8	34,8
0059572	EAST LONDON WO	-0,09	2,39	26,01	37,3	39,8	46,2
0061298	LANGEBAANWEG	-0,43	1,70	20,42	37,7	45,2	74,1
0063807	EXCELSIOR CERES	+0,06	1,92	20,00	26,6	27,7	29,9
0078227	FORT BEAUFORT	-0,34	1,87	24,96	40,3	46,0	65,6
0083572	LAMBERTSBAAI	+1,07	1,23	22,10	23,2	23,2	23,3
0092081	BEAUFORT-WES	-0,01	2,36	29,59	38,9	40,6	44,5
0096072	GRAAFF - REINET	+0,17	2,07	24,82	30,8	31,5	32,8
0123685	QUEENSTOWN	+0,47	1,66	27,82	30,8	31,0	31,2
0127272	UMTATA WO	-0,19	3,08	26,58	44,4	49,2	63,0
0134479	CALVINIA WO	+0,11	2,38	24,75	32,2	33,2	35,3
0144791	NOUPOORT	0,00	2,38	24,68	33,9	35,5	39,2

Station Number	Station Name	Distribution parameters			Annual maximum wind gust (m/s)		
		κ	α	β	X_{50}	X_{100}	X_{500}
0148517	JAMESTOWN	+0,17	2,55	28,33	35,6	36,4	38,1
0150620	ELLIOT	+0,32	3,39	29,64	37,2	37,8	38,8
0155394	PORT EDWARD	-0,12	1,79	23,25	32,2	34,4	40,0
0169880	DE AAR WO	-0,33	1,87	26,34	41,2	46,5	64,7
0182465	PADDOCK	+0,03	1,83	22,77	30,6	32,0	34,9
0182591	MARGATE	+0,01	1,70	24,16	30,7	31,8	34,5
0184491	KOINGNAAS	+0,23	1,74	21,62	26,1	26,5	27,3
0190868	BRANDVLEI	+0,36	2,52	25,33	30,6	31,0	31,6
0214700	SPRINGBOK WO	+0,45	2,07	26,67	30,5	30,7	31,0
0224400	PRIESKA	-0,02	2,26	24,55	33,8	35,5	39,6
0239698	PIETERMARITZBURG	-0,05	2,20	19,72	29,2	31,1	35,8
0239699	ORIBI AIRPORT	-0,25	2,47	22,51	39,0	44,0	59,8
0240808	DURBAN WO	-0,14	2,00	24,62	35,0	37,5	44,4
0241072	MT EDGECOMBE	+0,34	1,42	21,15	24,2	24,4	24,8
0241076	VIRGINIA	+0,17	2,08	21,40	27,3	28,0	29,3
0261516	BLOEMFONTEIN WO	-0,24	2,01	24,02	37,1	41,0	53,1
0268016	GIANTS CASTLE	-0,23	2,12	29,03	42,5	46,5	58,8
0270155	GREYTOWN	+0,37	3,18	23,31	29,9	30,3	31,0
0274034	ALEXANDERBAAI	+0,09	1,70	25,75	31,3	32,1	33,7
0290468	KIMBERLEY WO	+0,20	3,07	27,21	35,6	36,5	38,2
0300454	LADYSMITH	-0,27	2,26	25,32	40,8	45,7	61,1
0304357	MTUNZINI	+0,18	2,10	23,53	29,4	30,1	31,3
0317475	UPINGTON WO	-0,17	2,82	24,90	40,5	44,6	56,1
0321110	POSTMASBURG	+0,51	2,93	25,12	30,1	30,3	30,7
0331585	BETHLEHEM WO	-0,09	1,43	23,50	30,1	31,6	35,3
0333682	VAN REENEN	+0,45	3,09	26,83	32,5	32,9	33,3
0337738	ULUNDI	+0,04	1,94	23,56	30,5	31,6	34,1
0339732	CHARTERS CREEK	-0,06	1,94	18,59	27,2	28,9	33,3
0356880	KATHU	+0,07	2,61	23,51	32,4	33,8	36,7
0360453	TAUNG	+0,34	3,16	24,60	31,5	32,0	32,8
0362189	BLOEMHOF	-0,35	2,17	22,75	40,9	47,6	71,2
0364300	WELKOM	-0,04	3,42	26,47	40,9	43,8	50,6
0365398	KROONSTAD	+0,43	2,55	26,84	31,7	32,0	32,4
0370856	NEWCASTLE	+0,60	3,41	27,04	32,2	32,4	32,6

Station Number	Station Name	Distribution parameters			Annual maximum wind gust (m/s)		
		κ	α	β	X_{50}	X_{100}	X_{500}
0410175	PONGOLA	+0,22	2,63	22,24	29,1	29,9	31,2
0427083	VAN ZYLSRUS	+0,34	1,73	21,22	24,9	25,2	25,6
0438784	VEREENIGING	+0,35	3,44	24,18	31,5	32,1	32,9
0441416	STANDERTON	+0,28	3,82	23,96	33,0	33,8	35,1
0472278	LICHTENBURG	+0,18	3,38	22,96	32,5	33,6	35,7
0475879	JHB BOT TUINE	-0,08	2,32	18,22	28,9	31,2	37,0
0476399	JOHANNESBURG	-0,16	2,46	22,70	36,1	39,5	49,1
0479870	ERMELO WO	+0,56	1,87	24,47	27,4	27,6	27,7
0508047	MAFIKENG WO	+0,20	2,65	24,20	31,4	32,3	33,8
0511399	RUSTENBURG	+0,15	2,91	20,25	28,9	29,9	32,1
0513346	PRETORIA UNISA	+0,44	2,13	21,90	25,9	26,1	26,4
0513385	IRENE WO	+0,03	2,82	23,11	33,5	35,2	39,0
0515320	WITBANK	+0,12	2,88	21,64	30,6	31,8	34,3
0520691	KOMATIDRAAI	+0,13	3,19	20,58	30,4	31,7	34,2
0548375	PILANESBERG	-0,01	2,97	21,36	33,1	35,3	40,3
0554816	LYDENBURG	-0,03	3,39	20,11	34,3	37,0	43,6
0587725	THABAZIMBI	+0,49	3,15	21,52	27,0	27,2	27,6
0594626	GRASKOP	+0,69	4,40	21,17	27,1	27,3	27,5
0633882	POTGIETERSRUS	+0,16	3,33	22,69	32,0	34,1	39,6
0638081	HOEDSPRUIT	-0,04	2,28	22,30	32,0	33,9	38,5
0674341	ELLISRAS	-0,13	2,19	18,94	30,1	32,7	39,8
0675666	MARKEN	-0,35	1,35	19,86	31,2	35,4	50,4
0677802	PIETERSBURG WO	+0,36	3,43	23,39	30,5	31,1	31,8
0723664	THOHOYANDOU WO	+0,07	1,97	20,73	27,4	28,4	30,5

A.3. GEV distribution estimations of the maximum hourly mean quantiles X_T.

Station Number	Station Name	Distribution parameters			Annual maximum hourly wind speed (m/s)		
		κ	α	β	X_{50}	X_{100}	X_{500}
0003108	STRUISBAAI	-0,23	0,6	14,6	18,7	19,9	23,6
0005609	STRAND	+0,14	1,4	14,5	18,8	19,4	20,5
0006386	HERMANUS	+0,05	1,2	13,5	17,9	18,6	20,2
0007699	TYGERHOEK	+0,25	1,6	12,8	16,7	17,1	17,7
0010682	STILBAAI	+0,02	0,9	13,0	16,4	17,0	18,4
0012661	GEORGE WO	+0,27	2,2	14,6	20,0	20,5	21,3
0014123	KNYSNA	+0,07	1,0	10,8	14,2	14,7	15,8
0014545	PLETTENBERGBAAI	+0,16	1,5	11,4	15,7	16,2	17,2
0015692	TSITSIKAMMA	+0,01	1,8	11,7	16,3	16,9	18,0
0020618	ROBBENEILAND	+0,22	1,0	12,1	14,8	15,1	15,6
0021178	CAPE TOWN WO	-0,20	1,4	15,8	23,9	26,1	32,7
0021823	PAARL	+0,02	1,2	11,9	11,5	12,0	12,9
0022729	WORCESTER	+0,41	1,2	18,5	20,8	20,9	21,2
0031650	JOUBERTINA	+0,28	0,6	10,6	12,0	12,1	12,3
0033556	PATENSIE	+0,03	0,8	9,0	12,1	12,6	13,8
0034763	UITENHAGE	-0,18	0,8	12,7	17,4	18,6	22,2
0035209	PORT ELIZABETH	-0,11	1,5	18,5	25,8	27,4	31,9
0040192	GEELBEK	+0,27	0,9	13,5	15,6	15,8	16,1
0041388	MALMESBURY	-0,02	1,0	12,3	11,7	12,3	13,6
0041841	PORTERVILLE	-0,06	1,2	10,8	16,0	17,1	19,8
0045642	LAINGSBURG	+0,02	1,5	13,8	18,3	19,2	21,1
0056917	GRAHAMSTOWN	+0,06	1,1	13,2	17,2	17,8	19,2
0059572	EAST LONDON WO	+0,45	1,2	15,8	18,1	18,2	18,4
0061298	LANGEBAANWEG	-0,08	0,9	13,4	17,7	18,6	21,0
0063807	EXCELSIOR CERES	+0,30	1,3	8,7	11,7	11,9	12,3
0078227	FORT BEAUFORT	+0,31	1,0	13,3	15,6	15,8	16,1
0083572	LAMBERTSBAAI	+0,52	1,2	12,9	15,0	15,1	15,2
0092081	BEAUFORT-WES	-0,04	2,6	15,7	26,6	28,7	33,9
0096072	GRAAFF - REINET	+0,05	0,7	12,0	14,6	15,0	15,9
0123685	QUEENSTOWN	+0,12	1,0	13,0	16,0	16,4	17,2
0127272	UMTATA WO	-0,05	1,6	14,4	21,4	22,8	26,2
0134479	CALVINIA WO	+0,39	1,0	14,1	16,1	16,2	16,4
0144791	NOUPOORT	+0,38	0,6	14,2	15,3	15,4	15,5

Station Number	Station Name	Distribution parameters			Annual maximum hourly wind speed (m/s)		
		κ	α	β	X_{50}	X_{100}	X_{500}
0148517	JAMESTOWN	+0,11	1,0	10,8	13,9	14,3	15,2
0150620	ELLIOT	+0,10	1,4	12,9	17,3	17,9	19,2
0155394	PORT EDWARD	-0,05	1,3	12,7	18,4	19,6	22,4
0169880	DE AAR WO	-0,07	0,8	13,8	17,2	17,9	19,6
0182465	PADDOCK	+0,02	1,1	12,5	17,4	18,1	20,0
0182591	MARGATE	-0,03	0,8	12,0	16,7	17,2	18,5
0184491	KOINGNAAS	+0,09	0,5	14,5	16,1	16,3	16,8
0190868	BRANDVLEI	+0,25	1,2	12,9	16,0	16,3	16,8
0214700	SPRINGBOK WO	+0,37	1,7	15,9	19,4	19,6	20,0
0224400	PRIESKA	-0,10	1,2	11,4	17,3	18,6	22,0
0239698	PIETERMARITZBURG	-0,03	0,9	7,6	11,3	12,0	13,8
0239699	ORIBI AIRPORT	+0,31	1,3	11,2	14,2	14,4	14,8
0240808	DURBAN WO	-0,13	1,1	14,6	20,2	21,5	25,1
0241072	MT EDGECOMBE	+0,40	1,1	9,6	11,8	11,9	12,1
0241076	VIRGINIA	+0,13	0,5	10,6	12,2	12,5	12,9
0261516	BLOEMFONTEIN WO	+0,13	0,9	11,4	14,1	14,5	15,2
0268016	GIANTS CASTLE	-0,32	1,1	12,0	20,2	23,1	32,8
0270155	GREYTOWN	+0,32	1,2	10,1	12,8	13,0	13,3
0274034	ALEXANDERBAAI	+0,22	1,0	19,1	21,7	22,0	22,5
0290468	KIMBERLEY WO	+0,07	1,0	13,3	16,8	17,3	18,4
0300454	LADYSMITH	+0,01	1,1	12,0	16,0	16,7	18,3
0304357	MTUNZINI	-0,24	1,0	11,8	18,2	20,1	25,9
0317475	UPINGTON WO	+0,55	1,1	13,9	15,7	15,8	15,9
0321110	POSTMASBURG	-0,04	1,2	12,6	15,9	16,9	19,2
0331585	BETHLEHEM WO	+0,12	1,1	11,8	15,3	15,7	16,7
0333682	VAN REENEN	+0,12	1,2	13,4	17,2	17,7	18,8
0337738	ULUNDI	-0,18	0,9	11,6	16,8	18,2	22,3
0339732	CHARTERS CREEK	-0,34	0,4	8,2	11,1	12,1	15,8
0356880	KATHU	-0,03	1,0	9,9	13,9	14,7	16,5
0360453	TAUNG	+0,29	0,7	9,7	11,3	11,4	11,6
0362189	BLOEMHOF	+0,28	0,9	11,0	13,2	13,4	13,7
0364300	WELKOM	-0,04	1,8	14,5	21,9	23,3	26,8
0365398	KROONSTAD	-0,06	1,7	14,5	21,9	23,4	27,1
0370856	NEWCASTLE	+0,22	1,3	13,9	17,2	17,6	18,2

Station Number	Station Name	Distribution parameters			Annual maximum hourly wind speed (m/s)		
		κ	α	β	X_{50}	X_{100}	X_{500}
0410175	PONGOLA	-0,05	0,7	9,1	12,1	12,7	14,2
0427083	VAN ZYLSRUS	-0,34	0,6	8,1	13,3	15,2	21,8
0438784	VEREENIGING	-0,01	0,8	12,0	15,4	16,1	17,5
0441416	STANDERTON	+0,34	0,9	9,8	11,8	11,9	12,2
0472278	LICHTENBURG	+0,15	1,3	10,8	14,5	15,0	15,9
0475879	JHB BOT TUINE	+0,04	0,8	5,8	8,8	9,2	10,3
0476399	JOHANNESBURG	+0,11	1,1	11,7	15,3	15,8	16,8
0479870	ERMELO WO	-0,01	1,2	14,3	19,0	19,8	21,8
0508047	MAFIKENG WO	-0,04	1,3	14,2	19,6	20,7	23,3
0511399	RUSTENBURG	+0,28	0,8	7,9	9,8	10,0	10,3
0513346	PRETORIA UNISA	-0,27	0,5	10,3	13,9	15,1	18,9
0513385	IRENE WO	+0,11	1,1	12,4	15,9	16,4	17,4
0515320	WITBANK	+0,33	1,0	11,1	13,2	13,3	13,6
0520691	KOMATIDRAAI	+0,20	0,5	9,2	10,5	10,7	10,9
0548375	PILANESBERG	+0,38	1,0	9,0	11,1	11,2	11,4
0554816	LYDENBURG	-0,06	0,8	7,7	11,1	11,9	13,7
0587725	THABAZIMBI	-0,25	0,8	7,5	12,8	14,4	19,4
0594626	GRASKOP	+0,16	1,8	8,6	13,8	14,4	15,6
0633882	POTGIETERSRUS	+0,20	1,1	12,2	11,4	12,0	13,1
0638081	HOEDSPRUIT	+0,29	1,2	13,1	15,8	16,1	16,5
0674341	ELLISRAS	+0,06	0,5	6,7	8,5	8,8	9,4
0675666	MARKEN	-0,35	0,4	8,1	11,4	12,7	17,1
0677802	PIETERSBURG WO	+0,39	1,3	11,5	14,1	14,2	14,5
0723664	THOHOYANDOU WO	+0,00	0,7	10,4	13,1	13,6	14,7

A.4. POT method estimations of the wind gust quantiles X_T.

Station Number	Station Name	Distribution parameters					Annual maximum wind gust (m/s)		
		κ	α	β	n	λ	X_{50}	X_{100}	X_{500}
0003108	STRUISBAAI	-0,50	0,9	25,5	25	2,27	43,2	51,3	85,6
0005609	STRAND	-0,26	1,2	27,6	18	1,50	37,2	40,0	48,9
0006386	HERMANUS	+0,12	2,6	24,9	46	3,83	35,2	36,1	38,0
0007699	TYGERHOEK	-0,27	1,5	24,2	47	2,94	40,4	45,0	59,6
0010682	STILBAAI	-0,08	1,4	22,9	30	2,00	30,8	32,3	36,0
0012661	GEORGE WO	+0,19	2,7	22,4	62	3,88	31,3	32,0	33,2
0014123	KNYSNA	+0,35	2,9	20,0	43	3,58	26,9	27,2	27,7
0014545	PLETTENBERGBAAI	+0,60	3,4	22,7	30	1,88	28,0	28,1	28,3
0015692	TSITSIKAMMA	+0,04	2,1	22,5	41	2,56	31,8	33,0	35,7
0020618	ROBBENEILAND	+0,12	1,8	20,1	73	4,87	27,2	27,8	29,0
0021178	CAPE TOWN WO	-0,19	2,2	24,8	49	3,06	42,7	46,8	58,4
0021823	PAARL	+0,26	1,7	20,0	33	2,20	24,5	24,8	25,4
0022729	WORCESTER	+0,27	3,7	25,0	68	6,80	35,9	36,4	37,3
0031650	JOUBERTINA	-0,38	1,3	19,9	36	3,27	39,9	46,9	72,3
0033556	PATENSIE	-0,16	1,5	17,6	71	5,07	31,1	33,8	41,5
0034763	UITENHAGE	+0,03	2,1	20,0	105	9,46	32,1	33,3	36,1
0035209	PORT ELIZABETH	+0,21	2,8	25,1	193	12,06	35,2	35,7	36,6
0040192	GEELBEK	+0,00	1,8	20,0	36	3,27	29,0	30,2	33,1
0041388	MALMESBURY	-0,12	1,7	17,5	47	3,36	29,7	32,0	38,0
0041841	PORTERVILLE	+0,10	2,7	20,4	31	2,07	30,4	31,5	33,8
0045642	LAINGSBURG	+0,02	2,9	23,1	52	4,00	32,4	33,3	35,2
0056917	GRAHAMSTOWN	-0,10	1,7	20,2	79	5,64	33,2	35,4	41,1
0059572	EAST LONDON WO	+0,12	2,6	20,2	167	15,18	32,3	33,1	34,7
0061298	LANGEBAANWEG	-0,41	1,2	20,1	24	2,18	36,6	42,9	66,7
0063807	EXCELSIOR CERES	-0,08	1,8	17,7	66	4,13	29,8	31,8	36,8
0078227	FORT BEAUFORT	-0,12	2,0	20,2	120	10,91	39,1	42,2	50,3
0083572	LAMBERTSBAAI	+0,17	2,1	17,5	130	9,29	25,6	26,0	27,0
0092081	BEAUFORT-WES	+0,10	3,0	24,9	83	5,53	38,0	39,2	41,6
0096072	GRAAFF - REINET	+0,05	2,2	22,4	48	3,00	32,3	33,5	36,2
0123685	QUEENSTOWN	+0,39	3,8	22,5	87	7,25	31,1	31,3	31,6
0127272	UMTATA WO	+0,03	3,2	20,0	103	10,30	38,3	40,1	44,2
0134479	CALVINIA WO	0,09	2,6	22,4	42	2,63	32,7	33,9	36,2
0144791	NOUPOORT	0,00	2,4	22,5	159	11,36	37,2	38,8	42,5

Station Number	Station Name	Distribution parameters					Annual maximum wind gust (m/s)		
		κ	α	β	n	λ	X_{50}	X_{100}	X_{500}
0148517	JAMESTOWN	0,06	1,9	20,3	59	4,21	28,9	29,9	31,9
0150620	ELLIOT	0,03	4,2	22,3	76	6,91	44,5	46,8	52,1
0155394	PORT EDWARD	0,05	2,4	20,0	83	5,93	31,9	33,1	35,8
0169880	DE AAR WO	-0,04	3,4	22,6	70	4,67	43,2	46,1	53,2
0182465	PADDOCK	0,01	2,2	19,8	91	6,07	30,5	31,6	34,4
0182591	MARGATE	0,10	2,4	20,1	125	8,33	30,8	31,7	33,5
0184491	KOINGNAAS	0,02	1,2	20,1	58	3,87	26,4	27,2	29,0
0190868	BRANDVLEI	0,43	4,3	22,2	30	2,50	30,9	31,3	31,7
0214700	SPRINGBOK WO	0,21	2,7	22,5	72	5,14	31,4	31,9	32,9
0224400	PRIESKA	0,06	2,6	20,0	94	6,71	32,8	34,0	36,8
0239698	PIETERMARITZBURG	0,04	2,6	15,0	118	8,43	28,8	30,1	33,2
0239699	ORIBI AIRPORT	0,02	2,8	15,0	192	19,20	33,1	34,7	38,6
0240808	DURBAN WO	-0,05	2,0	20,0	151	9,44	34,3	36,2	40,8
0241072	MT EDGECOMBE	0,15	2,0	17,5	123	8,79	25,5	26,1	27,1
0241076	VIRGINIA	-0,10	1,6	17,6	132	9,43	31,7	33,9	39,7
0261516	BLOEMFONTEIN WO	0,03	2,8	20,1	112	8,00	35,1	36,6	40,0
0268016	GIANTS CASTLE	0,04	2,8	18,6	102	7,29	37,5	40,4	43,2
0270155	GREYTOWN	0,03	2,9	17,4	108	7,71	33,1	34,7	38,4
0274034	ALEXANDERBAAI	0,11	1,7	22,6	138	9,86	30,3	30,9	32,0
0290468	KIMBERLEY WO	0,00	2,9	20,0	158	11,29	38,0	40,0	44,5
0300454	LADYSMITH	0,11	2,9	20,1	131	9,36	33,4	34,4	36,5
0304357	MTUNZINI	0,02	2,2	20,0	76	5,43	31,4	32,7	35,7
0317475	UPINGTON WO	0,02	2,6	20,1	140	10,00	35,1	36,7	40,2
0321110	POSTMASBURG	-0,01	2,5	19,8	52	5,20	34,3	36,1	40,6
0331585	BETHLEHEM WO	0,01	1,6	22,7	23	1,92	29,6	30,6	32,9
0333682	VAN REENEN	0,29	3,5	22,4	76	5,85	32,1	32,5	33,3
0337738	ULUNDI	0,11	2,8	17,6	101	9,18	30,2	31,1	33,1
0339732	CHARTERS CREEK	-0,12	1,2	15,1	153	12,75	26,4	28,2	32,9
0356880	KATHU	0,02	2,5	17,7	123	11,18	32,4	33,9	37,4
0360453	TAUNG	0,08	3,4	17,5	141	12,82	34,5	35,9	38,7
0362189	BLOEMHOF	-0,27	1,5	20,0	72	5,14	38,9	43,9	59,9
0364300	WELKOM	0,04	3,2	20,2	151	11,62	38,0	39,7	43,4
0365398	KROONSTAD	0,13	3,2	20,3	133	11,08	34,3	35,2	37,1
0370856	NEWCASTLE	0,19	3,6	19,9	115	10,46	33,1	33,8	35,2

Station Number	Station Name	Distribution parameters					Annual maximum wind gust (m/s)		
		κ	α	β	n	λ	X_{50}	X_{100}	X_{500}
0410175	PONGOLA	0,03	2,8	17,4	45	4,50	31,5	33,2	36,9
0427083	VAN ZYLSRUS	0,25	2,5	17,6	88	7,33	25,3	25,7	26,3
0438784	VEREENIGING	0,05	2,5	20,1	70	5,83	32,4	33,7	36,5
0441416	STANDERTON	-0,13	2,2	17,5	45	10,46	38,5	42,0	51,4
0472278	LICHTENBURG	0,02	2,6	17,5	164	12,62	33,2	34,8	38,3
0475879	JHB BOT TUINE	-0,06	1,8	15,3	91	7,00	28,4	30,3	35,1
0476399	JOHANNESBURG	-0,05	2,2	17,8	158	11,29	34,3	36,4	41,7
0479870	ERMELO WO	0,33	2,8	20,0	120	8,57	27,2	27,4	27,8
0508047	MAFIKENG WO	-0,04	1,9	20,3	97	8,08	33,3	35,0	39,2
0511399	RUSTENBURG	-0,12	1,7	17,5	65	5,00	31,3	33,8	40,5
0513346	PRETORIA UNISA	0,15	2,3	17,5	167	15,18	27,0	27,6	28,7
0513385	IRENE WO	0,11	2,8	17,5	188	13,43	30,7	31,7	33,6
0515320	WITBANK	-0,01	2,2	17,7	123	8,79	31,5	33,1	36,9
0520691	KOMATIDRAAI	-0,08	1,9	15,2	171	11,40	31,1	33,4	39,3
0548375	PILANESBERG	-0,06	2,5	17,5	71	6,46	34,8	37,3	43,6
0554816	LYDENBURG	-0,18	1,8	15,0	114	8,77	34,3	38,1	49,0
0587725	THABAZIMBI	0,16	2,9	17,5	62	6,20	28,3	29,1	30,6
0594626	GRASKOP	-0,19	2,1	15,0	61	6,10	37,3	42,0	55,8
0633882	POTGIETERSRUS	0,02	2,0	17,8	58	5,27	31,6	31,7	36,4
0638081	HOEDSPRUIT	0,00	2,2	20,0	36	3,27	30,9	32,4	35,8
0674341	ELLISRAS	-0,05	1,9	15,2	156	11,14	29,1	30,9	35,4
0675666	MARKEN	-0,03	1,9	17,5	40	3,33	28,2	29,7	33,5
0677802	PIETERSBURG WO	0,19	3,7	17,4	117	9,00	30,7	31,4	32,9
0723664	THOHOYANDOU WO	0,14	2,6	15,0	154	12,83	25,9	26,6	27,9

A.5. EXP method estimations of the wind gusts quantiles X_T.

Station Number	Station Name	Distribution parameters				Annual maximum wind gust (m/s)		
		α	β	n	λ	X_{50}	X_{100}	X_{500}
0003108	STRUISBAAI	2,0	25,3	25	2,27	34,7	36,1	39,3
0005609	STRAND	1,5	27	18	1,50	33,6	34,7	37,1
0006386	HERMANUS	2,2	25,1	46	3,83	36,6	38,1	41,6
0007699	TYGERHOEK	2,9	22,7	47	2,94	37,3	39,3	44,0
0010682	STILBAAI	1,6	22,8	30	2,00	30,3	31,4	34,0
0012661	GEORGE WO	2,0	22,6	62	3,88	33,3	34,7	38,0
0014123	KNYSNA	2,1	20,1	43	3,58	30,8	32,3	35,6
0014545	PLETTENBERGBAAI	2,2	20,6	30	1,88	30,6	32,1	35,7
0015692	TSITSIKAMMA	1,8	22,7	41	2,56	31,6	32,9	35,9
0020618	ROBBENEILAND	1,6	20,1	73	4,87	28,7	29,8	32,3
0021178	CAPE TOWN WO	2,3	25,2	49	3,06	36,7	38,2	41,9
0021823	PAARL	1,2	20,1	33	2,20	25,7	26,5	28,4
0022729	WORCESTER	2,8	25,1	68	6,80	41,5	43,4	48,0
0031650	JOUBERTINA	1,9	20,1	36	3,27	29,6	30,9	33,9
0033556	PATENSIE	1,8	17,6	71	5,07	27,3	28,5	31,4
0034763	UITENHAGE	2,0	20,1	105	9,46	32,1	33,5	36,6
0035209	PORT ELIZABETH	2,4	25,1	193	12,06	40,4	42,1	45,9
0040192	GEELBEK	1,7	20,1	36	3,27	28,8	30,0	32,8
0041388	MALMESBURY	1,9	17,6	47	3,36	27,1	28,4	31,4
0041841	PORTERVILLE	2,8	20,1	31	2,07	32,9	34,9	39,3
0045642	LAINGSBURG	2,1	20,6	52	4,00	32,4	33,4	36,1
0056917	GRAHAMSTOWN	2,0	20,1	79	5,64	31,5	32,9	36,2
0059572	EAST LONDON WO	2,4	20,1	167	15,18	36,1	37,8	41,7
0061298	LANGEBAANWEG	2,0	20,1	24	2,18	29,4	30,8	34,0
0063807	EXCELSIOR CERES	2,1	17,6	66	4,13	28,7	30,2	33,5
0078227	FORT BEAUFORT	2,4	20,1	120	10,91	35,4	37,1	41,0
0083572	LAMBERTSBAAI	1,7	17,6	130	9,29	27,9	29,1	31,8
0092081	BEAUFORT-WES	2,5	25,1	83	5,53	39,0	40,7	44,7
0096072	GRAAFF - REINET	1,7	22,6	48	3,00	31,1	32,2	35,0
0123685	QUEENSTOWN	2,4	22,7	87	7,25	37,1	38,8	42,8
0127272	UMTATA WO	3,0	20,1	103	10,30	39,0	41,1	46,0
0134479	CALVINIA WO	2,2	22,6	42	2,63	33,4	34,9	38,4
0144791	NOUPOORT	2,3	22,5	159	11,36	37,4	39,0	42,8

Station Number	Station Name	Distribution parameters				Annual maximum wind gust (m/s)		
		α	β	n	λ	X_{50}	X_{100}	X_{500}
0148517	JAMESTOWN	2,2	20,1	59	4,21	31,9	33,5	37,0
0150620	ELLIOT	3,7	22,6	76	6,91	44,2	46,8	52,8
0155394	PORT EDWARD	2,2	20,1	83	5,93	32,6	34,2	37,7
0169880	DE AAR WO	3,6	22,5	70	4,67	42,3	44,8	50,7
0182465	PADDOCK	2,1	20,7	91	6,07	30,3	31,2	33,7
0182591	MARGATE	2,2	20,1	125	8,33	33,3	34,8	38,3
0184491	KOINGNAAS	1,2	20,1	58	3,87	26,3	27,2	29,1
0190868	BRANDVLEI	2,6	22,6	30	2,50	35,2	37,0	41,2
0214700	SPRINGBOK WO	2,2	22,6	72	5,14	34,6	36,1	39,6
0224400	PRIESKA	2,4	20,1	94	6,71	33,9	35,6	39,4
0239698	PIETERMARITZBURG	2,3	15,1	118	8,43	29,1	30,8	34,5
0239699	ORIBI AIRPORT	2,7	15,1	192	19,20	33,6	35,4	39,8
0240808	DURBAN WO	2,0	20,1	151	9,44	32,6	34,0	37,3
0241072	MT EDGECOMBE	1,7	17,6	123	8,79	27,7	28,9	31,5
0241076	VIRGINIA	1,9	17,6	132	9,43	29,1	30,4	33,5
0261516	BLOEMFONTEIN WO	2,7	20,1	112	8,00	36,3	38,2	42,5
0268016	GIANTS CASTLE	2,8	18,4	102	7,29	37,3	40,2	42,8
0270155	GREYTOWN	2,6	17,6	108	7,71	33,1	34,9	39,1
0274034	ALEXANDERBAAI	1,5	22,6	138	9,86	32,1	33,2	35,7
0290468	KIMBERLEY WO	2,8	20,1	158	11,29	37,7	39,6	44,1
0300454	LADYSMITH	2,7	20,1	131	9,36	36,4	38,3	42,5
0304357	MTUNZINI	2,1	20,1	76	5,43	31,6	33,0	36,3
0317475	UPINGTON WO	2,6	20,1	140	10,00	36,0	37,8	41,9
0321110	POSTMASBURG	2,3	20,1	52	5,20	32,7	34,3	38,0
0331585	BETHLEHEM WO	1,6	22,6	23	1,92	29,9	31,1	33,6
0333682	VAN REENEN	2,5	22,6	76	5,85	37,0	38,7	42,8
0337738	ULUNDI	2,5	17,6	101	9,18	32,9	34,7	38,7
0339732	CHARTERS CREEK	1,3	15,1	153	12,75	23,3	24,2	26,3
0356880	KATHU	2,5	17,6	123	11,18	33,3	35,0	39,0
0360453	TAUNG	3,0	17,6	141	12,82	36,9	39,0	43,8
0362189	BLOEMHOF	1,9	20,1	72	5,14	30,9	32,2	35,4
0364300	WELKOM	3,1	20,1	151	11,62	40,0	42,2	47,2
0365398	KROONSTAD	2,9	20,2	133	11,08	38,8	40,8	45,5
0370856	NEWCASTLE	2,9	20,1	115	10,46	38,2	40,2	44,9

Station Number	Station Name	Distribution parameters				Annual maximum wind gust (m/s)		
		α	β	n	λ	X_{50}	X_{100}	X_{500}
0410175	PONGOLA	2,5	17,6	45	4,50	31,2	33,0	37,0
0427083	VAN ZYLSRUS	2,0	17,6	88	7,33	29,2	30,5	33,7
0438784	VEREENIGING	2,3	20,2	70	5,83	33,4	35,0	38,8
0441416	STANDERTON	2,5	17,6	45	10,46	32,9	34,6	38,6
0472278	LICHTENBURG	2,4	17,6	164	12,62	33,0	34,7	38,6
0475879	JHB BOT TUINE	2,2	15,1	91	7,00	27,8	29,3	32,7
0476399	JOHANNESBURG	2,5	17,6	158	11,29	33,4	35,1	39,2
0479870	ERMELO WO	2,0	20,1	120	8,57	32,1	33,5	36,7
0508047	MAFIKENG WO	2,2	20,1	97	8,08	33,0	34,5	38,0
0511399	RUSTENBURG	1,9	17,6	65	5,00	28,2	29,5	32,6
0513346	PRETORIA UNISA	1,9	17,6	167	15,18	30,3	31,7	34,8
0513385	IRENE WO	2,5	17,6	188	13,43	33,6	35,3	39,3
0515320	WITBANK	2,3	17,6	123	8,79	31,5	33,1	36,7
0520691	KOMATIDRAAI	2,2	15,1	171	11,40	28,9	30,4	33,9
0548375	PILANESBERG	2,6	17,6	71	6,46	32,4	34,1	38,3
0554816	LYDENBURG	2,1	15,1	114	8,77	27,7	29,1	32,5
0587725	THABAZIMBI	2,4	17,6	62	6,20	31,1	32,7	36,5
0594626	GRASKOP	2,5	15,1	61	6,10	29,6	31,3	35,4
0633882	POTGIETERSRUS	2,1	17,9	58	5,27	31,4	31,6	36,0
0638081	HOEDSPRUIT	2,1	20,1	36	3,27	30,6	32,1	35,4
0674341	ELLISRAS	2,0	15,1	156	11,14	27,9	29,3	32,6
0675666	MARKEN	1,9	17,6	40	3,33	27,2	28,6	31,6
0677802	PIETERSBURG WO	2,9	17,6	117	9,00	35,0	37,0	41,6
0723664	THOHOYANDOU WO	2,1	15,1	154	12,83	29,0	30,4	33,9

A.6. Mixed distribution method estimations for the quantiles X_T.

Station Number	Station Name	Annual maximum wind gust (m/s)			Annual maximum hourly wind speed (m/s)		
		X_{50}	X_{100}	X_{500}	X_{50}	X_{100}	X_{500}
0003108	STRUISBAAI				18,1	18,7	20,4
0005609	STRAND	36,6	38,3	42,1	19,4	20,3	22,4
0006386	HERMANUS				17,7	18,5	20,2
0007699	TYGERHOEK						
0010682	STILBAAI						
0012661	GEORGE WO						
0014123	KNYSNA						
0014545	PLETTENBERGBAAI				16,4	17,4	19,6
0015692	TSITSIKAMMA						
0020618	ROBBENEILAND	29,7	31,3	34,9	15,4	16,1	17,7
0021178	CAPE TOWN WO	38,7	41,0	46,3	22,8	24,0	26,8
0021823	PAARL	26,1	27,1	29,2			
0022729	WORCESTER						
0031650	JOUBERTINA	34,3	36,9	43,1	12,9	13,3	14,4
0033556	PATENSIE	30,5	32,7	37,8	12,2	12,8	14,3
0034763	UITENHAGE	33,8	36,0	41,8			
0035209	PORT ELIZABETH						
0040192	GEELBEK	28,6	29,9	32,9	16,1	16,6	17,7
0041388	MALMESBURY	28,8	30,1	33,1	12,6	13,3	14,8
0041841	PORTERVILLE	32,8	35,0	40,0	16,1	17,2	19,8
0045642	LAINGSBURG	33,6	35,0	38,3			
0056917	GRAHAMSTOWN	34,0	36,4	42,2			
0059572	EAST LONDON WO						
0061298	LANGEBAANWEG	33,1	35,3	40,5	17,6	18,3	20,1
0063807	EXCELSIOR CERES				12,4	13,1	14,8
0078227	FORT BEAUFORT	37,2	39,6	45,2			
0083572	LAMBERTSBAAI	26,0	26,8	28,8	16,0	16,6	18,0
0092081	BEAUFORT-WES	38,8	40,4	44,1			
0096072	GRAAFF - REINET	31,9	33,3	36,6	15,1	15,7	17,2
0123685	QUEENSTOWN	33,1	34,2	36,7			
0127272	UMTATA WO	41,9	44,7	51,2			
0134479	CALVINIA WO	32,4	33,8	36,9	17,2	17,8	19,3
0144791	NOUPOORT	33,8	35,4	39,2	18,2	19,2	21,7

Station Number	Station Name	Annual maximum wind gust (m/s)			Annual maximum hourly wind speed (m/s)		
		X_{50}	X_{100}	X_{500}	X_{50}	X_{100}	X_{500}
0148517	JAMESTOWN	30,2	31,7	35,3			
0150620	ELLIOT	41,8	44,4	50,6			
0155394	PORT EDWARD						
0169880	DE AAR WO	41,2	43,1	47,7	20,0	20,6	22,3
0182465	PADDOCK	30,5	32,2	36,3	17,2	18,0	19,9
0182591	MARGATE						
0184491	KOINGNAAS	27,6	28,8	31,6	16,7	17,3	18,6
0190868	BRANDVLEI	35,0	37,1	41,9	16,3	16,9	18,5
0214700	SPRINGBOK WO	33,4	34,9	38,5	20,6	21,4	23,5
0224400	PRIESKA	33,4	34,9	38,5	17,3	18,2	20,4
0239698	PIETERMARITZBURG	28,6	30,1	33,6	11,0	11,6	13,0
0239699	ORIBI AIRPORT	35,4	37,7	43,0	14,6	15,2	16,7
0240808	DURBAN WO						
0241072	MT EDGECOMBE				12,6	13,1	14,5
0241076	VIRGINIA				12,7	13,0	14,0
0261516	BLOEMFONTEIN WO				14,4	14,9	16,1
0268016	GIANTS CASTLE						
0270155	GREYTOWN	32,7	34,6	38,9			
0274034	ALEXANDERBAAI	32,2	33,6	37,4			
0290468	KIMBERLEY WO				16,9	17,5	19,0
0300454	LADYSMITH	37,3	39,4	44,3			
0304357	MTUNZINI	32,3	34,2	38,7			
0317475	UPINGTON WO				17,0	17,7	19,2
0321110	POSTMASBURG				16,2	17,2	19,6
0331585	BETHLEHEM WO	30,7	32,1	35,2	15,3	15,9	17,4
0333682	VAN REENEN	35,5	37,4	42,0			
0337738	ULUNDI	30,7	32,0	35,2			
0339732	CHARTERS CREEK	26,5	28,2	32,3	10,3	10,7	11,7
0356880	KATHU				13,4	14,0	15,3
0360453	TAUNG				11,7	12,0	12,8
0362189	BLOEMHOF	36,0	38,3	43,7			
0364300	WELKOM	39,3	41,6	46,8	21,1	22,3	25,2
0365398	KROONSTAD	33,4	34,8	37,9	17,8	18,6	20,3
0370856	NEWCASTLE	34,6	36,2	39,8			

Station Number	Station Name	Annual maximum wind gust (m/s)			Annual maximum hourly wind speed (m/s)		
		X_{50}	X_{100}	X_{500}	X_{50}	X_{100}	X_{500}
0410175	PONGOLA	30,0	31,5	34,9			
0427083	VAN ZYLSRUS	26,0	26,6	28,5	12,4	13,1	14,8
0438784	VEREENIGING	33,2	34,8	38,6	15,5	16,1	17,6
0441416	STANDERTON	34,3	36,4	41,2	12,3	12,8	13,8
0472278	LICHTENBURG	32,6	34,4	38,5			
0475879	JHB BOT TUINE	27,6	29,2	33,1	8,5	8,9	10,0
0476399	JOHANNESBURG	34,6	36,8	41,7	15,8	16,5	18,2
0479870	ERMELO WO	28,8	29,7	31,8			
0508047	MAFIKENG WO	31,8	33,3	36,7			
0511399	RUSTENBURG	29,7	31,4	35,4			
0513346	PRETORIA UNISA	26,9	27,8	30,0			
0513385	IRENE WO	33,3	35,1	39,4	16,5	17,2	18,9
0515320	WITBANK	31,0	32,7	36,7			
0520691	KOMATIDRAAI						
0548375	PILANESBERG	32,3	34,2	38,8			
0554816	LYDENBURG	34,2	36,8	42,9	10,9	11,4	12,8
0587725	THABAZIMBI	29,2	30,6	34,0	11,9	12,7	14,6
0594626	GRASKOP	29,7	31,9	36,9			
0633882	POTGIETERSRUS	32,1	34,6	40,3	12,1	12,8	14,5
0638081	HOEDSPRUIT	31,9	34,0	39,0			
0674341	ELLISRAS	28,7	30,4	34,4	8,8	9,2	10,1
0675666	MARKEN	30,6	32,8	37,8			
0677802	PIETERSBURG WO				15,0	15,7	17,3
0723664	THOHOYANDOU WO	28,3	29,9	33,4	13,7	14,3	15,8

Appendix B

Standard deviations associated with the estimated quantiles by the Gumbel and EXP methods

B.1. The standard deviations for the Gumbel and EXP methods.

Station Number	Station Name	Gumbel			EXP		
		S_{50}	S_{100}	S_{500}	S_{50}	S_{100}	S_{500}
0003108	STRUISBAAI	3,9	4,5	5,9	1,9	2,2	2,8
0005609	STRAND	2,8	3,3	4,3	1,6	1,8	2,4
0006386	HERMANUS	1,6	1,9	2,4	1,7	1,9	2,5
0007699	TYGERHOEK	2,8	3,2	4,2	2,2	2,5	3,1
0010682	STILBAAI	1,5	1,8	2,3	1,4	1,6	2,1
0012661	GEORGE WO	1,6	1,8	2,4	1,4	1,6	2,0
0014123	KNYSNA	1,5	1,8	2,3	1,7	1,9	2,4
0014545	PLETTENBERGBAAI	1,7	1,9	2,5	1,9	2,1	2,8
0015692	TSITSIKAMMA	1,5	1,7	2,2	1,4	1,6	2,1
0020618	ROBBENEILAND	1,5	1,7	2,2	1,0	1,2	1,4
0021178	CAPE TOWN WO	2,8	3,2	4,2	1,7	1,9	2,4
0021823	PAARL	0,9	1,0	1,4	1,0	1,1	1,5
0022729	WORCESTER	2,2	2,6	3,3	2,0	2,2	2,8
0031650	JOUBERTINA	3,0	3,4	4,4	1,6	1,8	2,3
0033556	PATENSIE	1,9	2,2	2,8	1,2	1,3	1,6
0034763	UITENHAGE	1,8	2,1	2,7	1,2	1,3	1,6
0035209	PORT ELIZABETH	1,8	2,1	2,8	1,1	1,2	1,5
0040192	GEELBEK	1,7	2,0	2,5	1,5	1,7	2,1
0041388	MALMESBURY	1,7	1,9	2,5	1,4	1,6	2,0
0041841	PORTERVILLE	2,7	3,1	4,1	2,4	2,7	3,5
0045642	LAINGSBURG	1,8	2,1	2,7	1,6	1,7	2,0
0056917	GRAHAMSTOWN	2,2	2,5	3,2	1,3	1,5	1,8
0059572	EAST LONDON WO	2,1	2,4	3,2	1,3	1,4	1,7
0061298	LANGEBAANWEG	3,3	3,8	4,9	1,9	2,2	2,9
0063807	EXCELSIOR CERES	1,5	1,7	2,2	1,4	1,6	2,0
0078227	FORT BEAUFORT	3,0	3,4	4,4	1,4	1,6	1,9
0083572	LAMBERTSBAAI	0,8	1,0	1,3	0,9	1,0	1,3
0092081	BEAUFORT-WES	2,1	2,4	3,1	1,5	1,7	2,2
0096072	GRAAFF - REINET	1,5	1,7	2,2	1,2	1,4	1,8
0123685	QUEENSTOWN	1,1	1,3	1,7	1,6	1,7	2,2
0127272	UMTATA WO	3,8	4,3	5,7	1,9	2,1	2,6
0134479	CALVINIA WO	1,8	2,0	2,6	1,7	1,9	2,5
0144791	NOUPOORT	2,0	2,3	3,0	1,2	1,3	1,6

Station Number	Station Name	Gumbel			EXP		
		S_{50}	S_{100}	S_{500}	S_{50}	S_{100}	S_{500}
0148517	JAMESTOWN	1,8	2,1	2,7	1,6	1,8	2,2
0150620	ELLIOT	2,5	2,9	3,8	2,5	2,8	3,5
0155394	PORT EDWARD	1,8	2,1	2,7	1,4	1,6	1,9
0169880	DE AAR WO	2,0	2,3	3,0	2,4	2,7	3,4
0182465	PADDOCK	2,1	2,3	3,1	1,7	1,8	2,1
0182591	MARGATE	1,5	1,8	2,3	1,2	1,3	1,6
0184491	KOINGNAAS	1,2	1,4	1,8	0,8	0,9	1,2
0190868	BRANDVLEI	1,7	2,0	2,6	2,3	2,7	3,4
0214700	SPRINGBOK WO	1,4	1,6	2,1	1,4	1,6	2,0
0224400	PRIESKA	2,0	2,3	3,0	1,4	1,6	2,0
0239698	PIETERMARITZBURG	1,8	2,1	2,7	1,3	1,5	1,8
0239699	ORIBI AIRPORT	3,4	4,0	5,2	1,3	1,5	1,8
0240808	DURBAN WO	1,9	2,2	2,9	1,0	1,1	1,4
0241072	MT EDGECOMBE	0,9	1,1	1,4	0,9	1,0	1,3
0241076	VIRGINIA	2,3	2,6	3,4	1,0	1,1	1,4
0261516	BLOEMFONTEIN WO	2,4	2,8	3,7	1,6	1,7	2,1
0268016	GIANTS CASTLE	2,3	2,4	2,7	1,9	2,0	2,4
0270155	GREYTOWN	2,1	2,4	3,1	1,5	1,7	2,1
0274034	ALEXANDERBAAI	1,3	1,5	2,0	0,8	0,9	1,1
0290468	KIMBERLEY WO	2,3	2,6	3,4	1,4	1,6	1,9
0300454	LADYSMITH	2,8	3,2	4,2	1,4	1,6	2,0
0304357	MTUNZINI	1,5	1,7	2,3	1,3	1,5	1,9
0317475	UPINGTON WO	2,9	3,3	4,4	1,4	1,5	1,9
0321110	POSTMASBURG	2,1	2,4	3,2	1,8	2,0	2,5
0331585	BETHLEHEM WO	1,4	1,6	2,1	1,6	1,8	2,3
0333682	VAN REENEN	2,0	2,4	3,1	1,7	1,9	2,3
0337738	ULUNDI	1,8	2,1	2,7	1,5	1,7	2,1
0339732	CHARTERS CREEK	1,8	2,1	2,7	0,7	0,7	0,9
0356880	KATHU	2,3	2,7	3,5	1,4	1,6	1,9
0360453	TAUNG	2,3	2,7	3,5	1,6	1,8	2,2
0362189	BLOEMHOF	3,3	3,8	4,9	1,3	1,4	1,8
0364300	WELKOM	3,1	3,6	4,7	1,6	1,8	2,2
0365398	KROONSTAD	1,7	2,0	2,6	1,6	1,8	2,2
0370856	NEWCASTLE	2,3	2,7	3,5	1,7	1,9	2,3

Station Number	Station Name	Gumbel			EXP		
		S_{50}	S_{100}	S_{500}	S_{50}	S_{100}	S_{500}
0410175	PONGOLA	2,1	2,4	3,2	2,1	2,3	2,9
0427083	VAN ZYLSRUS	1,2	1,4	1,8	1,3	1,4	1,7
0438784	VEREENIGING	2,4	2,8	3,7	1,6	1,8	2,2
0441416	STANDERTON	2,9	3,3	4,3	2,3	2,6	3,2
0472278	LICHTENBURG	2,5	2,9	3,8	1,2	1,3	1,6
0475879	JHB BOT TUINE	2,2	2,6	3,4	1,3	1,5	1,9
0476399	JOHANNESBURG	2,6	3,0	3,9	1,3	1,4	1,7
0479870	ERMELO WO	1,1	1,3	1,7	1,1	1,2	1,5
0508047	MAFIKENG WO	2,0	2,3	3,0	1,3	1,5	1,8
0511399	RUSTENBURG	2,2	2,6	3,4	1,3	1,5	1,9
0513346	PRETORIA UNISA	1,5	1,7	2,2	1,0	1,1	1,3
0513385	IRENE WO	2,4	2,7	3,5	1,2	1,3	1,6
0515320	WITBANK	2,2	2,5	3,2	1,3	1,4	1,7
0520691	KOMATIDRAAI	2,5	2,8	3,7	1,1	1,2	1,5
0548375	PILANESBERG	2,9	3,3	4,3	1,8	2,0	2,5
0554816	LYDENBURG	3,1	3,6	4,7	1,2	1,3	1,6
0587725	THABAZIMBI	2,2	2,6	3,3	1,7	1,9	2,4
0594626	GRASKOP	3,1	3,6	4,7	1,9	2,1	2,6
0633882	POTGIETERSRUS	2,7	2,9	3,3	2,1	2,2	2,7
0638081	HOEDSPRUIT	2,3	2,7	3,5	1,8	2,0	2,6
0674341	ELLISRAS	2,3	2,6	3,4	1,0	1,2	1,4
0675666	MARKEN	2,4	2,8	3,7	1,6	1,8	2,2
0677802	PIETERSBURG WO	2,3	2,7	3,5	1,6	1,8	2,2
0723664	THOHOYANDOU WO	1,6	1,9	2,4	1,1	1,2	1,5

Appendix C

κ parameter estimations for the different strong wind mechanisms

C. 1. Values of the κ parameter for the different strong wind mechanisms, estimated by fitting of the GEV distribution.

Station Number	Station Name	Annual maximum wind gust (m/s)				Annual maximum hourly wind speed (m/s)		
		κ_{TS}	κ_{CF}	κ_{R}	κ_{OTHER}	κ_{CF}	κ_{R}	κ_{OTHER}
0003108	STRUISBAAI		-0,47			-0,13	+0,07	
0005609	STRAND		+0,47	+0,12		-0,16	+0,54	
0006386	HERMANUS		+0,50			-0,01	+0,20	
0007699	TYGERHOEK		-0,07			+0,25		
0010682	STILBAAI		-0,01			+0,02		
0012661	GEORGE WO		+0,23			+0,27		
0014123	KNYSNA		+0,26			+0,07		
0014545	PLETTENBERGBAAI		+0,65			+0,16		+0,15
0015692	TSITSIKAMMA		-0,01					
0020618	ROBBENEILAND		+0,29	-0,02		+0,43	-0,07	
0021178	CAPE TOWN WO		-0,04	-0,14		-0,16	-0,01	
0021823	PAARL		+0,16	+0,58				
0022729	WORCESTER		-0,15			+0,41		
0031650	JOUBERTINA	-0,20	-0,54		-0,26	+0,38		+0,71
0033556	PATENSIE	+0,24	-0,11		+0,28	-0,02	+0,93	+0,40
0034763	UITENHAGE	+0,03	+0,01			-0,18		
0035209	PORT ELIZABETH		-0,13			-0,11		
0040192	GEELBEK		-0,07	-0,03		+0,20	+0,33	
0041388	MALMESBURY		-0,01	+0,21				
0041841	PORTERVILLE		-0,11	+0,46	-0,41	+0,19	+0,10	-0,17
0056917	GRAHAMSTOWN	+0,09	-0,09			+0,06		
0059572	EAST LONDON WO		+0,59			+0,45		
0061298	LANGEBAANWEG		-0,39	+0,12		+0,10	-0,05	
0063807	EXCELSIOR CERES		+0,06			+0,07	+0,06	
0078227	FORT BEAUFORT	-0,15	+0,18			+0,31		
0083572	LAMBERTSBAAI		+0,34		+0,80	+0,29	+0,53	
0092081	BEAUFORT-WES	+0,32	-0,05		-0,30	-0,04		
0096072	GRAAFF - REINET	-0,21	+0,15		+0,23	+0,01		+0,66
0123685	QUEENSTOWN	+0,40	+0,33			+0,12		
0127272	UMTATA WO	-0,35	+0,57			-0,05		
0134479	CALVINIA WO		-0,13		+0,03	+0,21		+0,36

Station Number	Station Name	Annual maximum wind gust (m/s)				Annual maximum hourly wind speed (m/s)		
		K_{TS}	K_{CF}	K_R	K_{OTHER}	K_{CF}	K_R	K_{OTHER}
0144791	NOUPOORT	+0,20	-0,20		+0,05		+0,27	+0,04
0148517	JAMESTOWN	+0,57	+0,13		-0,06	+0,11		
0150620	ELLIOT	+0,58	+0,18			+0,10		
0155394	PORT EDWARD		-0,12			-0,14		
0169880	DE AAR WO	-0,03			-0,09	+0,03		-0,09
0182591	MARGATE		+0,01					
0184491	KOINGNAAS		+0,28	+0,11	-0,01		+0,05	+0,32
0190868	BRANDVLEI	+0,74			+0,06	+0,06		-0,03
0214700	SPRINGBOK WO		+0,51		+0,18	+0,22		+0,20
0224400	PRIESKA	+0,08	+0,16		+0,00	-0,07		-0,24
0239698	PIETERMARITZBURG	-0,13	-0,17		-0,24	-0,23		-0,03
0239699	ORIBI AIRPORT	-0,21	-0,05		+0,16	-0,19		+0,10
0240808	DURBAN WO		-0,14			-0,13		
0241072	MT EDGECOMBE		+0,34			+0,30	-0,06	
0241076	VIRGINIA		+0,09			+0,37	+0,02	
0261516	BLOEMFONTEIN WO	-0,24				+0,21		-0,09
0268016	GIANTS CASTLE		-0,23			-0,32		
0270155	GREYTOWN	+0,46	+0,08			+0,44		
0274034	ALEXANDERBAAI		+0,09		-0,04			+0,22
0290468	KIMBERLEY WO	+0,20				+0,21		-0,07
0300454	LADYSMITH	-0,39	-0,02			+0,01		
0304357	MTUNZINI	+0,49	+0,23			-0,24		
0317475	UPINGTON WO	-0,17				+0,23		+0,20
0321110	POSTMASBURG	+0,51						
0331585	BETHLEHEM WO	+0,24	+0,35	-0,30		+0,08	-0,12	
0333682	VAN REENEN	+0,04	+0,55			+0,12		
0337738	ULUNDI	-0,12	+0,12			-0,18		
0339732	CHARTERS CREEK	-0,28	+0,38	-0,12		-0,41	+0,05	
0356880	KATHU	+0,07				-0,04		+0,05
0360453	TAUNG	+0,34				+0,34		-0,10
0362189	BLOEMHOF	-0,33	-0,26			+0,28		
0364300	WELKOM	-0,19	+0,32			+0,05		
0365398	KROONSTAD	+0,35				-0,05		
0370856	NEWCASTLE	+0,41				+0,22		

Station Number	Station Name	Annual maximum wind gust (m/s)				Annual maximum hourly wind speed (m/s)		
		κ_{TS}	κ_{CF}	κ_{R}	κ_{OTHER}	κ_{CF}	κ_{R}	κ_{OTHER}
0410175	PONGOLA	+0,22				-0,05		
0427083	VAN ZYLSRUS	+0,36				-0,09		-0,22
0438784	VEREENIGING	+0,33				-0,20		+0,27
0441416	STANDERTON	+0,18				+0,21		+0,35
0472278	LICHTENBURG	+0,05				+0,15		
0475879	JHB BOT TUINE	-0,06				-0,11		-0,13
0476399	JOHANNESBURG	+0,01				+0,27		-0,03
0479870	ERMELO WO	+0,31				-0,01		
0508047	MAFIKENG WO	-0,12						-0,04
0511399	RUSTENBURG	+0,30				+0,28		
0513346	PRETORIA UNISA	+0,40					-0,27	
0513385	IRENE WO	+0,09				-0,15		+0,21
0515320	WITBANK	+0,16						+0,33
0520691	KOMATIDRAAI	+0,13				+0,20		
0548375	PILANESBERG	-0,01					+0,38	
0554816	LYDENBURG	-0,07				-0,45		+0,34
0587725	THABAZIMBI	+0,53				-0,19		-0,25
0594626	GRASKOP	-0,03				+0,16		
0638081	HOEDSPRUIT	-0,25		+0,44			+0,29	
0674341	ELLISRAS	-0,11				+0,14		+0,03
0675666	MARKEN	+0,03		+0,05			-0,35	
0677802	PIETERSBURG WO	+0,36				+0,24	-0,10	
0723664	THOHOYANDOU WO	+0,26				+0,51		+0,16

κ_{TS} is the shape parameter for the data set for thunderstorms, κ_{CF} for cold fronts and κ_{R} for ridging. κ_{OTHER} indicates another strong wind mechanism at a specific weather station, which can be found in Table 4.8.

Appendix D

Differences between the estimates for the quantiles estimated by the Mixed Distribution and Gumbel methods

Table D.1. Differences between the estimates for the quantiles X_T estimated by the mixed distribution and Gumbel methods.

Station Number	Station Name	Annual maximum wind gust (m/s)			Annual maximum hourly wind speed (m/s)		
		X_{50}	X_{100}	X_{500}	X_{50}	X_{100}	X_{500}
0003108	STRUISBAAI				0,3	0,3	0,8
0005609	STRAND	0,2	0,3	0,4	0,4	0,5	0,8
0006386	HERMANUS				0,1	0,2	0,1
0007699	TYGERHOEK						
0010682	STILBAAI						
0012661	GEORGE WO						
0014123	KNYSNA						
0014545	PLETTENBERGBAAI				0,5	0,6	1,0
0015692	TSITSIKAMMA						
0020618	ROBBENEILAND	1,3	1,7	2,8	0,3	0,4	0,7
0021178	CAPE TOWN WO	0,4	0,5	0,7	0,4	0,5	0,6
0021823	PAARL	1,0	1,4	1,9			
0022729	WORCESTER						
0031650	JOUBERTINA	2,1	2,8	4,7	0,7	0,9	1,3
0033556	PATENSIE	4,5	5,5	7,9	0,2	0,4	0,7
0034763	UITENHAGE	2,1	3,1	6,3			
0035209	PORT ELIZABETH						
0040192	GEELBEK	0,4	0,6	0,9	0,2	0,3	0,4
0041388	MALMESBURY	0,4	0,5	0,6	0,9	1,2	1,6
0041841	PORTERVILLE	0,0	0,2	0,4	0,6	0,9	1,6
0045642	LAINGSBURG	1,2	1,5	2,4			
0056917	GRAHAMSTOWN	1,8	2,7	4,8			
0059572	EAST LONDON WO						
0061298	LANGEBAANWEG	-0,1	0,1	0,3	0,4	0,4	0,7
0063807	EXCELSIOR CERES				0,1	0,2	0,4
0078227	FORT BEAUFORT	0,8	1,3	2,3			
0083572	LAMBERTSBAAI	1,1	1,3	1,9	0,0	0,1	0,1
0092081	BEAUFORT-WES	0,2	0,3	0,3			
0096072	GRAAFF - REINET	0,7	0,9	1,6	0,3	0,4	0,7
0123685	QUEENSTOWN	1,2	1,5	2,2			
0127272	UMTATA WO	1,4	1,8	2,7			

Station Number	Station Name	Annual maximum wind gust (m/s)			Annual maximum hourly wind speed (m/s)		
		X_{50}	X_{100}	X_{500}	X_{50}	X_{100}	X_{500}
0134479	CALVINIA WO	0,0	0,1	0,0	0,6	0,7	1,2
0144791	NOUPOORT	0,6	0,7	1,1	-0,6	-0,4	0,1
0148517	JAMESTOWN	2,0	2,4	3,4			
0150620	ELLIOT	3,0	3,9	6,3			
0155394	PORT EDWARD						
0169880	DE AAR WO	1,5	1,8	2,8	0,1	0,1	0,3
0182465	PADDOCK	-0,3	0,0	0,9	-0,2	-0,2	-0,3
0182591	MARGATE						
0184491	KOINGNAAS	1,0	1,3	2,0	0,6	0,9	1,6
0190868	BRANDVLEI	3,1	4,0	6,0	0,0	-0,1	0,0
0214700	SPRINGBOK WO	1,3	1,8	3,1	0,1	0,1	0,2
0224400	PRIESKA	0,1	0,1	0,1	0,7	0,7	0,8
0239698	PIETERMARITZBURG	1,6	1,8	2,2	0,0	0,0	0,0
0239699	ORIBI AIRPORT	0,4	0,6	0,9	-0,1	-0,1	-0,1
0240808	DURBAN WO						
0241072	MT EDGECOMBE				0,2	0,2	0,3
0241076	VIRGINIA				0,3	0,3	0,5
0261307	BLOEMFONTEIN				0,1	0,2	0,3
0261516	BLOEMFONTEIN WO				0,2	0,2	0,2
0268016	GIANTS CASTLE						
0270155	GREYTOWN	1,1	1,4	2,2			
0274034	ALEXANDERBAAI	0,9	1,3	2,8			
0290468	KIMBERLEY WO				0,1	0,1	0,2
0300454	LADYSMITH	-0,1	-0,1	0,0			
0304357	MTUNZINI	2,5	3,3	5,2			
0317475	UPINGTON WO				0,4	0,6	0,9
0321110	POSTMASBURG				0,4	0,5	0,8
0331585	BETHLEHEM WO	1,5	2,0	2,8	0,0	0,0	0,0
0333682	VAN REENEN	0,7	1,1	2,2			
0337738	ULUNDI	0,6	0,8	1,3			
0339732	CHARTERS CREEK	0,6	1,0	2,2	-0,1	0,0	0,1
0356880	KATHU				-0,1	-0,1	-0,3
0360453	TAUNG				0,2	0,1	0,1
0362189	BLOEMHOF	-0,7	-0,8	-0,9			

Station Number	Station Name	Annual maximum wind gust (m/s)			Annual maximum hourly wind speed (m/s)		
		X_{50}	X_{100}	X_{500}	X_{50}	X_{100}	X_{500}
0364300	WELKOM	0,0	0,0	0,0	0,0	0,1	0,3
0365398	KROONSTAD	0,1	0,3	0,6	0,7	1,0	1,4
0370856	NEWCASTLE	-0,4	-0,3	-0,3			
0410175	PONGOLA	0,3	0,5	0,8			
0427083	VAN ZYLSRUS	0,0	0,0	0,0	0,3	0,3	0,5
0438784	VEREENIGING	0,0	0,0	0,0	0,4	0,5	0,7
0441416	STANDERTON	-0,1	0,1	0,5	0,0	0,1	0,0
0472278	LICHTENBURG	-0,5	-0,5	-0,5			
0475879	JHB BOT TUINE	0,2	0,2	0,4	-0,1	-0,2	-0,2
0476399	JOHANNESBURG	0,6	0,9	1,2	0,4	0,4	0,6
0479870	ERMELO WO	-0,1	-0,1	0,1			
0508047	MAFIKENG WO	-0,1	0,0	0,2			
0511399	RUSTENBURG	0,5	0,7	1,0			
0513346	PRETORIA UNISA	-0,3	-0,4	-0,5			
0513385	IRENE WO	0,4	0,5	0,8	0,5	0,6	0,8
0515320	WITBANK	0,3	0,4	0,7			
0520691	KOMATIDRAAI						
0548375	PILANESBERG	0,3	0,3	0,7			
0554816	LYDENBURG	1,5	1,9	2,9	0,1	0,0	0,2
0587725	THABAZIMBI	0,1	0,1	0,2	0,2	0,3	0,5
0594626	GRASKOP	-1,5	-1,2	-0,8			
0633882	POTGIETERSRUS	0,0	0,1	0,2	0,2	0,2	0,2
0638081	HOEDSPRUIT	1,0	1,6	3,1			
0674341	ELLISRAS	0,1	0,2	0,2	0,4	0,5	0,6
0675666	MARKEN	1,1	1,7	2,8			
0677802	PIETERSBURG WO				0,1	0,2	0,4
0723664	THOHOYANDOU WO	1,1	1,6	2,4	0,8	0,9	1,3

Appendix E

Summaries of weather station exposures

0003108A7 STRUISBAAI 34°48'0.74"S, 20° 3'24.80"E

The climate station is situated on the northern side of a peninsula extending into the Atlantic Ocean. The village of Struisbaai covers the peninsula, and consists of low-rise buildings. The station is situated to the north of a parking area, with a low-rise building about 25 m south-east of the anemometer. The residential area is situated from about 60 m to the south-west, covering a distance of between 650 m and 1,4 km. Strong winds are from south-west to north-west, or from the north-east to east.

0005609 8 STRAND 34° 8'27.90"S, 18°50'55.93"E

The climate station is situated about 120 m from the coast line in a north-easterly direction. There are some isolated low-rise structures close to the station, especially in a westerly direction. The built-up residential area, which is mainly low-rise, is situated about 200 m to the north-east. The built-up area stretches for long distances along the coast, but in the region of the station is only 1 to 2 km wide. In the vicinity of the station the built-up area does not reach too close to the coastline. However, the built-up areas which stretch to the coastline start about 700 m to the north-west and 350 m to the south-east. A small clump of low trees and shrubs is situated about 50 m to the east. The strong winds are from the south-east, 9or south-west to north-west.

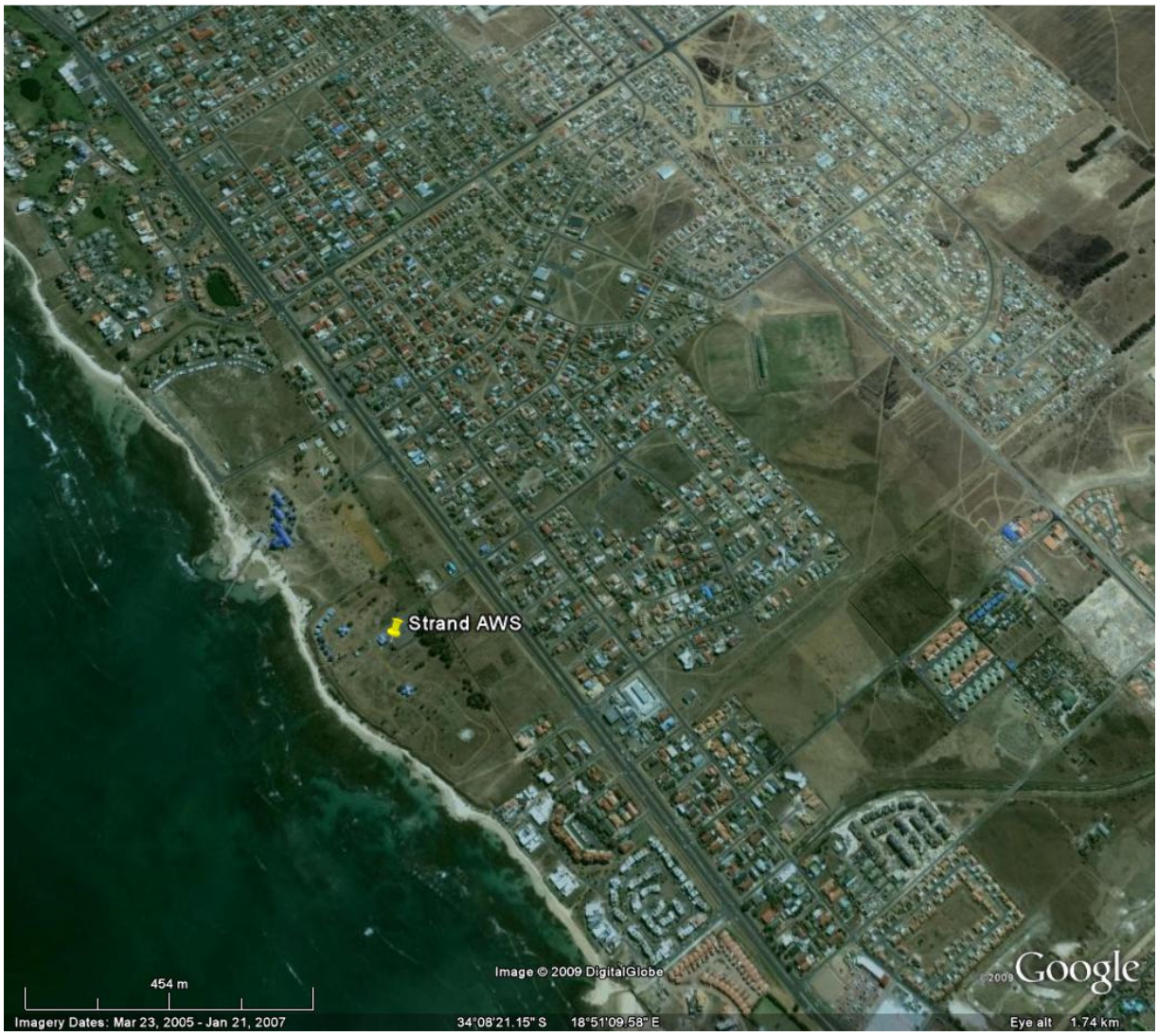

0006386A7 HERMANUS 34°25'56.18"S, 19°13'28.59"E

The AWS is situated about 100 m to the west of the coastline. Some low-rise buildings, about 15 to 30 m from the station, obstruct the view to the ocean. Low-rise developments start about 150 m to the south and south-west, and 50 m to the west, north and north-east. The built-up areas are interspersed with open land but is extensive, averaging about 1,5 km in breadth but extending several kilometers to the west-north-west to north-east. Mountainous areas exist towards the north-west to north-east, reaching a maximum height of about 450 m to the north-west at a distance of about 6 km from the weather station. The strong winds are from the north-east to east, and from the west to north-west.


Hermanus AWS
202 m
Image © 2009 DigitalGlobe
©2009 Google
Imagery Dates: Apr 7, 2004 - Aug 19, 2004
34°25'57.18" S 19°13'26.26" E elev 15 m
Eye alt 795 m

0007699A0 TYGERHOEK 34° 8'58.74"S, 19°54'7.89"E

The AWS is situated 600 m to the west of the village of Tygerhoek. To the north an extensive mountain range reaches heights of more than 700 m at a distance of 5 km from the station. The remainder of the terrain around the station is quite flat. Low buildings are situated at various distances in the immediate vicinity of the station, the most prominent being a shed of about 30 m wide at a distance of about 20 m east of the anemometer. The strong winds are from the south-west to north-west.


Tygerhoek AWS
Image © 2009 DigitalGlobe
©2009 Google
312 m
Imagery Date: Mar 3, 2003
34°08'58.41" S 19°54'10.72" E elev 156 m
Eye alt 1.35 km

0010682 0 STILBAAI 34°22'8.91"S, 21°23'27.86"E

The AWS is situated west of the coastal village of Stilbaai. The terrain is gently sloping upwards from east to west. No significant obstructions are situated close to the anemometer. The exposure of the AWS is regarded to be very good. The strong winds are from the south-west to north-west.

0012661 7 GEORGE WO 34° 00'20.99"S, 22°23'21.55"E

The AWS is situated at the P W Botha Airport, which is about 6 km to the west from the urbanized area of George. Although there are some bushy river valleys to the east and west of the airport, the terrain can be described as almost flat. Cultivated lands surround the airport. The anemometer is close to the edge of one of the runways, with the closest airport buildings about 650 m away to the north-west. The exposure of the AWS is considered to be very good. The strong winds are from the west to north-west.

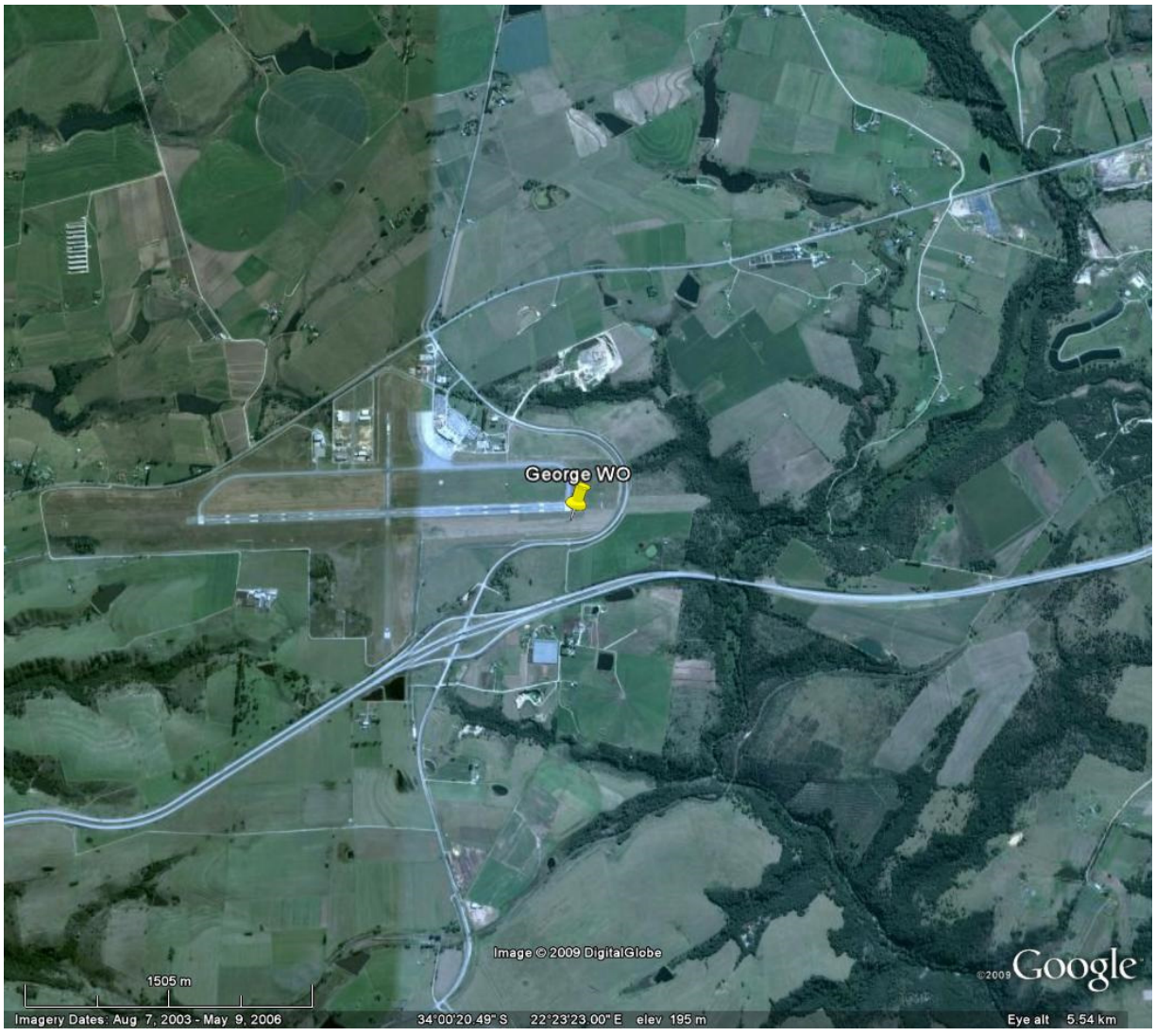

0014123 3 KNYSNA 34° 2'52.82"S, 23° 4'43.89"E

The AWS is situated in cemetery grounds, just south of an industrial area. Residential areas are located about 300 m to the east and south. Only winds from the south-western quadrant will not be significantly affected by built-up areas. A mountain range with height just over 200 m is located 1 km to the north. This anemometer is not ideally situated for wind measurements. The strong winds are from the west to north-west.

0014545 4 PLETTENBERGBAAI 34° 5'18.13"S, 23°19'22.84"E

The AWS is situated at the airstrip, which is situated about 3 km to the west and south of the town of Plettenberg Bay, and 1,2 km north of the coastline. A township is situated about 2 km to the west. There are a number of hangars about 30 m to the south-east. The terrain is somewhat hilly, but definitely not mountainous. Except for the hangars, the exposure is good. The strong winds are from the south-west to north.

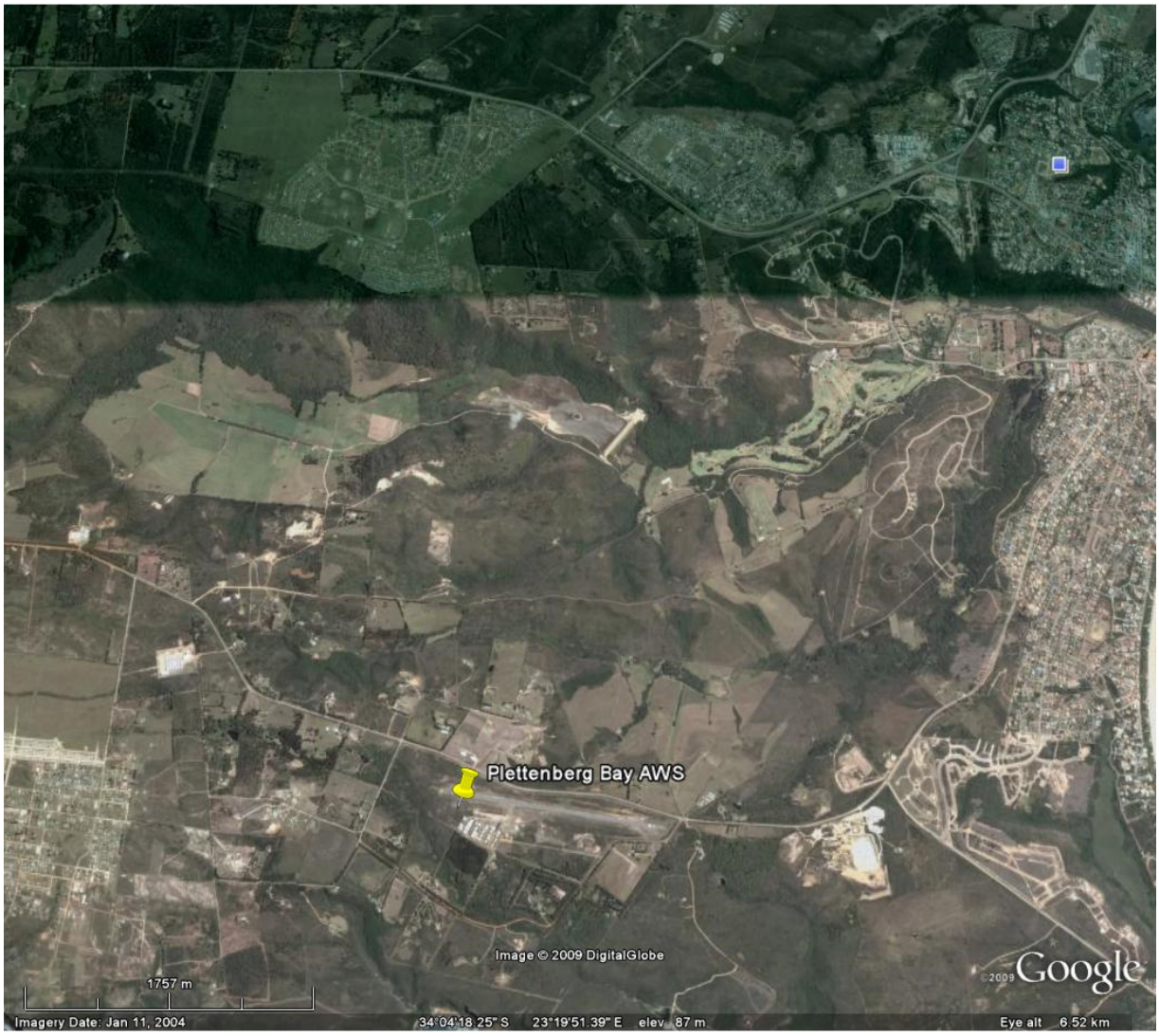

0015692A4 TSITSIKAMMA 34° 01' 22.04" S, 23° 53' 54.68" E

The National Parks building is situated about 30 m to the north-west of the AWS. The instrumentation is surrounded by low shrubs, except towards the west, which would not unduly influence the wind measurements. The ocean is at the north-easterly to west-south-westerly sector. The sector from west-south-west to north-east is forested, With dense vegetation starting at a distance of between 60 and 200 m. with the shortest distance to the north-west. Therefore especially north-westerly winds will be lower than the theoretical basic wind speed. The steepest slope is also towards the north-west, of about 15º upwards from the station, over a distance of about 200 m. The strong winds are from the south-west to north-west.

0020618 X ROBBENEILAND 33°47'56.08"S, 18°22'28.16"E

Buildings are situated at a distance of about 15 to 20 m in the north-easterly to south-easterly sector from the AWS. About 180 m to the south-west another building complex is situated. Both these complexes are one-storey, which is about 10 m or lower in height. Isolated buildings are situated 100 to 150 m to the north-west. The terrain on the island is flat, and surrounded by ocean. The strong winds are south-easterly or south-westerly to north-westerly.

0021178A3 CAPE TOWN WO 33°58'43.34"S, 18°35'59.28"E

The weather office at Cape Town Airport is not ideally exposed, but wind is measured by the instrumentation situated in the south of the runways. The exposure in most directions is fine, except from the west, where some airport buildings are situated.
The terrain is flat. The strong winds are south-east to south and from the north-west.

0021823 0 PAARL 33°43'18.81"S, 18°58'20.02"E

The AWS is situated in the town of Paarl. The town itself is quite flat, but hilly, mountainous terrain starts at about 1,5 km to the west, reaching a height of about 600 m above the station elevation. There are not many high buildings in Paarl. However, the built up area almost surrounds the station, but at various distances, from about 100 m to the east to 800 m to the north. The strong winds are from the east to south-east and from the south-west to north-west.

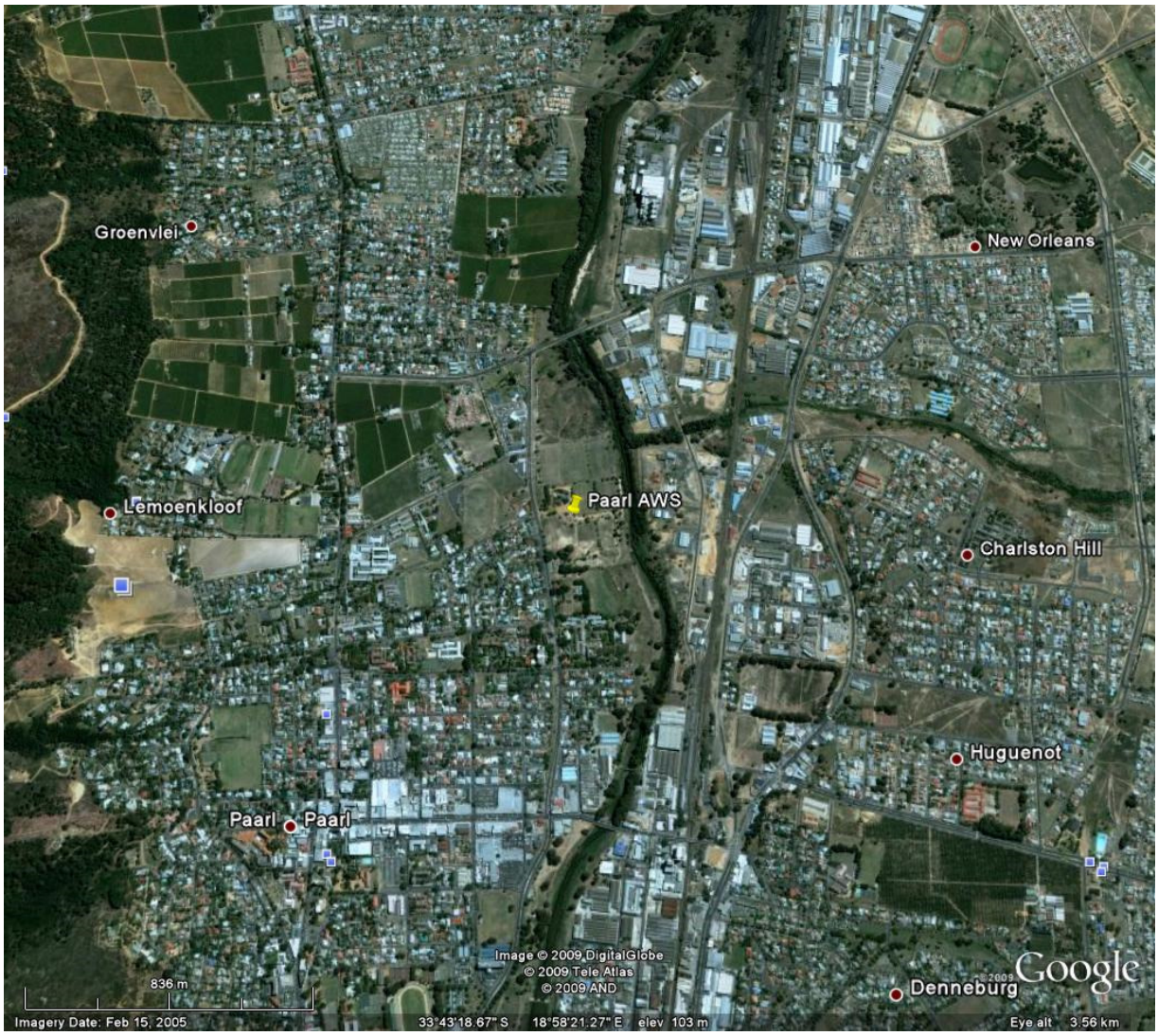


Paarl AWS
Image © 2009 DigitalGlobe
© 2009 Tele Atlas
© 2009 AND
224 m
Imagery Date: Feb 15, 2005
33°43'18.69" S 18°58'21.27" E elev 103 m
Eye alt 980 m
©2009 Google

0022729 X WORCESTER 33°39'50.47"S, 19°25'7.37"E

The AWS in Worcester is one of the best positioned weather stations amongst those identified to be utilized in this study. It is located at a small airport, in a large open valley with the dominant topography being several kilometres away from the site. Few airport hangars are located to the east of the anemometer as well as an extensive built-up terrain towards the north-east with a length of between 1,5 and 3 km. However, these buildings are very low and will not influence the wind speed significantly. The strong winds are from the north-west.


Worcester AWS
Image © 2009 DigitalGlobe
© 2009 Tele Atlas
© 2009 AND
157 m
Imagery Date: May 24, 2006
33°39'50.50" S 19°25'06.94" E elev 204 m
Eye alt 805 m
Google

0031650A4 JOUBERTINA AWS 33 50' 0.2'' S, 23 51' 52.0''E

The exact location of the AWS could not be established, except that it is located in the water works area to the east of the small town of Joubertina. From photographs it can be seen that there is a building located very close to the anemometer, with a height of about 3 to 4 m. There are some isolated trees around the water works. The town (and the anemometer) is located in a valley between two ridges. The ridge to the south is about 1 km away with a height of about 140 m, while the ridge to the north is also about 1 km away with a height of about 160 m. These ridges can cause the wind to be channeled through the valley, causing a strengthening of wind above the basic wind speed as well as altering of the general wind direction in some cases. The position of the anemometer is therefore not ideal for wind measuring purposes. The strong winds are from the south to north-west.

0033556 5 PATENSIE 33°46'0.22"S, 24°49'28.44"E

The station is situated in farmland. About 200 m the north-east is the foothills of a mountain range which reaches heights of about 250 m. To the north is a small settlement. There are no significantly high buildings close to the anemometer. Apart from the topography already mentioned the exposure seems to be good. The stron winds are from south-east to north-west.

0034763 X UITENHAGE 33°42'51.00"S, 25°26'6.40"E

The AWS is situated 40 m to the south of a small complex of low-rise buildings. The nearest built-up area is residential, about 2,3 km to the south-west. About 2 km to the north-west is the foothills of an extensive mountain range, which reaches heights of about 400 m at a distance of 5 km from the weather station. Apart from the topography, the exposure seems good. The strong winds are from the south-west to north-west.

0035209B1 PORT ELIZABETH WO 33°59'11.56"S, 25°37'0.48"E

The AWS is situated close to the runways of Port Elizabeth Airport. The closest buildings are about 450 m to the north-west and 300 m to the south. There are however some residential areas 1 km to the north-west and 350 m to the east. There are no obstructions close to the anemometer and the terrain is flat. The strong winds are from the south-west to west.

0040192 4 GEELBEK 33°11'46.57"S, 18° 7'26.25"E

The climate station is situated at the West Coast National Park, next to the Langebaan Lagoon. The lagoon stretches for an appreciable distance in a north-westerly direction. The Atlantic Ocean is about 6 km in a south-westerly direction. Low and flat one-storey buildings are situated about 30 m to the north, but this will not have a significant impact on wind flow. The exposure of the station can be considered to be very good. The strong winds are south-easterly, and south-westerly to north-westerly.

0041388 0 MALMESBURY 33°28'21.04"S, 18°43'6.73"E

The AWS is situated at the water works of the town of Malmesbury. Some buildings are situated at a distance of about 100 m to the north. The urbanized built up areas are in the northern sector, at a distance of about 400 m. The southern sector consists of mainly cultivated land. The strong winds are southerly, clockwise to north-north-easterly.


Malmesbury AWS
Image © 2009 DigitalGlobe
1308 m
Imagery Dates: Mar 23, 2005 - Jul 9, 2005
33°28'20.16" S 18°43'07.17" E
Eye alt 4.89 km
©2009 Google

0041841 X PORTERVILLE 33° 0'45.82"S, 18°58'37.91"E

The AWS is situated about 1 km to the west of the town of the small town of Porterville. The town has no high buildings. This is a wheat growing area. The terrain is flat, with some scrubland to the south. Strong winds are possible from any wind direction.

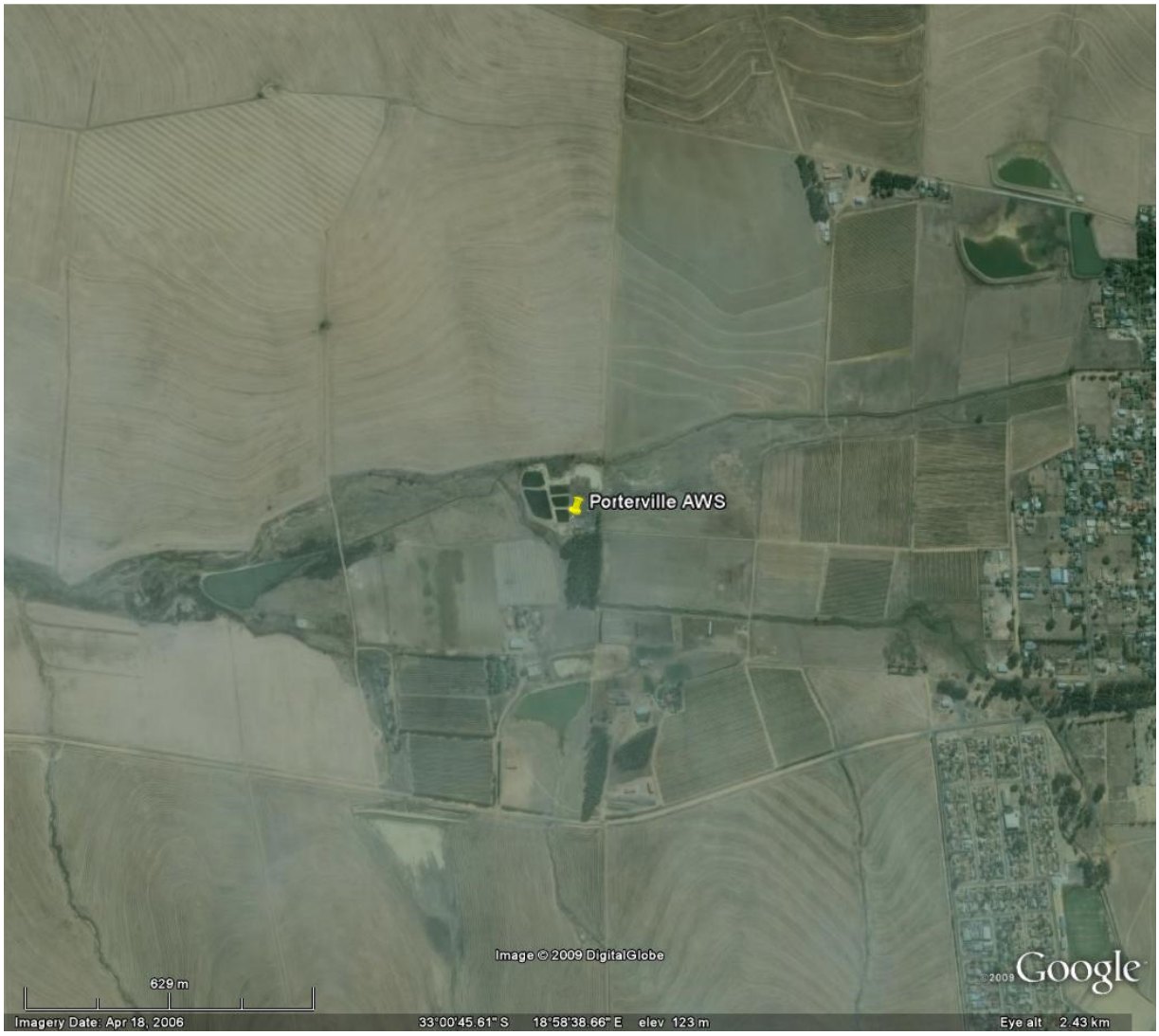

0045642 0 LAINGSBURG 33°11'26.80"S, 20°51'47.20"E

The AWS is positioned in a narrow (150 m wide) valley between two ridges with heights of about 50 m, extending to the north and south of the station, and other prominent topography located further away. Several buildings and tall trees are located within the close vicinity to the south of the anemometer, and a built-up area extends to the west, south-west, south and south-east. Wind speeds will predominantly be reduced but in some specific instances or directions could also be accelerated. The positioning of the wind meter is totally unsuitable for any reliable representation of wind speed measurements in a flat terrain. The strong winds are northwesterly.

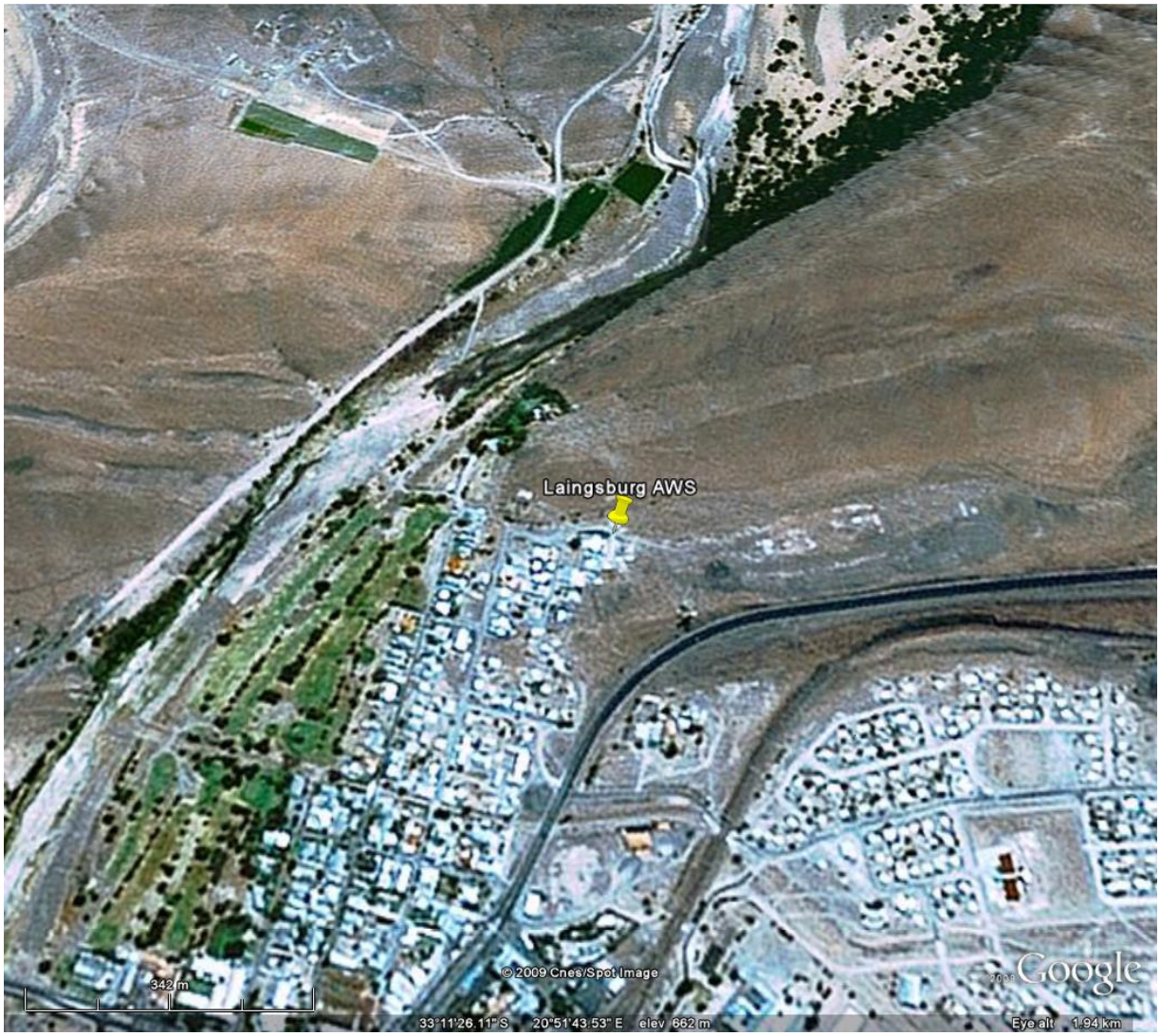

0056917 8 GRAHAMSTOWN 33°17'26.60"S, 26°30'9.80"E

The AWS is located about 1 km northwest of Grahamstown, at the airfield. Some low buildings at the airfield are located from 100 m to the north-west of the AWS, and a cluster of low-rise buildings are located about 600 m to the north of the AWS. The terrain is quite flat. The strong winds are westerly to northerly.

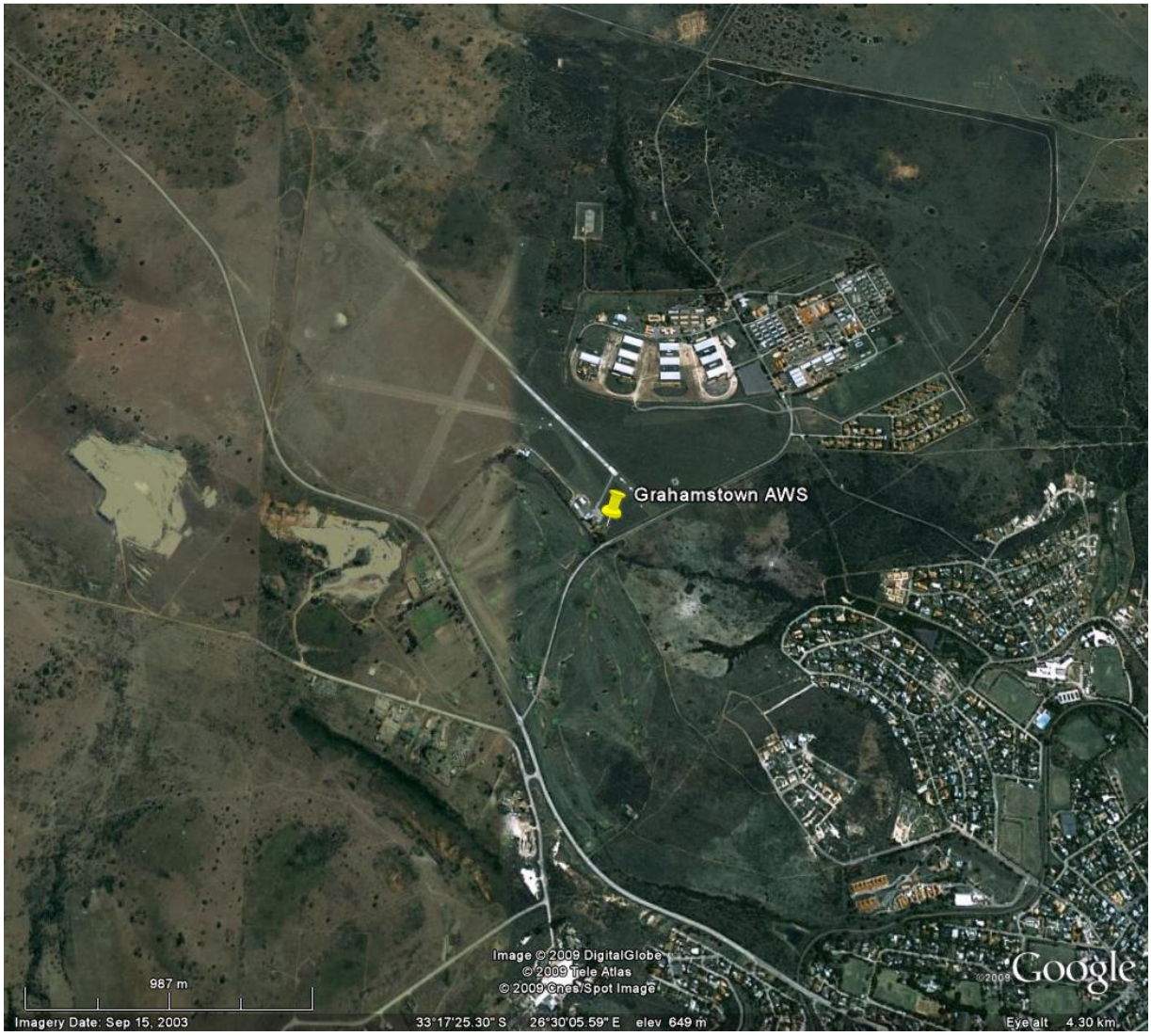

0059572B8 EAST LONDON WO 33° 2'9.36"S, 27°49'47.34"E

The AWS is located between runways at the East London Airport. The main airport buildings are about 240 m to the south. Patches of residential areas surround the airport at a distance of about 1 km or further. The terrain is quite flat, sloping slightly in a south-east to north-westerly direction. The strong winds are south-westerly to north-westerly.

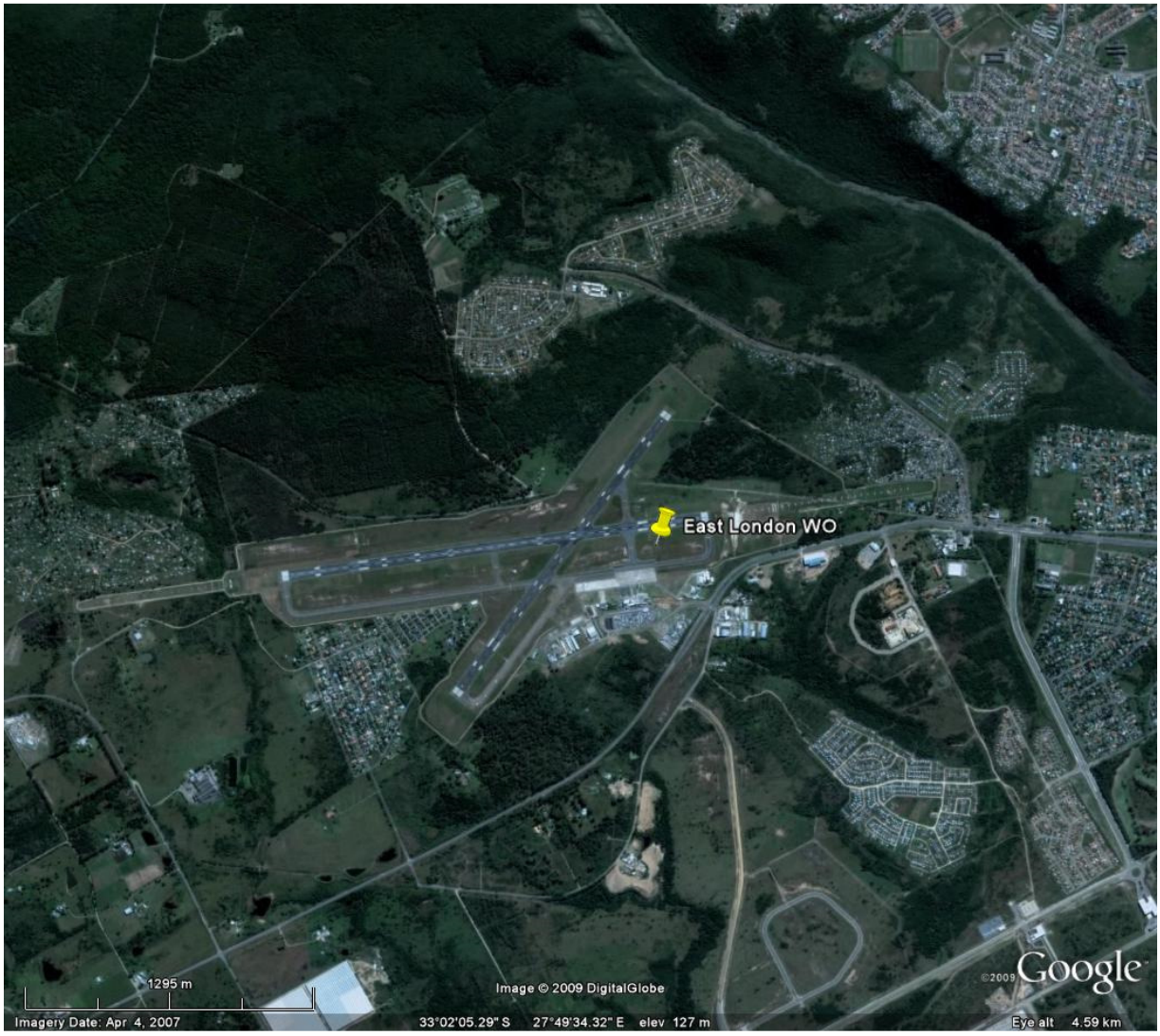

0061298 8 LANGEBAANWEG AWS 32°58'20.82"S, 18° 9'27.72"E

The AWS is situated at the Langebaan airport. The terrain surrounding the airport is flat. Hangars are situated 150 m to the north-west, and 200 m to the south-west. A small built-up area is situated about 300 m from the station. Small isolated buildings are located close to the station, on average about 30 m, while the main airport building is about 70 m away. The strong winds are south-easterly to north-north-westerly.

0063807 2 EXCELSIOR CERES 32°57'48.47"S, 19°25'50.36"E

The locality of the AWS is not ideal for wind measurements. Several buildings are positioned in the close proximity of the anemometer (to the east and north), within distances of about 50 m and heights between 4 m and 6 m, while to the south and south-east a plantation of apple trees (with heights of about 3 m) is present. To the west and north-west two rugged/rocky ridges (with heights of 150m and 300m) are present within a distance of between 300 m and 2 km of the AWS. The strong winds are south-easterly and south-westerly to north-westerly.

0078227A3 FORT BEAUFORT 32°47'17.20"S, 26°37'46.00"E

The AWS is situated about 1 km south of the town of Fort Beaufort. The terrain surrounding the station is quite flat. Some buildings are located at between 100 and 200 m from the AWS. The strong winds are from most directions, but especially westerly to north-westerly.

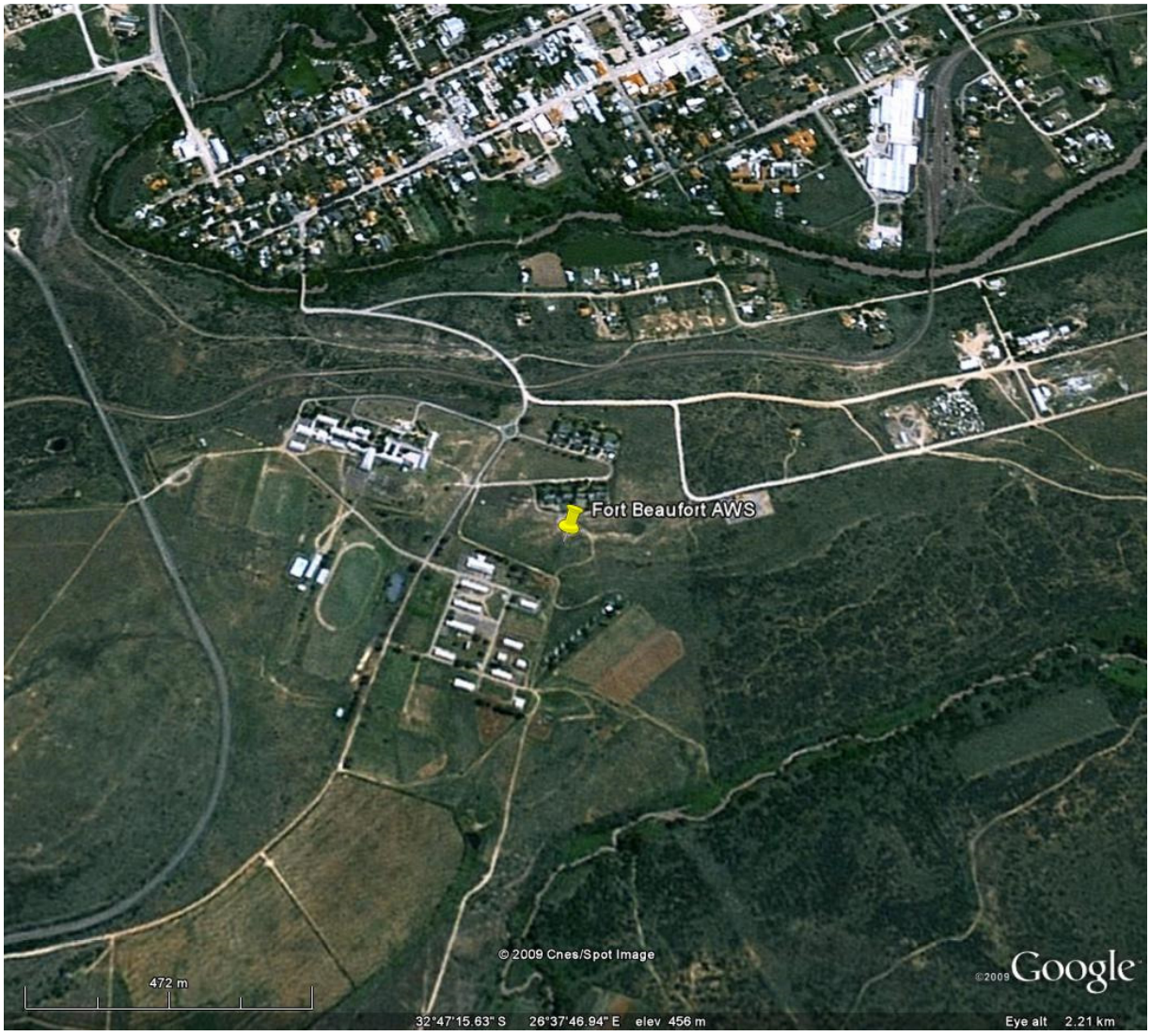

0083572 8 LAMBERTSBAAI NORTIER 32° 2'8.15"S, 18°19'52.77"E

There are some low buildings in the vicinity of the anemometer, the closest about 40 m, as the AWS is on the grounds of the offices of the Nortier agricultural research farm, about 4 km north-north east of the coastal town of Lamberts Bay. The surrounding terrain is flat, with sparse vegetation. The strong winds are north-easterly to easterly, and south-westerly to north-westerly.

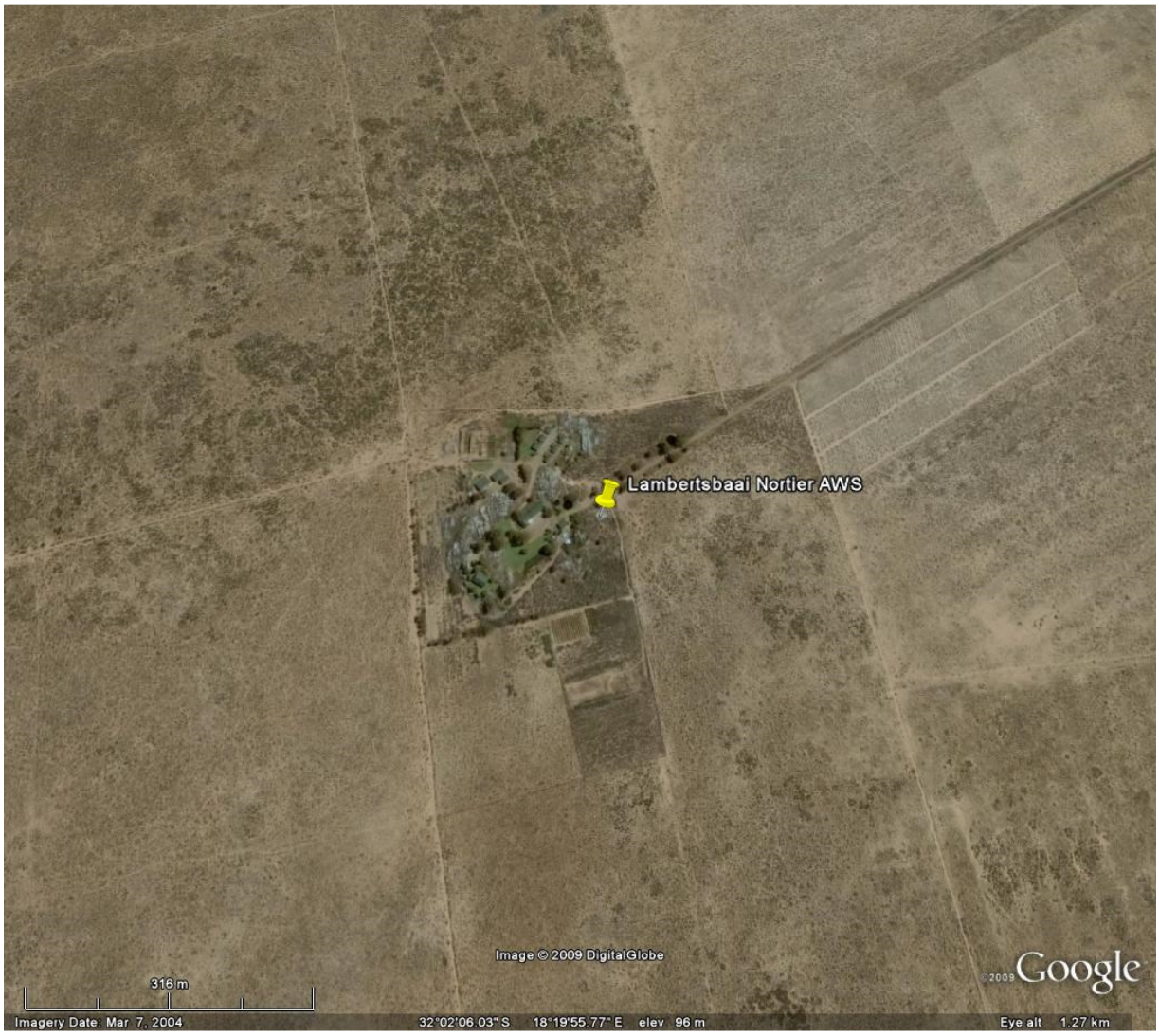

0092081 5 BEAUFORT-WES 32°20'51.32"S, 22°34'23.79"E

The location of the AWS in Beaufort West is not ideally suited for wind measurements due to the local topography, presence of prominent building structures within the immediate vicinity to the north, as well as the proximity of the suburban terrain. The station is located on top of a ridge (with an elevation of about 100 m above the surrounding ground level) and, therefore, will overestimate the measured wind speeds. On the other hand, presence of urban terrain between the azimuths of 70° and 225° will decelerate wind speeds at low elevations. A group of three large concrete tanks are located at a distance of about 50 m away from the AWS, to the south and south-east. The strong winds are from the west to north-west.

0096072 5 GRAAFF – REINET 32°11'33.92"S, 24°32'36.76"E

This AWS is well situated in a large valley with surrounding ridges with elevations between 500 m and 700 m, and distance of more than 5 km. From certain directions the site is surrounded by dense vegetation, consisting of 2 to 3 m trees. The town is located about 7 km to the south. Few building structures are situated in the vicinity of the anemometer, within a distance of about 30 m away and height of about 5 m - a 10 m wide building is situated in a south-south-westerly direction, and some buildings in a north-easterly direction. The strong winds are from most directions, but mainly north-westerly.

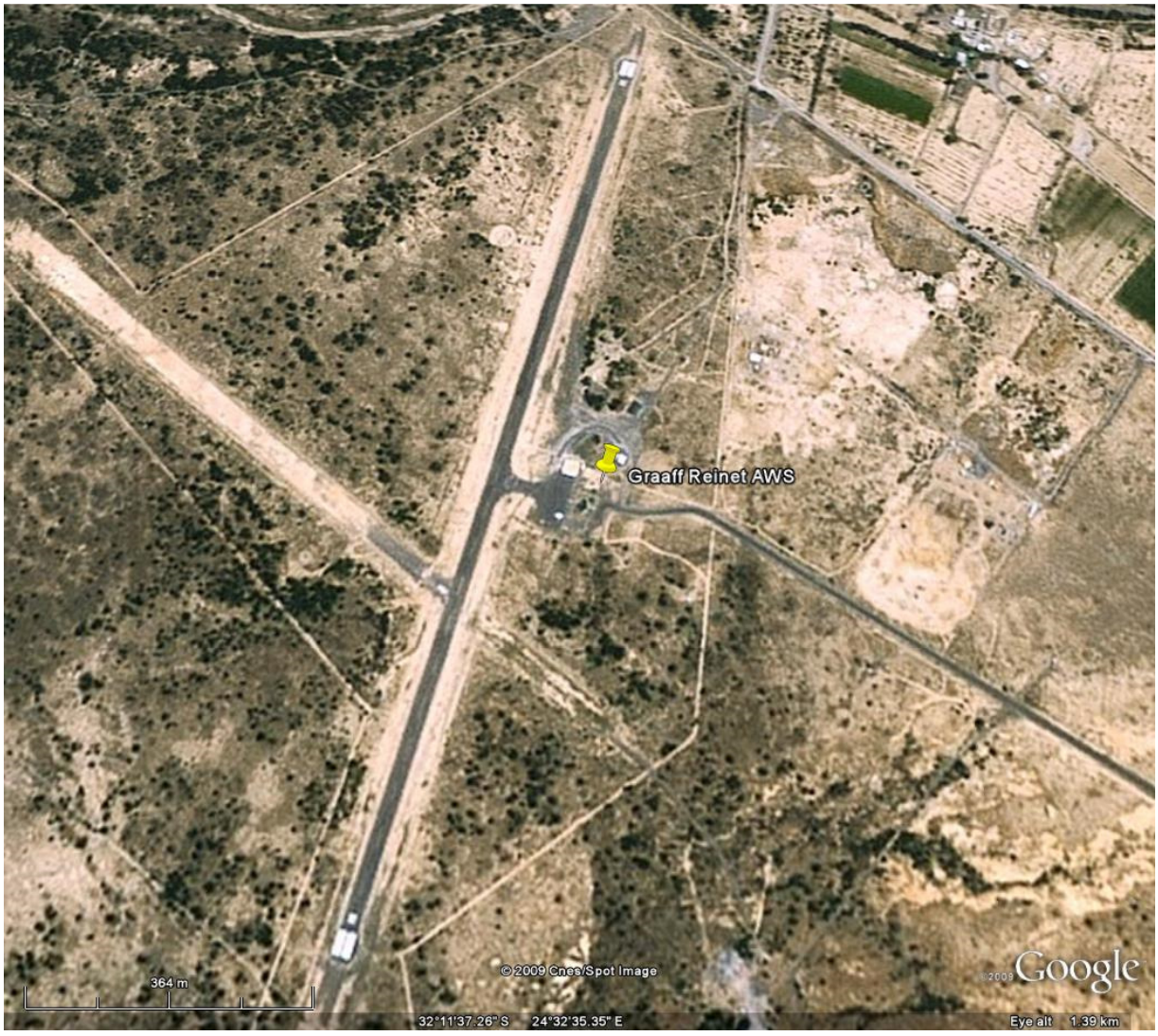

0123685 X QUEENSTOWN 31°55'4.36"S, 26°52'41.41"E

The AWS is located at the Queenstown airstrip. The few buildings at the airstrip, such as the hangar, are situated about 30 m to the north-west to north-east. There is a residential area just to the north of the airport buildings, while other residential areas are scattered around the airstrip, with a closest distance about 650 m to the south-west. The terrain is flat. Due to these built-up areas the exposure seems to be only fair. The strong winds are mainly south-westerly to north-westerly, but with some strong winds from the east as well.

0127272A4 UMTATA WO

The AWS is situated at the K D Matanzima Airport, about 10 km north-west of the city of Umtata. The airport buildings are situated about 70 m to the west, and can therefore have some influence on the wind measurements. The terrain surrounding the airport is flat. Apart from the close vicinity to the airport buildings, the exposure of the AWS can be considered to be good. Strong winds are from most directions, but mainly south-westerly.

0134479A3 CALVINIA WO 31° 28’ 55.26” S, 19° 45’ 41.97” E

This weather office has a fairly good locality surrounded by open terrain. The town is located about 1,5 km to the north and north-east of the AWS. A relatively large building (25 m long and 4 m high), housing the Weather Service office, is positioned about 30 m to the south of the anemometer. Several mountains are present between north-west and north-east azimuths. Their heights vary between 300m and 650m and the distance between 3km and 8km away from the station. The strong winds are westerly to north-westerly.

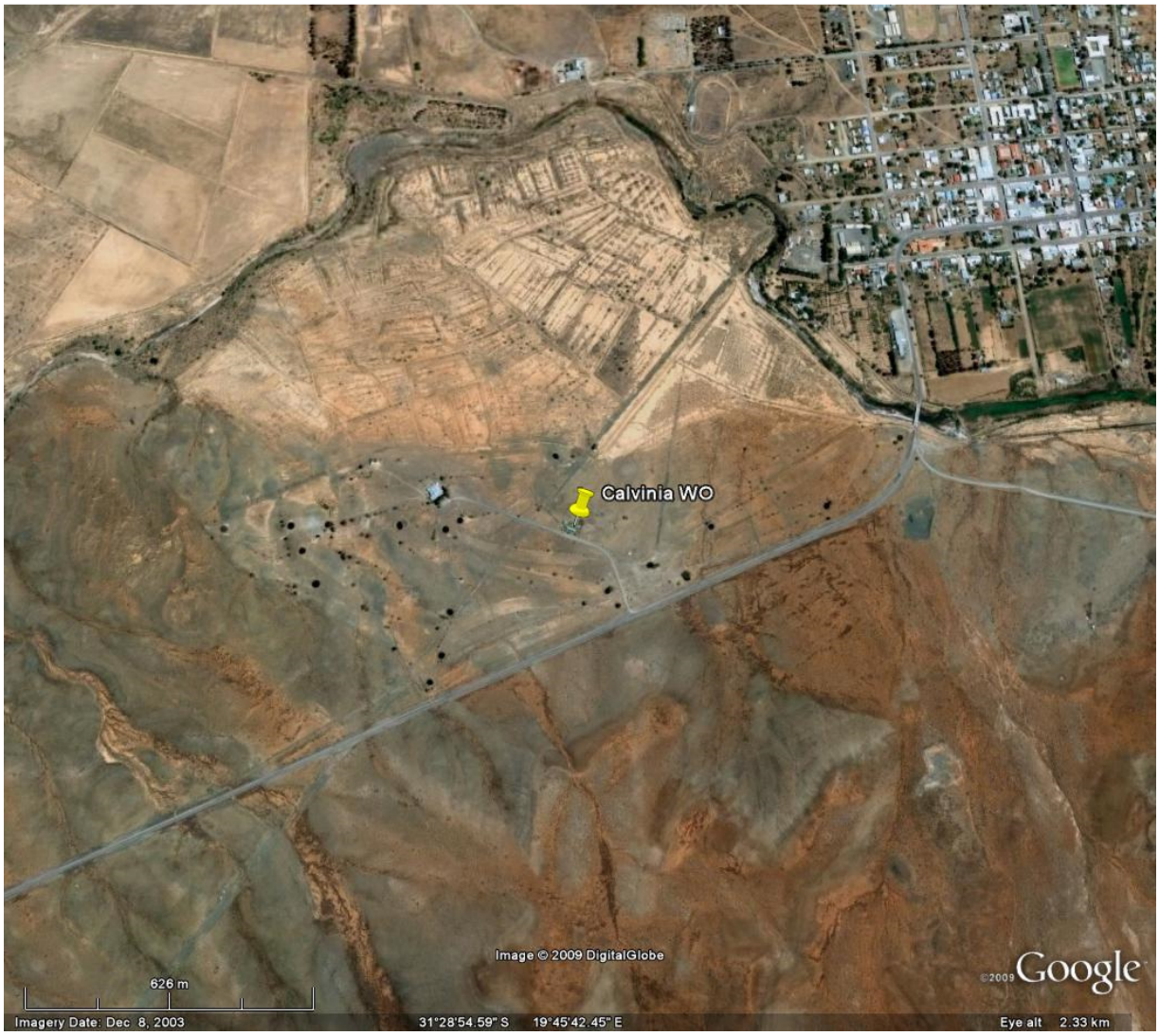

0144791 2 NOUPOORT 31°11'11.00"S, 24°57'40.00"E

The AWS is located at a distance of approximately 1 km to the east of the small town of Noupoort. Two significant mountains are located at distances of 3 km to the east and 4 km to the south, both with an elevation of about 250 m above the terrain. Two buildings (one of them prominent) are situated 15 and 50 meters away from the AWS, in a south-westerly direction. The strong winds are possible from any direction.

0148517A9 JAMESTOWN 31° 7'15.41"S, 26°48'35.49"E

The AWS is located in the west of the small town of Jamestown. The closest low-rise building is about 25 m to the north, with others about 40 m to the west and north-east. The town in the western sector might have a small influence on the wind speed. The terrain is quite flat, apart for some ridges, from about 350 m to the east, which are up to 60 m high. Due to the buildings close by, the exposure is fair to poor. The strong winds are westerly to north-westerly, but also south-easterly in a few cases.

0150620AX ELLIOT

The AWS is situated 150 m south-west of the small town of Elliot, which has an approximate size of one square kilometer. The terrain is flat, and there are no significant structures in the close vicinity to the station. The strong winds are south-westerly to north-westerly.

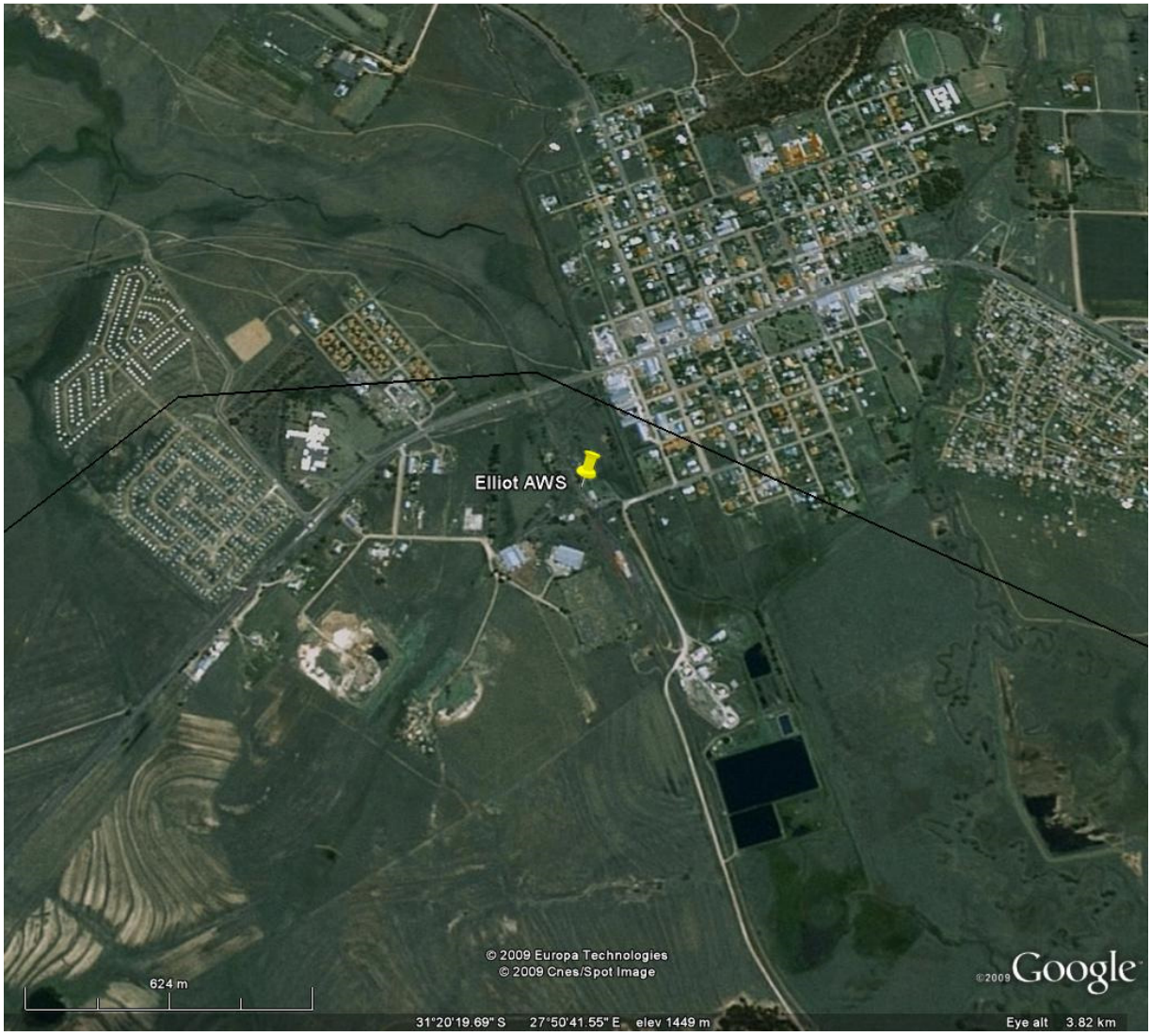

0155394A5 PORT EDWARD 31° 3'28.60"S, 30°13'40.46"E

The AWS is located very close to the coastline. The closest buildings are isolated and from about about 60 m to the west. The terrain is flat. and the exposure is good. The strong winds are south-westerly to westerly.

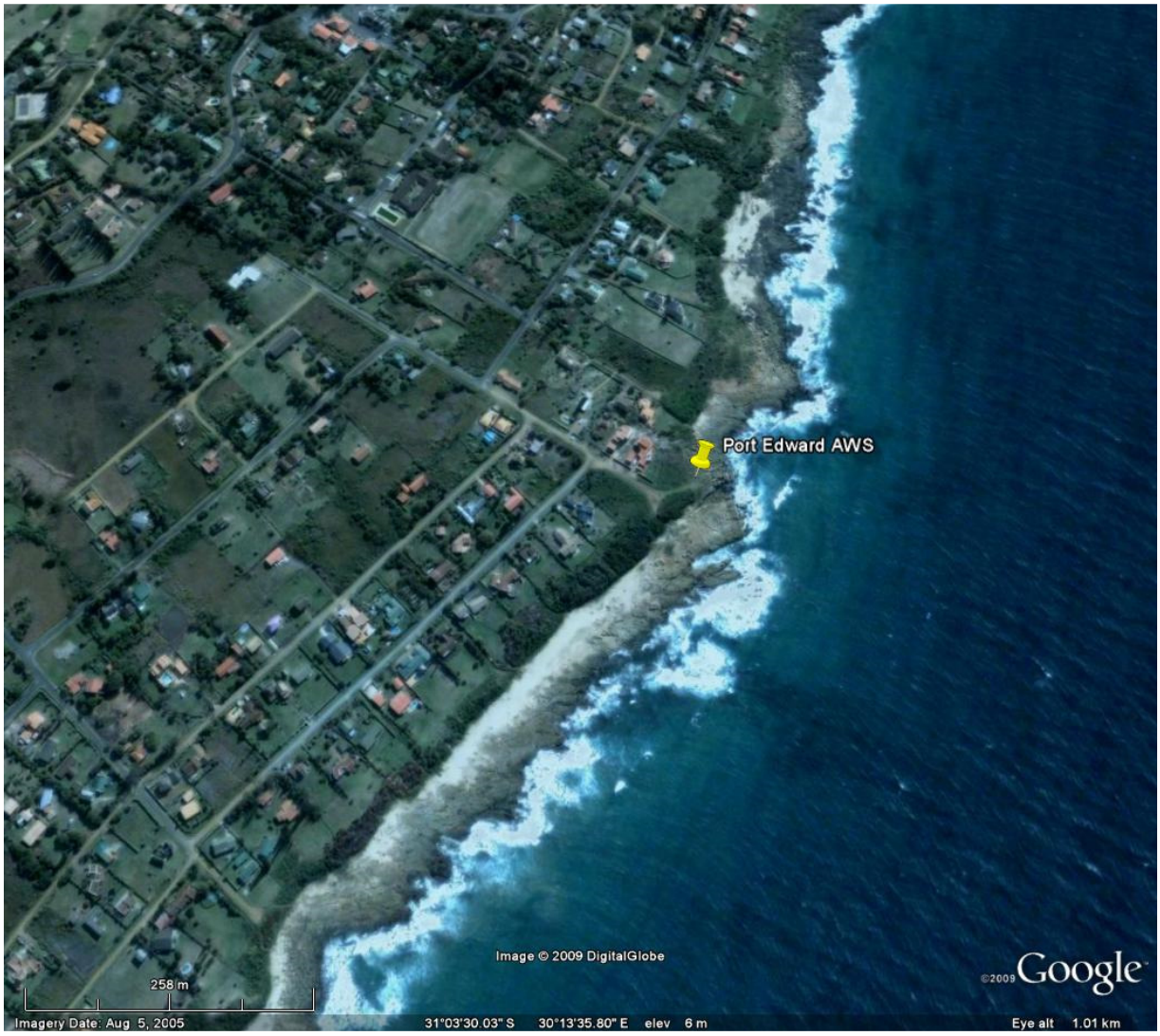

0169880 1 DE AAR WO 30°39'54.20"S, 23°59'33.40"E

The weather office is located on a hill approximately 30 m high at the north-west outskirts of the town. Because of its elevation the wind measurements will be overestimated. The weather office building, with a height of about 8 m is positioned at a distance of about 20 m towards the north of the station. For other wind azimuths the hill is surrounded by open terrain. The strong winds are south-westerly to north-westerly.

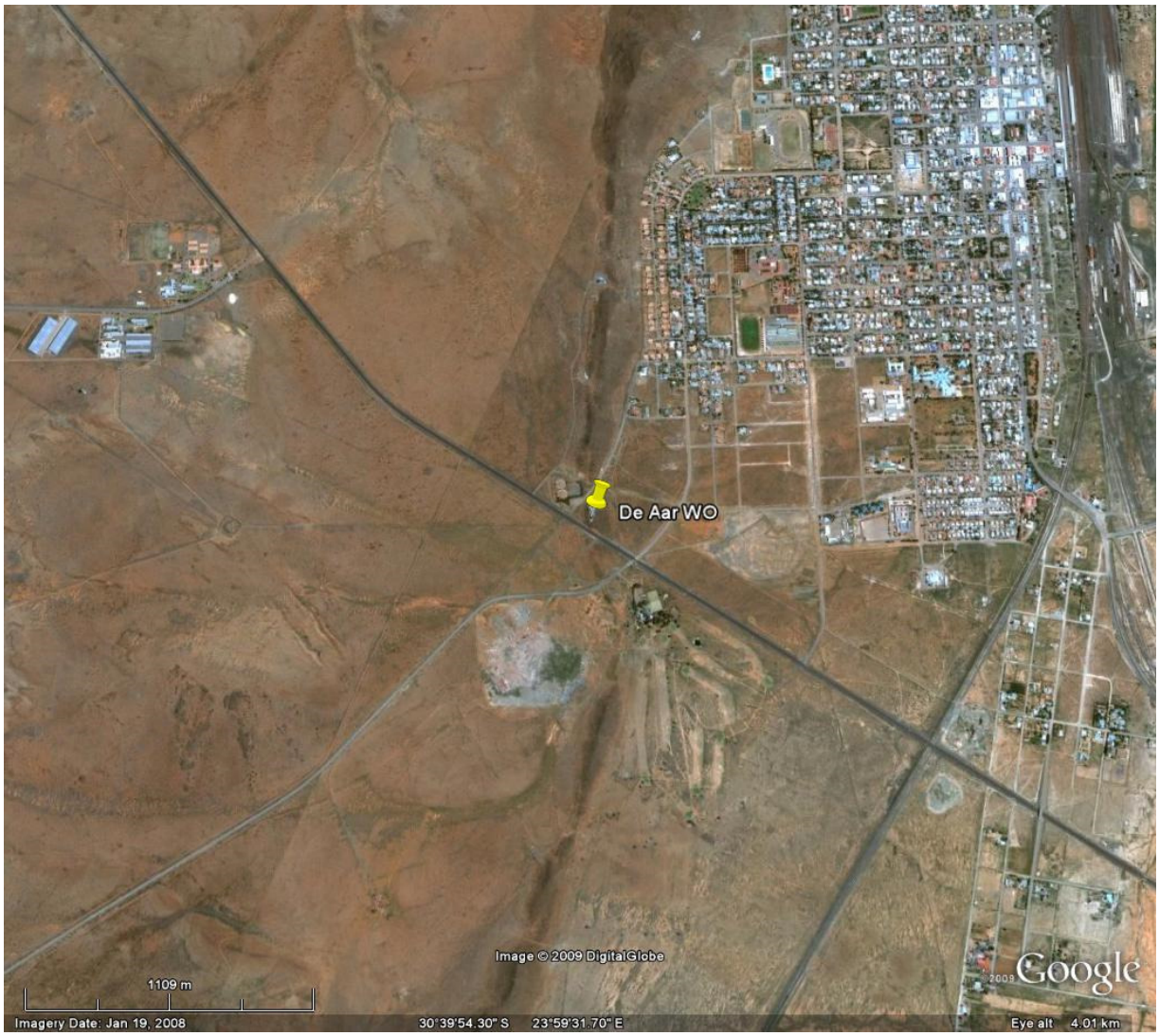


De Aar WO
Image © 2009 DigitalGlobe
84 m
Imagery Date: Jan 19, 2008
30°39'54.27" S 23°59'33.49" E
Eye alt 317 m
Google

0182465 7 PADDOCK 30°45'16.10"S, 30°15'29.54"E

The AWS is located in the small railway siding/village of Paddock, the closest house being about 50 m away from the site to the east, but with most buildings located about 350 m to the west-south-west. There is a river valley to the south at a distance of about 600 m, which is 50 m below station level. Sugarcane fields surround the area around the AWS but do not obstruct the wind flow. The strong winds are southerly to south-westerly.

0182591A4 MARGATE 30°53'36.38"S, 30°19'30.72"E

The AWS is located west of the coastal town of Margate, at the airport. From photographs it is apparent that there are no buildings close to the anemometer in the prevailing wind directions. Although the terrain is quite hilly the area surrounding the airport is flat. Winds from the east can be significantly influenced by the proximity of the town. Strong winds are south-westerly.

0184491 4 KOINGNAAS 30°11'43.74"S, 17°17'24.50"E

The AWS is situated at the small mining village of Koingnaas about 5 km east of the West Coast. All the buildings in the vicinity of the AWS is mostly residential, the closest being about 100 m away. The terrain is flat, with sparse vegetation. Strong winds are north-easterly to southerly, as well as westerly to north-westerly.

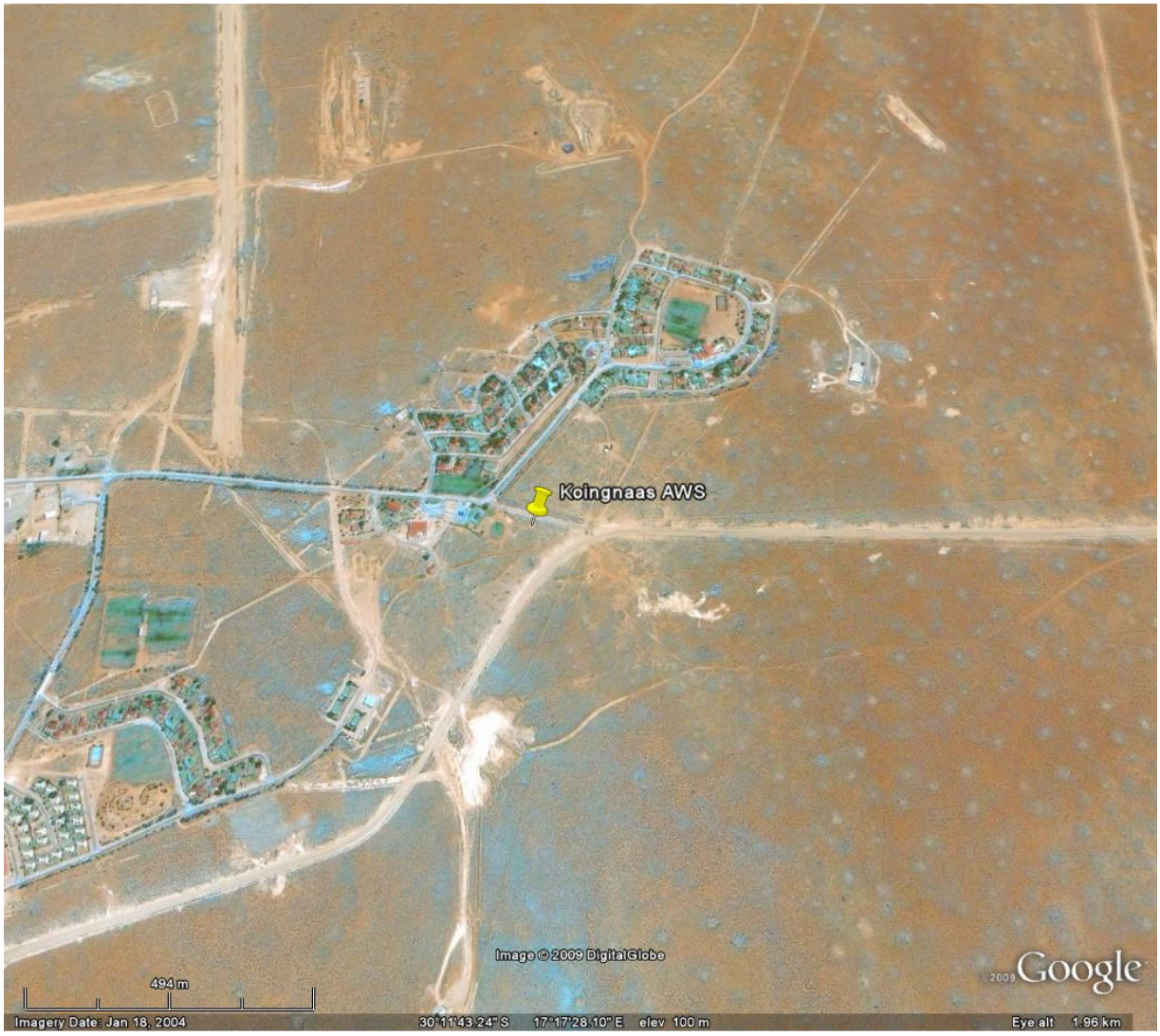

0190868 1 BRANDVLEI 30°27'53.21"S, 20°28'42.76"E

The AWS at Brandvlei is well positioned in a flat terrain with a large salt-pan to its south-west. To the east, a 2 km long fetch terrain of sparsely spaced one storey buildings is present. A 3 m high building is located about 20 m to the west of the meter, but its influence on the recorded wind speeds will likely be small. The strong winds are mainly westerly to north-westerly, but also possible from other directions.

0214700B2 SPRINGBOK WO 29°40'10.17"S, 17°52'45.38"E

The AWS is at the Springbok Weather Office on the outskirts of town. The terrain is quite hilly, with a drop of about 70 m over a distance of 300 m to the east into a sort of valley, and a steep hill of about 150 m, over a distance of 1 km to the north-west. The anemometer is quite close to the weather office building, which can have an influence on wind measurements. The main built-up area is about 300 m to the north-east, and stretches over a distance of about 1 km. This site is not ideal for wind measurements. The strong winds are westerly to easterly in a clockwise direction.

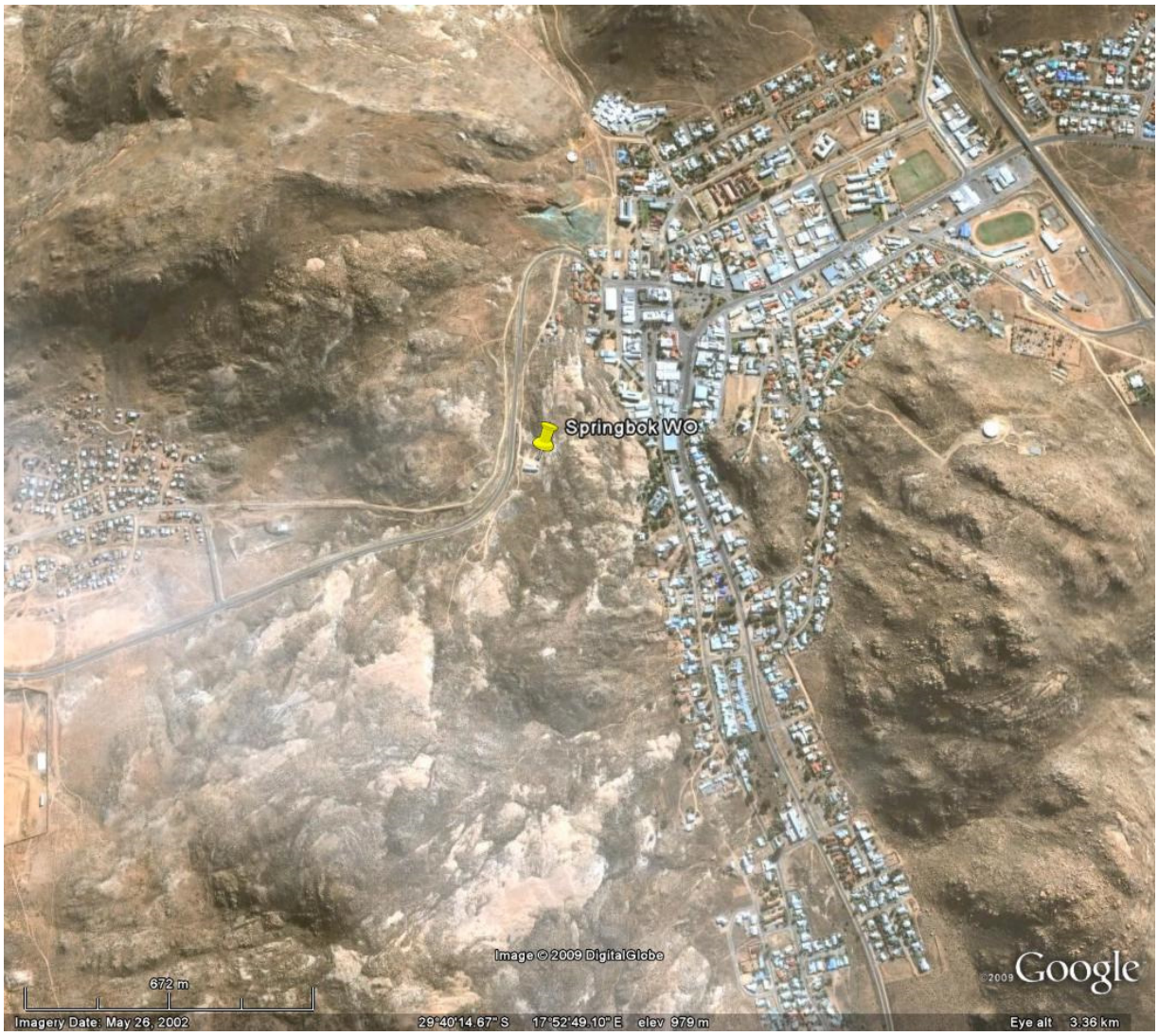

0224400 8 PRIESKA 29°40'21.10"S, 22°44'8.57"E

The AWS is located at the water works, on the outskirts of the small mining town of Prieska. The closest residential areas are about 500 m away to the north-west and east, but are low-rise and widely spaced. Some buildings are in the immediate vicinity, the closest being about 60 m away to the south-east. The terrain is flat. The strong winds are south-westerly to north-westerly.

0239698 5 PIETERMARITZBURG 29°37'39.83"S, 30°24'12.24"E

The AWS is located on the grounds of the Agriculture Department of the University of KwaZulu-Natal, in the city of Pietermaritzburg. The terrain is quite flat around the weather station. According to photographs of the immediate vicinity there are no significantly high buildings close to the anemometer. However, being in a city the weather station is surrounded by built-up areas which will significantly influence wind speed measurements. Therefore the position of the anemometer is not ideal for wind measurements. Strong winds are mainly south-westerly to north-westerly, but also north-easterly to easterly.

0239699 7 ORIBI AIRPORT 29°38'52.41"S, 30°24'0.92"E

The AWS lies about 2,5 km to the south of the Pietermaritzburg AWS. The closest buildings are about 600 m away as it lies close to the runway of the Oribi Airport. This weather station has a much better exposure than the Pietermaritzburg AWS. The exposure is good, apart from the surrounding built up areas. Strong winds are mainly south-westerly to north-westerly, but also easterly to south-easterly.

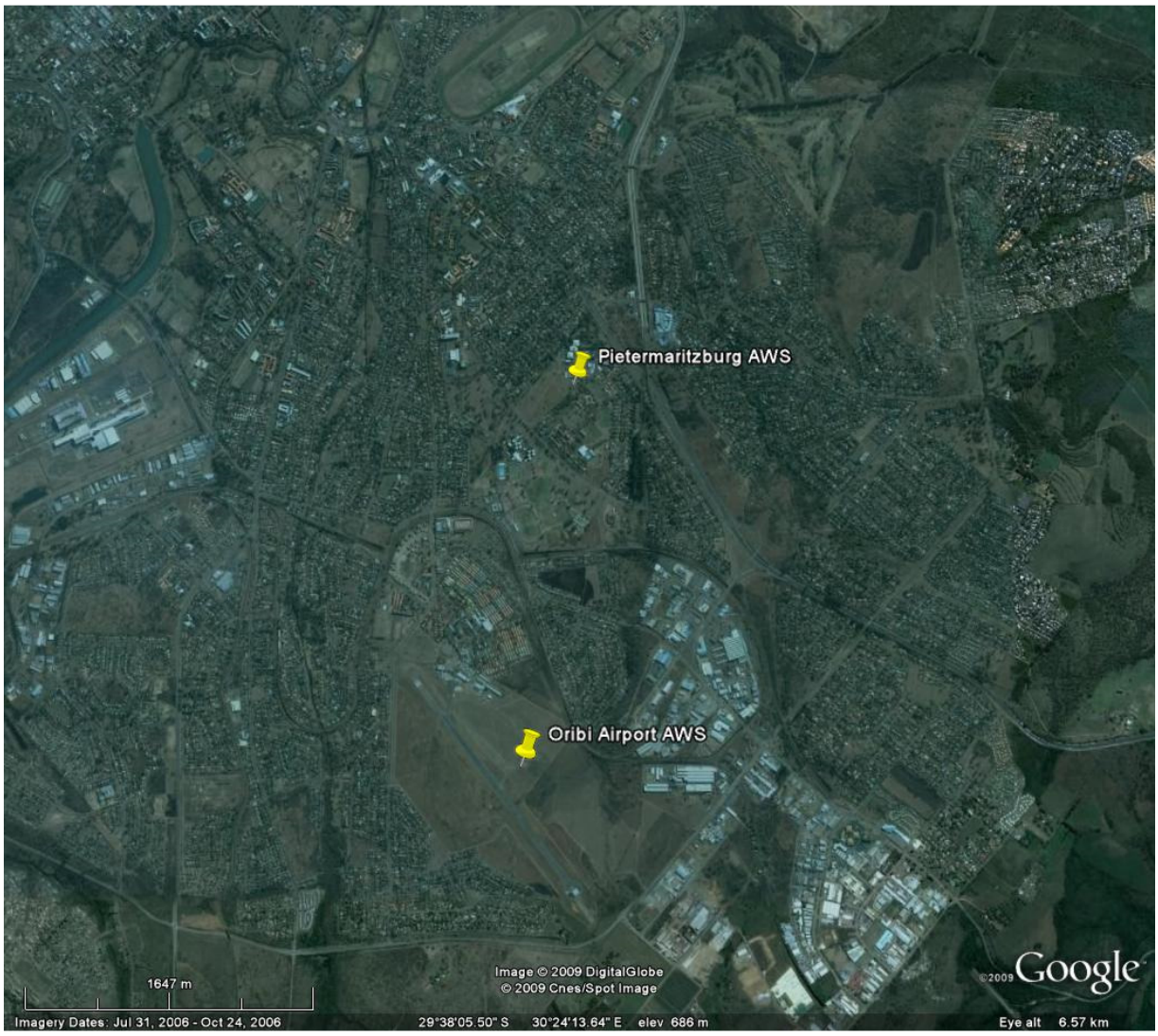

0240808A2 DURBAN WO 29°57'50.92"S, 30°57'21.70"E

The AWS is located at Durban International Airport. The terrain is flat and the closest buildings are those of the airport, of which the closest are about 500 m away. The areas surrounding the airport are mainly urbanized. The strongest winds are from the south to south-west, which is clear from buildings for about 3 km.

0241072 9 MOUNT EDGECOMBE 29°42'24.49"S, 31° 2'45.24"E

The weather station is surrounded by buildings and/or trees and tall shrubs. It is difficult to have even a vague idea of the effect of the vegetation and buildings in the vicinity of the anemometer. The exposure of the AWS seems to be poor. Strong winds are north-easterly, and south-easterly to south-westerly.

0241076 6 VIRGINIA 29°46'31.79"S, 31° 3'20.44"E

The AWS is located next to the coastline at the Viginia Airport in the north of the city of Durban. From photographs it seems that there are no significantly high buildings close by. The terrain is flat but there are some shrubs of about 3 m high in the vicinity of the anemometer. The exposure seems to be good in the direction of strong winds, i.e. south-westerly and north-easterly.

0261307A4 BLOEMFONTEIN STAD 29° 7'13.80"S, 26°11'14.92"E

The AWS is located next to sports fields in the city centre. The open field where the weather station is located is surrounded by mostly residential developments, the closest being about 40 m to the north. There are no obstructions close to the anemometer. However, the surrounding developments may significantly reduce wind speeds. The strong winds are possible from almost any wind direction.

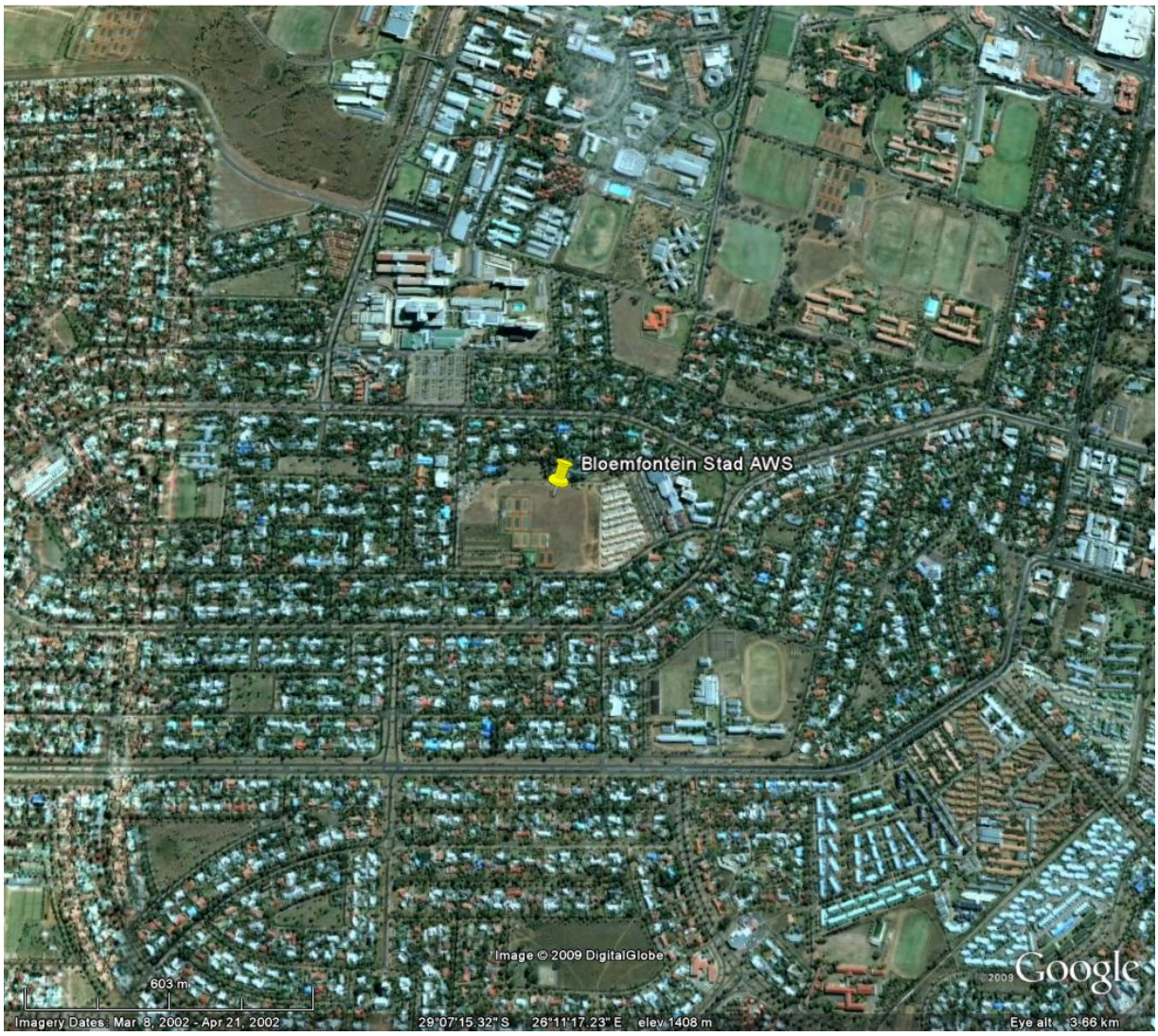

0261516B0 BLOEMFONTEIN WO 29° 6'14.37"S, 26°17'52.89"E

The AWS is located a short distance from the weather office close to the runway of Bloemfontein Airport on the outskirts of the city. The terrain is flat and there are no nearby obstacles, apart from the weather office building about 40 m away to the west, which can influence the wind measurements significantly. The strong winds are mainly north-westerly, but possible from any direction.

0268016AX GIANTS CASTLE 29°16'12.06"S, 29°31'11.99"E

This AWS is situated in a valley in the Drakensberg mountain range. To the west the slope is about 60 m high over a distance of 250 m to the bottom of the valley. To the east the hills are about 120 m high at a distance of about 400 m. The station is surrounded by trees and buildings, which will also influence the wind measurements. The strong winds are mainly south-westerly to north-westerly, but possible from any direction except south-easterly.

0270155 9 GREYTOWN 29°04'59.53"S, 30°36'11.99"E

The AWS is located close to some buildings to the west, but it is clear to the east. Although the region is quite hilly the terrain around the weather station is flat. A residential development is situated at about 500 m to the north and north-east, while the proper town is about 1,5 km away to the north-west. The buildings close to the anemometer will significantly influence winds from the south-west to the north-west, which are the main wind directions for strong winds.

0274034A4 ALEXANDERBAAI 28°34'13.51"S, 16°31'41.69"E

The AWS is situated at the Alexander Bay airstrip. Two small low-rise isolated buildings are situated close to the anemometer, 20 to 30 m to the east and west. These buildings might have a small impact on the wind readings. The terrain is flat. The strong winds are from all directions except from the north-east to east.

0290468A9 KIMBERLEY WO 28°48'3.05"S, 24°46'1.49"E

The AWS is situated close to the crossing of two runways at the airport of the city of Kimberley. The main built-up area commences about 3 km to the north. The airport buildings and a close-by military base is about 1 km to the north-east, which might have a small influence on the wind measurements. The terrain is flat. The strong winds are almost always south-westerly to north-westerly.

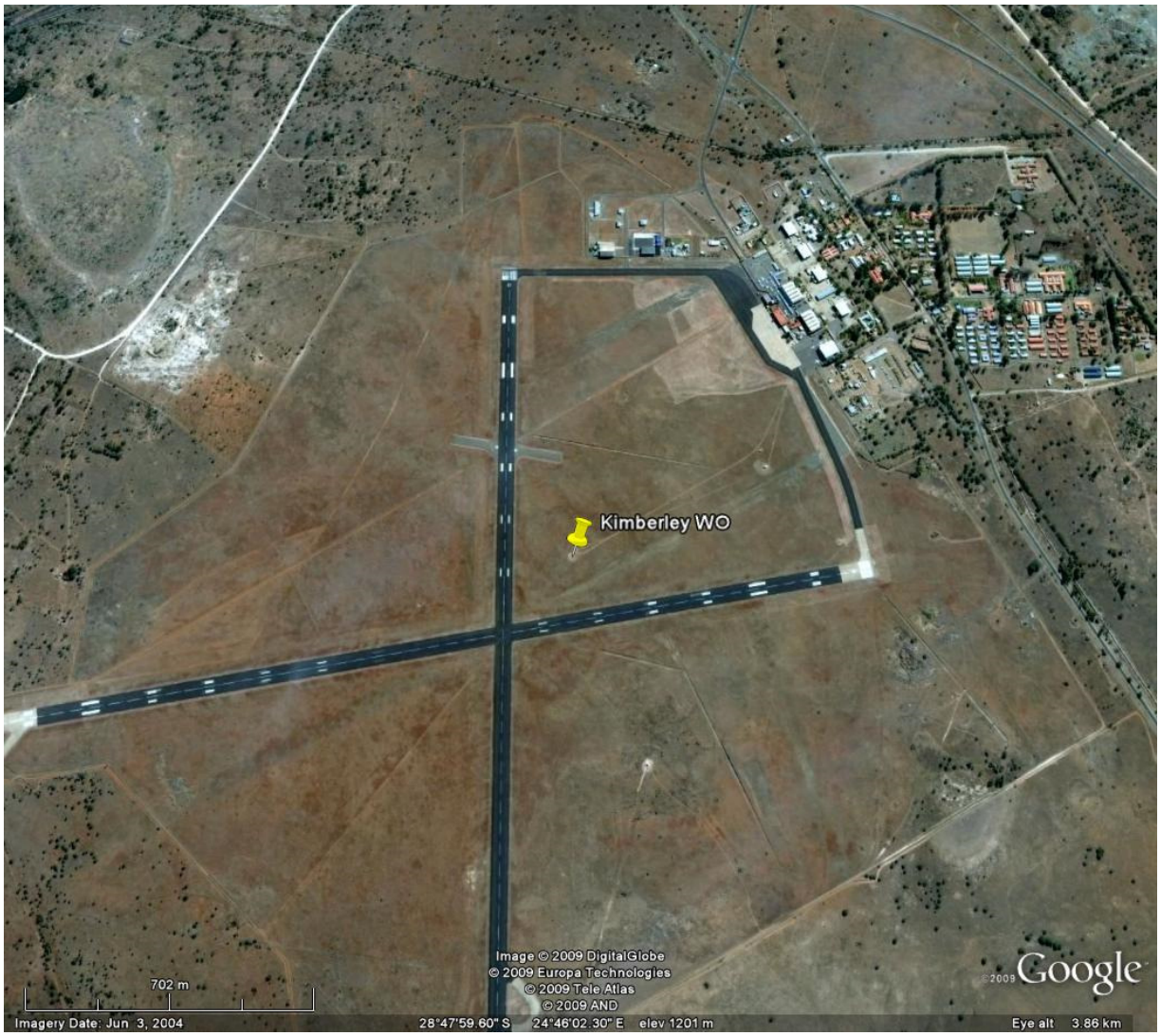
Kimberley WO
Image © 2009 DigitalGlobe
© 2009 Europa Technologies
© 2009 Tele Atlas
© 2009 AND
©2009 Google
702 m
Imagery Date: Jun 3, 2004
28°47'59.60" S 24°46'02.30" E elev 1201 m
Eye alt 3.86 km

0300454 3 LADYSMITH 28°34'29.20"S, 29°45'1.85"E

The exact position of the AWS could not be located, but it is situated at the Ladysmith airport, about 2 km to the west of the town. In some directions there are of the airport buildings which will influence the wind measurements. The terrain is flat, but the location of the anemometer is not ideal for wind measurements. The strong winds are south-westerly to north-westerly.

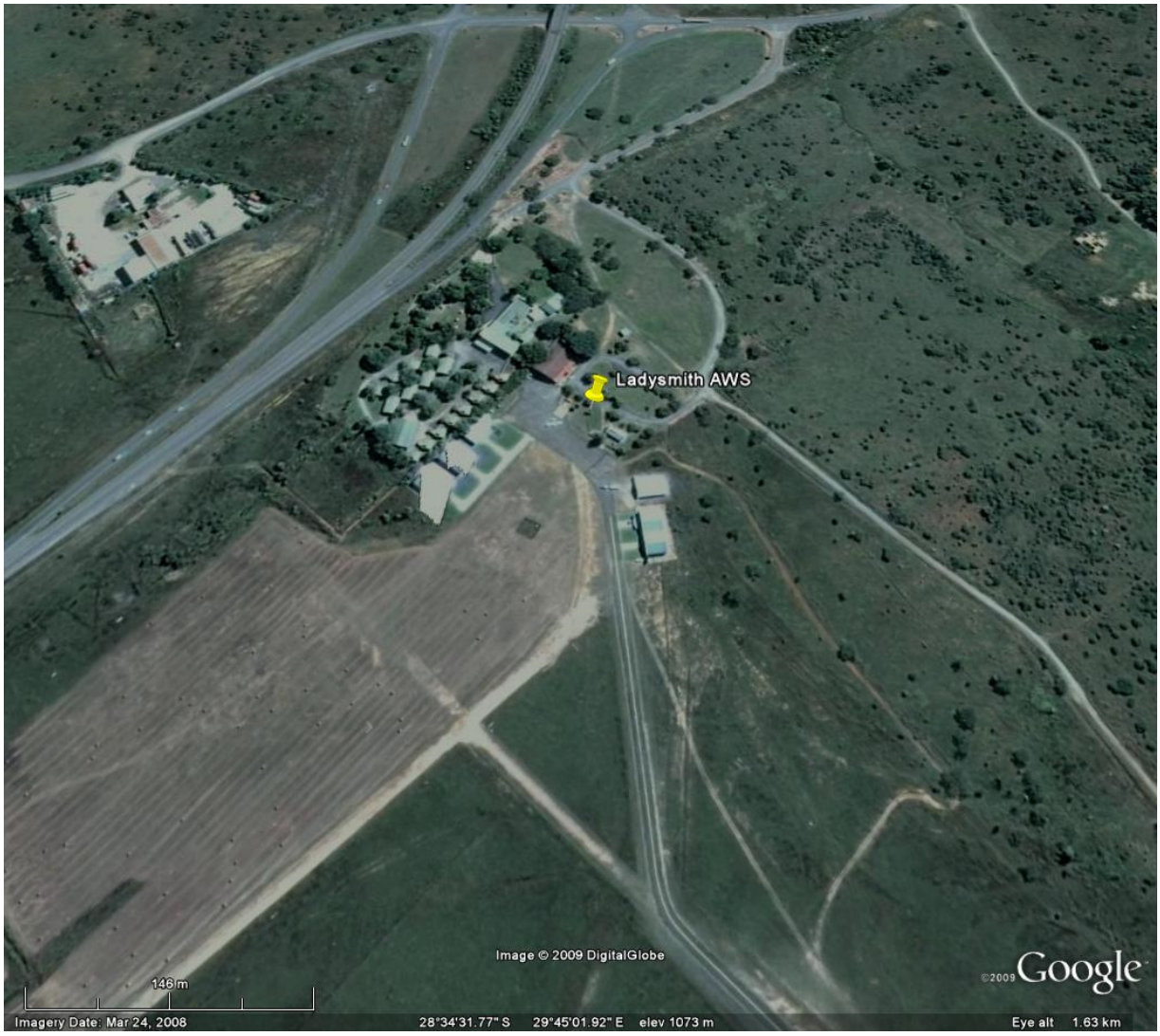

0304357 6 MTUNZINI 28°56'50.40"S, 31°42'28.39"E

The AWS is located on a sugarcane farm. There are some low-rise buildings and shrubs to the north-west, north, east and south-east of the anemometer, but these are about 2 m high at the most and will therefore not affect the wind measurements significantly. The terrain is quite flat. The exposure is therefore adequate, but possibly not ideal. The strong winds are mainly south-westerly, but also possible from other directions.

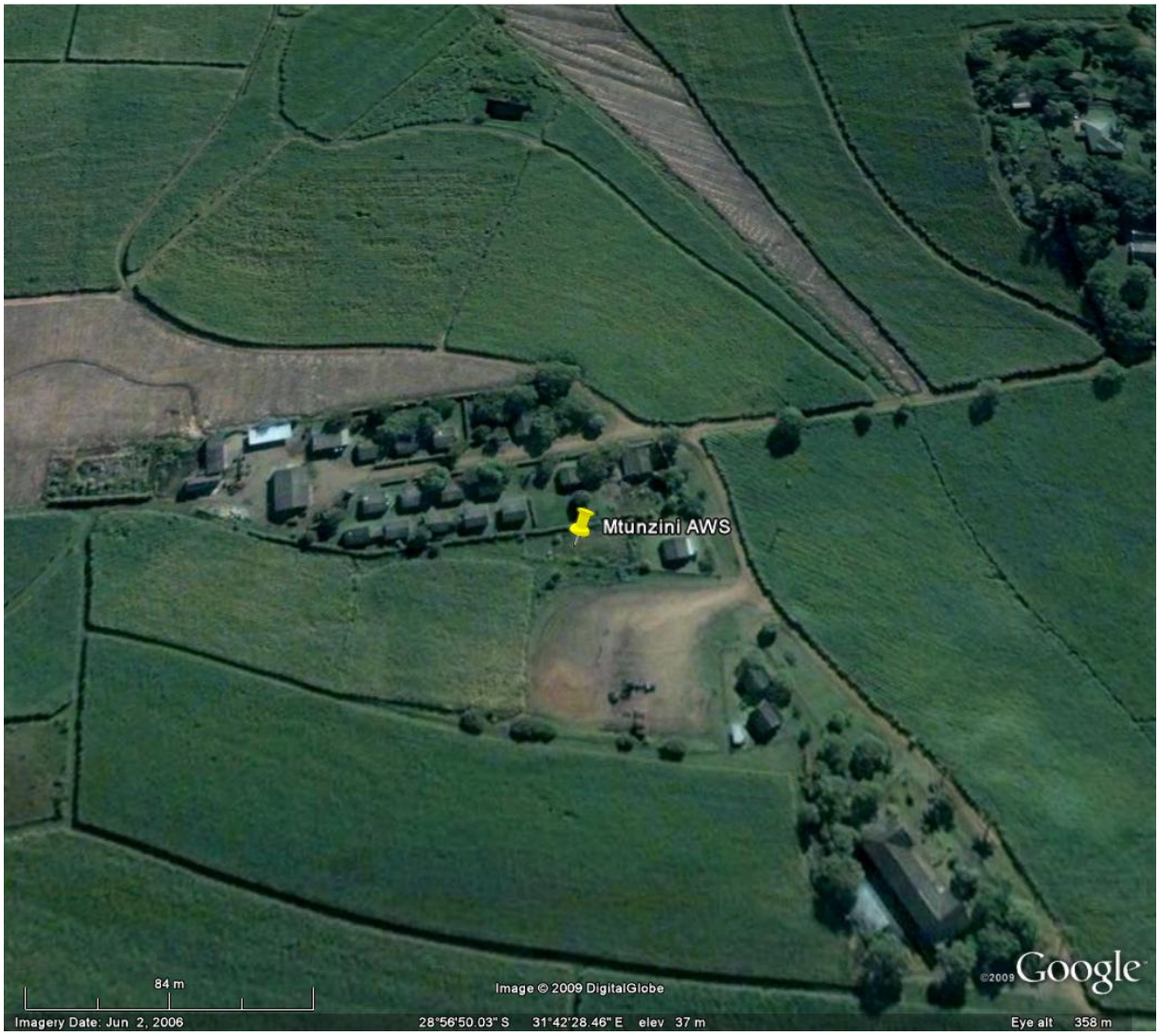

0317475A8 UPINGTON WO 28°24'26.12"S, 21°15'24.55"E

The AWS is located about 150 m north-east of the buildings of the airport, 3 km north of the town of Upington. The terrain is flat, and exposure very good. The strong winds are mainly south-westerly to north-westerly, but also possible form other directions.


Upington WO
Image © 2009 DigitalGlobe
© 2009 Google
79 m
Imagery Date: May 21, 2004
28°24'32.71" S
21°15'24.69" E
elev 836 m
Eye alt 1.14 km

0321110 7 POSTMASBURG 28°20'25.65"S, 23° 3'42.35"E

The AWS is at the sports grounds of the small town of Postmasburg, which is located about 350 m to the north. The buildings of the sports grounds are also about 100 m to the north. Except for this the terrain is flat and the location good. The strong winds are almost always south-westerly to north-westerly.

0331585 9 BETHLEHEM WO 28°14'56.66"S, 28°20'1.39"E

The AWS is situated about 20 m north of the weather office and other airport buildings, which are quite low but might have a significant impact on the wind readings. No significant obstructions exist towards the other directions. The terrain is flat, but there are extensive residential areas, at distance of about 1 km from the AWS, in the westerly and northerly directions. The strong winds are possible from any directions.

0333682A9 VAN REENEN 28°22'42.60"S, 29°23'10.00"E

The AWS is located close to the N3 highway between Gauteng and Durban. There are a few building in the vicinity of the anemometer, but these are all low-rise. However, the buildings to the west of the anemometer might have a small impact on the wind measurements. The terrain around the anemometer is quite flat, but in general the topography in this region (the escarpment) is complex. For example, towards the south the elevation falls more than 100 m over a distance of about 500 m. However, it will always be difficult here to find an ideal spot for wind measurements. The strong winds are almost always south-westerly to north-westerly.

0337738 2 ULUNDI 28°18'45.94"S, 31°25'14.22"E

The AWS is located close to the runway of the Ulundi airport. The terrain is quite flat. No obstructions close to the anemometer is evident. Around the airport there are extensive developments, but these buildings are as a rule quite small, low-rise and widely spaced and therefore will not affect the wind measurements significantly. The strong winds are southerly to north-westerly.

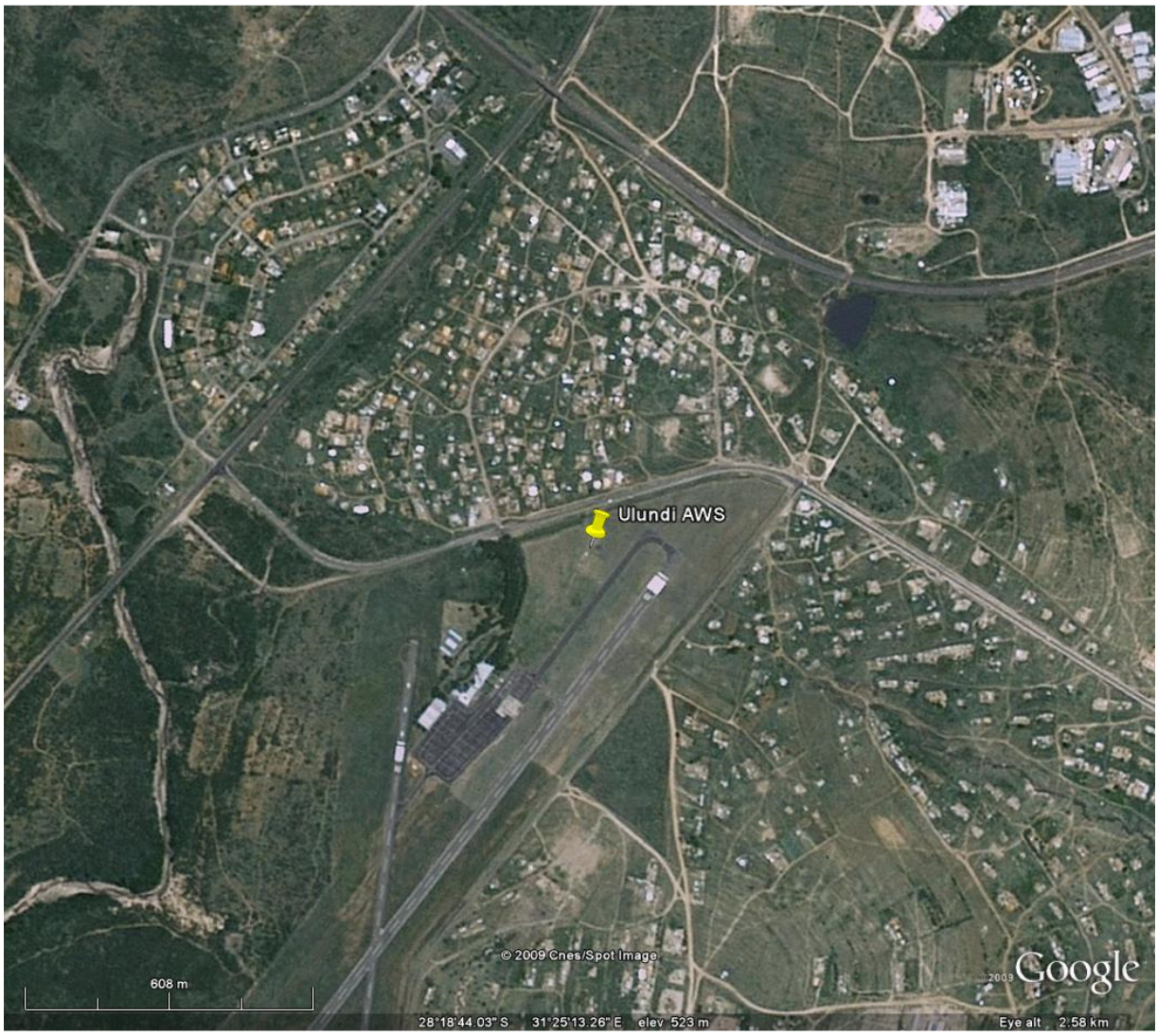

0339732A9 CHARTERS CREEK 28°11'52.00"S, 32°24'50.80"E

The AWS is situated at about 250 m west of the St. Lucia Lake. In other directions the station is surrounded by coastal bush, at distances of 100 m or further. Especially from the southerly through to the north-westerly directions, the dense vegetation will definitely have some influence on the wind readings. The strong winds are possible from any directions.

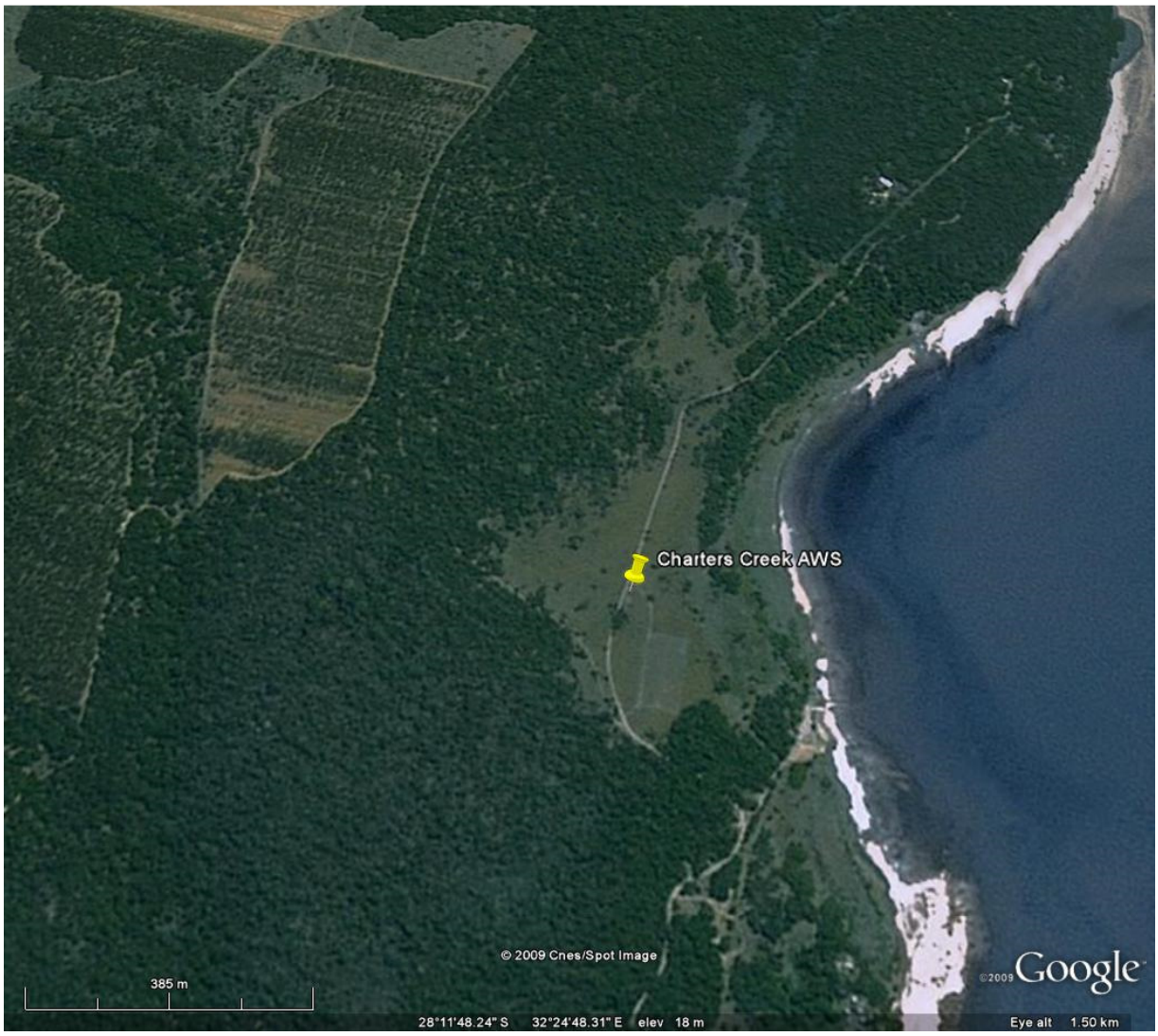

0356880 4 KATHU 27°40'14.57"S, 23° 0'21.94"E

The AWS is located about 4 km to the north-west of the small mining town of Kathu. The closest buildings are those of the abattoir, which are 200 m away. A new residential development is located about 2 km to the south-west. The terrain is quite flat. The strong winds are possible from any directions.

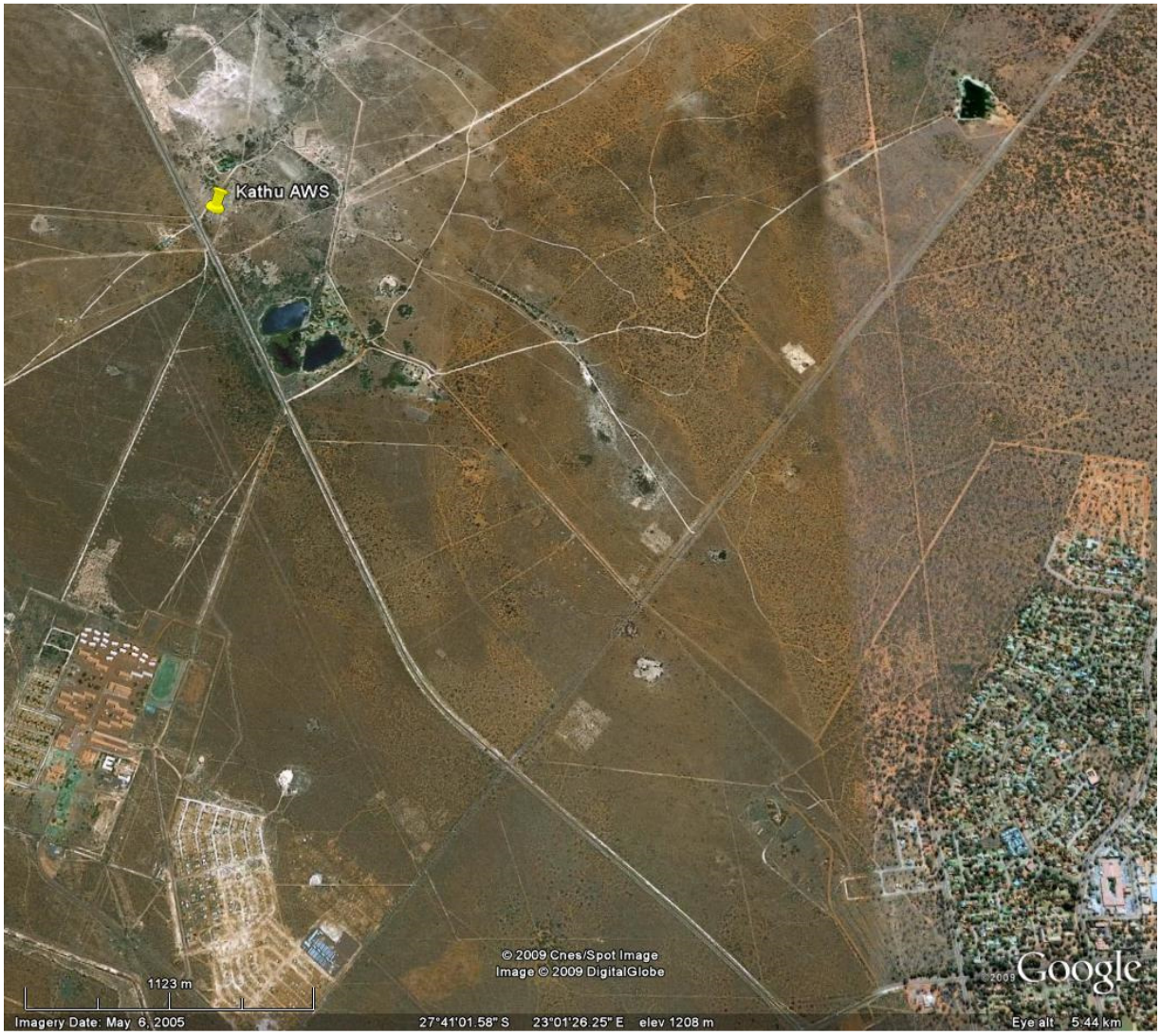

0360453A0 TAUNG 27°32'45.01"S, 24°46'9.44"E

The exact location of the AWS could not be determined, but it is on the grounds of an agricultural college, about 1 km southwest of the town of Taung. According to available photographs the closest building in the vicinity of the anemometer is about 150 m away. The terrain is flat. The strong winds are almost always south-westerly to north-westerly, but also possible from other directions.

0362189 7 BLOEMHOF 27°39'04"S, 25°37'19"E

The AWS is located about 700 m north-west of the Bloemhof Dam. The town of Bloemhof, which consists mostly of widely spaced, low-rise buildings, is about 700 m north-west of the AWS, and is developed in more or less a square with sides of about 1,5 km in length. Some isolated buildings are located about 30 m to the east. The AWS is considered to be well situated. The strong winds are almost always north-westerly, but also possible from other directions.

0364300 1 WELKOM 27°59'40.7"S, 26°39'57.2"E

The climate station is located at the Welkom Airport. Some hangars and other airport buildings are located 120 to 130 m to the south-west and south of the AWS, but will not have a significant influence on the anemometer readings. The exposure can be rated as very good, but bare soil around the airport, especially during wintertime, might influence the wind measurements significantly. The strong winds are mainly westerly to north-westerly, but possible from most directions.

0370856 3 NEWCASTLE 27°46'7.57"S, 29°58'44.18"E

The exact location of the AWS could not be established. However, it is next to the airstrip of the town of Newcastle. There is no buildings close to the anemometer, the closest being about 300 m away to the east. The closest development is about 1 km to the south, but it is quite small and will not affect the wind measurements significantly. The exposure of this weather station is very good. The strong winds are possible from any directions.

0410175 X PONGOLA 27°24'49.93"S, 31°35'32.46"E

The AWS is located on the grounds of a sugarcane research station, and is mostly surrounded by sugarcane fields. About 60 m to the north-west there are some short trees and isolated buildings which might have a small affect on the wind measurements. The terrain is quite flat. The strong winds are almost always south-easterly to south-westerly.

0427083B8 VAN ZYLSRUS 26°52'35.95"S, 22° 2'49.95"E

The AWS is located about 70 m from the closest building. There are not many buildings in the hamlet of Van Zylsrus and the terrain is very flat with sparse vegetation. The exposure of the anemometer is very good. The strong winds are possible from any directions.

0438784 3 VEREENIGING 26°34'7.48"S, 27°57'29.73"E

The AWS is located close to the runway of the Vereeniging airstrip. There is one low-rise building about 60 m to the south. However, beyond this building all the aerodrome buildings are situated between 130 and 400 m from the anemometer. The closest residential areas are about 500 m to the north-west but it is not significant, and might have a small influence on the wind measurements. The terrain is flat. The exposure is good, except towards the south. The strong winds are possible from all directions, but rarely from the south.

0441416B5 STANDERTON 26°56'15.34"S, 29°14'14.41"E

The AWS is in a recreational area in Standerton, on the edge of the older urban area of the town. Built-up areas are situated in all directions except towards the west-south-west to north-west. A building, with what seems to be a substantial height, is situated at about 100 m to the north. Some trees surround the AWS site. The terrain is flat. The strong winds are possible from all directions.

0472278 0 LICHTENBURG 26° 8'50.07"S, 26° 7'42.04"E

The exact location of the AWS could not be located, but it is situated about 2 km west of the town of Lichtenburg. The terrain is quite flat. From photographs it seems that there are no significant buildings or obstructions in the vicinity of the AWS, except for a water tower and associated building at a distance of maybe about 100 m. The strong winds are possible from almost all directions.

0475879 0 JHB BOTANICAL GARDENS 26° 9'36.91"S, 27°59'53.09"E

The exact location of the AWS could not be established. However, from photographs it is clear that there are tall trees in the vicinity. The weather station is located in the central parts of the city of Johannesburg. The surrounding built up areas will influence the wind measurements significantly, and therefore this weather station is not ideally situated for wind measurements. The strong winds are possible from all directions.

0476399 0 JHB INTERNATIONAL WO 26° 8'36.87"S, 28°14'11.80"E

The AWS is located next to one of the runways of the O R Tambo International Airport. The airport buildings and hangars are located to the west, the closest being a distance of about 650 m from the anemometer. The airport is basically surrounded by built up areas. Those to the west are mainly high-rise while those to the east are low-rise, mainly residential, and more than 2 km away. The terrain is flat. It is concluded that the exposure is fine, but that measurements will definitely be affected for winds from the south-western to north-western sectors from which most strong winds are forthcoming.

0479870 X ERMELO WO 26°29'51.36"S, 29°59'1.66"E

The AWS is situated 30 m north-west of the weather office building at the airstrip. The weather office is located at about 600 m north-east of the closest built-up area and about 1 km north of the town of Ermelo. Due to the proximity of the built-up areas as well as the position of the weather office building, some influence on wind readings from the south-east through to the west-north-west can be expected. The terrain is somewhat hilly. The strong winds are almost always south-westerly to north-westerly.

0508047 0 MAFIKENG WO 25°48'18.00"S, 25°32'26.31"E

The AWS is situated about 100 m south-east of the airport building at Mmabatho Airport. The airport is located 6 km north-west of the city. The terrain is flat. The strong winds are mostly north-easterly, but possible from other wind directions as well.


Mafikeng WO
Image © 2009 DigitalGlobe
167 m
Imagery Date: May 2005
25°48'18.91" S 25°32'27.59" E elev 1287 m
Eye alt 1.93 km
Google

0511399 X RUSTENBURG 25°39'37.73"S, 27°13'55.26"E

This AWS is located almost in the middle of the city of Rustenburg. Winds from the south-west will be the least affected by the urbanization, due to a golf course about 300 m away in that direction. The positioning of this station is poor. The strong winds are southerly to north-westerly.

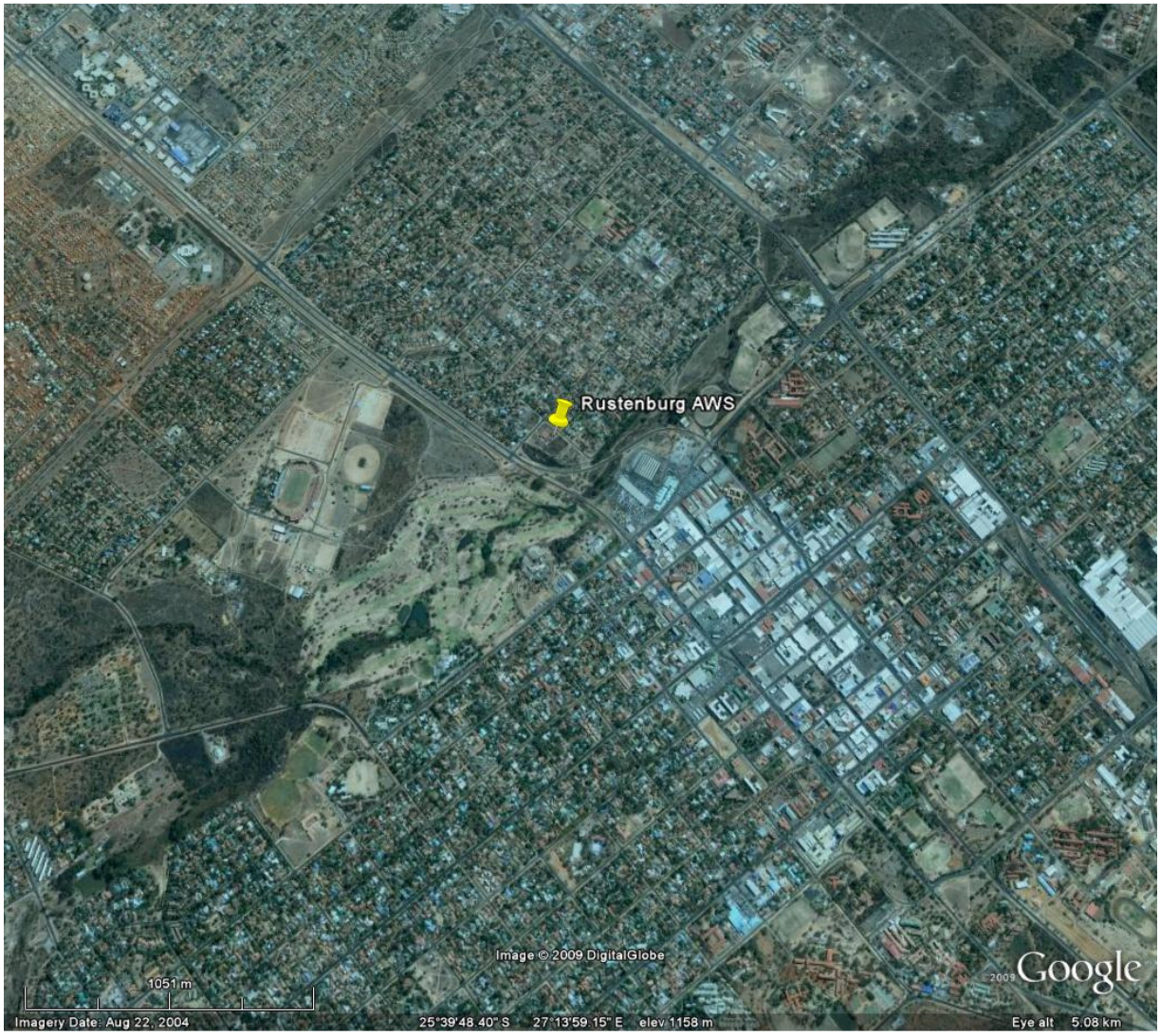

0513346 0 PRETORIA UNISA 25°45'55.85"S, 28°12'11.83"E

The exact location of the AWS could not be established. Shrubs and trees with a height of about 2 m surround the weather station, which is located on a hill to the south of the Pretoria CBD. There is about a 100 m drop in elevation in the westerly to south-westerly directions, over a distance of 800 m to 1,3 km. Towards the other directions the drop in elevation is more gradual. In most of the wind directions the weather station is surrounded by built-up areas at various distances from the anemometer. All the above factors, which can influence the wind measurements, have the effect that it is impossible to guess how the wind measurements will be influenced. This weather station is not ideally situated for wind measurements. The strong winds are possible from any directions.

0513385A2 IRENE WO 25°54'37.79"S, 28°12'38.16"E

The AWS is situated about 40 m to the north of the weather office complex. Closer, to the east, there is a parking bay with a low roof. A new residential area is situated at about 500 m to the south-west. The terrain is flat. Apart from wind measurements from the south, which might be influenced by the office complex, the exposure is good. The strong winds are possible from any directions.

0515320 8 WITBANK 25°50'15.65"S, 29°11'30.40"E

The exact location of the AWS could not be established, but according to the approximate position and available photographs the anemometer should be located at least 50 m north of the ATC tower of the Witbank Aerodrome. The terrain is flat, and the closest built up area, which is low rise residential, is about 650 m to the north-west. The exposure seems to be good. The strong winds are possible from any directions.

0520691 2 KOMATIDRAAI 25°30'49.72"S, 31°54'44.16"E

The AWS is located close to the offices of an agricultural estate. According to available photographs there are a few trees in the vicinity of the anemometer, at most 3 m high. The office building is located at about 50 to 100 m to the east, but low. The area is surrounded by farmland and the terrain is flat. The strong winds are possible from any directions, but not often from the east.

0548375A4 PILANESBERG 25°15'13.52"S, 27°13'7.30"E

The exact position of the AWS could not be determined from the available information. The instruments are located at the first rest camp of the Pilanesberg Nature Reserve. There are no tall buildings in the camp and from available photographs the exposure seems to be good. The terrain in the vicinity of the AWS is flat. The strong winds are mainly south-westerly to westerly, but possible from other directions as well.

0587725CX THABAZIMBI 24°34'41.19"S, 27°24'53.63"E

The exact position of the AWS, which is located next to an airstrip, could not be determined. However, it is assumed, from available photographs, that there are no significant structures in the immediate vicinity. There are mountains to the west and north which reach height of about 250 m or more above station level. To the south the town of Thabazimbi stretches over a distance of about 2 km. South of the town a mountain range reaches heights of almost 500 m above station level. The combination of town and mountain can severely slow down winds from the south. The positioning of the AWS is not ideal for wind measurements. The strong winds are possible from all directions.


Thabazimbi AWS
© 2009 Tele Atlas
© 2009 Cnes/Spot Image
1093 m
24°35'08.03" S 27°24'42.09" E elev 970 m
Eye alt 4.90 km
©2009 Google

0594626B9 GRASKOP 24°55'51.98"S, 30°50'36.90"E

The AWS is basically close to the centre of the rural town of Graskop. Some low isolated buildings are situated close-by, the closest probably about 30 m away. The surrounding buildings, although quite low, will probably have some influence on the wind readings. A gradual increase in altitude from west to east is observable. The strong winds are southerly to north-westerly, but also possible from other directions.

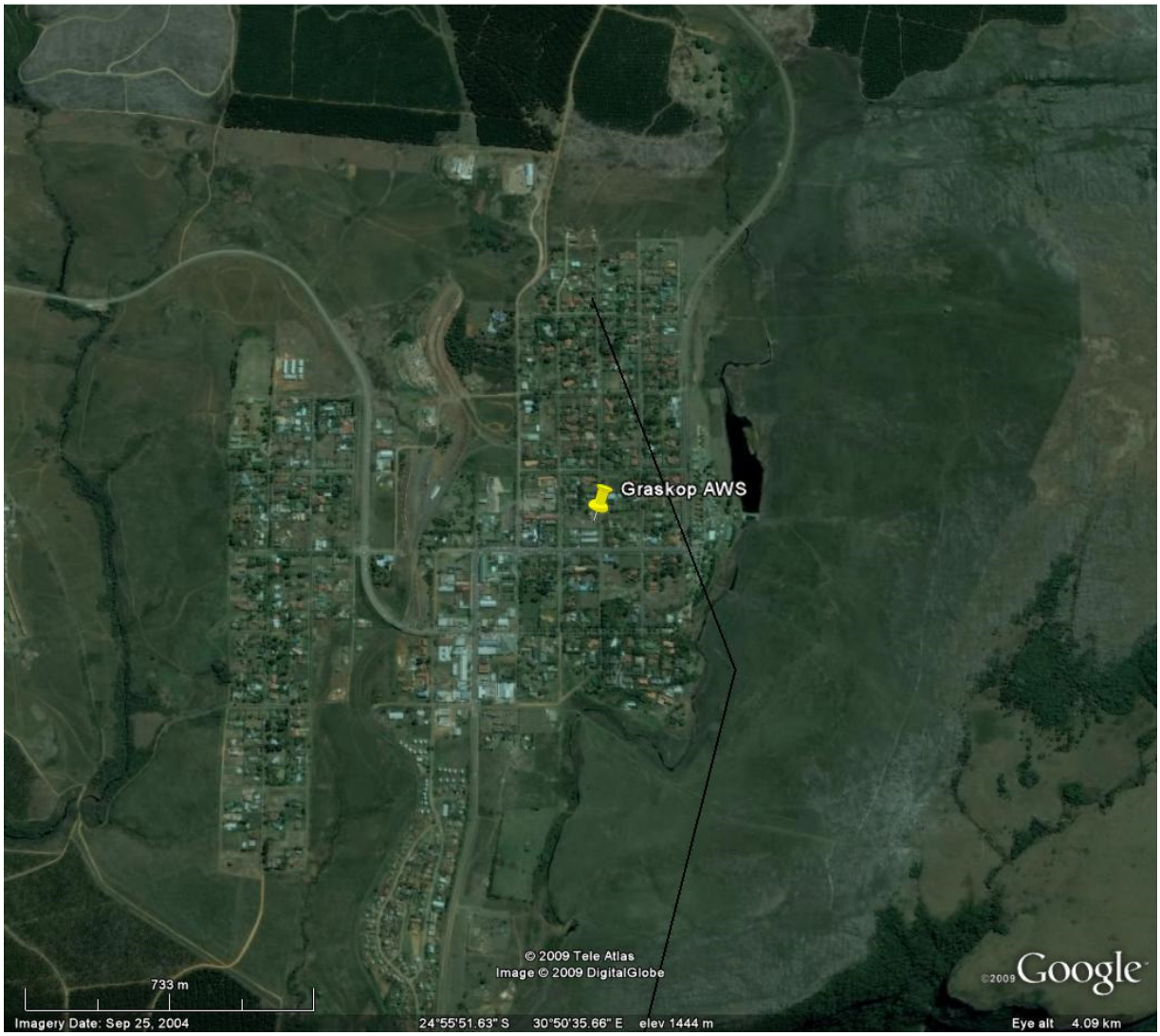
Graskop AWS
© 2009 Tele Atlas
Image © 2009 DigitalGlobe
733 m
Imagery Date: Sep 25, 2004
24°55'51.63" S 30°50'35.66" E elev 1444 m
Eye alt 4.09 km
©2009 Google

0633882 7 POTGIETERSRUS 24°11'36.81"S, 29° 0'11.19"E

The AWS is situated next to an abandoned air strip, just south of the main town area of Mokopane (formerly Potgietersrus). From the Google maps it is not possible to locate the exact position of the station, but available photographs indicate some trees in the vicinity with heights of about 5 m. There are no buildings of significant height in the immediate vicinity of the AWS. However, the proximity to built-up areas indicates possible influences such as reduced wind speeds, from most directions. The strong winds are possible from all directions.


Potgietersrus AWS
Image © 2009 DigitalGlobe
© 2009 Cnes/Spot Image
© 2009 Tele Atlas
© 2009 Europa Technologies
1557 m
Imagery Dates: Jul 30, 2004 - Jun 20, 2007
24°11'34.69" S 29°00'10.08" E elev 1104 m
Eye alt 6.76 km
©2009 Google

0638081 1 HOEDSPRUIT 24°21'15.90"S, 31°2'59.13"E

The exact location of the AWS could not be determined. However it is situated in the vicinity of the ATC tower of the Hoedspruit Air Force Base. From photographs it can be estimated that the distance from any significant structures are far enough not to influence the anemometer readings significantly. The terrain is quite flat. The strong winds are usually south-easterly to south-westerly.

0674341 8 ELLISRAS 23°40'37.85"S, 27°42'24.71"E

The AWS is situated close to the village of Onverwacht, which is about 4,5 km west of Lephalale (formerly Ellisras). The exact position of the AWS could not be determined, but from photographs it seems that there are no significant buildings closer than about 100 m. The terrain is flat and typical Bushveld, i.e. grass or soil interspersed with trees of about 5 m in height. From the available information the exposure seems to be good. The strong winds are possible from any directions.

0675666 2 MARKEN 23°35'45.23"S, 28°23'16.02"E

The AWS is situated on school grounds, far enough from any significant +buildings. A small building, about 2 m high, is situated next to the anemometer but this will not influence the wind measurements significantly. The terrain is flat. The strong winds are possible from any directions.

0677802BX PIETERSBURG WO 23°51'27.83"S, 29°27'7.71"E

The AWS is situated close to the weather office next to the runway of the Gateway International Airport at Polokwane. Winds from the southern sector might be influenced by the built up area of the airport, as well as the city of Polokwane to the south of it. The terrain is flat. The strong winds are possible from any directions.


Pietersburg WO
397 m
© 2009 Cnes/Spot Image
Google
23°51'36.19" S 29°27'09.89" E elev 1237 m
Eye alt 2.64 km

0723664 6 THOHOYANDOU WO 23º04'48"S, 30º23'01.50"E

Thohoyandou Weather Office is located at the P R Mphephu Airport. Except towards the south-west, the station is surrounded by low-rise residential developments, at various distances. The closest development is directly to the south, but the density is so low that it should not have a significant effect on the anemometer readings. However, the ATC tower is about 50 m directly north of the weather station. These buildings are usually tens of meters high, and therefore will significantly influence the anemometer readings, by creating a sheltering effect for winds from the north. What seems to be an isolated low-rise building is situated about 30 m to the west of the anemometer. The strong winds are almost always south-easterly to south-westerly.